Host-microbe relationships: impacts on the mother and offspring

Maternal-microbiome relationships in pregnancy and impact on offspring intestinal development

By Katherine M. Kennedy,

A Thesis Submitted to the School of Graduate Studies

in the Partial Fulfillment of the Requirements for the Degree

Doctor of Philosophy

McMaster University

McMaster University

Doctor of Philosophy (2021)

Hamilton, Ontario (Department of Biochemistry and Biomedical Sciences)

TITLE: Maternal-microbiome relationships in pregnancy and impact on offspring intestinal development

AUTHOR: Katherine M. KENNEDY BSc., MSc. SUPERVISOR: Dr. Deborah SLOBODA

NUMBER OF PAGES: xxi, 280

Abstract

Fetal intestinal and immune development prepares the neonate for life in a microbial world, and the environment within which this development occurs has implications for lifelong health and the prevention of chronic diseases. We hypothesized that obesity-associated shifts in the maternal gut microbiota contribute to a pro-inflammatory milieu through impaired maternal gut barrier function, resulting in altered fetal gut development, neonatal microbial colonization, and offspring intestinal structure and function. In Chapter 3, we found that microbial gut colonization does not occur before birth in healthy term infants. In Chapter 4, we investigated the normal course of microbial profiling in human pregnancy and the impact of pre-pregnancy body mass index (BMI) and gestational weight gain (GWG) on this profiling. We found that the maternal gut microbiota composition changed less over the course of pregnancy in participants with higher pre-pregnancy BMI and that pre-pregnancy overweight/obesity was associated with a decreased relative abundance of short-chain fatty acid (SCFA) producers. In Chapter 5, we used an *in vivo* mouse model of high-fat (HF) diet-induced obesity during pregnancy and found that HF diet intake increased maternal intestinal permeability and increased levels of maternal circulating proinflammatory factors at term gestation, and induced fetal intestinal inflammation. In Chapter 6, we aimed to investigate the role of tumour necrosis factor (TNF) in inducing endoplasmic reticulum (ER) stress in maternal intestinal adaptations to pregnancy as well as fetal intestinal development in the context of diet-induced obesity. We found that pregnancy and HF diet-induced shifts in the gut microbiota were modestly modulated by TNF and that maternal

HF diet-induced fetal intestinal inflammation was dependent on TNF. In Chapter 7, we investigated the relationship between early-life exposure to maternal HF diet and the offspring gut microbiota, as well as offspring gut permeability and susceptibility to postnatal HF challenge. We found that maternal HF diet intake resulted in changes in gut microbiota community composition that persisted to adulthood and that offspring born to HF mothers were predisposed to increased gut barrier permeability. Collectively, our data provide new insights into host-microbe relationships and their impact on the mother and offspring.

Acknowledgements

I am grateful to have worked with, learned from, and been supported by many remarkable individuals throughout my time as a PhD student. Thank you to Dr. Deborah Sloboda for your unwavering guidance and encouragement, for creating a collaborative and supportive lab environment, for your inspiring enthusiasm, for your mentorship and sponsorship. Thank you my committee members Dr. Michael Surrette and Dr. Dawn Bowdish for your support and guidance, for your invaluable perspectives and contributions to this research.

Thank you to the amazing members of the Sloboda Lab that I have been fortunate to work with, learn with, and learn from. Thank you to Wajiha Gohir, Violet Patterson, Jessica Wallace, Dr. Tatiane Ribeiro, Dr. Luseadra McKerracher, Dr. Jessica Breznik, Erica Yeo, Patrycja Jazwiec, Christian Bellissimo, Brianna Kennelly, and Ana Chouvalov. Thank you also to the undergraduate students that I have had the privilege of working with: Emily Moon, Alexandria Amadasun, Jade Schneider, Harshini Ramesh, Megane Bouchard, and William Hum. Thank you to the members of the Schertzer Lab, the Bowdish Lab and the Surette Lab, thank you to Michelle Shah and Laura Rossi.

Thank you to Dr. Thorsten Braun and the Braun Lab for your collaboration, upon which a large part of this thesis is built. Thank you to Dr. Stephanie Atkinson and Caroline Moore for your collaboration and all your work supporting the BUGS in BHIP study. Thank you to all of the participants in the studies within this thesis, for your generous contributions.

Table of Contents

List of Figures

List of Tables

List of Abbreviations

ASV amplicon sequence variant

Atf activating transcription factor

AUC area under the curve

BMI body mass index

BMP bone morphogenic protein

C control

C-section Cesarean section

cDNA complementary deoxyribonucleic acid (DNA)

Chop CCAAT-enhancer-binding protein homologous protein

Cp crossing point

CYP7A1 cholesterol 7α-hydroxylase

DIO diet-induced obesity

DNA deoxyribonucleic acid

DSS Dextran sulphate sodium

E embryonic day

eIF2α Eukaryotic translation initiation factor 2α

ER endoplasmic reticulum

FITC fluorescein isothiocyanate

g grams

GC goblet cell

GC/MS gas chromatography-mass spectroscopy

GDM gestational diabetes mellitus

gDNA genomic DNA

Gpr G protein-coupled receptor

Grp78 78-kDa glucose-regulated protein

GWG gestational weight gain

HF high-fat

IBD inflammatory bowel disease

IEC intestinal epithelial cell

Ig immunoglobulin

IL interleukin-

IRE1 Inositol-requiring enzyme 1

ISC intestinal stem cell

JAK Janus kinase

JNK c-Jun N-terminal kinase

Klf4 Kruppel like factor 4

Lgr5 leucine-rich repeat-containing G protein-coupled receptor 5

LPS lipopolysaccharide

mRNA messenger ribonucleic acid (RNA)

MUB mucin-binding protein

Muc mucin

Myd88 myeloid differentiation primary response 88

NF-κB nuclear factor kappa B

NOD non-obese diabetic

P postnatal day

PCoA principal coordinate analysis

PCR polymerase chain reaction

Pdgf platelet-derived growth factor

PERK Protein kinase R-like endoplasmic reticulum kinase

PERMANOVA permutational multivariate analysis of variance

pHFD post-HF diet challenge

qPCR quantitative polymerase chain reaction

RCT randomized controlled trial

RNA ribonucleic acid

rRNA ribosomal RNA

SCFA short-chain fatty acid

SM sample: maternal

SPF specific-pathogen-free

STAT signal transducer and activator of transcription

Th T helper

Tjp1 tight junction protein 1

Tlr toll-like receptor

TNF tumour necrosis factor

TNF$^{-/-}$ TNF knockout

TRAF2 TNF receptor-associated factor 2

UPR unfolded protein response

V3-V4 variable 3 and 4

W0 week 0

WBG whole blood glucose

Wt wildtype

Xbp1 X-box binding protein 1

Declaration of Academic Achievement

I, Katherine M. KENNEDY, declare that this thesis titled, "Maternal-microbiome relationships in pregnancy and impact on offspring intestinal development" and the work presented in it are my own. I confirm that:

- For all microbiota profiling, genomic DNA extraction was performed by Michelle Shah of the Surette Lab, 16S ribosomal RNA (rRNA) gene amplification and processing of raw sequencing data was performed by Laura Rossi of the Surette lab, and amplicon sequencing was performed by the Farncombe Genomics Facility.

- Chapter 1: Excerpts of the introduction were adapted from a previously published Conference Proceeding (1) written in collaboration with Dr. Johanna Selvaratnam and Dr. Deborah Sloboda.

- Chapter 3: I am the primary author of this paper. The study was done in collaboration with the Braun Lab at the Charite University in Berlin Germany, who collected the participant samples and performed the microbial cultures. I processed all the meconium samples and analyzed all the data and wrote the manuscript.

- Chapter 4: This study was done in collaboration with the Braun Lab at the Charite University in Berlin Germany, who recruited participants and collected samples. I processed all samples and analyzed all data.

- Chapter 5: I am a co-primary author of this paper. The study was completed equally by the candidate and by Wajiha Gohir, a former MSc Student of the Sloboda Lab. Wajiha Gohir completed the animal experiments, performed maternal in vivo permeability tests and maternal and placental inflammatory profiling, and processed fecal samples for bacterial sequencing, and participated in manuscript editing. I processed cecal samples for short-chain fatty acid (SCFA) quantification, contributed to gut microbiota analyses, assisted in lipopolysaccharide (LPS), tumour necrosis factor (TNF), and interleukin- (IL)6 quantification in maternal serum, prepared placental for Nanostring analysis, performed all fetal gut analyses and wrote the main manuscript.

- Chapter 6: I performed all experiments and analyzed all data, with the following exceptions. Christian Bellissimo, Erica Yeo, Dr. Jessica Breznik, Jessica Wallace, Patrycja Jazwiec, Dr. Tatiane Ribeio, and Violet Patterson assisted with maternal and fetal dissections. Maternal intestinal histology analyses were assisted by undergraduate thesis students in the Sloboda Lab: Emily Moon and Jade Schnarr.

- Chapter 7: I performed all experiments and analyzed all data, with the following exceptions. Erica Yeo, Patrycja Jazwiec, and Dr. Tatiane Ribeiro assisted with in vivo intestinal permeability experiments. Offspring intestinal histology analyses were assisted by an undergraduate thesis student in the Sloboda Lab, William Hum.

- Appendix A: I am the primary author of this Letter to the Editor and

performed the reanalysis of published data and wrote the manuscript with assistance from all listed co-authors.

- Appendix B: This study was done in collaboration with the Atkinson Lab at McMaster University in Hamilton, Ontario, who recruited participants and collected fecal samples. I processed all samples and analyzed all data.

- Appendix C: I performed all experiments and analyzed all data, with the following exceptions. Generation of littermates and littermate genotyping was performed by the Bowdish Lab. Christian Bellissimo, Erica Yeo, Dr. Jessica Breznik, Patrycja Jazwiec and Dr. Tatiane Ribeio assisted with maternal and fetal dissections.

- Appendix D: I performed all experiments and analyzed all data, with the following exception. Analysis of video recordings for offspring behaviour experiments was assisted by undergraduate thesis students in the Sloboda Lab: Brianna Kennelly and Megane Bouchard.

Chapter 1

Introduction

1.1 The gut microbiota

1.1.1 The healthy gut microbiota

The human gastrointestinal tract is colonized by over 10^{13} microbes, collectively known as the human gut microbiota (2). The gut is one of the most densely colonized microbial ecosystems (3) and participates several foundational physiological functions. Within the gastrointestinal tract, microbial diversity and density increase along two axes: from proximal to distal and from the tissue to the lumen (4) and the composition of this microbial community is associated with health and disease risk (5). When and how environmental factors impact this community composition is still unclear but under intense investigation.

Over the (postnatal) life-course, gut microbial community composition is relatively stable over time within individuals (6), with much greater variability

between individuals (7, 8) and is characterized by shallow diversity with representation of relatively few abundant phyla but many species and subspecies (8, 9). This may be due to the competing selective pressures that exist within the gut: the host favours stability through functional redundancy and microbes favour functional specialization to reduce interspecies competition for nutrients (10). Typically, a healthy gut microbiota is characterized by a high diversity of microbial taxa (8), but measures of richness can also be affected by transit time and stool consistency (11, 12).

Functionally, gut microbes synthesize essential amino acids and vitamins, detoxify potentially harmful xenobiotics (13), and metabolize energy sources otherwise inaccessible to their hosts, such as cellulose and resistant starches (14, 15). Beyond its metabolic contributions, the gut microbiota also influence immune development and function (16) and intestinal barrier function (17–19) through the production of metabolites such as short-chain fatty acids (SCFAs) (20, 21). SCFAs are primarily produced in the colon (and cecum in rodents (22)) from the fermentation of undigested carbohydrates (23). Acetate, propionate, and butyrate are the most abundant SCFAs produced in the colon (23), where they act as an energy source for colonocytes (24) and stimulate β-oxidation and oxygen consumption to maintain an anaerobic gut lumen (25). SCFAs act primarily through binding to G protein-coupled receptor (Gpr)41 and Gpr43 (26). Gpr43 preferentially binds acetate and propionate, while Gpr41 preferentially binds butyrate and has a lower affinity for acetate (27). Most available evidence to data supports a beneficial role for SCFAs in host metabolism (22, 23, 28, 29) although some studies have also linked SCFAs production to obesity (30).

Importantly, SCFAs are key regulators of intestinal barrier function (31).

1.1.2   The gut barrier: host-microbe interactions

The intestinal mucosa is a selectively permeable physical and immunological barrier comprised of a mucus layer, antimicrobial peptides and immunoglobulin (Ig)A, a single layer of intestinal epithelial cells, and the lamina propria (32). The intestinal epithelial barrier is mediated by tight junctions, multi-protein complexes that limit diffusion of solutes across the epithelium. Tight junctions are comprised of transmembrane proteins including occludin and members of the claudin family, and peripheral membrane proteins such as tight junction protein 1 (Tjp1) (also known as zona occludens 1) which play a key role in tight junction assembly and maintenance (32). The intestinal epithelium is protected by a mucus layer formed by heavily glycosylated mucin proteins, which prevents direct contact with lumenal microbes (33).

Microbes can stimulate host mucin secretion through the production of SCFAs (34). The SCFA butyrate can increase both transcription (35) and translation of the principle mucin of the mucus barrier, mucin (Muc)2 (34), though this effect is concentration-dependent, with inhibition seen at higher butyrate concentrations (35). Pathogens (36), lipopolysaccharide (LPS) (37), and pro-inflammatory cytokines (38) can also stimulate mucin expression, and many pathogens have evolved invasion mechanisms that exploit properties of the mucus layer (36). Colonization of the mucus layer by commensal microbes can prevent pathogens from exploiting this niche (39). Microbial colonization of the mucus layer is mediated by mucin glycosylation (40–42). The mucus-binding properties

of commensal bacteria have been most extensively studied in Lactobacilli, which possess mucin-binding proteins (MUBs) that bind mucin glycans through terminal sialic acid and sulphate residues (43). While host mucin glycosylation patterns can select for beneficial microbes to promote intestinal homeostasis (42), microbes can also influence mucin glycosylation patterns (44–46). Mucin glycosylation patterns impact the microbial degradation of mucins due to functional specialization between microbial species (47), and while some microbes are mucolytic-specialists (e.g. *Akkermansia* (48)) others, such as *Bacteroides*, adapt their metabolism according to the availability of exogenous and host-derived glycans (14). Variation in mucin glycosylation may explain why some mucin-degrading taxa can have beneficial or harmful effects in different contexts.

The production of SCFAs by microbial mucin degradation can also impact the gut barrier by regulating tight junction assembly (49). A recent study suggested that butyrate-induced increases in tight junction and mucin expression may be particularly important in preventing early-life intestinal inflammation (50).

1.1.3 The gut microbiota in early-life

Microbial colonization of the human intestine is a key developmental process as the order and timing of microbial exposures shape the development of the gut microbiome (51, 52). Altered patterns of microbial colonization during this window of development have been associated with immune and metabolic impairments later in life (53–55). The neonatal gut microbiota is impacted by both host selection (56, 57) and exogenous factors, including delivery mode, diet,

4

and environmental exposures (58).

Shortly after birth, maternal vaginal, skin, and gut microbes can be detected in the infant gut microbiota (59). The gut microbiota of vaginally-delivered infants is initially enriched in *Lactobacillus* species common in the maternal vaginal microbiota (59), while Cesarean section (C-section) infants have a greater abundance of skin microbes including *Staphylococcus*, *Streptococcus*, and *Propionibacteria* (60). As only specific gut-adapted microbes such as *Bifidobacteria* and *Bacteroides* persistently colonize the infant gut (61), differences in the gut microbiota due to delivery mode gradually decrease (60) but the effect of delivery mode can be detected up to at least 2 years of age (62). Interestingly, a recent study found that a decreased abundance of *Bacteroides*, the most reproducible effect of C-section (60, 62–66), was initiated during the second week of life, suggesting that this decrease may be due to host-factors or microbial competition (67).

Transfer of microbiota from mother to child continues after birth with lactic acid bacteria including *Lactococcus* and *Lactobacillus* species transferred through breast milk (68, 69). The microbiota of exclusively breastfed infants is characterized by a lower diversity than that of partially formula-fed infants due to lower diversity within the Firmicutes, and also by a higher relative abundance of *Bifidobacterium* (70). *Bifidobacterium* species are important members of the healthy infant gut microbiota due to their ability to metabolize both human milk oligosaccharides and host mucins to produce lactate, thereby engaging in cross-feeding with other beneficial microbes (71) including the butyrate-producer *Anaerostipes* (72).

As the gut microbiota of infants develops into its climax community around 3 years of age (64, 73), the influence of these early factors is obscured, but not eliminated. The instability of the microbiota during early life makes it more susceptible to modification (74). Early colonizers can shape their environment to be more favourable for their growth by regulating gene expression in epithelial cells and thereby influence the composition and structure of the developing microbiota (75). For example, *Bacteroides thetaiotaomicron* can induce fucosylation of host glycans (76), increasing the availability of fucose as a food source (14), and expanding commensal populations of *Ruminococcaceae* and *Bacteroides* species (77). The enduring influence of the initial colonizers is exemplified by the fact that the microbiota can reflect kinship relationships, with inherited genotypes acting on early colonizers received from the mother and environmental sources (10).

Shifts in early-life gut microbial communities can also have enduring impacts due to the role of the microbiota in immune education, impacting intestinal homeostasis and tolerance later in life (78). Disruption of the gut microbiota in early-life has been associated with an increased risk of inflammatory bowel disease (IBD) (79, 80), asthma (81), and obesity (82, 83). *Bacteroides* in particular may be important for early-life immune education due to structural differences in its LPS, which has been suggested to explain population-level differences in the prevalence of autoimmune diseases (84). There is some evidence to suggest that microbes can also impact development prenatally (85, 86), and that maternal gut microbes may regulate fetal neurodevelopment (87) and intestinal development (88) in preparation for postnatal life.

1.1.4 The gut microbiota in pregnancy

Pregnancy requires physiological, metabolic, and immune adaptations to support fetal growth and development (89). These adaptations may influence and/or be influenced by shifts in the gut microbiota. Most studies investigating the human gut microbiota during pregnancy are cross-sectional, only including pregnancy samples from the second (90) or third trimester (91, 92), while a growing number have investigated the maternal gut microbiota over the course of pregnancy.

In one of the first studies of the gut microbiota during pregnancy, Koren et al. reported an increase in beta diversity and a decrease in alpha diversity in otherwise normal pregnant individuals during the third trimester of pregnancy compared to the first trimester (93). These changes were accompanied by an increase in Proteobacteria, typical of inflammatory conditions (94), and increased levels of pro-inflammatory cytokines including tumour necrosis factor (TNF) (93). Transfer of third-trimester microbiota into germ-free mice also led to greater weight gain and insulin resistance than first-trimester microbiota (93). As these physiological changes are also observed in pregnancy, the authors hypothesized that shifts in the gut microbiota over the course of pregnancy may mediate maternal metabolic adaptations (93).

Maternal metabolic adaptation to pregnancy may also lead to shifts in the gut microbiota. A recent study found the abundance of *Bifidobacterium* was increased in the third trimester of pregnancy compared to the first and was also increased by progesterone (95), levels of which increase in maternal circulation over the course of pregnancy (96). Given the importance of Bifidobacteria in the neonatal gut microbiota, the authors hypothesized this increase may improve

maternal-infant transmission of this genus (95). Probiotic supplementation of *B. breve* and *B. longum* in pregnant women prior to delivery and infants postnatally has been shown to decrease the risk of atopic dermatitis at 18 months of age (97), so increased maternal-infant transmission during delivery may have similar benefits.

Others have found the maternal gut microbiota to be stable over the course of healthy pregnancy (98–100). DiGiulio et al. collected weekly samples from 40 participants and found no significant changes to alpha or beta diversity over the course of pregnancy (98). The authors suggested early reports of a shift in the maternal microbiota were confounded by probiotic and antibiotic consumption and may be due to dietary intervention between the first and second trimester (98). A study of 20 participants by Kumbhare et al. similarly found no difference between first and third-trimester microbiota (99). A recent large cross-sectional study of 1479 pregnant participants also showed limited associations with gestational age, though this study was limited by the lack of longitudinal sampling that could have detected shifts in the microbiota within individuals (100). This inconsistency in the reported impact of pregnancy on the maternal gut microbiota highlights the need for more studies and for accounting for factors such as parity (101), diet (102), and gestational diabetes mellitus (GDM).

Studies of the maternal gut microbiota in cases of GDM have found similar shifts to those seen in type 2 diabetes (91, 103, 104), including decreases in beneficial microbes such as *Bifidobacterium*, *Alistipes* (103), and *Bacteroides*, and increases in *Collinsella* (91). Crusell et al. additionally found *Akkermansia* to be associated with decreased insulin sensitivity (91). While most studies of GDM

have investigated the gut microbiota in the third trimester, Mokkala et al. found an increased abundance of *Ruminococcaceae* in the first trimester was associated with an increased risk of GDM later in pregnancy (105).

To date, a few studies have investigated the impact of pre-pregnancy body mass index (BMI) or gestational weight gain (GWG) on the maternal microbiota (91, 106–109). Collado et al. found pre-pregnancy overweight and excess GWG were each associated with a higher abundance of *Bacteroides* and a lower abundance of *Bifidobacteria* in the first and third trimester (106). Pre-pregnancy overweight was also found to be associated with enrichment of *Bacteroides*, as well as decreases *Akkermansia*, by Crusell et al. (91). Conversely, Santacruz et al. found pre-pregnancy overweight was associated with decreased *Bacteroides*, but reproduced the previous association of decreased *Bifidobacterium* and additionally found *Akkermansia* to be decreased by excess GWG at 24 weeks of gestation (107). Stanislawski et al. also found pre-pregnancy overweight to be associated with a decreased abundance of *Bacteroidaceae* in the third trimester of pregnancy (108). How maternal BMI and/or excess GWG impact gut microbial community shifts over the course of pregnancy and whether these shifts influence fetal and neonatal development is still unclear.

1.2   Early-life intestinal development

1.2.1   Maternal microbiota: impacts on fetal intestinal development

It is possible that shifts in the maternal gut microbiota over the course of pregnancy, and with excess adiposity during pregnancy, impact offspring intestinal development in two ways: through altered maternal-infant microbial transfer during and after birth and/or by impacting fetal intestinal development prior to birth—via their impacts on maternal adaptations to pregnancy or more directly through circulating microbial products. Despite a lack of understanding of pregnancy-related changes in the maternal gut microbiota, there is some evidence to suggest maternal microbes impact fetal gut development via microbial antigens or metabolites (88, 110).

Normal gut development is key to ensuring a niche for commensal bacteria postnatally (10). Although the intestinal epithelium is not the largest surface through which we interact with the external environment (111, 112), it is the most densely populated by microbes. Prenatal intestinal development must appropriately prepare the gut for colonization to promote gut homeostasis. A landmark study by Gomez de Agüero et al. used a transient colonization model during pregnancy to demonstrate the impact of the maternal gut microbiota on fetal intestinal development (88). They found that maternal colonization during pregnancy, in the absence of offspring colonization, increased offspring intestinal epithelial messenger RNA (mRNA) levels of antibacterial peptides, and decreased splenocyte production of TNF in response to LPS (88). These effects

were mediated by the antibody-assisted transfer of microbial fragments or molecules (88). The authors hypothesized that fetal intestinal development may also be shaped by SCFAs produced by the maternal microbiota. This possibility was recently investigated by Kimura et al., who found offspring of germ-free mothers fostered by specific-pathogen-free (SPF) mothers, or SPF mothers fed a low-fibre diet, were more susceptible to high-fat (HF) diet-induced metabolic syndrome, including obesity and glucose intolerance, and had an altered gut microbiota at postnatal day (P)14 (113). These metabolic effects were rescued by treatment with the SCFA propionate during pregnancy. As they found maternal SCFAs were present at similar concentrations in maternal and fetal plasma and phenotypic rescue by maternal propionate treatment was dependent on SCFA receptors Gpr41 and Gpr43, the authors concluded that SCFAs produced by the maternal gut microbiota influenced prenatal metabolic development, though they did not investigate intestinal development specifically (113).

1.2.2   Mechanisms of intestinal development

Prenatal preparation for postnatal colonization requires appropriate development of the intestinal epithelium. Intestinal epithelial cells can be broadly classified as absorptive or secretory, reflecting the dual roles of the intestinal epithelium: nutrient absorption and barrier function. The majority of intestinal epithelial cells are absorptive in both the small and large intestine, where they are termed enterocytes and colonocytes respectively. The most abundant secretory cell types are goblet cells, which secrete mucus to form a protective barrier against lumenal microbes, and Paneth cells, which secrete antimicrobial peptides.

Intestinal development is similar in mice and humans, though in humans it occurs relatively earlier in gestation, primarily within the first trimester, while in mice intestinal maturation continues postnatally until approximately P14 (114). During embryonic development, the gut tube is formed following gastrulation and initially consists of endoderm-derived simple epithelium surrounded by mesoderm. The epithelium then transitions to become pseudostratified as the gut tube grows in length and circumference. Ultimately, the epithelium reorganizes into its simple columnar form. At this time mesoderm-derived mesenchymal cells cluster beneath the epithelium and coordinate the emergence of villi which project into the lumen, increasing intestinal surface area, in a rostral-to-caudal wave (115). This occurs around week 7-9 of gestation in humans and embryonic day (E)14.5-E15.5 in mice (116). The mechanisms behind villus formation are not well known in humans. In mice, the pseudostratified epithelium secretes platelet-derived growth factor (Pdgf) which stimulates the aggregation and proliferation of underlying mesenchymal cells, but it is unclear what factors then initiate villus formation (117). As villi form, the proliferative cells of the intestine become restricted to the intervillus region. Completion of intestinal morphogenesis is marked by the appearance of crypts in between villi around week 11-12 of gestation in humans and P7-P14 in mice. Intestinal stem cells (ISCs) are restricted to these crypts and produce transit-amplifying progenitor cells, which proliferate and differentiate as they move from the crypt to the tip of the villus (118). The formation of crypts coincides with the emergence of Paneth cells (117). Interestingly, although intestinal development in mice is not completed prenatally, a study of allotransplantation of small intestine and colon into the kidney capsule found that this development is intrinsically regulated, as

it is in humans, and not a response to food intake (119).

This is consistent with the conservation, in mice and humans, of critical pathways directing intestinal epithelial differentiation which influence cell fate determination through the timing and extent of exposure to stimuli. The Notch pathway plays a role in balancing secretory and absorptive lineages, as activation is required for enterocyte differentiation and inhibition promotes secretory differentiation (120). Wnt signalling through β-catenin promotes secretory cell differentiation and is antagonized by Notch (121). Activation of the Wnt pathway also promotes intestinal proliferation and stem cell renewal (122).

Wnt activity exists on a gradient opposite to bone morphogenic protein (BMP) signalling, which is lowest at the crypt base and promotes differentiation (123). ISCs of the crypts marked by the Wnt pathway-associated receptor leucine-rich repeat-containing G protein-coupled receptor 5 (Lgr5) (124) are critical for intestinal homeostasis, and depletion of these ISCs has recently been shown to impair intestinal barrier integrity (125). One regulator of Wnt activity is the transcription factor Kruppel like factor 4 (Klf4) as deletion of Klf4 from the intestinal epithelium increases activation of the Wnt pathway (126). Klf4 also is critical for the differentiation of goblet cells (127) and maturation of enterocytes (126), as well as the positioning of Paneth cells at the crypt base (126). Lgr5 has also been shown to influence the differentiation of Paneth cells: deletion of Lgr5 increases Wnt signalling and induces precocious Paneth cell differentiation (128).

Intestinal epithelial cell metabolism also contributes to intestinal development, with a shift towards oxidative phosphorylation and away from glycolysis at the

time of villus formation (129). Interestingly, in mice the timing of villus formation coincides with the detection of SCFAs in fetal circulation (113) and the SCFA butyrate, a major energy source for intestinal epithelial cells (IECs), is metabolized by oxidative phosphorylation (130). It is possible that SCFAs produced by the maternal microbiota contribute to the metabolic regulation of fetal intestinal development. While enterocyte differentiation is impaired by inhibition of this shift towards oxidative phosphorylation, goblet cell differentiation appears to be unaffected (129). In the adult intestine, a gradient of glycolysis-to-oxidative phosphorylation exists along the crypt-villus axis (131), and decreased oxidative phosphorylation has been associated with necrotizing enterocolitis (129), indicating intestinal metabolic regulation may be critical in preparing the intestine for postnatal life.

1.3 Maternal impacts on fetal and offspring gut and offspring microbiota

It is now well established that the environment within which we develop as embryos, fetuses, and infants sets the stage for health later in life. Adverse events occurring during these critical developmental windows can increase disease risk later in life. Such adversity includes poor maternal or infant nutrition (malnutrition, caloric restriction or caloric excess), stress, or exposure to maternal disease. Many pre-clinical and clinical studies have shown that developmental responses to these early life events are inextricably linked to chronic diseases later in life. This framework of perinatal disease risk programming, termed the Developmental Origins of Health and Disease

(DOHaD), has its foundations in early epidemiological studies conducted by Dr. David Barker who, over three decades ago, demonstrated an association between weight at birth and mortality due to ischemic heart disease in adulthood (132). This initial observation led to the formation of the "Barker hypothesis"— a hypothesis founded on the concept that adverse environmental stimuli that occur during prenatal life induce developmental adaptations that later result in the increased risk of what we otherwise assumed were lifestyle-associated diseases, including glucose intolerance, hypertension, and type 2 diabetes (133). A marker of an adverse developmental environment, low birth weight, has since been associated with increased risk of many adult disorders including glucose intolerance (134), insulin resistance (135), and obesity (136).

Adversity during developmental critical windows requires the fetus to make adaptations to maximize its survival postnatally. The developing fetus processes cues or signals from the maternal environment via the placenta to predict which adaptations are most beneficial for postnatal survival. This concept—predictive adaptive response (137) proposes that the degree of mismatch between the pre- and postnatal environments is a major determinant of subsequent disease. While these changes in fetal physiology may be beneficial for short-term survival in utero, they may be maladaptive postnatally, contributing to poor health outcomes. Many animal models of prenatal caloric restriction have also shown associations between fetal growth restriction and offspring obesity (138, 139), insulin resistance, leptin resistance, and altered appetite (140). Interestingly, similar effects on offspring disease risk have been shown in models of maternal diet-induced obesity. HF-diet intake during pregnancy results in increased

adiposity, leptin resistance, and insulin resistance in the offspring, independent of postnatal diet (139). The role of the gut microbiota in mediating the effects of maternal obesity or HF diet on offspring development is currently an active topic of investigation.

1.3.1 Maternal obesity

The role of the gut microbiota in energy extraction and storage has also been linked to the etiology of obesity (15, 141). Globally, 39% of adults are overweight and 13% are obese, and almost half of women enter pregnancy overweight or gain more weight than is recommended over the course of pregnancy (142). Maternal obesity is a key predictor of offspring obesity (143), but the mechanisms behind this association are complex and not fully understood.

Maternal metabolic adaptations to pregnancy mirror changes seen in non-pregnant obesity and the gut microbiota have been implicated in mediating these adaptations (93). A few studies have investigated the relationship between pregnancy-associated maternal microbial shifts and pre-pregnancy BMI or GWG (106–109). Excess maternal adiposity during pregnancy is associated with elevated levels of pro-inflammatory mediators (TNF, interleukin- (IL)6) (144), and reports suggest that some of these associations may be mediated by the gut microbiome and the "dysbiosis" of obesity during pregnancy (92, 107). Maternal obesity has also been linked to shifts in the offspring gut microbiota in humans infants (145) and mice (146), as well as offspring gut inflammation (147). The mechanistic signalling pathways governing these associations are still unclear, and under intense investigation in both clinical and experimental models.

1.3.2 Impacts on offspring microbiota

The microbial community that colonizes the infant gut interacts with its host to influence host metabolism (148) and immune education (78, 149). Early life is a particularly crucial period for the microbiota to influence development (150), so it is important to understand the determinants of microbial community composition. While the gut microbiome is influenced by environmental factors during and after birth including delivery mode (59), feeding method (60), and antibiotic usage (151), the influence of prenatal factors is less clear.

Recently, strain-level metagenomic profiling provided additional evidence of the importance of the maternal microbiota in shaping the infant microbiota (61, 152–154). Ferretti et al. found that during the first day of life, half of the infant gut microbiota belonged to species found in the maternal microbiota (153). The maternal origin of infant gut microbes was further supported as the proportion of shared species that were found to be the same strain was more than 22-fold higher in mother-infant pairs than between unrelated mothers and infants. Maternally transmitted strains were also more likely than to colonize the infant gut, with 70% being retained in the infant gut across repeated sampling compared to 27% retention of strains that were not found in the maternal microbiome. This may indicate maternally-derived strains have greater fitness in the infant gut (153) or differ in their transmission strategy compared to non-maternally derived strains (61).

Although the maternal microbiota is a key source of the early colonizers of the infant gut, the overall microbiota composition of infants differs from that of their mothers (61, 153, 154) due to different selective pressures in the developing gut

(155). As prenatal adversities such as maternal obesity influence both the maternal microbiota and fetal gut development, offspring colonization and host-microbe interactions are likely shaped by each of these factors.

The complexity of interactions between these factors may explain inconsistent findings regarding the impact of maternal overweight and obesity on the offspring gut microbiome. In a longitudinal study of 181 infants from birth to 2 years of age, maternal pre-pregnancy overweight/obesity was not associated with altered infant microbiota composition (108). This may be confounded by GWG, as only a third of non-overweight/obese controls were within the recommended limits for weight gain over the course of pregnancy.

Collado et al. found that both maternal pre-pregnancy overweight and excessive GWG were associated with lower numbers of *Bacteroides* at one month and *Bifidobacterium* at 6 months, and higher numbers of *Clostridium histolyticum* at six months (156). Similarly, Chu et al. reported a relative decrease in *Bacteroides* in neonates of mothers who consumed a high-fat diet compared to those who consumed a low-fat diet (157). However, when Mueller et al. stratified by birth-mode maternal overweight and obesity was associated with relative increases in *Bacteroides* in vaginally-delivered but not C-section neonates (158). Similarly, in a study of 935 mother-infant pairs, Tun et al. found higher relative abundances of *Bacteroides* and *Lachnospiraceae* in vaginally-delivered infants of overweight or obese mothers (159). Previous work has found the abundance of *Bacteroides* to be greater in pregnant women who were overweight or obese prior to pregnancy (106). An increase in the relative abundance of *Bacteroides* in the infant gut microbiota likely influences early immune education, as *Bacteroides*

LPS can inhibit innate immune signalling and endotoxin tolerance (84).

1.3.3   Impacts on intestinal development

One of the most frequently reported driving factors underpinning maternal obesity-induced changes in fetal development is inflammation. In a study of the effects of combined maternal and paternal HF diet, Myles et al. showed increased LPS-induced inflammation in the offspring gut was rescued by cohousing (160), suggesting that inheritance of the microbiota plays a role in the effects of maternal HF diet. Notably, the microbiome of HF offspring was enriched in *Clostridiales*, which have been linked to T helper (Th)17 cell differentiation (161), potentially contributing to the increased LPS-induced IL17 production observed. In sheep, Yan et al. also found that maternal obesity increased colonic IL17 levels in fetuses and offspring and that this was associated with increased nuclear factor kappa B (NF-κB) activity (162), which may contribute to Th17 differentiation (163). As these increases were observed in both the fetal and offspring colon they are not dependent on the inheritance of the maternal microbiota. While IL17 acts on IECs to reduce permeability through regulation of the tight-junction protein occludin (164), IL22, which is also produced by Th17 cells, has recently been shown to increase intestinal permeability by increasing the expression of pore-forming tight-junction protein claudin-2 through the Janus kinase (JAK)/signal transducer and activator of transcription (STAT) pathway (165). Xue et al. showed that maternal diet-induced obesity in non-obese diabetic (NOD) mice increased offspring intestinal permeability and ileal expression of claudin-2, as well as markers of oxidative stress (166).

Oxidative stress due to intestinal inflammation may increase neutrophil infiltration to deplete tissue oxygen by activating the respiratory burst response (167). When combined with a postnatal high-fat diet, maternal obesity is associated with increased neutrophil infiltration in mice that are genetically susceptible to Crohn's disease-like ileitis due to TNF overexpression (168) and in wildtype mice after Dextran sulphate sodium (DSS)-induced colitis (169). Neutrophils contribute to repair and antimicrobial defence following intestinal epithelial damage through the production of IL-22 (170), which acts on intestinal epithelial cells to induce proliferation (171) and antimicrobial peptide production (172). Intestinal inflammation is intricately linked to endoplasmic reticulum (ER) stress, and studies have found that ER stress can be both the cause and a consequence of inflammation (173). Efficient function of the ER, where proteins are translated and undergo post-translational modification, is essential for cell survival. The ER is sensitive to cellular stresses such as inflammation, which hinder protein folding causing an accumulation of immature proteins, resulting in ER stress (174). As the intestinal epithelium is a rapidly proliferating, highly metabolic tissue and must produce many proteins including heavily glycosylated mucins and tight junction proteins, ER homeostasis is critical to its structure and function.

The unfolded protein response (UPR) is a homeostatic mechanism triggered by ER stress that results in signalling through multiple transcription factors and protein-related pathways (Fig. 1.1): Inositol-requiring enzyme 1 (IRE1), cleaves X-box binding protein 1 (Xbp1) mRNA into the transcription factor Xbp1s; Protein kinase R-like endoplasmic reticulum kinase (PERK) phosphorylates

Eukaryotic translation initiation factor 2α (eIF2α), blocking protein synthesis and increasing translation of activating transcription factor (Atf)4, inducing CCAAT-enhancer-binding protein homologous protein (Chop); Atf6 is shuttled to the Golgi and cleaved to release the transcription factor Atf6f. When the UPR fails to restore normal ER function, prolonged activation triggers apoptosis (174, 175). One mechanism behind this is the recruitment of TNFR1 and activation of TNF-independent c-Jun N-terminal kinase (JNK) signalling (176) by IRE1. Deletion of the IRE1 pathway, the most conserved among species, has been shown to impair intestinal barrier integrity in association with increased PERK pathway activation and expression of pro-inflammatory cytokines including TNF (177).
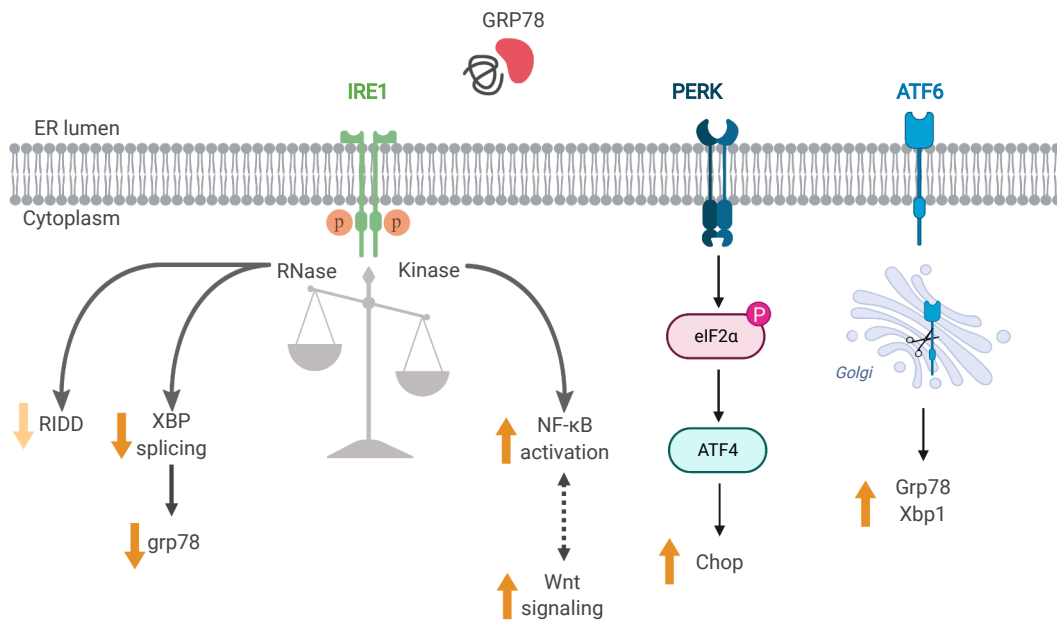
Figure 1.1. The Unfolded Protein Response stress sensors IRE1, PERK, and Atf6 are activated by unbinding of the chaperone protein 78-kDa glucose-regulated protein (Grp78) due to unfolded proteins within the ER.

Obesity is associated with increased ER stress in metabolic tissues (178, 179). Within the gut, ER stress causes under-glycosylation of secreted mucins, decreasing barrier integrity (180), and impaired UPR signalling has been associated with the intestinal inflammatory disorder ulcerative colitis (181). There is also some evidence to suggest that specific microbes impact intestinal ER stress: *Lactobacillus* species have been shown to inhibit intestinal inflammation through modulation of ER stress pathways (182, 183). Currently, the role of inflammation and ER stress in the relationship between maternal obesity, the gut microbiota, and fetal gut development is unclear.

1.4 Rationale

Over the past two decades, the gut microbiota has become one of the most studied factors mediating the impact of the environment on human health and disease throughout our lives (5). The composition of our gut microbiota is influenced by mode of birth and infant feeding in early life (62, 184), and by diet (185, 186), sex, age, host genetics (187), and health status (188) in adulthood. The gut microbiota has important roles in energy extraction (141), intestinal homeostasis (189, 190), and immune education (191, 192). An accumulation of evidence has also implicated gut microbiota as a mediator of obesity in adulthood (15, 193–195), and perturbations of the gut microbiota in early life have been linked to increased risk of obesity in childhood (196–200).

To understand how microbes influence early-life development, we must know how and when we are colonized. Although recent studies have challenged the long-held view that the prenatal environment is sterile (201–204), and suggested

microbial colonization may occur before birth, these data have been criticized (205–208) and concurrent studies have found contamination to be the source of bacterial DNA detected in these sites (209–213). If colonization does not occur before birth, the maternal gut microbiota may indirectly influence fetal development through its impact on maternal physiology. However, little is currently known about the relationship between maternal gut microbes and maternal metabolism during pregnancy, and how changes in maternal pregnancy adaptation influence fetal development.

Maternal metabolic adaptations to pregnancy mirror changes seen in non-pregnant obesity and the gut microbiota have been implicated in mediating these adaptations (93). Few studies have investigated the relationship between pregnancy-associated maternal microbial shifts and pre-pregnancy BMI or GWG (106–109). Excess maternal adiposity during pregnancy is associated with elevated levels of pro-inflammatory mediators (TNF, IL6) (144), and reports suggest that some of these associations may be regulated by the gut microbiome and the "dysbiosis" of obesity during pregnancy (92, 107). Maternal obesity has been linked to shifts in the offspring gut microbiota in humans infants (145) and mice (146), as well as offspring gut inflammation and immune dysfunction (147). These impairments likely stimulate signalling pathways that govern the known relationship between maternal obesity and offspring metabolic and immune dysfunction. However, the signalling pathways governing these associations are still unclear and therefore were the subject of this thesis investigation.

Note: the impact of the COVID-19 pandemic on this investigation is outlined in Appendix E.

1.5 Central Hypothesis

We hypothesize that obesity-associated shifts in the maternal gut microbiota contribute to a pro-inflammatory milieu through impaired maternal gut barrier function, resulting in altered fetal gut development, neonatal microbial colonization, and offspring intestinal structure and function.
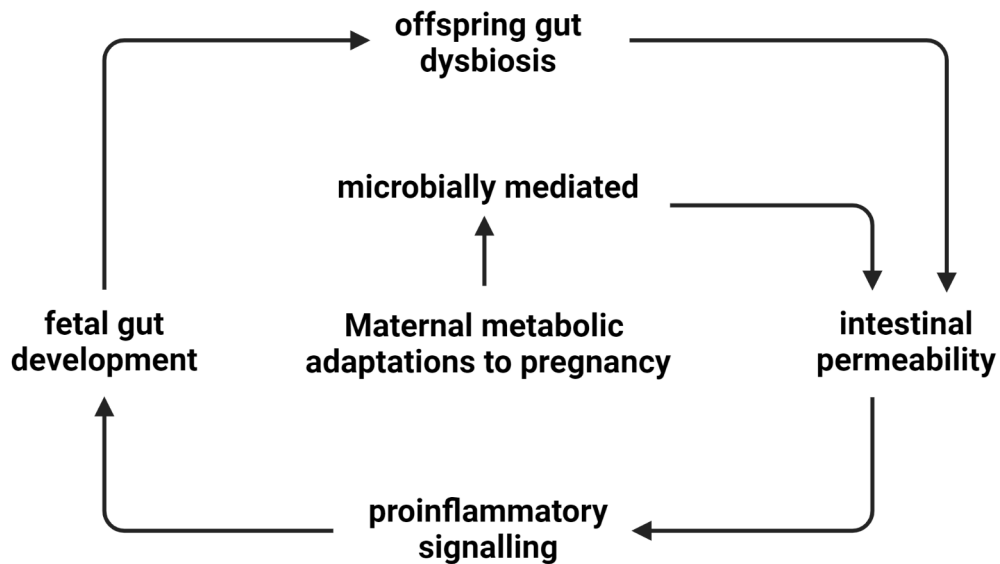
Figure 1.2. Central thesis.

1.6 Overall Aim

We aim to understand host-microbe relationships in the context of excess adiposity during pregnancy and their impact on fetal gut development and offspring gut dysbiosis.

1.7   Specific Aims

1. Determine whether microbial colonization occurs prior to birth in healthy human pregnancies (Chapter 3).

2. Characterize the impact of BMI and GWG on shifts in the maternal gut microbiota over the course of pregnancy and on the infant gut microbiota (Chapter 4).

3. Assess the role of TNF-mediated inflammation in the impact of high-fat diet-induced obesity on maternal gut microbiota and maternal and fetal intestinal ER stress (Chapters 5 and 6)

4. Investigate the relationship between early-life exposure to maternal HF diet and the offspring gut microbiota, as well as offspring gut permeability and susceptibility to postnatal HF challenge (Chapter 7).

Chapter 2

Methods

Methods for Chapters 3 and 5 are within the manuscripts in those chapters.

2.1   Ethical approval

All animal procedures for the present study were approved by the McMaster University Animal Research Ethics Board (Animal Utilization Protocol 12-10-38) in accordance with the guidelines of the Canadian Council of Animal Care.

2.2   Human studies

Healthy pregnant females >18 years of age with singleton pregnancies (nulliparous or multiparous), were recruited between 9-17 weeks gestation. Women with severe chronic gastrointestinal diseases or conditions; any significant heart, kidney, liver or pancreatic diseases; pre-existing diabetes; who were currently smoking and will not discontinue smoking during the pregnancy; or

identified previously with depression were excluded. Participants were be evaluated 4 times: at end of the first (10-17wks), second (26-28wks) and third trimesters (>36wks) of pregnancy and 6 months postpartum. Body mass index (BMI) of mothers will be obtained from measured height and weight at recruitment and BMI categorized into; healthy (18.5-24.9kg/m2); overweight (25-29.9 kg/m2), obese (>30<40 kg/m2). At each visit, participants completed a standard 3-day food and supplement intake record. Also at this time, women completed the Bristol Stool Chart, a diagnostic tool to evaluate gut function. Maternal stool samples were collected at end of each trimester of pregnancy, at delivery, and maternal and infant stool samples at 6 months postpartum. Data on pregnancy and infant outcomes were obtained from clinic charts including; impaired fasting and glucose intolerance, pre-eclampsia, mode of delivery; birth weight, gestational age, birth trauma including shoulder dystocia, and 5-minute Apgar score.

2.3   Animal studies

wildtype (Wt) C57BL/6J female and male mice (RRID: IMSR_JAX:000664), and TNF knockout (TNF$^{-/-}$) C57BL/6J female and male mice (RRID: IMSR_JAX:003008), were bred at the McMaster University Central Animal Facility under specific-pathogen-free (SPF) conditions. Pathogen-free status was ensured through continuous monitoring of sentinel mice and specific testing of fecal samples for common murine pathogens. Female mice were randomly assigned to a control diet (17% kcal fat, 29% kcal protein, 54% kcal carbohydrate, 3.40 kcal/g; HT8640 Teklad 22/5 Rodent Diet; Harlan, Indianapolis, IN, USA) or

high-fat (HF) diet (60% kcal fat, 20% kcal protein, 20% kcal carbohydrates, 5.24 kcal/g; D12492; Research Diets Inc., New Brunswick, NJ, USA). Females were housed two per cage with food and water available ad libitum at a constant temperature (22 °C) under a 12:12 light/dark cycle.

Chapter 6: Pregnancy and fetal experiments

Following 6 weeks of dietary intervention female mice were co-housed with a control-fed male of the same genotype and mating was confirmed by visualization of a vaginal plug. Maternal fecal samples were collected before dietary randomization (week 0 (W0)), before mating (embryonic day (E)0) and at term gestation E18.5. At E18.5, maternal serum was collected via tail vein blood and stored at –80°C for future analyses. Pregnant mice were killed by cervical dislocation. Maternal cecal contents and intestinal tissue from the duodenum, jejunum, ileum and colon were snap-frozen in liquid nitrogen and stored at –80°C. Fetuses were dissected free and fetal weights were recorded. Fetal intestinal tissues were dissected free and small and large intestines were snap-frozen in liquid nitrogen and stored at –80°C. All sample sizes in the study represent a litter or dam as a biological replicate, with one female and one male being randomly selected from each litter for each tissue of interest.

Chapter 7: Offspring experiments

Following 2 weeks of dietary intervention female mice were co-housed with a control-fed male of the same genotype and mating was confirmed by visualization of a vaginal plug. Pregnant females were housed individually, and gestational weight and food intake were recorded throughout pregnancy and lactation. Dams

were allowed to deliver and surviving litters were normalized to 6 offspring at postnatal day (P)3 with equal numbers of female and male offspring where possible. Maternal fecal samples were collected at P3, P14, and P28 during lactation. Offspring were weaned onto a control diet at P28 and were housed in same-sex pairs with ad libitum food and water. Offspring weights were recorded at P3, P7, P14, and P21 before weaning, and weights and food intake were recorded weekly from weaning onward until sacrifice. Tissues were collected from a maximum of one male and one female offspring per dam at P3, P14, and P120. Adult offspring remaining after P120 collections were challenged with a HF diet (60% kcal fat) and sacrificed for tissue collection after 6 weeks of dietary intervention (post-HF diet challenge (pHFD)). Offspring were sacrificed by decapitation (P3 and P14) or cervical dislocation (P120 and pHFD). Offspring serum was collected and stored at -80℃ for future analysis. Offspring fecal samples, cecal contents, and intestinal tissue from the duodenum, jejunum, ileum, and colon were fixed in Carnoy's fixative and stored in 70% ethanol or snap-frozen in liquid nitrogen and stored at -80℃.

2.3.1   In vivo experiments

Metabolic and body composition assessment

Blood glucose was measured via tail vein using the Accu-Chek Inform II system glucometer and test strips (Roche Diagnostics). Adiposity was measured as percent body fat calculated from whole-body Echo-MRI imaging (Bruker Minispec LF90-II).

In vivo intestinal permeability assessment

Mice were placed in a clean cage and fasted for 4 hours (lactation study: 8 am – 12 pm). Blood was collected via tail nick in a heparinized capillary tube before gavage with 4 kDa fluorescein isothiocyanate (FITC)-dextran (cat:46944, Sigma-Aldrich) diluted in PBS (pH 7.4; 8 mg/kg body weight), and post-gavage at 30, 60, 90, 120, and 240 minutes. Acid-citrate dextrose (15% v/w; cat: C3821, Sigma-Aldrich) was added to blood samples after collection to prevent clotting. Plasma was collected post centrifugation (8000 rpm, 10 minutes) after each time point and stored on ice until all samples were collected. Whole-intestinal permeability was assessed by measuring fluorescence in plasma diluted 1:10 in PBS in duplicate on a plate reader with excitation at 585 nm and emission at 530 nm (Synergy H4 Hybrid Microplate Reader, BioTek Instruments, Inc.). Intestinal permeability was calculated by subtracting the average baseline fluorescence values and average fluorescence of triplicate wells of PBS (sample blank) from the average post-gavage fluorescence values at each time point in each mouse and was expressed as relative fluorescence units.

2.3.2 Intestinal histology

Intestinal sections were fixed in Carnoy's fixative (60% ethanol, 30% chloroform, 10% glacial acetic acid) at room temperature for 4 hours and processed and embedded into paraffin. Tissue sections were cut at 4 μm thickness on charged glass slides.

PAS staining

Following deparaffinization, slides were immersed in Periodic Acid
(Sigma-Aldrich, 3951-100 ml) for 5 minutes then rinsed in several changes of
distilled water and immersed in Schiff's reagent (Sigma-Aldrich, 3952-50 ml) for
15 minutes and then washed in running tap water for 5 minutes. Slides were
counterstained with hematoxylin for 60 seconds and rinsed in running tap water
for 5 min. Following staining, slides were dehydrated and mounted with
Permount (Fisher Sci, SP50-500).

PAS analysis

Stained tissue sections were imaged with the Nikon Eclipse NI microscope
(960122, Nikon Eclipse NI-S-E). Images were captured using the Nikon DSQi2
Colour Microscope Camera and Nikon NIS Elements Imaging Software
(v4.30.02). Image analysis was performed in ImageJ. For each tissue section, 10
villi and crypt were randomly selected for measurements. Villus and crypt
lengths were measured and the goblet cells in those villi and crypts were counted.

2.3.3   Intestinal gene expression

RNA extraction

Maternal intestinal, placental, and fetal small intestinal tissue was homogenized
by bead beating in 900 μL of TRIzol (Life Technologies) and centrifuged at
12,000 g for 10 minutes at 4°C. The supernatant was removed and added to 300
μL of chloroform. The solution was thoroughly mixed and incubated at room
temperature for 3 minutes. Samples were centrifuged for 10 minutes at 12,000 g

at 4°C. The aqueous phase of the sample was removed and added to 500 μL of isopropanol. Samples were mixed thoroughly, incubated for 20 minutes at room temperature, after which they were centrifuged at 12,000 g for 10 minutes at 4°C. The supernatant was removed and the resulting pellet was washed twice with 75% ethanol. ribonucleic acid (RNA) was reconstituted in 20 μL of ultrapure water. RNA was quantified using the NanoDrop 2000 spectrophotometer (Thermo Scientific, Waltham, MA, USA) with NanoDrop 2000/2000c software (Thermo Scientific). The A260/A280 and A260/A230 ratios for all samples were >2.0 and >1.5, respectively. All RNA samples were stored at –80°C until experimentation. As a result of the small amount of starting material, fetal small intestine RNA was extracted using the RNeasy Mini Kit (Qiagen, Valencia, CA, USA) per the manufacturer's instructions.

cDNA synthesis

Following extraction, 2 μg of RNA was used for complementary DNA (cDNA) synthesis using the Superscript VILO™ cDNA Synthesis Kit (Life Technologies) per the manufacturer's instructions. Each reaction consisted of 4 μL of 5 $\times$ VILO™ Reaction Mix, 2 μL of 10 $\times$ SuperScript Enzyme Mix, 4 μL of RNA (concentration of 250 ng μL–1) and 12 μL of ultrapure water for a total reaction volume of 20 μL. Tubes were incubated in a thermocycler (C1000 Touch; Bio-Rad, Hercules, CA, USA) at 25°C for 10 minutes, followed by 42°C for 1 h, and then 85°C for 5 minutes. cDNA was stored at –20°C until quantitative polymerase chain reaction (PCR) assays were performed.

qPCR

To quantify transcript levels, quantitative polymerase chain reaction (qPCR) was performed using the LightCycler 480 II (Roche, Basel, Switzerland) and LightCycler 480 SYBR Green I Master (catalogue no. 04887352001; Roche). Primers were designed using Primer-BLAST software (blast.ncbi.nlm.nih.gov) and manufactured by Life Technologies (Table 1). The PCR cycling conditions used for each assay were enzyme activation at 95°C for 5 min; amplification of the gene product through 40 successive cycles of 95°C for 10 s, 60°C for 10 s and 72°C for 10 s. Specificity of primers was tested by dissociation analysis and only primer sets producing a single peak were used. Each plate for a gene of interest contained a standard curve (10-fold serial dilution) generated using pooled cDNA. Each sample and standard curve point was run in triplicate. The crossing point (Cp) of each well was determined via the second derivative maximum method using LightCycler 480 Software, version 1.5.1.62 (Roche). An arbitrary concentration was assigned to each well based on the standard curve Cp values by the software. The geometric mean of housekeeping genes was determined to use as reference gene value for each intestinal sample. β-actin, cyclophilin and hypoxanthine ribosyltransferase (HPRT)were used as housekeepers for maternal intestines; cyclophilin and HPRT for fetal intestines; and β-actin and UBC for placentae. Housekeeper mRNA levels did not differ significantly between groups. Relative messenger RNA (mRNA) levels for each sample were determined by dividing the geometric mean of the triplicate for each sample by that sample's reference gene value.

2.3.4   NF-KB activity

Maternal and fetal intestinal tissue was homogenized with ceramic beads using a Precellys 24 homogenizer (Bertin Technologies SAS, Montigny-le-Bretonneux, France) at 5 m s–1 for 60 s in buffer containing 50 mM KH2PO4, 5 mM EDTA, 0.5 mM dithiothreitol and 1.15% KCl with cOmplete protease inhibitor tablets (Roche). Protein concentrations were determined using the BCA method in the supernatant after homogenates were centrifuged for 10 min at 10,000 g at 4°C. nuclear factor kappa B (NF-κB) activity was measured in maternal and fetal intestinal homogenates using the TransAMTM NF-κB p65 Transcription Factor Assay Kit per the manufacturer's instructions (catalogue no. 40096; Active Motif, Carlsbad, CA, USA).

2.3.5   Western blot

Western blot analyses were performed on 15 μg of protein using SDS-PAGE of varying percentage depending on the protein of interest. Each western blot analysis used a separate protein aliquot and membrane for each protein of interest. After transfer onto or polyvinylidene difluoride membrane, blots were blocked for 1 h at room temperature in5% BSATris-Tween 20 and incubated with the following primary antibodies overnight: β-actin (dilution 1:5000; Cell Signaling Technology; catalogue no. 5125; RRID: AB_1903890). Blots were washed in Tris-Tween 20 and incubated with HRP-conjugated goat anti-rabbit IgG secondary antibody (Abcam; catalogue no. ab6721; RRID: AB 955447) for 1 h at room temperature. Blots were developed using BioRad ClarityTM Western enhanced chemiluminescence (ECL; Bio-Rad, 170–5061), images captured using a

Bio-Rad ChemiDoc MP System and densitometric quantification was carried out using ImageLab software (Bio-Rad) relative to β-actin internal controls.

2.4 Microbiome profiling

2.4.1 gDNA extraction

Genomic DNA (gDNA) was extracted from fecal samples as described previously (214) with the addition of a mechanical lysis step using 0.2 g of 2.8 mm ceramic beads to improve extraction efficiency and without mutanolysin.

2.4.2 16S rRNA gene sequencing

V3 16S rRNA gene sequencing

PCR amplification of the variable 3 region of the 16S ribosomal RNA (rRNA) gene was subsequently performed on the extracted deoxyribonucleic acid (DNA) from each sample independently using methods described previously (214, 215). Each reaction contained 5 pmol primer, 200 mM dNTPs, 1.5 μL of 50 mM MgCl2, 2 μL of 10 mg mL–1 bovine serum albumin (irradiated with a transilluminator to eliminate contaminating DNA) and 0.25 μL of Taq polymerase (Life Technologies, Carlsbad, CA, USA) for a total reaction volume of 50 μL. 341F and 518R rRNA gene primers were modified to include adapter sequences specific to the Illumina technology and 6 bp barcodes were used to allow multiplexing of samples as described previously. 16S DNA products of the PCR amplification were subsequently sequenced using the Illumina MiSeq

platform (2 × 150 bp) at the Farncombe Genomics Facility (McMaster University, Hamilton, ON, Canada).

V3-V4 16S rRNA gene sequencing

PCR amplification of the variable 3 and 4 (V3-V4) regions of the 16S rRNA gene was performed on the extracted DNA from each sample using methods previously described (215). Each reaction contained 5 pmol of primer (341F – CCTACGGGNGGCWGCAG, 806R – GGACTACNVGGGTWTC-TAAT), 200 mM of dNTPs, $1.5\mu l$ 50 mM MgCl2, 2 μl of 10 mg/ml bovine serum albumin (irradiated with a transilluminator to eliminate contaminating DNA) and $0.25\mu l$ Taq polymerase (Life Technologies, Canada) for a total reaction volume of 50 μl. 341F and 806R rRNA gene primers were modified to include adapter sequences specific to the Illumina technology and 6-base pair barcodes were used to allow multiplexing of samples. 16S DNA products of the PCR amplification were subsequently sequenced using the Illumina MiSeq platform (2x300bp) at the Farncombe Genomics Facility (McMaster University, Hamilton ON, Canada).

2.4.3   Processing of 16S data

Primers were trimmed from FASTQ files using Cutadapt (216) (RRID: SCR_011841) and DADA2 (217) was used to derive amplicon sequence variants (ASVs). Taxonomy was assigned using the Silva 132 reference database (218). Non-bacterial ASVs were culled (kingdom Eukaryota, family Mitochondria, order Chloroplast, or no assigned phylum), as was any ASV to which only 1 sequence was assigned.

2.4.4   SCFA quantification

SCFA levels were measured in maternal cecal samples by the McMaster Regional Centre of Mass Spectrometry. A weight equivalent amount of 3.7% HCl, 10 μL of internal standard and 500 μL of diethyl ether was added to each cecal sample and vortexed for 15 minutes. After vortexing, 400 μL of diethyl ether fecal extract was transferred to a clean 1.5 mL Eppendorf tube. In a chromatographic vial containing an insert, 20 μL of N-tert-butyldimethylsilyl-N-methyltrifluoroacetamide was added, after which 60 μL of diethyl ether fecal extract was added. The mixture was incubated at room temperature for 1 h and analyzed using gas chromatography-mass spectroscopy (GC/MS) (6890N GC, coupled to 5973N Mass Selective Detector; Agilent Technologies, Santa Clara, CA, USA).

2.5   Statistical analysis

All statistical analyses were performed in R (RRID: SCR_001905). For analyses of fetal and offspring intestines, sample size represents the number of litters analyzed; a representative male and female were analyzed from each litter. Excluding 16S analyses, all other data were analyzed by linear models or mixed linear models for data with repeated measures, wherein the experimental unit was used as a random effect. Details of these analyses are included in the text and figure captions.

Analysis of 16S data

We performed alpha and beta diversity analyses in R using phyloseq (219)
(RRID: SCR_013080) and tested for whole community differences across groups
using vegan's (220) (RRID: SCR_011950) implementation of permutational
multivariate analysis of variance (PERMANOVA) in the adonis command. These
results were visualized via Principal Coordinate Analysis (PCoA) ordination
using R's ggplot2 package (RRID: SCR_014601 (221)). Differential abundance
analysis was performed in DESeq2 (RRID: SCR_015687).

Chapter 3

Fetal meconium does not have a detectable microbiota before birth

This chapter contains a paper published in Nature Microbiology[1]. Since its publication, other reports showing contradictory results have been published and as a result a Letter to the Editor has also been submitted to Cell and is currently under review (Appendix A).

Our gut microbes affect our health and wellbeing throughout our lives. Recent data suggest that our relationship with intestinal commensals is greatest in early life, during critical stages of immunological and physiological development (55, 223). However, how our gut microbes participate in shaping our earliest development is still unclear. In order to understand how microbes influence early-life development, first we must know how and when we are colonized.

---

[1]Originally published Nature Microbiology: (222) Copyright © 2021 by The Authors.

Recent studies have sparked controversy by claiming that we are colonized by bacteria before birth. Reports suggest that the prenatal environment including reproductive tissues like the placenta, the amniotic fluid, and indeed the fetus are colonized before birth and that fetal immune development may be driven by the presence of live microbes in intrauterine sites(224, 225). However, studies such as these are fraught with confounders, and methods for controlling for contamination are often not as robust as needed . A number of concurrent studies point to experimental contamination dominating low-microbial biomass sequencing data as the source of microbial DNA in the intrauterine environment (209, 211, 226, 227). Therefore, we set about to develop stringent methods to control for contamination and to test whether the fetal gut is actually colonized before birth. The study was done in collaboration with the Braun Lab at the Charite University in Berlin Germany, who collected the participant samples, and performed the microbial cultures. The candidate processed all the meconium samples and analysed all the data and wrote the manuscript. The following is the published manuscript resulting from this work.

Check for updates

Fetal meconium does not have a detectable microbiota before birth

Katherine M. Kennedy [1,2], Max J. Gerlach[3], Thomas Adam[4], Markus M. Heimesaat[5], Laura Rossi[2,6], Michael G. Surette [1,2,6], Deborah M. Sloboda [1,6,7,8 ✉] and Thorsten Braun [3,8 ✉]

Microbial colonization of the human intestine impacts host metabolism and immunity; however, exactly when colonization occurs is unclear. Although many studies have reported bacterial DNA in first-pass meconium samples, these samples are typically collected hours to days after birth. Here, we investigated whether bacteria could be detected in meconium before birth. Fetal meconium ($n = 20$) was collected by rectal swab during elective breech caesarean deliveries without labour and before antibiotics and compared to technical and procedural controls ($n = 5$), first-pass meconium (neonatal meconium; $n = 14$) and infant stool ($n = 25$). Unlike first-pass meconium, no microbial signal distinct from negative controls was detected in fetal meconium by 16S ribosomal RNA gene sequencing. Additionally, positive aerobic ($n = 10$ of 20) and anaerobic ($n = 12$ of 20) clinical cultures of fetal meconium (13 of 20 samples positive in at least one culture) were identified as likely skin contaminants, most frequently *Staphylococcus epidermidis*, and not detected by sequencing in most samples (same genera detected by culture and sequencing in 2 of 13 samples with positive culture). We conclude that fetal gut colonization of healthy term infants does not occur before birth and that microbial profiles of neonatal meconium reflect populations acquired during and after birth.

Microbial colonization of the human intestine is a key developmental process since the order and timing of microbial exposure shape the development of the gut microbiome[1] and impact host metabolism and immunity later in life[2]. In humans, maturation of both intestinal barrier function and immunity occurs prenatally[3]. The fetal intestine is more permeable to macromolecules[4] and less tolerant of antigens[5] than that of term infants. Transfer of maternal immunoglobulin G (IgG) across the placenta and uptake in the fetal intestine increase near term gestation[6], shaping neonatal gut immune responses after birth[7]. Thus the intrauterine environment has the capacity to shape health well beyond fetal life and can influence long-term health trajectories[8]; recently, it has been suggested that early-life colonization with specific microbes can predict health outcomes including asthma[9] and obesity[10]. To understand the mechanisms by which microbial colonization influences health later in life, we must know when colonization occurs. Several research groups using sequencing-based methods have reported bacterial DNA in the placenta[11,12] and amniotic fluid[13] and have suggested that this reflects microbial populations that initiate gut colonization in utero[14]. However, recent studies accounting for the high risk of contamination in low-biomass samples[15] have failed to detect a placental[16–18] or amniotic fluid microbiome[19–21]. Thus, this issue is highly controversial.

Since neonatal (first-pass) meconium is formed before birth, it has been used as a proxy for the in utero environment[22,23] but this does not account for microbial acquisition that occurs during and/ or immediately after birth. Recent metagenomic evidence[24] and previous culture data[25] have shown a correlation between the time from birth to collection and bacterial detection in neonatal meconium.

Only one previous study evaluated the presence of microbes in fetal meconium before birth[26] and found that at mid-gestation most fetal meconium bacterial profiles did not differ from procedural and kidney controls[26]. Those that differed were dominated by *Micrococcus* and *Lactobacillus* species, likely originating from the maternal cervicovaginal microbiota during sample collection[27]. In this study, we characterized the bacterial profiles of human fetal meconium before birth. We show that unlike neonatal meconium, fetal meconium is indistinguishable from negative controls, indicating that colonization of the human gut likely does not occur before birth. These data substantially extend our understanding of the establishment of our intestinal microbiome and shed light on which early-life influences may impact postnatal gut health.

Results

Pilot study: sampling protocol optimization. We recruited a pilot cohort of 22 participants (pilot cohort 1a, $n = 10$; pilot cohort 1b, $n = 12$) to optimize sample collection methods and minimize the risk of contamination (Extended Data Fig. 1). Only non-laboured, elective caesarean deliveries were included to avoid the vertical transmission of bacteria during a vaginal birth, during which the child is exposed to the maternal bacterial flora. Pilot study samples were analysed by aerobic and anaerobic culture (Supplementary Table 1).

Pilot cohort 1a. An initial attempt of sample collection by flushing with a rectal tube was unsuccessful (T01) and all subsequent samples were collected by eSwab. Of the 16 pilot meconium cultures (8 aerobic + 8 anaerobic), 11 showed bacterial detection (68.8%),

[1]Department of Biochemistry and Biomedical Sciences, McMaster University, Ontario, Hamilton, Canada. [2]Farncombe Family Digestive Health Research Institute, McMaster University, Hamilton, Ontario, Canada. [3]Department of Obstetrics and Experimental Obstetrics, Charité-Universitätsmedizin Berlin, Freie Universität Berlin and Humboldt-Universität zu Berlin, Berlin, Germany. [4]Labor Berlin, Charité Vivantes GmbH, Berlin, Germany. [5]Institute for Microbiology, Infectious Diseases and Immunology, Charité-Universitätsmedizin Berlin, Freie Universität Berlin and Humboldt-Universität zu Berlin, Berlin, Germany. [6]Department of Medicine, McMaster University, Hamilton, Ontario, Canada. [7]Departments of Pediatrics, Obstetrics and Gynecology, McMaster University, Hamilton, Ontario, Canada. [8]These authors jointly supervised this work: Deborah M. Sloboda, Thorsten Braun. ✉e-mail: sloboda@mcmaster.ca; thorsten.braun@charite.de

Table 1 | Participant characteristics

Characteristic	Fetal (*n* = 20)	Neonatal (*n* = 14)
Maternal age, years, mean (s.d.)	32.3 (5.1)	33.2 (4.4)
Gestational age, days, mean (s.d.)[a]	271.4 (5.6)	276.7 (6.0)
Birth weight, g, mean (s.d.)	3,240 (380)	3,384 (557)
Sex, *n* (%)		
Female	14 (70)	7 (47)
Male	6 (30)	8 (53)
Delivery, *n* (%)[b]		
Vaginal	0 (0)	9 (60)
Caesarean	20 (100)	8 (40)

[a]*P* < 0.05 indicated by a *t*-test. [b]*P* < 0.05 indicated by a chi-squared test.

2 of which were more than one species (T02, T10). Both anaerobic and aerobic cultures were negative for only 1 of the 8 pilot fetal meconium samples (T05). Only anaerobic cultures were positive for 3 of 8 samples (T02, T06, T08; 37.5%). Both anaerobic and aerobic cultures were positive for 4 of 8 samples (T03. T04, T07, T10; 50%). Positive cultures had a median incubation time of 20 h until detection. The 13 detected microbial populations were assigned to the following species in decreasing frequency: *Staphylococcus epidermidis* (5); *Staphylococcus lugdunensis* (3); *Staphylococcus capitis* (2); *Staphylococcus caprae, Propionibacterium* (*Cutibacterium*) *acnes* and *Propionibacterium avidum* (1 each).

Pilot cohort 1b. To investigate maternal skin as a potential source of contamination, we cultured a set of pilot swabs of maternal skin around the caesarean section area both preoperatively after disinfection and post-operatively after the end of wound care. Anaerobic preoperative swab cultures were positive for *S. lugdenensis, Bacillus licheniformis* and *Clostridium perfringens*. Post-operative swab cultures were positive for *S. epidermidis* (both anaerobic and aerobic) and *B. licheniformis* (anaerobic) and *S. lugdunensis* (aerobic). To reduce maternal skin contamination, we expanded the area of disinfection and designed a model of draping (Methods). Of the 22 pilot 1b meconium cultures, 9 showed bacterial detection (40.9%), none of which were more than one species. Both anaerobic and aerobic cultures were negative for 5 of 11 samples (T13, T16, T18, T19, T21; 45.5%). Only anaerobic cultures were positive for 3 of 11 samples (T12, T14, T22; 27.3%). Both anaerobic and aerobic cultures were positive for 3 of 11 samples (T15, T17, T20; 27.3%). The nine detected microbial populations could be assigned to the following species in decreasing frequency: *S. epidermidis* (4); *S. capitis* (3); *P. acnes* (2). Since our stringent procedures (expanded area of disinfection, modified draping design) reduced the frequency of contamination, these procedures were implemented for the principal study cohort.

Participant characteristics. To investigate the possible colonization of the fetal gastrointestinal tract in utero, we analysed meconium samples collected from 20 term fetuses during caesarean section before birth after an intensive method establishment (Table 1). Fetal meconium was sampled during elective caesarean section deliveries with no signs of labour, preterm labour or rupture of membranes to prevent vertical transmission during labour (Fig. 1 and Extended Data Fig. 2). Since others previously detected a microbiome in first-pass (neonatal) meconium[2,22], we also included neonatal meconium from term deliveries and infant stool samples collected at six months of age as positive controls. As often seen during breech
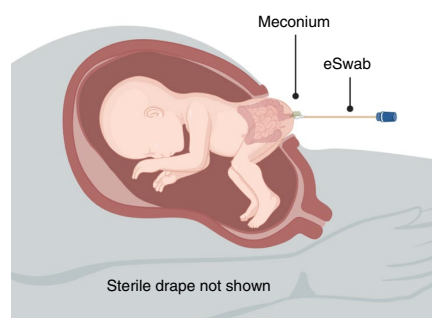
Fig. 1 | Diagram of the collection method for fetal meconium samples. After advanced physical disinfection of maternal skin from maternal armpits to knees, the surgical area was covered using a specialized sterile drape, with the film remaining intact until the incision. After caesarean section and exposure of the fetal buttocks before birth, meconium was rectally sampled using sterile eSwabs. Image created with BioRender.com.

delivery C-sections, meconium is spontaneously expelled via abdominal pressure; thus, we were able to collect similar quantities of material for each sample across sample types. We included multiple negative controls: a swab exposed to operating theatre air during caesarean delivery (sampling negative, collected in triplicate for sequencing and cultures during collection of M213), genomic prep reagents either exposed to PCR hood air during sample preparation or not exposed (extraction negative) and V3–V4 PCR amplifications without added template DNA (PCR negative).

Fetal and neonatal participants did not differ significantly in maternal age or birth weight. The gestational age of fetal participants at birth was less than that of neonatal participants (*P* = 0.0010; Welch's *t*-test), likely due to differences in mode of delivery (*P* = 0.00029, chi-squared test).

Clinical culture results. Fetal meconium samples and the sampling negative control were cultured under both aerobic and anaerobic conditions (Table 2). Of the 20 fetal meconium samples, 7 were negative for both aerobic and anaerobic cultures after 120 h, as was the sampling negative control. Additionally, three samples had negative aerobic cultures but positive anaerobic cultures (M208, *S. epidermidis*; M210, *P. acnes*; M217, *P. acnes*) and one sample had a negative anaerobic culture but positive aerobic culture (M219, *S. epidermidis*). Despite growth of *S. epidermidis* under both aerobic and anaerobic conditions, only three meconium samples had positive cultures under both conditions, while five had positive cultures under only one. Since *P. acnes* and coagulase-negative staphylococci are common skin contaminants in clinical cultures, we attempted to confirm positive results in the sequencing data.

16S rRNA marker gene sequencing. We assessed the bacterial DNA present in the samples using 16S ribosomal RNA gene sequencing of combined variable 3 and 4 region (V3–V4) amplicons from 30 cycles of PCR amplification (Supplementary Tables 2 and 3). Additionally, all meconium samples and negative controls were sequenced after 40 PCR cycles to confirm the presence of any genera detected at 30 cycles. We first looked at the number of amplicons sequenced in each sample (read count). Fetal meconium samples were dominated by host-associated reads before removal of host sequences (pruning) (median read count of 109.5; min = 23; max = 1,316; *n* = 20), after which they had a median read count of 76.5 (min = 16, max = 202, *n* = 20). Read counts of neonatal

Table 2 | Fetal meconium culture results

Sample ID	Anaerobic culture		Aerobic culture	
	Result	Incubation time (h)	Result	Incubation time (h)
M201[a]	*S. epidermidis*	18.64	*S. epidermidis*	23.2
M202	*S. epidermidis*	18.68	*S. lugdunensis*	20.67
M203[b]	*S. epidermidis*	20.12	*S. epidermidis*	14.92
M204[a,b]	*S. epidermidis*	18.59	*S. epidermidis*	17.09
M205[a]	Negative	120.07	Negative	120.07
M206	*Staphylococcus saprophyticus*	26.09	*S. saprophyticus*	17.96
M207[a]	*S. epidermidis*	19.06	*S. lugdunensis*	18.69
M208	*S. epidermidis*	22.05	Negative	120.08
M209	Negative	120.07	Negative	120.08
M210	*P. acnes*	79.21	Negative	120.08
M211	Negative	120.08	Negative	120.09
M212	*S. epidermidis*	19.94	*Staphylococcus hominis*	24.29
M213	*P. acnes*	102.77	*S. capitis*	36.68
Neg	Negative	120.02	Negative	120.03
M215	Negative	120.13	Negative	120.13
M216	Negative	120.16	Negative	120.15
M217	*P. acnes*	66.24	Negative	120.17
M219	Negative	120.08	*S. epidermidis*	17.41
M221	Negative	120.08	Negative	120.08
M222	Negative	120.08	Negative	120.09
M223	*P. avidum*	80.85	*P. avidum*	99.05

[a]Not breech presentation. [b]Monochorionic diamniotic twins. Bacterial species detected in fetal meconium by anaerobic and aerobic culture. Cultures were maintained until detection or for a maximum of 120 h.

meconium samples were much more variable: two samples did not have any reads and the remaining samples had a median read count of 130 (min = 4, max = 63,079, n = 12) before pruning and a median read count of 191 after (min = 9, max = 63,079, n = 11). Negative controls had a median of 74 reads (min = 6, max = 396) before pruning and a median of 46 reads after (min = 6, max = 99). As expected, infant stool samples had much higher read counts than other samples (median read count of 53,207; min = 5,505; max = 105,212; n = 25) before and after pruning.

Looking at within-sample diversity, fetal meconium had lower alpha diversity (observed amplicon sequence variants (ASVs), Shannon and Simpson indices; Fig. 2a) than infant stool (P = 0.0016, P = 0.0001 and P = 0.0086, respectively). Neonatal meconium alpha diversity did not differ from that of infant stool (P = 0.7503, P = 0.6401 and P = 0.7762, respectively). To investigate differences in overall community composition between samples (beta diversity) we performed principal coordinate analysis (PCoA) of Bray–Curtis dissimilarity and found that fetal meconium samples clustered with negative controls, while neonatal meconium samples were more variable and more similar to infant stool samples (Fig. 2b). Overall, the beta diversity of fetal meconium was indistinguishable from that of negative controls (Fig. 2c) since Bray–Curtis dissimilarity between samples was similar within negative controls, within fetal meconium and between negative controls and fetal meconium. Compared to fetal meconium, neonatal meconium was more dissimilar to negative controls (P < 0.001).

The most prevalent genera detected in fetal meconium samples were *Halomonas* (20 out of 20 samples), *Rhodanobacter* (19 out of 20 samples, only detected in 1 of 2 sequencing runs for 4 samples) and *Pseudomonas* (15 out of 20 samples, only detected in 1 of 2 sequencing runs for 6 samples), all of which were also detected in

negative controls (Fig. 3). The only genera detected in more than 1 fetal meconium sample and not detected in negative controls were *Bacteroides* (4 out of 20 samples, only detected in 1 of 2 sequencing runs for 2 samples) and *Staphylococcus* (4 out of 20 samples, only detected in 1 of 2 sequencing runs for 2 samples). *Bacteroides* was only consistently detected across sequencing runs and with both 30 and 40 cycles of amplification in 1 of 20 samples (M202; Extended Data Fig. 3). *Staphylococcus* was not consistently detected with both 30 and 40 cycles of PCR amplification in any sample and was only detected by sequencing in 2 of 11 samples with positive *Staphylococcus* culture results (M201 positive for *S. epidermidis* and M207 for both *S. epidermidis* and *S. lugdunensis*). The only other genus consistently detected in a sample with both 30 and 40 cycles of PCR amplification and across sequencing runs was *Escherichia/Shigella* (M202, M203, M207), which was also detected in an extraction negative control (Extended Data Fig. 3). Overall, agreement between sequencing runs (Cohen's kappa) was moderate or high for genera that were detected in more than one negative control as expected for contaminants (Supplementary Table 4). The only genus not detected in negative controls that showed any agreement between sequencing runs was *Bacteroides*, indicating that other genera detected may be the result of stochastic sequencing noise. Despite culture results being positive for *Propionibacterium* species, no members of this genus were detected in sequencing data from any fetal meconium sample.

Discussion

The role of the microbiome in controlling host metabolism and its relationship to metabolic dysfunction and obesity[28] has led investigators to question whether our microbial signatures early in life could be used to predict chronic disease risk[29]. Because of this, how
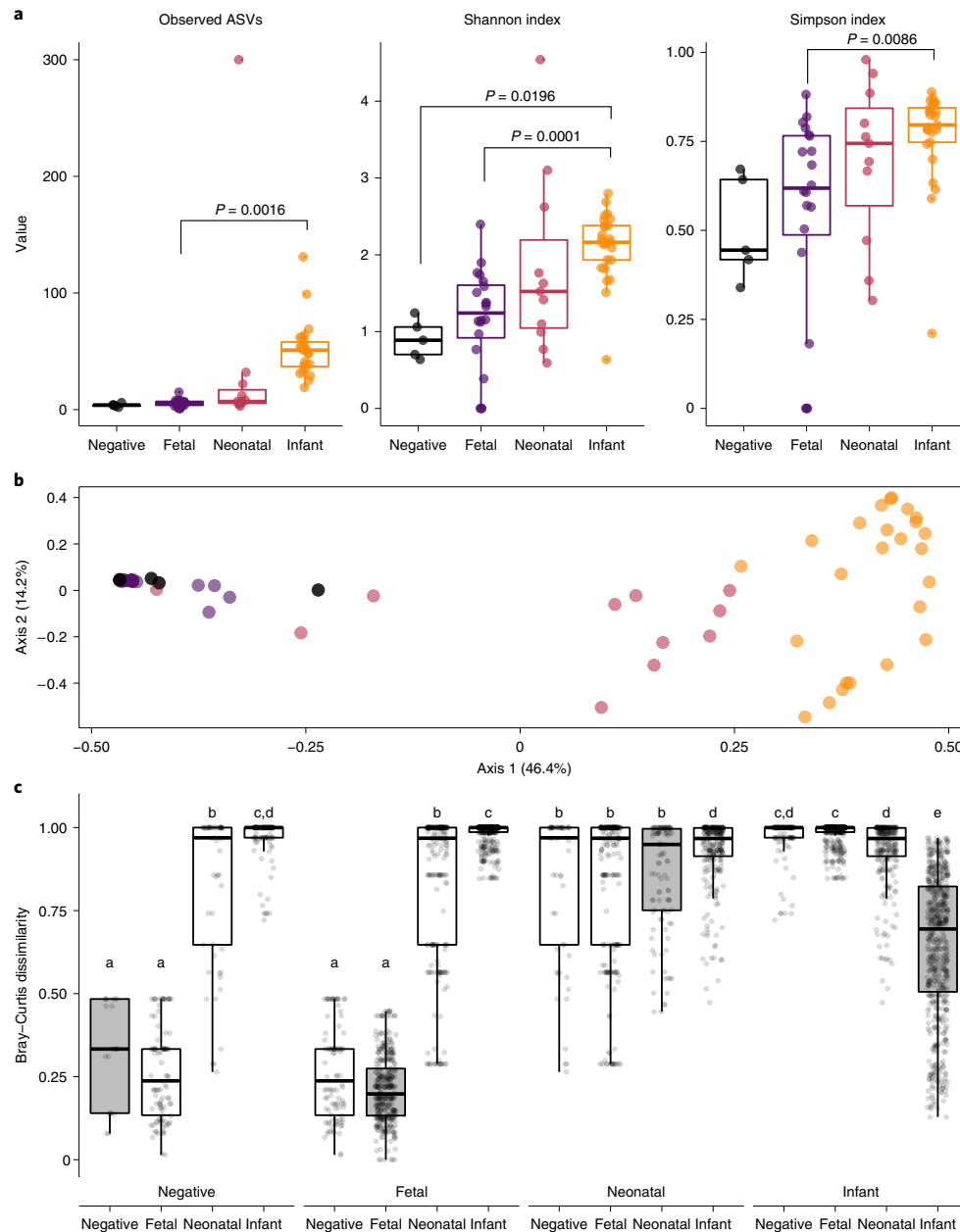
Fig. 2 | Fetal meconium alpha and beta diversity do not differ from those of sampling negative controls. a, Box plots of alpha diversity measures by sample type (negative control, $n=5$), fetal meconium ($n=20$), neonatal meconium ($n=11$) and infant stool ($n=25$). Fetal meconium had lower alpha diversity (observed ASVs, Shannon and Simpson indexes) than infant stool ($P=0.0016$, $P=0.0001$ and $P=0.0086$, respectively), as did the negative controls (Shannon index, $P=0.0196$). Neonatal meconium alpha diversity did not differ from that of infant stool ($P=0.7503$, $P=0.6401$ and $P=0.7762$, respectively). Significance assessed by a linear mixed model (Kenward–Roger d.f. with Tukey adjustment for multiple comparisons), with sample type as a fixed effect and participant ID as a random effect. **b**, PCoA of Bray–Curtis distances at the genus level show that fetal meconium samples (purple) cluster with sampling negative controls (black), indicating that their community composition is similar, while neonatal meconium samples (pink) are more variable and more similar to infant stool (yellow). **c**, Box plots of Bray–Curtis dissimilarities within (grey fill) (where *x* is the sample size for that sample type) and between (white fill) sample types show that fetal meconium samples are less dissimilar to each other and are similar to negative controls. Sample-to-sample dissimilarities are grouped by sample type-to-sample type comparisons (negative–negative, $n=20$; negative–fetal, $n=100$; negative–neonatal, $n=55$; negative–infant, $n=125$; fetal–fetal, $n=380$; fetal–neonatal, $n=220$; fetal–infant, $n=500$; neonatal–neonatal, $n=110$; neonatal–infant, $n=275$). Comparisons are bidirectional (negative–fetal data are the same as fetal–negative data). Significance was assessed by linear mixed model with sample type comparison as a fixed effect (for example, negative–negative, negative–fetal) and participant ID as a random effect. Different letters indicate a statistically significant difference between groups. The box plot centre line represents the median; the box limits represent the upper and lower quartiles; the whiskers represent the 1.5× interquartile range; the points represent the outliers.
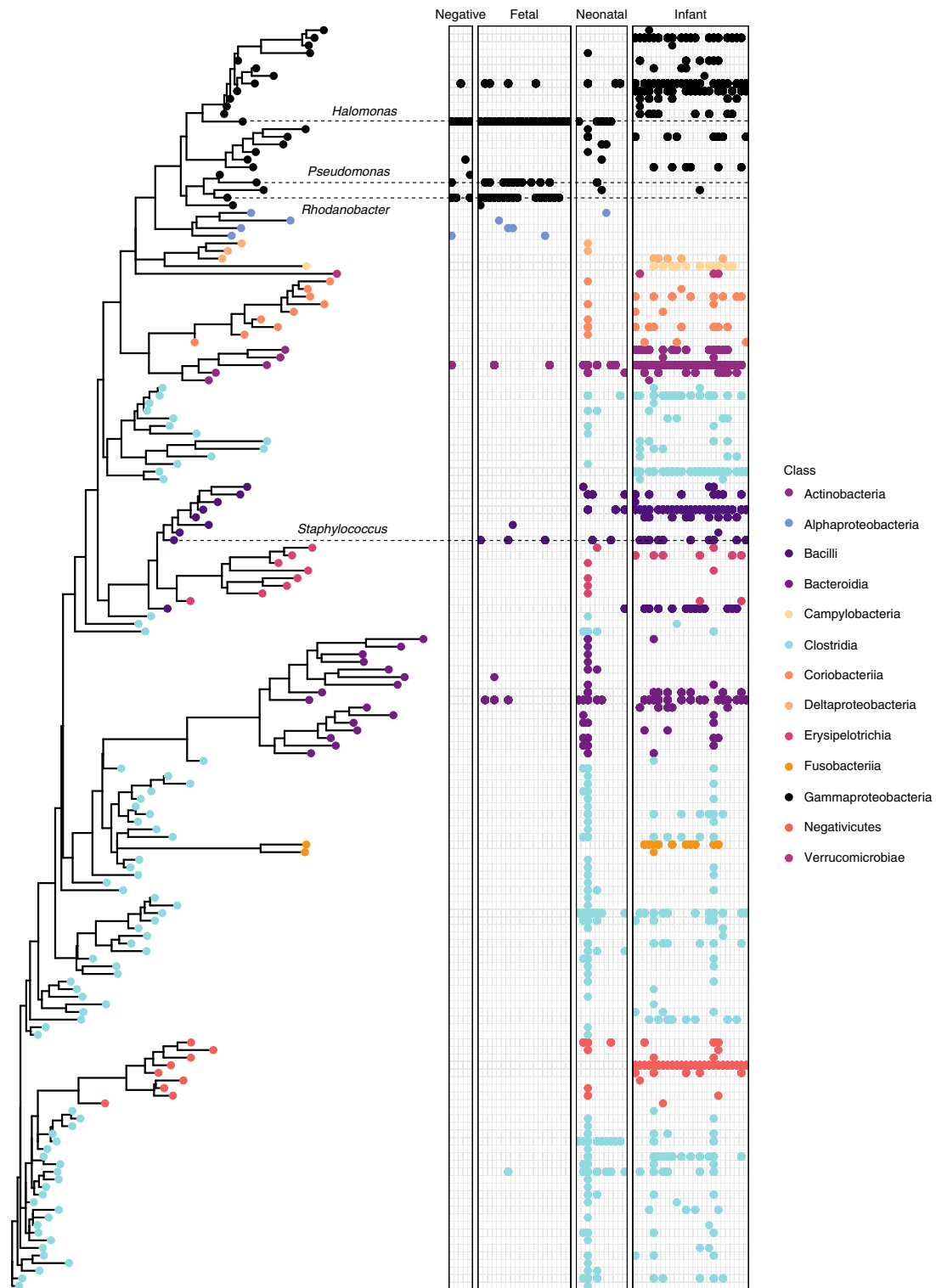
Fig. 3 | Neighbour-joining phylogenetic tree of all genera and presence/absence in each sample. Taxonomy was assigned using the Silva 132 reference database. ASV sequences were aligned using DECIPHER and a GTR + G + I (generalized time-reversible with gamma rate variation) maximum likelihood phylogenetic tree was constructed with phangorn using a neighbour-joining tree as a starting point. The dots indicate the presence of the genera at any abundance in the given sample. Gammaproteobacteria prevalent in fetal meconium are also prevalent in sampling and extraction negative controls. The microbial profiles of first-pass neonatal meconium share more genera with those of infant stool than fetal meconium.

early in life host–microbe interactions are established has become a topic of intense investigation. In neonates, several microbial species are known to regulate intestinal function[30] and are key in immune development[31]. Recent studies reporting that colonization may be initiated in utero[11,12,14] have been the subject of vigorous debate and have been criticized for potential contamination[16,17,21]. Despite our extensive sample collection optimization to reduce potential contamination (Methods and Extended Data Fig. 2), more than half of fetal meconium samples had at least one culture test positive for a likely skin contaminant (22 out of 40 total cultures) despite implementation of stringent procedures to reduce risk of contamination; this highlights the difficulty in avoiding contamination in these types of studies. Contaminating bacteria or bacterial DNA may be introduced by maternal skin or blood during sampling, the environment or investigators during sample handling and culturing or reagents during DNA extraction and PCR. Therefore, negative controls are necessary at each of these stages to rule out contamination. We analysed fetal meconium collected immediately before birth and compared term fetal meconium to appropriate negative controls[32], to neonatal meconium and to infant stool samples. This was a particular strength of our study. Additionally, we used a combination of clinical culture and 16S rRNA gene sequencing to identify a fetal microbial signature. Despite all efforts, we were unable to detect a microbial signature in fetal meconium that was distinct from the negative controls. Overall, the lack of a consistent bacterial signal in our data indicates that fetal meconium does not have a microbiome before birth.

Staphylococcus was the dominant genus in culture results (17 cultures) and *S. epidermidis* was the most prevalent species (11 cultures). In our pilot cohort, post-operative swabs of maternal skin around the incision were also positive for *S. epidermidis*. While it is not possible to know if positive cultures were the result of contamination by skin microbes, the absence of cultured genera in sequencing data make this a likely possibility. Although *S. epidermidis* DNA has also been reported in amniotic fluid[14] and neonatal meconium[24], it is most frequently associated with the skin microbiota[33] suggesting that despite especially stringent efforts to control for contamination, some element of contamination may always exist with current technologies and protocols. This makes the strong case for ensuring that a robust set of controls is in place when performing these types of investigations.

Although sequencing cannot prove the absence of bacterial DNA in a sample, we used robust negative controls and technical replicates to distinguish contamination signals from stochastic sequencing noise. Additionally, we included neonatal meconium as a positive control of our extraction and amplification of bacterial DNA from these low-biomass samples. No sample avoids contamination during collection and processing[34] and this contamination can dominate the composition of low-biomass samples[35]. As contaminating bacteria and/or bacterial DNA are introduced during sample collection, the genomic DNA extraction and PCR amplification sequencing data of samples must be compared to that of sampling, extraction and amplification negative controls. When investigating the existence of in utero colonization, it is essential to show the sequencing data of negative controls alongside that of samples since post hoc decontamination does not remove all contaminating signals[35].

While previous studies have reported the existence of bacterial DNA in amniotic fluid and the placenta, these studies did not compare sample sequencing data to those of one or more of these negative controls (Supplementary Table 5) and therefore could not rule out contamination[15]. Most recently, Rackaityte et al.[26] reported 17 taxa in fetal meconium that they did not attribute to contamination, although re-analysis of these data by de Goffau et al.[36] identified a batch effect that was not accounted for in the previous analysis and concluded that colonization was not supported by these data. Additionally, these fetal samples (20 ± 2 weeks of gestation) were

collected from pregnancy terminations in mid-pregnancy, which require passage through the vaginal canal, thus resulting in considerable potential contamination. Although the authors included fetal kidney samples as negative controls, the isolation of the kidney control was through punch biopsy (excluding surface contamination), which unfortunately biased their results. These limitations are consistent with the fact that the dominant taxa Rackaityte et al.[26] found to be enriched in fetal meconium—*Micrococcus* and *Lactobacillus*—are commonly detected in the vaginal microbiome[37]. We did not find either taxon in fetal meconium (Extended Data Fig. 3 and Supplementary Table 2) samples in our study because our collection protocol completely avoided vaginal contamination (Fig. 1); our culture method would have recovered these organisms if they were present[38,39]. Additionally, we directly compared sample sequencing data to those of negative controls collected during sampling, extraction and PCR amplification without removing putative contaminants. Post hoc decontamination by statistical methods inherently assumes the presence of a bacterial community in the samples being decontaminated and is not well suited to answering the question of bacterial presence since the stringency of the methods are set by the investigator and any decrease in the probability of false negatives increases the probability of false positives. Davis et al.[40] showed that post hoc decontamination of placental samples requires a true signal—ASVs mapping to *Homo sapiens*–to identify other ASVs as contaminants[40]. Therefore, targeted depletion of host DNA before sequencing or removal of host reads by taxon filtering hinders the identification of contaminants by post hoc methods. Additionally, post hoc decontamination methods are only effective for common-source contaminants and cannot address cross-contamination between samples. Thus, we believe that our approach captures a truer representation of the fetal meconium than post hoc decontamination. Direct comparison of samples to these negative controls allowed us to identify the most prevalent and abundant genera as likely contaminants introduced during extraction (*Halomonas* and *Rhodanobacter*) or sampling (*Pseudomonas*).

Even when sequencing data from appropriate negative controls are included, low-biomass samples are especially sensitive to stochastic amplification[41] and sequencing[32] noise. Determination of a true bacterial signal requires its presence across technical replicates. In this study, we ran the PCR products of each amplification on two separate sequencing runs. Excluding likely contaminants, almost all genera detected were only found in one of two sequencing runs for each sample. *Bacteroides* was the only genus consistently detected across technical replicates and this was only true in 1 of 20 fetal meconium samples. This is likely due to the mixed biomass nature of this study since abundant taxa from high-biomass samples are most likely to appear in low-biomass samples[42]. Thus, when comparing across sequencing runs, we found that bacterial signals in fetal meconium that are not also detected in negative controls are likely due to stochastic sequencing noise.

In terms of overall community composition, fetal meconium beta diversity was similar to that of negative controls and lower than that of neonatal meconium. Neonatal meconium community composition was highly variable with some samples more closely resembling infant stool. The high intra-sample type dissimilarity of neonatal meconium is due to the high variability we see in the level of colonization, which likely depends on multiple factors including time from birth to collection, mode of delivery and infant feeding. The biomass of our infant stool samples was relatively high but the community composition of these samples was variable. In contrast, negative controls and fetal meconium have much lower intra-sample dissimilarity; we predict this is because these samples are dominated by contamination, resulting in a more homogeneous community composition. Thus, microbial profiles of neonatal meconium reflect populations acquired during and after birth and not populations that exist before birth.

In this study, we investigated the meconium microbiome in term human neonates before birth and controlled for both contamination during sampling and DNA extraction and stochastic noise during sequencing (Supplementary Table 5). While it is not possible to prove the absence of bacteria in fetal meconium before birth and it is possible our methods were not sensitive enough to detect bacteria present at very low abundances, our data do not support in utero colonization. These data suggest that colonization more likely occurs either during birth via maternal skin/vaginal/fecal seeding or post-birth via environmental seeding.

Methods

Study design and sample collection. *Implementation phase.* The pilot study protocols were reviewed and approved by the Charité ethics committee (EA 04/059/16). Informed consent was obtained from all study participants. A pilot cohort of 22 participants was recruited to optimize the sample collection methods and minimize the risk of contamination. It consisted of two pilot cohorts as described below (pilots 1a and 1b). Only caesarean deliveries were included to avoid the vertical transmission of bacteria during a vaginal birth, during which the child is exposed to the maternal bacterial flora. In addition to the duration of the birth process itself, a further disadvantage of spontaneous delivery is the variable time within which the newborn engages its first bowel movement (neonatal meconium, which is of prenatal origin). Study inclusion was further restricted to elective caesarean sections before labour due to potential microbial influences on unplanned section deliveries and to guarantee the presence of an operator familiar with the study protocol and an equally trained researcher who was able to carry out the immediate transport and further processing of the sample in the nearby laboratory. Breech presentations were preferred to ensure that the rectum was immediately accessible for sampling after sectioning and before delivery and to minimize manipulation of the child before sampling (Fig. 1). This ensured a reduced risk of contamination since a swab could be taken before the neonate was fully removed from the uterus. Finally, to avoid false negative results, a preoperative prophylactic antibiotic was administered after meconium sample collection.

Pilot cohort 1a (establishment of sampling procedures). Swabs with nylon flock fibre (eSwab; Copan Diagnostics) were used to collect the fetal meconium samples. In the event of meconium leakage (spontaneous since it is a side effect of breech presentation), a sample was either taken up with a swab or a careful rectal smear was performed. Pilot samples were transferred to blood culture bottles (BACTEC; BD) and brought to Labor Berlin for culturing. Initially, the inoculation of the blood culture bottles was not carried out under sterile conditions but the use of a sterile workbench was quickly considered and tested. An amniotic fluid sample and fetal perianal swabs were also cultured to identify possible sources of contamination. The Head of Clinical Advice in Microbiology from Labor Berlin was consulted for an external review of the study design and protocol. Maternal skin was considered as the potential source of contamination; therefore, a second pilot study was performed to minimize skin contamination during sampling.

Pilot cohort 1b. Samples were collected and cultured as in pilot 1a. To reduce contamination from maternal skin microbes, we expanded the area of disinfection with Softasept N coloured from the maternal armpits to the knees. To reduce the chance of contamination due to amniotic fluid dampening the surgical draping, a model of draping was designed and used that had a wider design, better adhesive properties and a thinner film. The thinner film helped in cases where the mother had repeated caesarean sections, where the prior model sometimes required the film to be slit to visualize the existing scar. The film of the new sheet remained intact and the aseptic area was undisturbed up to the skin incision. Lateral drapes were also introduced and the remaining pilot samples were used to observe the resistance of the seal, to identify possible points susceptible to film detachments.

Principal study cohort. Participants ($n = 19$ mothers) were recruited during routine antenatal counselling at $36 + 0$ weeks gestation when patients presented with planned caesarean section and breech presentation (18 singleton pregnancies and 1 twin pregnancy; Extended Data Fig. 1). The study protocol was reviewed and approved by the Charité ethics committee. Informed consent was obtained from all study participants.

Advanced physical disinfection of maternal skin was performed (as described in pilot 1b), covering the area from the maternal armpits to the knees and the surgical area was covered using the specialized sterile drape, with the film remaining intact until the incision. After caesarean section and exposure of the fetal buttocks before birth, meconium was rectally sampled using sterile ESwabs. An operating theatre negative control (swab exposed to operating theatre air) was also taken. Triplicate samples were collected; two were cultured immediately (anaerobic and aerobic) and one was flash-frozen in liquid nitrogen for future sequencing.

Neonatal meconium and infant stool sample collection. Neonatal meconium ($n = 14$) and infant stool ($n = 25$) samples used as positive controls were collected as part of

a separate ongoing study (reviewed and approved by the Charité ethics committee). Informed consent was obtained from all study participants. Neonatal meconium samples were collected from nappies (diapers) within 48 h of birth and frozen at −80 °C before processing for sequencing. Infant stool samples were collected at 6 months of age by parents and frozen at −20 °C before being stored at −80 °C before processing for sequencing. Neonatal meconium and infant stool samples were not included in bacterial culturing.

Bacterial culturing. Samples were transferred in a sterile hood to anaerobic and aerobic point bottles (BACTEC; BD) and supplemented (BACTEC FOS; BD) to improve the growth conditions for more demanding bacterial species. Cultures were maintained for a maximum of 120 h. Positive cultures were subcultured on standard agar plates (Columbia, Chocolate, Schaedler, MacConkey, Sabouraud) and identified using a matrix-assisted laser desorption/ionization-time-of-flight mass spectrometer (VITEK MS; bioMérieux).

DNA extraction and amplification. Sample aliquots were transferred to genomic prep tubes in a sterile PCR hood using sterile biopsy punches; gloves were changed between handling each sample. In addition to the sampling negative control collected in the operating theatre, an extraction negative control (an opened prep tube in the PCR hood during sample aliquoting) was included. Neonatal meconium and infant stool samples did not have specific sampling negative controls because these samples were positive controls themselves. An additional extraction negative control prep tube remained closed during sample aliquoting. Genomic DNA was extracted as described previously[43] with the addition of a mechanical lysis step using 0.2 g of 2.8-mm ceramic beads to improve extraction efficiency and without mutanolysin. PCR amplification of the V3–V4) regions of the 16S rRNA gene was performed subsequently on the extracted DNA from each sample using methods described previously[44]. In addition to the typical 30 cycles of amplification, each sample was also independently amplified for 40 cycles to confirm any signals detected. These additional amplifications were not used for general analysis since amplification beyond 30 cycles is known to bias sequencing data[45]. For 30 cycles of amplification, 80 ng of template DNA was used in each reaction; for 40 cycles of amplification, 20 ng of DNA was used in each reaction. Each reaction contained 5 pmol of primer (341F-CCTACGGGNGGCWGCAG, 806R-GGACTACNVGGGTWTC-TAAT), 200 mM of deoxyribonucleotide triphosphate, 1.5 μl of 50 mM of MgCl$_2$, 2 μl of 10 mg ml^{-1} BSA (irradiated with a transilluminator to eliminate contaminating DNA) and 0.25 μl of Taq polymerase (Thermo Fisher Scientific) for a total reaction volume of 50 μl. 341F and 806R rRNA gene primers were modified to include adaptor sequences specific to the Illumina technology and six-base pair barcodes were used to allow multiplexing of samples. The 16S DNA products of the PCR amplification were subsequently sequenced twice on two separate runs of the Illumina MiSeq platform (2×300 base pairs) at the Farncombe Genomics Facility (McMaster University).

16S rRNA gene sequencing and analysis. Primers were trimmed from FASTQ files using Cutadapt (v.1.18)[46] (RRID: SCR_011841) and DADA2 (v.1.14)[47] was used to derive ASVs. Taxonomy was assigned using the Silva 132 reference database[48]. Non-bacterial ASVs were culled (kingdom Eukaryota, family Mitochondria, order Chloroplast or no assigned phylum) as was any ASV to which only one sequence was assigned.

We performed alpha and beta diversity analyses in R using phyloseq[49] (RRID: SCR_013080; v.1.32.0) and tested for whole-community differences across groups using vegan[50] (RRID: SCR_011950; v.2.5-7) implementation of permutational multivariate analysis of variance in the adonis command. These results were visualized via PCoA ordination using the R package ggplot2 (RRID: SCR_014601; v.3.3.3)[51]. ASV sequences were aligned using DECIPHER (v.2.16.1)[52]; a GTR + G + I (generalized time-reversible with gamma rate variation) maximum likelihood phylogenetic tree was constructed with phangorn (v.2.5.5)[53] using a neighbour-joining tree as the starting point. The significance of alpha diversity was analysed by linear mixed model with sample type as a fixed effect and participant ID as a random effect. The significance of Bray–Curtis dissimilarity between and within sample types was assessed by linear mixed model with sample type comparison as the fixed effect (for example, negative–negative, negative–fetal) and participant ID as a random effect.

Reporting Summary. Further information on research design is available in the Nature Research Reporting Summary linked to this article.

Data availability
All sequencing data associated with this study have been made publicly available in the National Center for Biotechnology Information Sequence Read Archive under project ID PRJNA666699. Source data are provided with this paper.

Code availability
Custom scripts for the microbiome analyses are available from the GitHub repository at https://github.com/kennek6/Kennedyetal2021.

References

1. Sprockett, D., Fukami, T. & Relman, D. A. Role of priority effects in the early-life assembly of the gut microbiota. *Nat. Rev. Gastroenterol. Hepatol.* **15**, 197–205 (2018).
2. Durack, J. et al. Delayed gut microbiota development in high-risk for asthma infants is temporarily modifiable by *Lactobacillus* supplementation. *Nat. Commun.* **9**, 707 (2018).
3. Weström, B., Arévalo Sureda, E., Pierzynowska, K., Pierzynowski, S. G. & Pérez-Cano, F.-J. The immature gut barrier and its importance in establishing immunity in newborn mammals. *Front. Immunol.* **11**, 1153 (2020).
4. Axelsson, I. et al. Macromolecular absorption in preterm and term infants. *Acta Paediatr. Scand.* **78**, 532–537 (1989).
5. Nanthakumar, N. et al. The mechanism of excessive intestinal inflammation in necrotizing enterocolitis: an immature innate immune response. *PLoS ONE* **6**, e17776 (2011).
6. Chen, K., Magri, G., Grasset, E. K. & Cerutti, A. Rethinking mucosal antibody responses: IgM, IgG and IgD join IgA. *Nat. Rev. Immunol.* **20**, 427–441 (2020).
7. Yoshida, M. et al. Human neonatal Fc receptor mediates transport of IgG into luminal secretions for delivery of antigens to mucosal dendritic cells. *Immunity* **20**, 769–783 (2004).
8. Hanson, M. A. & Gluckman, P. D. Developmental origins of health and disease: new insights. *Basic Clin. Pharmacol. Toxicol.* **102**, 90–93 (2008).
9. Fujimura, K. E. et al. Neonatal gut microbiota associates with childhood multisensitized atopy and T cell differentiation. *Nat. Med.* **22**, 1187–1191 (2016).
10. Soderborg, T. K. et al. The gut microbiota in infants of obese mothers increases inflammation and susceptibility to NAFLD. *Nat. Commun.* **9**, 4462 (2018).
11. Aagaard, K. et al. The placenta harbors a unique microbiome. *Sci. Transl. Med.* **6**, 237ra65 (2014).
12. Antony, K. M. et al. The preterm placental microbiome varies in association with excess maternal gestational weight gain. *Am. J. Obstet. Gynecol.* **212**, 653.e1–653.e16 (2015).
13. Stinson, L. et al. Comparison of bacterial DNA profiles in mid-trimester amniotic fluid samples from preterm and term deliveries. *Front. Microbiol.* **11**, 415 (2020).
14. Collado, M. C., Rautava, S., Aakko, J., Isolauri, E. & Salminen, S. Human gut colonisation may be initiated in utero by distinct microbial communities in the placenta and amniotic fluid. *Sci. Rep.* **6**, 23129 (2016).
15. Salter, S. J. et al. Reagent and laboratory contamination can critically impact sequence-based microbiome analyses. *BMC Biol.* **12**, 87 (2014).
16. Lauder, A. P. et al. Comparison of placenta samples with contamination controls does not provide evidence for a distinct placenta microbiota. *Microbiome* **4**, 29 (2016).
17. Theis, K. R. et al. Does the human placenta delivered at term have a microbiota? Results of cultivation, quantitative real-time PCR, 16S rRNA gene sequencing, and metagenomics. *Am. J. Obstet. Gynecol.* **220**, 267.e1–267.e39 (2019).
18. Olomu, I. N. et al. Elimination of 'kitome' and 'splashome' contamination results in lack of detection of a unique placental microbiome. *BMC Microbiol.* **20**, 157 (2020).
19. Lim, E. S., Rodriguez, C. & Holtz, L. R. Amniotic fluid from healthy term pregnancies does not harbor a detectable microbial community. *Microbiome* **6**, 87 (2018).
20. Rehbinder, E. M. et al. Is amniotic fluid of women with uncomplicated term pregnancies free of bacteria? *Am. J. Obstet. Gynecol.* **219**, 289.e1–289.e12 (2018).
21. de Goffau, M. C. et al. Human placenta has no microbiome but can contain potential pathogens. *Nature* **572**, 329–334 (2019).
22. Wang, J. et al. Dysbiosis of maternal and neonatal microbiota associated with gestational diabetes mellitus. *Gut* **67**, 1614–1625 (2018).
23. Hu, J. et al. Diversified microbiota of meconium is affected by maternal diabetes status. *PLoS ONE* **8**, e78257 (2013).
24. Bittinger, K. et al. Bacterial colonization reprograms the neonatal gut metabolome. *Nat. Microbiol.* **5**, 838–847 (2020).
25. Hall, I. C. & O'Toole, E. Bacterial flora of first specimens of meconium passed by fifty new-born infants. *Am. J. Dis. Child.* **47**, 1279–1285 (1934).
26. Rackaityte, E. et al. Viable bacterial colonization is highly limited in the human intestine in utero. *Nat. Med.* **26**, 599–607 (2020).
27. Chen, C. et al. The microbiota continuum along the female reproductive tract and its relation to uterine-related diseases. *Nat. Commun.* **8**, 875 (2017).
28. Moreno-Indias, I., Cardona, F., Tinahones, F. J. & Queipo-Ortuño, M. I. Impact of the gut microbiota on the development of obesity and type 2 diabetes mellitus. *Front. Microbiol.* **5**, 190 (2014).
29. Gohir, W., Ratcliffe, E. M. & Sloboda, D. M. Of the bugs that shape us: maternal obesity, the gut microbiome, and long-term disease risk. *Pediatr. Res.* **77**, 196–204 (2015).
30. Singer, J. R. et al. Preventing dysbiosis of the neonatal mouse intestinal microbiome protects against late-onset sepsis. *Nat. Med.* **25**, 1772–1782 (2019).
31. Galazzo, G. et al. Development of the microbiota and associations with birth mode, diet, and atopic disorders in a longitudinal analysis of stool samples, collected from infancy through early childhood. *Gastroenterology* **158**, 1584–1596 (2020).
32. Erb-Downward, J. R. et al. Critical relevance of stochastic effects on low-bacterial-biomass 16S rRNA gene analysis. *mBio* **11**, e00258-20 (2020).
33. Stacy, A. & Belkaid, Y. Microbial guardians of skin health. *Science* **363**, 227–228 (2019).
34. Weyrich, L. S. et al. Laboratory contamination over time during low-biomass sample analysis. *Mol. Ecol. Resour.* **19**, 982–996 (2019).
35. Karstens, L. et al. Controlling for contaminants in low-biomass 16S rRNA gene sequencing experiments. *mSystems* **4**, e00290-19 (2019).
36. de Goffau, M. C., Charnock-Jones, D. S., Smith, G. C. S. & Parkhill, J. Batch effects account for the main findings of an in utero human intestinal bacterial colonization study. *Microbiome* **9**, 6 (2021).
37. Dominguez-Bello, M. G. et al. Partial restoration of the microbiota of cesarean-born infants via vaginal microbial transfer. *Nat. Med.* **22**, 250–253 (2016).
38. Valdivia-Arenas, M. A. Bloodstream infections due to *Micrococcus* spp and intravenous epoprostenol. *Infect. Control Hosp. Epidemiol.* **30**, 1237 (2009).
39. Oudiz, R. J. et al. *Micrococcus*-associated central venous catheter infection in patients with pulmonary arterial hypertension. *Chest* **126**, 90–94 (2004).
40. Davis, N. M., Proctor, D. M., Holmes, S. P., Relman, D. A. & Callahan, B. J. Simple statistical identification and removal of contaminant sequences in marker-gene and metagenomics data. *Microbiome* **6**, 226 (2018).
41. Kennedy, K., Hall, M. W., Lynch, M. D. J., Moreno-Hagelsieb, G. & Neufeld, J. D. Evaluating bias of Illumina-based bacterial 16S rRNA gene profiles. *Appl. Environ. Microbiol.* **80**, 5717–5722 (2014).
42. Sinha, R. et al. Assessment of variation in microbial community amplicon sequencing by the Microbiome Quality Control (MBQC) project consortium. *Nat. Biotechnol.* **35**, 1077–1086 (2017).
43. Whelan, F. J. et al. The loss of topography in the microbial communities of the upper respiratory tract in the elderly. *Ann. Am. Thorac. Soc.* **11**, 513–521 (2014).
44. Bartram, A. K., Lynch, M. D. J., Stearns, J. C., Moreno-Hagelsieb, G. & Neufeld, J. D. Generation of multimillion-sequence 16S rRNA gene libraries from complex microbial communities by assembling paired-end Illumina reads. *Appl. Environ. Microbiol.* **77**, 3846–3852 (2011).
45. Sze, M. A. & Schloss, P. D. The impact of DNA polymerase and number of rounds of amplification in PCR on 16S rRNA gene sequence data. *mSphere* **4**, e00163-19 (2019).
46. Martin, M. Cutadapt removes adapter sequences from high-throughput sequencing reads. *EMBnet.J.* **17**, 10–12 (2011).
47. Callahan, B. J. et al. DADA2: high-resolution sample inference from Illumina amplicon data. *Nat. Methods* **13**, 581–583 (2016).
48. Quast, C. et al. The SILVA ribosomal RNA gene database project: improved data processing and web-based tools. *Nucleic Acids Res.* **41**, D590–D596 (2013).
49. McMurdie, P. J. & Holmes, S. phyloseq: an R package for reproducible interactive analysis and graphics of microbiome census data. *PLoS ONE* **8**, e61217 (2013).
50. Oksanen, J. et al. Vegan: Community ecology package. R package version 2.0-10 https://cran.r-project.org/web/packages/vegan/index.html (2013).
51. Wickham, H. *ggplot2: Elegant Graphics for Data Analysis* (Springer, 2016).
52. Wright, E. S. RNAconTest: comparing tools for noncoding RNA multiple sequence alignment based on structural consistency. *RNA* **26**, 531–540 (2020).
53. Schliep, K. P. phangorn: phylogenetic analysis in R. *Bioinformatics* **27**, 592–593 (2011).

Additional information

Extended data is available for this paper at https://doi.org/10.1038/s41564-021-00904-0.

Supplementary information The online version contains supplementary material available at https://doi.org/10.1038/s41564-021-00904-0.

Correspondence and requests for materials should be addressed to D.M.S. or T.B.

Peer review information *Nature Microbiology* thanks the anonymous reviewers for their contribution to the peer review of this work. Peer reviewer reports are available.

Reprints and permissions information is available at www.nature.com/reprints.

Publisher's note Springer Nature remains neutral with regard to jurisdictional claims in published maps and institutional affiliations.

Chapter 4

Maternal and infant gut microbiota in humans and the impact of excess adiposity during pregnancy

4.1 Introduction

Since we have established that the fetus acquires intestinal commensal bacteria during and after birth (see Chapter 3), the relationship between the maternal microbiome and offspring microbiome is likely mediated by fetal gut development. How this occurs, however, is still unclear, although there are data to suggest that effects may be via changes to the metabolic adaptations that the mother makes over the course of pregnancy. Maternal metabolic adaptations to

pregnancy mirror changes seen in non-pregnant metabolic syndrome; including hyperglycemia and hyperinsulinemia in addition to increased adiposity. Given the association between metabolism and the gut microbiota, it is likely that some relationship between intestinal commensals and maternal metabolism during pregnancy exists. However, currently, little data exist to explain this relationship and we lack even the foundational understanding of whether the maternal microbiome does indeed change over the course of pregnancy. The impact of pregnancy on the gut microbiome in humans is challenging to assess due to the large effect of interpersonal variation (228). In one of the first studies of the gut microbiome during pregnancy, Koren et al. reported a qualitative increase in beta diversity and decrease in alpha diversity in otherwise normal pregnant individuals during the third trimester of pregnancy compared to the first (93). Others have found the maternal gut microbiota to be stable over the course of pregnancy (98, 99, 229). Most studies investigating the human gut microbiota during pregnancy are cross-sectional, including only pregnancy samples from the second (90) or third trimester (91, 92), and a few studies have investigated the relationship between pregnancy-associated maternal microbial shifts and pre-pregnancy body mass index (BMI) or gestational weight gain (GWG) (106–109). Whether maternal BMI and/or excess GWG together with pregnancy-associated shifts in the maternal gut microbiota influence fetal and neonatal development is still unclear.

Previous work shows that high maternal BMI and excess GWG are significantly associated with both pregnancy complications (230) and impairments in offspring metabolism (231, 232). High maternal BMI is

associated with elevated levels of maternal glucose and insulin, and pro-inflammatory mediators (tumour necrosis factor (TNF), interleukin- (IL)6) (144) as well as changes in the maternal microbiome.

Reports suggest that some of these associations may be mediated by the gut microbiome and the "dysbiosis" of obesity during pregnancy (92, 107). Indeed, in healthy pregnancies, shortly after birth, maternal vaginal, skin, and gut microbes can be detected in the infant gut microbiota (59), but only specific gut-adapted microbes such as *Bifidobacteria* and *Bacteroides* persist (61). As temporary shifts in the microbiota during critical developmental windows can have long-term effects on offspring (53) and priority effects influence gut microbiota community composition (52), the initial seeding of the infant gut by maternal microbes can have long-term effects in the absence of persistent colonization. Thus we set out to investigate the normal course of microbial profiling in pregnancy and determine how maternal pre-pregnancy BMI and GWG influenced this profiling. We also investigated how these factors were associated with changes in the infant gut microbiota.

4.2 Results

4.2.1 Participant characteristics

We investigated the relationship between pre-pregnancy BMI, GWG, and the maternal gut microbiota in collaboration with the Braun Lab in Berlin, Germany. The maternal gut microbiota was assessed in the first (sample: maternal (SM)1; 10-17 weeks gestation), second (SM2; 26-28 weeks gestation), and third (SM3;

>36 weeks gestation) trimester, and at delivery (SM4). Both the maternal and infant gut microbiota were additionally assessed at 6 months postpartum (SM5). A second cohort in collaboration with the Atkinson Lab at McMaster University in Hamilton, Canada was also assessed but due to time constraints associated with acquiring randomized controlled trial (RCT) metadata, a full analysis was not completed. An initial analysis of this cohort is appended (Appendix B).

After excluding participants who reported antibiotic use during the first, second, or third trimester, maternal samples from 65 Berlin participants were analyzed. Pre-pregnancy BMI was used as a continuous variable or by BMI category: optimal (18.5-24.9, n=38), overweight (25-29.9, n=12) or obese (>30, n=15). GWG was categorized by pre-pregnancy BMI category into below (n=9), within (n=18), or above (n=38) the recommended range according to Institute of Medicine guidelines (233).

The majority of participants with pre-pregnancy overweight (10 of 12; 83%) or obesity (12 of 15; 80%) had GWG above the recommended range, compared to less than half of participants with an optimal pre-pregnancy BMI (16 of 38; 42%). Participants predominantly delivered vaginally overall (51/65; 78%) and within each pre-pregnancy BMI category: optimal (31/38; 82%), overweight (10/12; 83%), obese (10/15; 67%). Of maternal participants who had matched infant samples included in our analyses, a greater proportion delivered vaginally overall (40/43; 93%) and within each pre-pregnancy BMI category—optimal (26/28; 93%), overweight (7/8; 88%), obese (7/7; 100%)—likely due to the exclusion of infants exposed to antibiotics during delivery (11/14 c-section and 6/46 vaginally delivered).

4.2.2 Pre-pregnancy BMI and GWG impact the maternal microbiota

We assessed the maternal and infant gut microbiota using 16S ribosomal RNA (rRNA) gene sequencing of the combined variable 3 and 4 region (V3-V4). After removing host-associated sequences and removing taxa present in less than 5% of samples, the median read count in maternal samples was 55,208 (minimum 13,052; maximum 116,095). To evaluate differences in within-sample alpha diversity, the Shannon Index was used as a measure of richness and evenness (234). The impacts of pre-pregnancy BMI, GWG category, and sample time point on alpha diversity were assessed by a mixed linear model with those factors as interacting fixed effects and participant ID as a random effect. Consistent with previous studies (98), sample alpha diversity was similar across sample time points (main effect of sample time, p=0.17; Fig. 4.1) and the effects of pre-pregnancy BMI and GWG did not change across sample time points (interaction effects, p=0.17 and p=0.17 respectively). Alpha diversity was decreased by GWG below or above the recommended range compared to within the recommended range (p=0.043; Fig. 4.2). Sample alpha diversity was positively correlated with pre-pregnancy BMI (R^2=0.050, p=0.023). This effect was driven by participants whose GWG was above the recommended range for their pre-pregnancy BMI, (R^2=0.082, p=0.014; Fig. 4.2). This correlation was absent in participants within their recommended gestational weight gain range (R^2=0.0040, p=0.73) and participants whose gestational weight gain was below the recommended range (R^2=0.023, p=0.62), but this may be due in part to limited sample size as 22 of 27 participants with a pre-pregnancy BMI greater
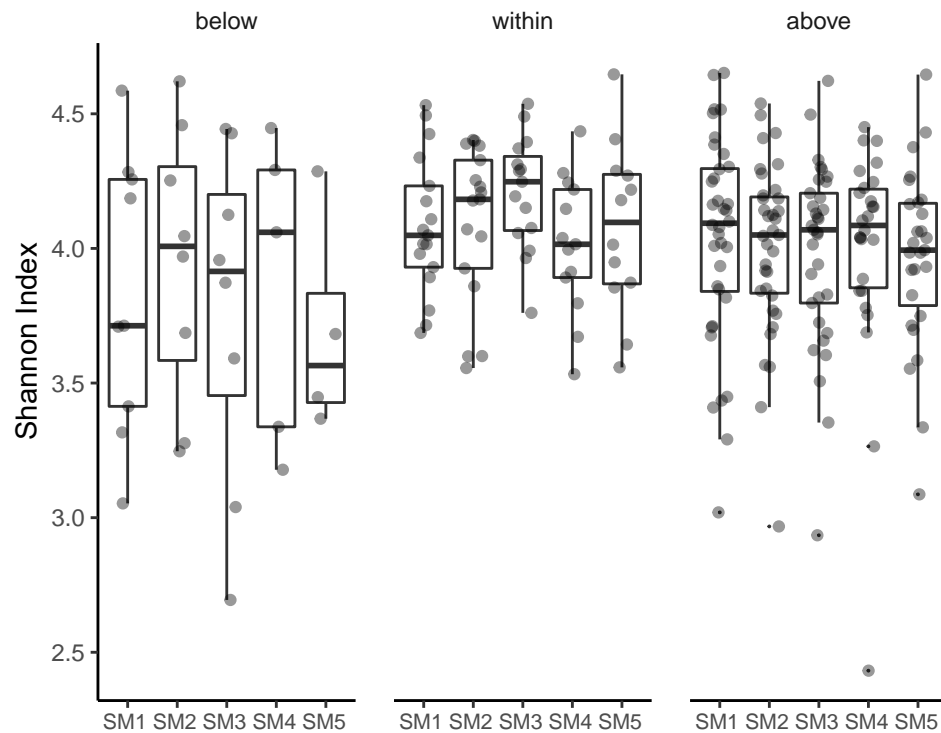
Figure 4.1. Alpha diversity is similar across sample time points. Boxplots of alpha diversity (Shannon Index) measures by sample time point (SM1 n=62; SM2 n=60; SM3 n=56; SM4 n=44; SM5 n=43) and GWG category (below n=34; within n=74; above n=157). Alpha diversity was similar across sample time points overall and within GWG categories. Significance was assessed by mixed linear model with pre-pregnancy BMI, GWG category, and sample time point as interacting fixed effects, and individual participant ID as a random effect. The boxplot centre line represents the median; the box limits represent the upper and lower quartiles; the whiskers represent the 1.5x interquartile range; the points represent individual values.

than 25 had excess gestational weight gain.
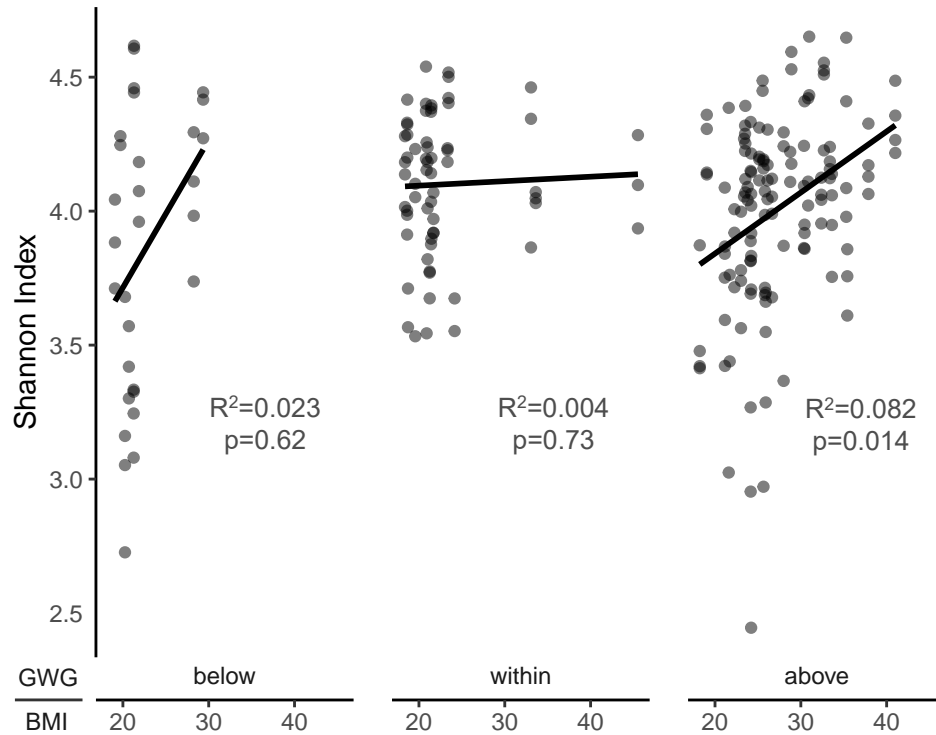
Figure 4.2. Alpha diversity is positively correlated with pre-pregnancy BMI in participants with excess GWG. Scatter plots of alpha diversity (Shannon Index) measures GWG category (below n=34; within n=74; above n=157). Alpha diversity was positively correlated with pre-pregnancy BMI in participants with excess GWG. Significance was assessed by mixed linear model within each GWG category with pre-pregnancy BMI as a fixed effect, and individual participant ID as a random effect.

Differences in overall microbiota community composition between samples (beta diversity) were assessed by Bray-Curtis dissimilarity and visualized by principal coordinate analysis (PCoA). Across all sample time points, pre-pregnancy BMI category had a small effect on beta-diversity (R^2=0.027, p=0.0001; Fig. 4.3). Within sample time points, pre-pregnancy BMI had a significant effect on beta diversity in the first trimester of pregnancy (SM1;

R^2=0.023, p=0.036). Sample time (SM1, SM2, etc.) also explained a small but significant percentage of the variation between samples (R^2=0.010, p=0.0001), as did GWG category (below, within, or above recommended GWG; R^2=0.023, p=0.0001; Fig. 4.4). Within sample time points, the effect of gestation weight gain category on beta diversity was only significant at 6-months postpartum (SM5; R^2=0.059, p=0.0499). Individual variation between participants explained the largest percentage of variation between samples (R^2=0.64, p=0.0001).

To investigate whether pre-pregnancy BMI impacts beta diversity within participants, we grouped samples by participant and calculated the mean distance to the centroid within each group (beta dispersion) using Bray-Curtis dissimilarity. Pre-pregnancy BMI was negatively correlated with mean beta dispersion across all sample time points. (R^2=0.077, p=0.0067; Fig. 4.5). This was driven by increased dissimilarity of samples at the time of delivery (delivery; SM4) as this correlation was not significant when this sample time point was excluded (R^2=0.031, p=0.089), but was significant if any other sample time point was excluded.

The effect of pre-pregnancy BMI on sample beta diversity within each participant was assessed by mixed linear model with pre-pregnancy BMI, GWG category, and sample time point as interacting fixed effects and participant ID as a random effect. Overall, beta-diversity within participants is negatively correlated with pre-pregnancy BMI across all sample time points (R^2=0.034, p=0.0044; Fig. 4.6), and differed by sample time point (p=0.00069), but did not differ by GWG category (p=0.39). These data suggest that the gut microbiota shift changes less over the course of pregnancy in participants who are overweight
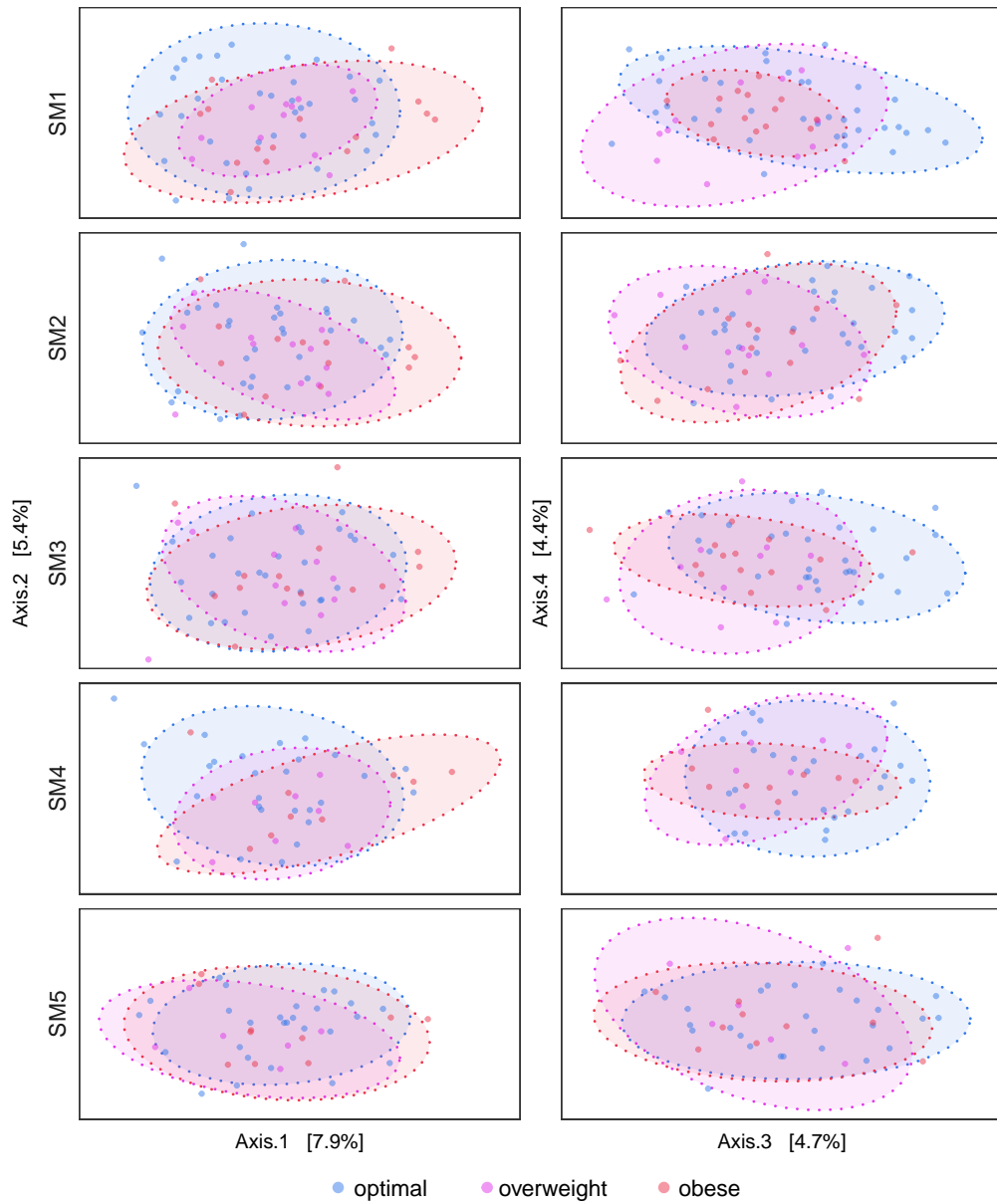
Figure 4.3. Beta diversity varies with pre-pregnancy BMI category. Principle coordinate analysis plots of Bray-Curtis dissimilarities show samples from participants with a pre-pregnancy BMI 18.5-24.9 (optimal n=36; blue), 25-29.9 (overweight n=11; purple) or greater than 30 (obese n=15; red). Significance was assessed by permutational multivariate analysis (adonis; vegan) with pre-pregnancy BMI category, GWG category, and sample time point as interacting fixed effects and participant ID as an additive fixed effect. Ellipses are shown for 90% confidence level.
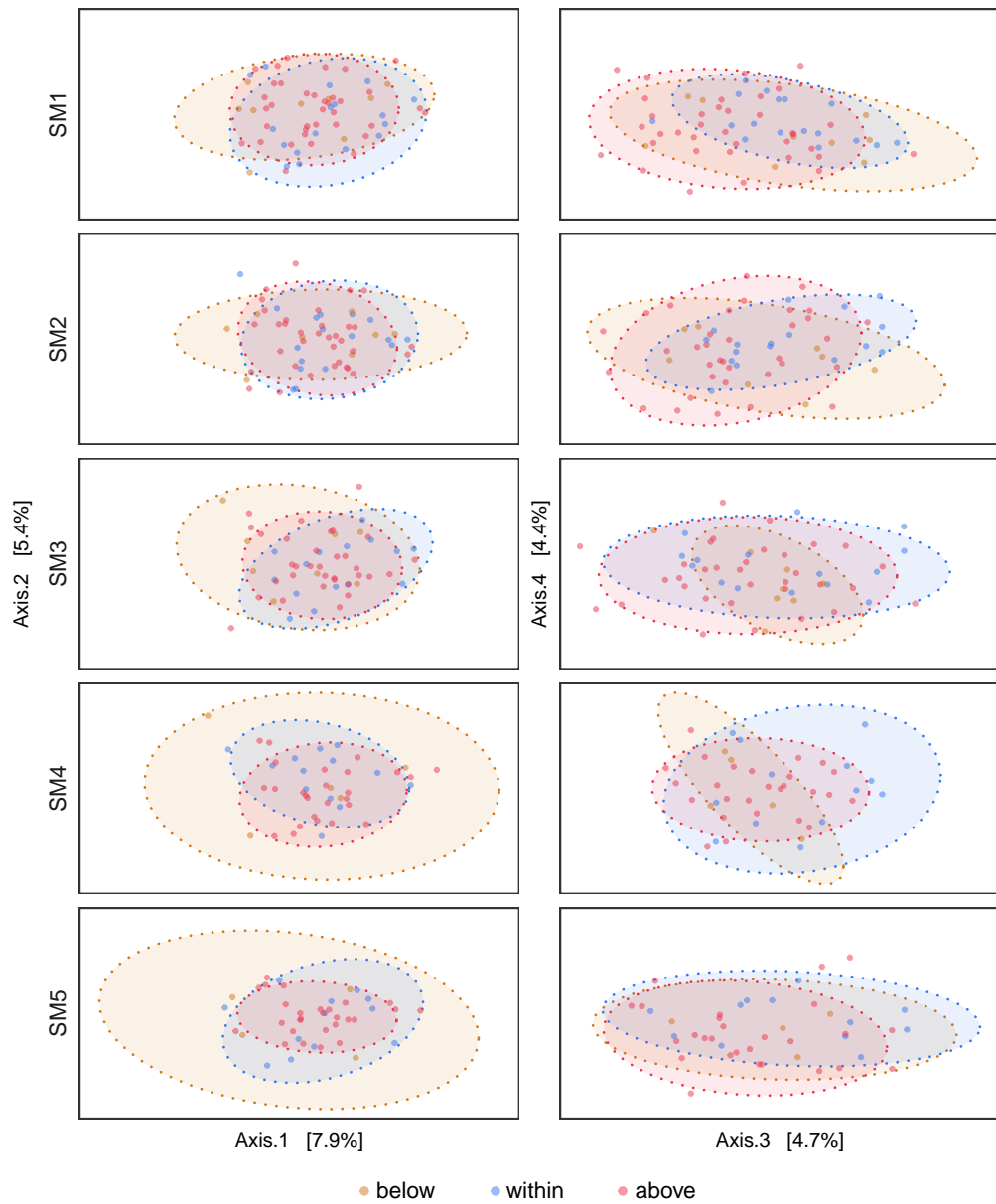
Figure 4.4. Beta diversity varies with gestational weight gain category. Principle coordinate analysis plots of Bray-Curtis dissimilarities show samples from participants with GWG below (n=9; orange), within (n=17; blue) or above (n=36; red) the recommended range for their pre-pregnancy BMI. Significance was assessed by permutational multivariate analysis (adonis; vegan) with pre-pregnancy BMI category, GWG category, and sample time point as interacting fixed effects and participant ID as an additive fixed effect. Ellipses are shown for 90% confidence level.
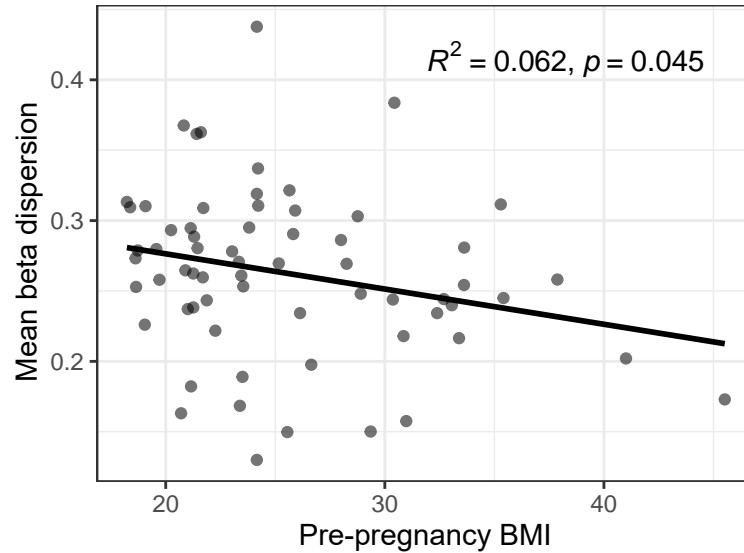
Figure 4.5. Beta dispersion within participants within participants is negatively correlated with pre-pregnancy BMI. A scatter plot of the mean distance to the centroid of each participant's samples (mean beta dispersion) by pre-pregnancy BMI show that mean beta dispersion is negatively correlated with pre-pregnancy BMI (R^2=0.079, p=0.0057); Pearson correlation, n=65.

or obese prior to pregnancy.

To investigate specific taxa affected by pre-pregnancy BMI and GWG category, differential abundance testing was performed using DESeq2 (RRID: SCR_015687). As all but 2 participants with pre-pregnancy overweight and 3 participants with pre-pregnancy obesity experienced excess GWG the impact of pre-pregnancy BMI category was assessed within participants who experienced excess GWG and the impact of excess GWG was assessed within participants with an optimal pre-pregnancy BMI.

Overall, pre-pregnancy obesity was associated with a decreased relative abundance of *Bacteroidaceae*, *Rikenellaceae*, *Christensenellaceae* and an
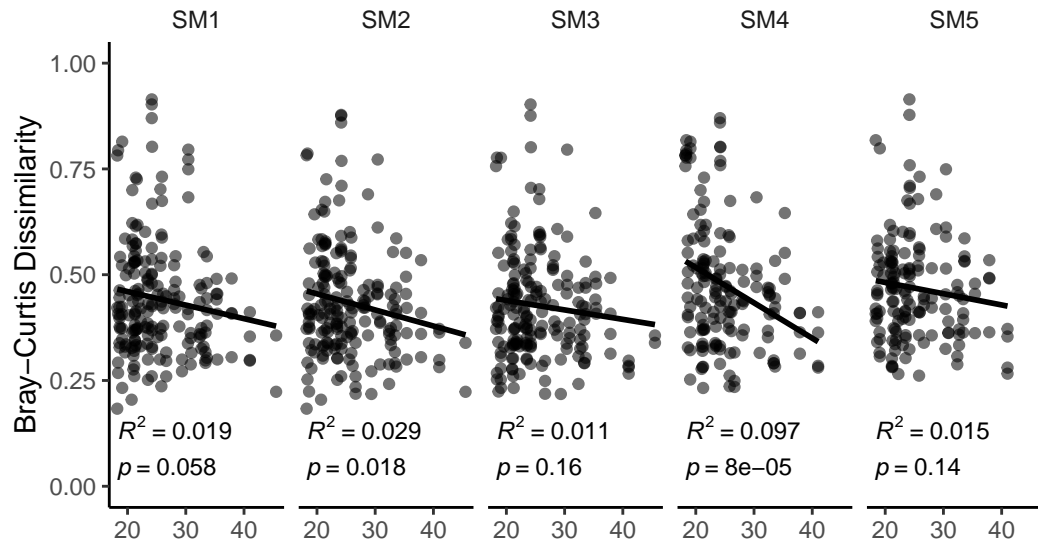
Figure 4.6. Beta diversity within participants is negatively correlated with pre-pregnancy BMI. Scatter plots of Bray-Curtis dissimilarities within participants by pre-pregnancy BMI show that beta-diversity within participants is negatively correlated with pre-pregnancy BMI. Significance was assessed by mixed linear model with pre-pregnancy BMI as a fixed effect and individual participant ID as a random effect (SM1 n=191; SM2 n=189; SM3 n=188; SM4 n=155; SM5 n=135).

unknown member of the order *Rhodospirillales* as well as an increased relative abundance of *Enterobacteriaceae* (Fig. 4.7; Table 4.1). Both pre-pregnancy overweight and obesity, as well as excess GWG ("above"), were associated with a decreased relative abundance of *Clostridiales vadin BB60 group*. Pre-pregnancy overweight and excess GWG were also each associated with an increased relative abundance of *Erysipelotrichaceae*. Excess GWG was also associated with an increased relative abundance of *Bifidobacteriaceae* and *Peptostreptococcaceae*.
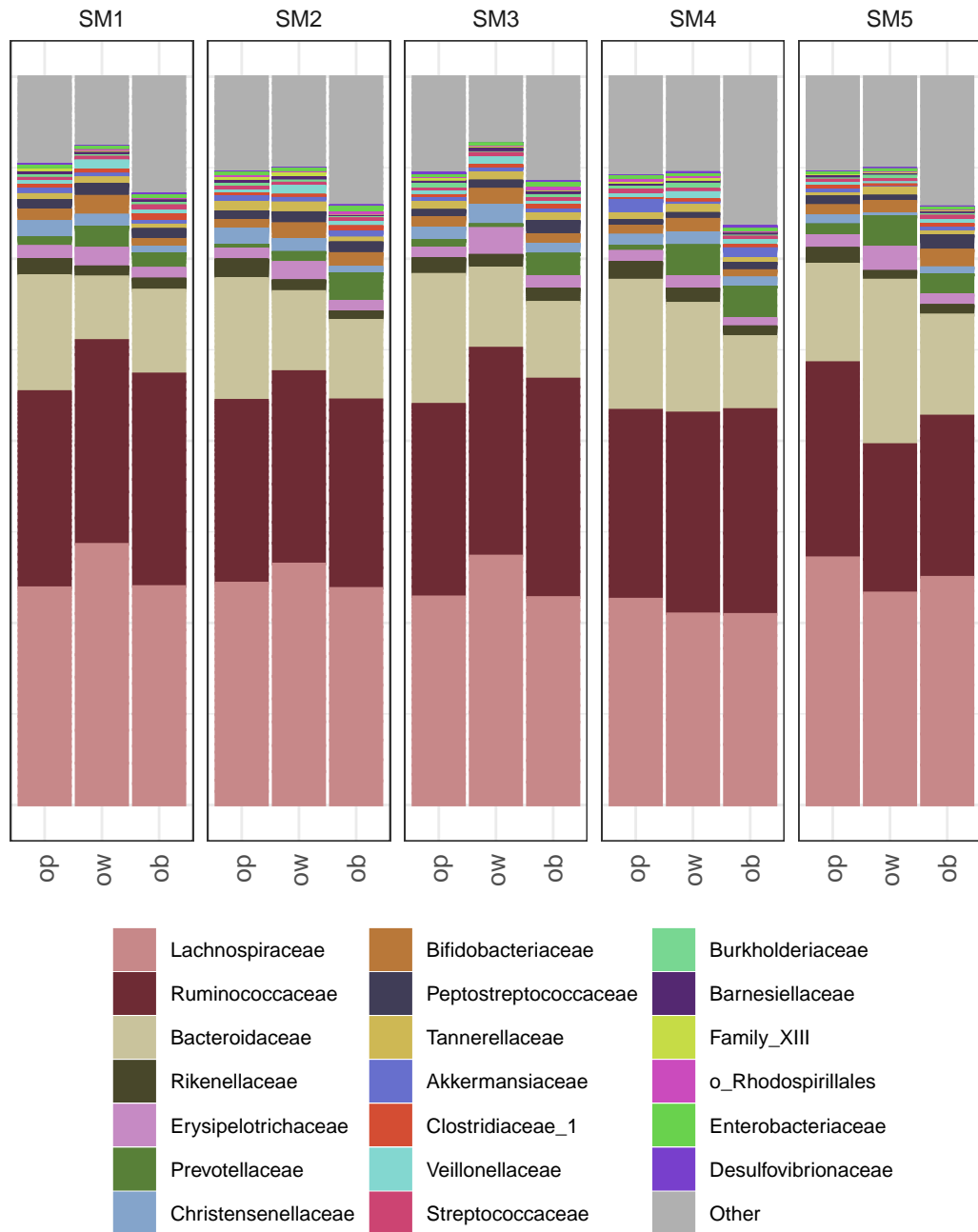
Figure 4.7. Taxonomic summary of top 20 families by pre-pregnancy BMI category and sample time point. The mean relative abundance of the 20 most abundant bacterial families was calculated within each combination of sample time point and pre-pregnancy BMI category (optimal/op n=36; overweight/ow n=11; obese/ob n=15) is shown in a stacked bar plot coloured by family.
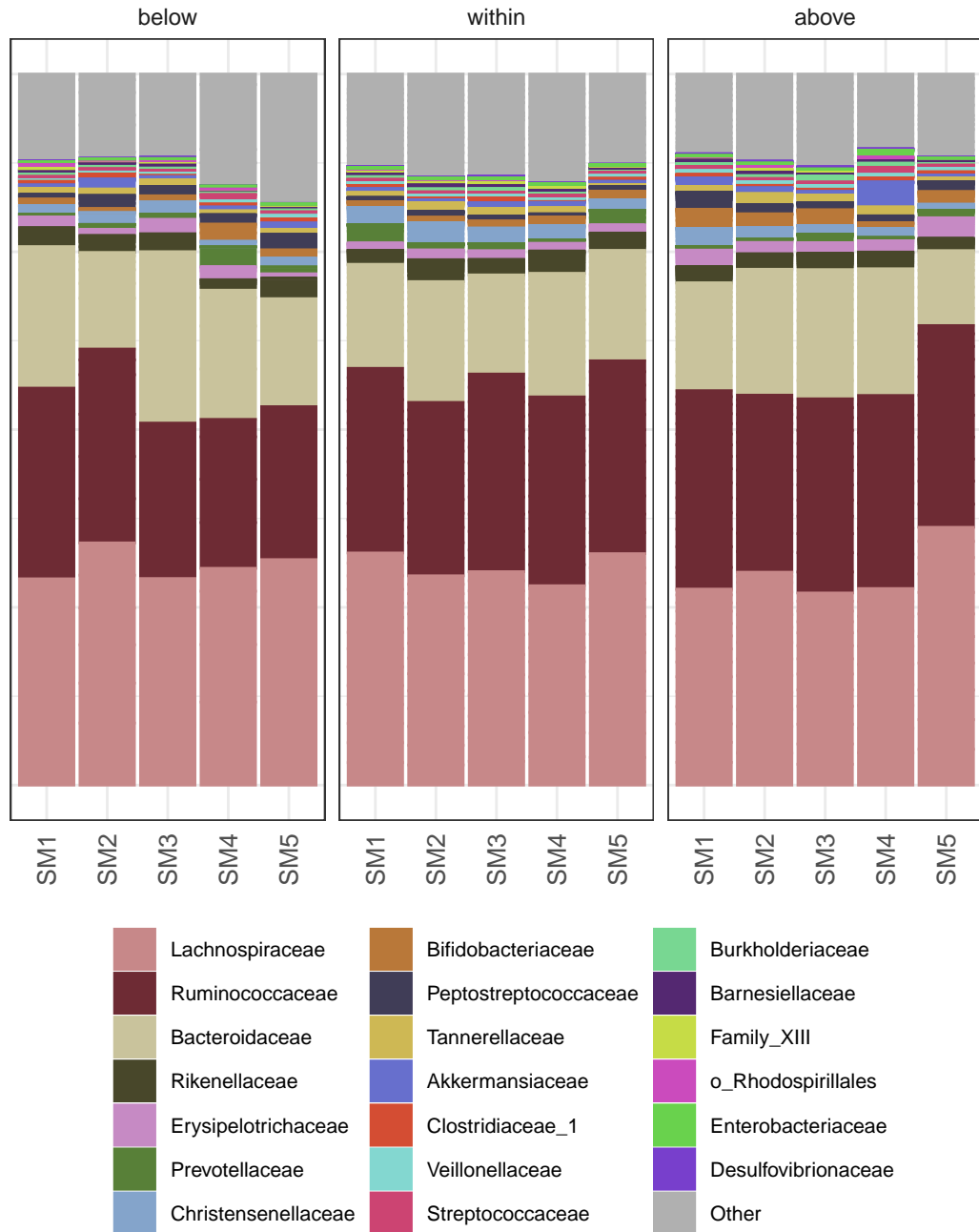
Figure 4.8. Taxonomic summary of top 20 families by GWG category and sample time point. The mean relative abundance of the 20 most abundant bacterial families was calculated within each combination of sample time point and GWG category (below n=9; within n=17; above n=36) is shown in a stacked bar plot coloured by family.

Within sample time points, pre-pregnancy overweight or obesity was associated with a significantly increased relative abundance of *Prevotella 9* in the first (SM1) and second trimester (SM2) and at delivery (SM4; Fig. 4.9, Table 4.2). Pre-pregnancy obesity was also associated with an increased relative abundance of *Escherichia/Shigella* in the third trimester (SM3), and also *Ruminococcaceae NK4A214 group* and *Coprococcus 1* at delivery (SM4). In the first trimester (SM1), pre-pregnancy obesity was associated with a decreased relative abundance of *Ruminococcaceae* genera *UCG-004*, *Oscillibacter*, and *UBA1819*, which was also decreased with pre-pregnancy overweight.

Excess GWG was associated with an increased relative abundance of an unknown member of the *Ruminococcaceae* in the first trimester (SM1), as well as increases in *Peptostreptococcaceae* members *Intestinibacter* and *Romboutsia*. The relative abundances of *Erysipelotrichaceae* members *Turicibacter* and *Holdemanella* were also increased with excess GWG at SM1, and *Holdemanella* was additionally increased at SM2 and SM3. GWG below the recommended range was associated with an increased relative abundance of *Holdemanella* at SM1 and a decreased relative abundance of *Holdemanella* at 6 months postpartum (SM5). *Lachnospiraceae* member *ND3007 group* was also decreased in relative abundance at 6 months postpartum (SM5) with GWG below the recommended range.

Table 4.1. Differentially abundant families in maternal microbiota by pre-pregnancy overweight (ow) or obesity (ob) compared to optimal (op) and by GWG above the recommended range compared to within the recommended range. Taxa with a mean abundance less than 40 were excluded. Mean, base mean abundance, log2FC, log2 fold change; SE, standard error.

Comparison	Phylum	Order	Family	Mean	log2FC	SE	p adjusted
ow v. op	Firmicutes	Erysipelotrichales	Erysipelotrichaceae	1,003.67	0.59	0.16	0.0077
ow v. op	Firmicutes	Clostridiales	vadin BB60 group	43.76	−2.03	0.51	0.0037
ob v. op	Bacteroidetes	Bacteroidales	Bacteroidaceae	10,442.27	−0.87	0.23	0.0021
ob v. op	Firmicutes	Clostridiales	Christensenellaceae	1,077.34	−0.89	0.32	0.032
ob v. op	Proteobacteria	Enterobacteriales	Enterobacteriaceae	140.12	1.43	0.44	0.012
ob v. op	Bacteroidetes	Bacteroidales	Rikenellaceae	1,360.65	−0.99	0.23	0.00061
ob v. op	Proteobacteria	Rhodospirillales	unknown	189.96	−2.02	0.66	0.017
ob v. op	Firmicutes	Clostridiales	vadin BB60 group	43.76	−2.73	0.47	<0.0001
above v. within	Actinobacteria	Bifidobacteriales	Bifidobacteriaceae	949.55	1.3	0.33	0.001
above v. within	Firmicutes	Erysipelotrichales	Erysipelotrichaceae	883.65	0.86	0.18	<0.0001
above v. within	Firmicutes	Clostridiales	Peptostreptococcaceae	672.8	1.25	0.31	0.001
above v. within	Firmicutes	Clostridiales	vadin BB60 group	54.95	−2.82	0.52	<0.0001
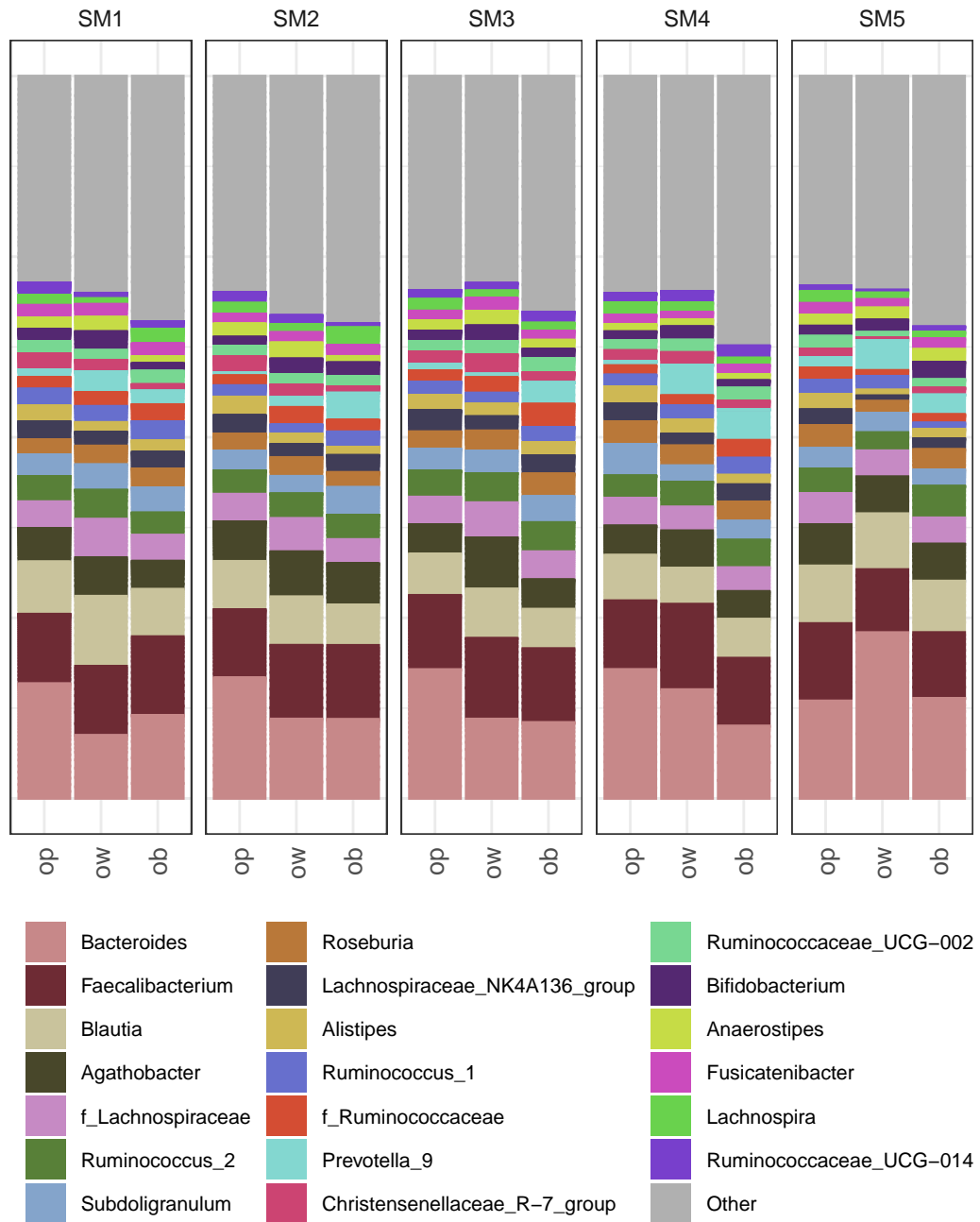
Figure 4.9. Taxonomic summary of top 20 genera by pre-pregnancy BMI category and sample time point. The mean relative abundance of the 20 most abundant bacterial genera was calculated within each combination of sample time point and pre-pregnancy BMI category (optimal/op n=36; overweight/ow n=11; obese/ob n=15) is shown in a stacked bar plot coloured by genus.
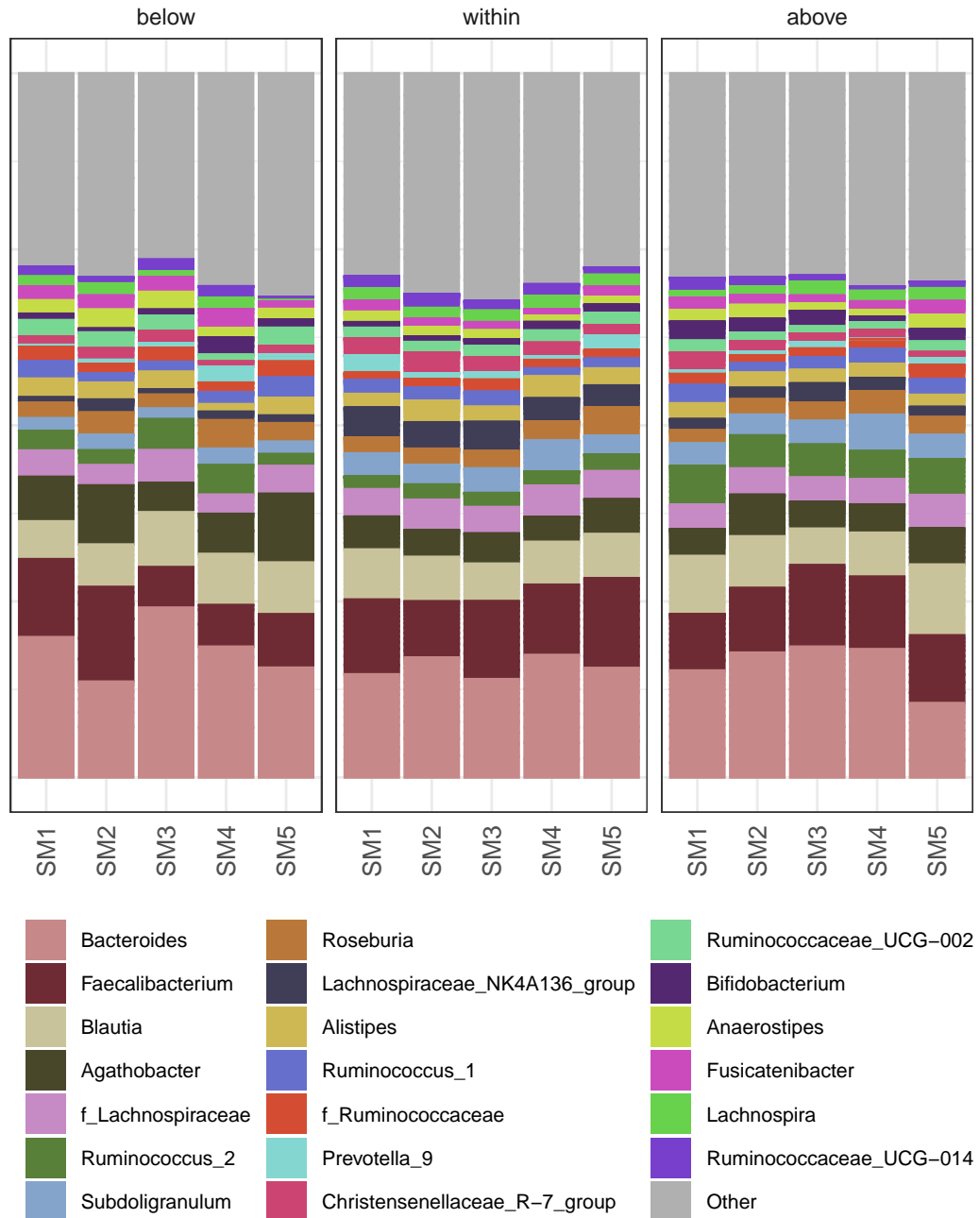
Figure 4.10. Taxonomic summary of top 20 genera by GWG category and sample time point. The mean relative abundance of the 20 most abundant bacterial genera was calculated within each combination of sample time point and GWG category (below n=9; within n=17; above n=36) is shown in a stacked bar plot coloured by genus.

Table 4.2. Differentially abundant genera in maternal microbiota within each sample time point by pre-pregnancy overweight (ow) or obesity (ob) compared to optimal (op) and by GWG above and below the recommended range compared to within the recommended range. Taxa with a mean abundance of less than 40 were excluded. Mean, base mean abundance, log2FC, log2 fold change; SE, standard error.

| Comparison	sample	Family	Genus	Mean	log2FC	SE	padj
above v. within	SM1	Erysipelotrichaceae	Holdemanella	108.38	41.82	3.01	<0.0001
below v. within	SM1	Erysipelotrichaceae	Holdemanella	108.38	15.91	3.8	0.0015
above v. within	SM1	Erysipelotrichaceae	Turicibacter	74.2	3.71	1.13	0.017
above v. within	SM1	Lachnospiraceae	AC2044 group	83.45	−25.18	3.26	<0.0001
above v. within	SM1	Peptostreptococcaceae	Intestinibacter	417.49	2.89	0.86	0.015
above v. within	SM1	Peptostreptococcaceae	Romboutsia	244.51	2.46	0.75	0.017
above v. within	SM1	Prevotellaceae	Prevotella 9	225.54	−28.07	3.26	<0.0001
ob v. op	SM1	Prevotellaceae	Prevotella 9	208.58	12.16	2.7	0.00018
ow v. op	SM1	Prevotellaceae	Prevotella 9	208.58	11.31	2.93	0.0034
ob v. op	SM1	Ruminococcaceae	Oscillibacter	105.72	−2.19	0.72	0.036
ob v. op	SM1	Ruminococcaceae	UBA1819	54.22	−3.41	0.83	0.00087
ow v. op	SM1	Ruminococcaceae	UBA1819	54.22	−3.14	0.9	0.012
ob v. op	SM1	Ruminococcaceae	UCG-004	120.94	−2.98	0.93	0.026
above v. within	SM1	Ruminococcaceae	unknown	1,155.07	1.73	0.57	0.036
above v. within	SM2	Erysipelotrichaceae	Holdemanella	79.96	30.02	2.89	<0.0001
ob v. op	SM2	Prevotellaceae	Prevotella 9	805.58	10.69	2.68	0.0052
ob v. op	SM3	Enterobacteriaceae	Escherichia-Shigella	157.35	4.04	1.11	0.045
above v. within	SM3	Erysipelotrichaceae	Holdemanella	78.53	28.61	3.27	<0.0001
above v. within	SM3	vadinBB60 group	unknown	108.66	−5.7	1.07	<0.0001
ob v. op	SM4	Lachnospiraceae	Coprococcus 1	156.27	2.55	0.82	0.034
ob v. op	SM4	Prevotellaceae	Prevotella 9	3,145.52	10.25	3.23	0.031
ob v. op	SM4	Ruminococcaceae	CAG-352	42.27	23.79	3.44	<0.0001
ow v. op	SM4	Ruminococcaceae	CAG-352	42.27	18.49	3.69	<0.0001
ob v. op	SM4	Ruminococcaceae	NK4A214 group	288.98	3.99	1.14	0.013
below v. within	SM5	Erysipelotrichaceae	Holdemanella	116.57	−20.37	4.45	0.00067
below v. within	SM5	Lachnospiraceae	ND3007 group	293.12	−2.56	0.79	0.028

4.2.3 Maternal gestational weight gain impacts the infant microbiota

Many studies have reported that maternal BMI is significantly associated with changes in infant microbial communities (108, 158, 159, 235–237). We evaluated the independent and combined impacts of maternal pre-pregnancy overweight or obesity and excess GWG on the gut microbiota of infants at 6 months of age (female n=30; male n=30). Our initial analysis showed that exposure to antibiotics during delivery was associated with a decrease in infant microbiota alpha diversity (p=0.039) and a decreased relative abundance of *Bifidobacterium*, *Escherichia/Shigella*, *Enterococcus*, *Staphylococcus*, *Sutterella*, *Akkermansia*, *Actinomyces*, and *Collinsella* (Table 4.3).

To avoid these confounding effects, antibiotic-exposed infants were excluded from further analyses (female n=8; male n=8 excluded). In addition to infants exposed to maternal antibiotics during delivery, infants from mothers who used nicotine during pregnancy were excluded (1 female and 3 male infants; female n=21; male n=19 included in analyses) due to the known impacts of nicotine use during pregnancy on the infant microbiota (238, 239) and childhood overweight and obesity (240, 241). As the infant microbiota was assessed in only 3 participants (1 male, 2 female) with maternal pre-pregnancy overweight or obesity who did not experience excess GWG, the impact of pre-pregnancy BMI was assessed within participants who experienced excess GWG and the impact of excess GWG was assessed within participants with an optimal pre-pregnancy BMI.

Table 4.3. Differentially abundant genera in infant microbiota at 6 months of age by maternal antibiotics at delivery (antibiotics vs. no antibiotics). Mean, base mean abundance, log2FC, log2 fold change; SE, standard error.

Phylum	Family	Genus	Mean	log2FC	SE	stat	padj
Actinobacteria	Actinomycetaceae	Actinomyces	48,446.6	−2.33	0.81	−2.89	$4.43 \cdot 10^{-2}$
Verrucomicrobia	Akkermansiaceae	Akkermansia	6,562.98	−2.32	0.89	−2.61	$4.55 \cdot 10^{-2}$
Actinobacteria	Bifidobacteriaceae	Bifidobacterium	2,582.62	−2.8	0.85	−3.3	$1.64 \cdot 10^{-2}$
Proteobacteria	Burkholderiaceae	Sutterella	177.35	−4.35	1.61	−2.69	$4.43 \cdot 10^{-2}$
Actinobacteria	Coriobacteriaceae	Collinsella	99.42	−7.42	2.72	−2.73	$4.43 \cdot 10^{-2}$
Proteobacteria	Enterobacteriaceae	Escherichia/Shigella	84.35	−8.99	3.23	−2.78	$4.43 \cdot 10^{-2}$
Firmicutes	Enterococcaceae	Enterococcus	76.07	−3.56	1.39	−2.56	$4.82 \cdot 10^{-2}$
Firmicutes	Staphylococcaceae	Staphylococcus	51.05	−10.16	2.65	−3.83	$3.22 \cdot 10^{-3}$

In participants with an optimal pre-pregnancy BMI (18.5-24.9), infant microbiota alpha diversity was increased by GWG above the recommended range (p=0.046; main effect of GWG category, p=0.043) and decreased by GWG below the recommended range (p=0.038). Infant microbiota alpha diversity was not significantly correlated with maternal pre-pregnancy BMI (R^2=0.16, p=0.091; Fig. 4.11), and was similar between male and female infants (p=0.56) and between infants delivered by Cesarean section (C-section) and infants delivered vaginally (p=0.22). This is consistent with previous reports that infant alpha diversity varies by delivery mode in the first 2 months of life but not at 6 months of age (242).
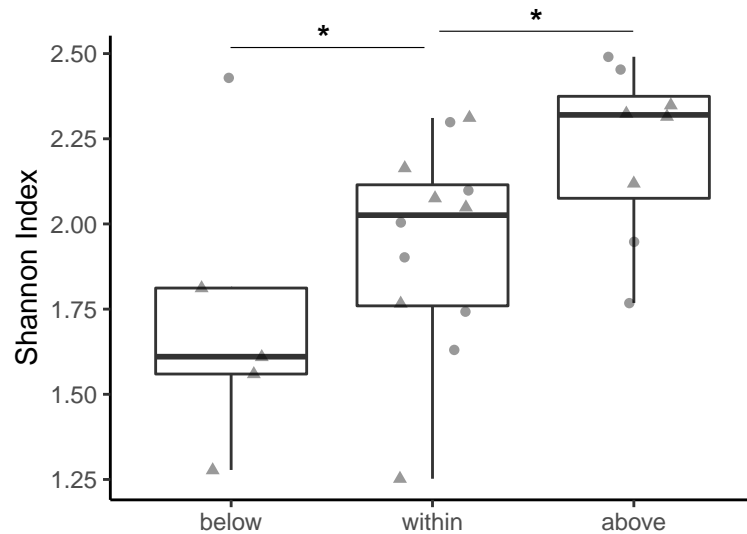
Figure 4.11. Maternal GWG impacts infant gut microbiota alpha diversity within participants with an optimal pre-pregnancy BMI (18.5-24.9). Infant microbiota alpha diversity was decreased by GWG below the recommended range (n=5) and increased by GWG above the recommended range (n=8) compared to GWG within the recommended range (n=12). Significance was assessed by linear model with maternal GWG category and infant sex as fixed effects (* p<0.05).

Infant beta diversity was calculated at the genus level using Bray-Curtis

71

dissimilarity and visualized by PCoA. Significance was assessed by permutational multivariate analysis (adonis; vegan) with infant sex, pre-pregnancy BMI category, and GWG category interacting fixed effects. Infant beta diversity differed by GWG (R^2=0.10, p=0.014) category, but was similar across maternal pre-pregnancy BMI categories (R^2=0.026, p=0.48) and between male and female infants (R^2=0.030, p=0.27; Fig. 4.12). Consistent with our alpha diversity data, these results suggest that the infant gut microbiota is more impacted by maternal GWG than by pre-pregnancy BMI.

To investigate specific taxa affected by pre-pregnancy BMI and GWG category, differential abundance testing was performed using DESeq2 (RRID: SCR_015687). Within the family *Enterobacteriaceae*, *Enterobacter* was increased by maternal pre-pregnancy overweight and *Escherichia/Shigella* was decreased in infants of participants with GWG below the recommended range compared to within the recommended range. Maternal pre-pregnancy overweight was also associated with increased *Streptococcus*. *Bacteroides* was also decreased in infants of participants with GWG below the recommended range compared to within the recommended range. *Bacteroides*, *Enterobacter*, *Escherichia/Shigella*, and *Streptococcus* are all early colonizers of the vaginally delivered infant gut transmitted from the maternal microbiota (60). This suggests that changes in these taxa could be due to differences in the initial colonization of the infant gut during and shortly after birth.

Maternal pre-pregnancy overweight or obesity and GWG categories were also associated with changes in bacterial genera more typically acquired after birth (60), including increased *Veillonella* and *Granulicatella* and decreased
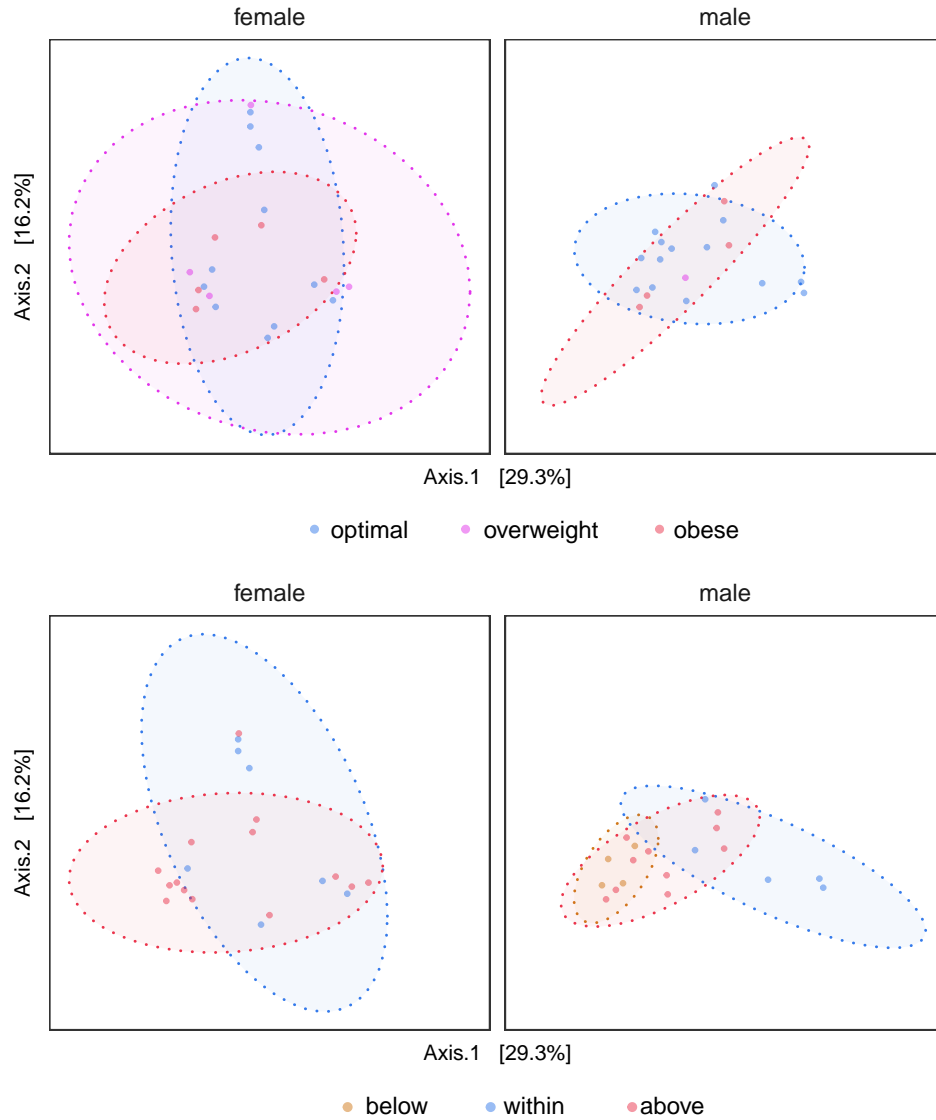
Figure 4.12. Infant microbiota beta diversity. Principle coordinate analysis plots of Bray-Curtis dissimilarity at the genus level. Infant beta diversity varied by maternal GWG below (n=4, orange), within (n=12, blue) and above (n=24, red) the recommended range. Infant beta diversity was similar between maternal pre-pregnancy BMI categories (optimal n=25, blue; overweight n=6, purple; obese n=9, red). Significance was assessed by permutational multivariate analysis (adonis; vegan) with pre-pregnancy BMI category, GWG category, and sample time point as interacting fixed effects and participant ID as an additive fixed effect. Ellipses are shown for 90% confidence level.

Anaerostipes with maternal pre-pregnancy overweight, and increased *Collinsella* with GWG below or above the recommended range. GWG below the recommended range was also associated with decreased *Lachnoclostridium*, a genus previously been linked to butyrate production in the 3-month-old infant gut microbiota (243).

Only the butyrate-producing genus *Clostridioides* was significantly affected by both maternal pre-pregnancy BMI and GWG, as it was decreased by pre-pregnancy overweight and GWG below the recommended range. The only genus impacted by maternal pre-pregnancy overweight or obesity in both the maternal and the infant gut microbiota was *Prevotella 9*, which was significantly increased in the maternal gut microbiota at delivery, and also increased in the infant gut microbiota at 6 months of age. Although our data show largely independent effects of maternal pre-pregnancy BMI and GWG, this may be due to the limited sample size of participants with high pre-pregnancy BMI without excess GWG.
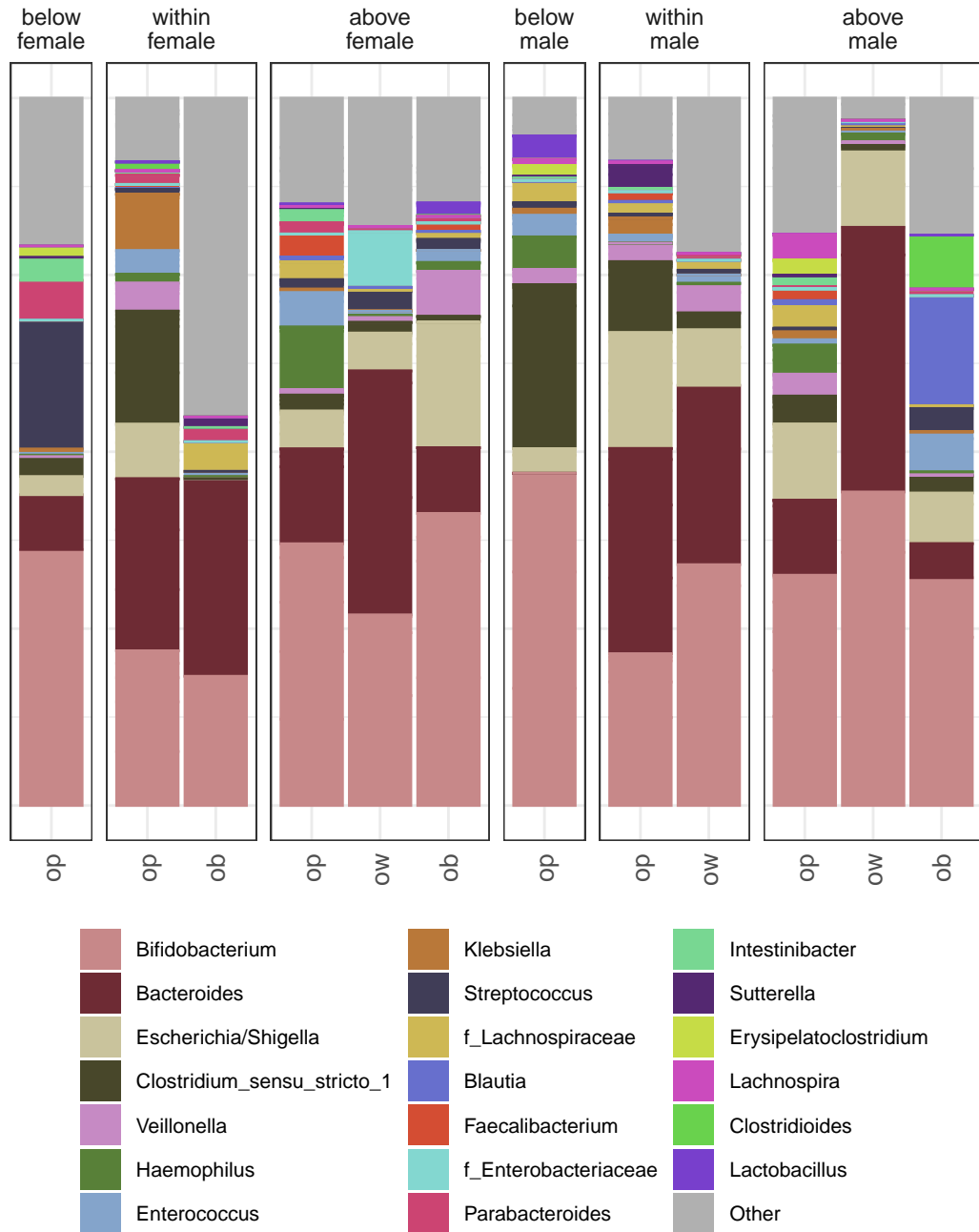
Figure 4.13. Taxonomic summary of top 20 genera in infant microbiota by GWG category, pre-pregnancy BMI category, and infant sex. The mean relative abundance of the 20 most abundant bacterial genera was calculated and is shown in a stacked bar plot coloured by genus.

Table 4.4. Differentially abundant genera in infant microbiota at 6 months of age by pre-pregnancy overweight (ow) or obesity (ob) compared to optimal (op) and by GWG above and below the recommended range compared to within the recommended range.

Comparison	Class	Family	Genus	Mean	log2FC	SE	padj
ow vs. op	Bacilli	Carnobacteriaceae	Granulicatella	66.52	5.55	1.85	$1.65 \cdot 10^{-2}$
ow vs. op	Bacilli	Streptococcaceae	Streptococcus	2,584.85	4.14	1.15	$2.4 \cdot 10^{-3}$
below v. within	Bacteroidia	Bacteroidaceae	Bacteroides	7,216.32	−13.72	2.91	$2.54 \cdot 10^{-5}$
ob v. op	Bacteroidia	Prevotellaceae	Prevotella 9	2.15	23.05	3.57	$2.07 \cdot 10^{-9}$
ow vs. op	Clostridia	Lachnospiraceae	Anaerostipes	205.28	−25.11	4.23	$1.62 \cdot 10^{-7}$
below v. within	Clostridia	Lachnospiraceae	Lachnoclostridium	357.55	−23.2	4.12	$4.64 \cdot 10^{-7}$
ob v. op	Clostridia	Lachnospiraceae	Lachnospira	10.79	−23.52	3.61	$2.07 \cdot 10^{-9}$
ow vs. op	Clostridia	Lachnospiraceae	Lachnospira	10.79	−20.95	4.23	$8.16 \cdot 10^{-6}$
below v. within	Clostridia	Lachnospiraceae	Roseburia	31.87	−23.54	5.37	$9.45 \cdot 10^{-5}$
below v. within	Clostridia	Peptostreptococcaceae	Clostridioides	65.18	−30	5.37	$4.64 \cdot 10^{-7}$
ow vs. op	Clostridia	Peptostreptococcaceae	Clostridioides	65.18	−23.37	4.23	$9.11 \cdot 10^{-7}$
ob v. op	Clostridia	Peptostreptococcaceae	Terrisporobacter	4.13	−21.95	3.62	$1.74 \cdot 10^{-8}$
ow vs. op	Clostridia	Peptostreptococcaceae	Terrisporobacter	4.13	−19.87	4.23	$2.48 \cdot 10^{-5}$
below v. within	Coriobacteriia	Coriobacteriaceae	Collinsella	47.29	23.93	4.39	$6.82 \cdot 10^{-7}$
above v. within	Coriobacteriia	Coriobacteriaceae	Collinsella	47.29	25.21	2.73	$1.02 \cdot 10^{-18}$
ob v. op	Gammaproteobacteria	Burkholderiaceae	Parasutterella	13.4	−23.44	3.61	$2.07 \cdot 10^{-9}$
ow vs. op	Gammaproteobacteria	Burkholderiaceae	Parasutterella	13.4	−21.43	4.23	$5.63 \cdot 10^{-6}$
ow vs. op	Gammaproteobacteria	Burkholderiaceae	Sutterella	13.74	−21.33	4.18	$5.63 \cdot 10^{-6}$
ow vs. op	Gammaproteobacteria	Enterobacteriaceae	Enterobacter	19,460.44	9.96	2.85	$3.24 \cdot 10^{-3}$
below v. within	Gammaproteobacteria	Enterobacteriaceae	Escherichia/Shigella	5,330.86	−6.1	1.86	$6.97 \cdot 10^{-3}$
ow vs. op	Negativicutes	Veillonellaceae	Veillonella	1,053.02	2.31	0.83	$3.12 \cdot 10^{-2}$

4.3   Discussion

In this study, we investigated the independent and combined impacts of maternal pre-pregnancy BMI and GWG on the maternal gut microbiota over the course of pregnancy and during lactation, and the infant gut microbiota at 6 months of age. We found that maternal pre-pregnancy BMI was positively correlated with maternal alpha diversity and that the microbiota of participants with higher pre-pregnancy BMI changed less over the course of pregnancy. We also found that the effect of pre-pregnancy BMI was greatest in the first trimester and the effect of GWG was greatest during lactation and that the overall diversity of the infant gut microbiota was affected by maternal GWG category but not by maternal pre-pregnancy BMI.

Previous studies of the gut microbiota during pregnancy have found alpha diversity to decrease (93) or remain stable (98, 99, 229) over the course of pregnancy. In this study, alpha diversity was similar across all sample time points (p=0.54) and across pregnancy time points (p=0.91). Alpha diversity was decreased by GWG outside the recommended range (p=0.043) but positively correlated with pre-pregnancy BMI in participants with excess GWG across all sample time points. As GWG recommendations vary by pre-pregnancy BMI category, participants within an optimal pre-pregnancy BMI who experienced excess GWG would have gained more weight over the course of gestation than participants with pre-pregnancy overweight or obesity. Thus, this correlation may be driven by greater metabolic shifts in participants with optimal pre-pregnancy BMIs who experience excess GWG.

Infant alpha diversity increased by excess GWG and decreased by insufficient GWG in participants within an optimal pre-pregnancy BMI range. Previous studies of the infant microbiota at 5-13 weeks of age (244) and 3-4 months of age (159) found maternal pre-pregnancy obesity, but not overweight to be associated with modestly increased alpha diversity in vaginally delivered infants. As the gut microbiota changes dynamically and is most strongly affected by birth mode in early infancy and by diet from around 3 months of age onward (245), the discrepancy between our data and these previous studies may be due to infant age at sampling.

In maternal samples, beta diversity between samples was modestly affected by pre-pregnancy BMI category, most strongly in the first trimester (SM1), and GWG category, most strongly at 6 months postpartum (SM5). The effect of individual participants was the largest contributor to beta diversity, accounting for 64% of the variation between individual samples, similar to the high interpersonal variability seen in non-pregnant populations (246). The variation observed between sample time points is also similar to the variation observed over time in non-pregnant individuals (247), indicating any microbial adaptations to pregnancy are not associated with consistent major shifts in community composition.

Within individual participants, we found higher pre-pregnancy BMI was associated with less variation (decreased mean beta dispersion) between sample time points, indicating the gut microbiome changed less over the course of pregnancy in participants who started pregnancy with an elevated BMI and that this effect was strongest at the end of pregnancy (SM4). If the gut microbiome

shifts over the course of pregnancy to mediate maternal metabolic adaptations to pregnancy, this decrease in beta dispersion may reflect a reduced requirement for metabolic adaptations in individuals with overweight or obesity prior to pregnancy.

No differences were found in infant gut microbiota beta diversity due to maternal pre-pregnancy BMI or infant sex, consistent with previous studies (108, 248). This lack of significance is consistent with the large effect of diet relative to in utero exposures or delivery mode at this time point (245).

In maternal samples, pre-pregnancy obesity was associated with decreased relative abundances of the bacterial family *Bacteroidaceae* and the genus *Bacteroides.* This is consistent with previous data showing decreased *Bacteroides* in the first and third trimester with pre-pregnancy overweight (107), though other studies have reported increased levels in the third trimester with pre-pregnancy overweight but not obesity (106, 248). *Bacteroides* has a high capacity to adapt to its environment and can degrade both dietary and host-derived glycans (14), and together with another member of the *Bacteroidales* order, *Prevotella*, is the largest contributor to propionate production (249). Although our data found pre-pregnancy overweight and obesity were also associated with an increased relative abundance of *Prevotella 9*, this genus is predicted to be *Prevotella copri* (250), which is unable to produce propionate. In independent studies, *Prevotella* has been associated with improved glucose tolerance (251), impaired glucose tolerance and insulin resistance (252), and increases susceptibility to colitis induced by Dextran sulphate sodium (DSS) (253). This functional diversity mirrors that of *Bacteroides* and indicates the

impact of both species likely depends on environmental factors.

Pre-pregnancy obesity was also associated with a decreased relative abundance of the family *Rikenellaceae* and its member *Alistipes*, which has previously been shown to be decreased in gestational diabetes (103) and non-pregnant obesity (254). As *Alistipes* is a key producer of the short-chain fatty acid (SCFA) acetate (255), decreases in its relative abundance may lead to decreases in the production of other SCFA due to reduced cross-feeding.

The link between overweight or obesity and a decreased relative abundance of the family *Christensenellaceae*, as found in this study, is one of the most supported associations between the gut microbiome and BMI (256). In pregnant individuals, a decreased relative abundance of *Christensenellaceae* has been associated with hyperglycemia (257). Importantly, *Christensenellaceae* also has a high heritability (258) and ferments glucose to acetate and butyrate under anaerobic conditions (259).

In infants, we found that maternal overweight/obesity and excess GWG impacted the relative abundances of both early-colonizers and genera acquired during infancy. This included an increased abundances of *Veillonella* and of the pathobiont *Enterobacter*, which has previously been associated with necrotizing enterocolitis (260, 261), as well as a decreased abundance of *Bacteroides* and *Anaerostipes*. *Bacteroides* has been hypothesized to drive butyrate production in the infant gut through cross-feeding with *Anaerostipes* (262). Previous studies have reported both decreased (156) and increased (159) abundances of *Bacteroides* in infants of overweight or obese mothers, and that this association

varies by birth mode (244). As only 5 female and 4 male infants in our cohort were delivered by C-section we were unable to assess whether these effects were modified by birth mode. *Veillonella*, which we was increased in the infant microbiota by maternal pre-pregnancy overweight, is a keystone genus in microbial lactate cross-feeding in the infant gut, and its production of hydrogen (H_2) has been linked to the etiology of colic (263), a functional gastrointestinal disorder that affects up to 20% of infants (264). Together, these data suggest that maternal overweight/obesity or excess GWG shift the infant gut microbiota. It is possible that these shifts negatively impact infant gut homeostasis.

In conclusion, this study extends our previous understanding of the impact of pre-pregnancy BMI and GWG on the maternal gut microbiome during pregnancy and postpartum, and on the infant gut microbiome. Pre-pregnancy BMI was positively correlated with alpha diversity of the maternal microbiota, and negatively correlated with mean beta-dispersion within participants. Pre-pregnancy overweight or obesity was also associated with decreases in the relative abundances of SCFA-producing taxa. These shifts may impact the health of offspring directly, due to differential colonization of neonates during birth and lactation, or indirectly, through impacts on maternal gut or circulating inflammatory factors or fetal exposure to microbial components and metabolites including SCFAs.

Chapter 5

High-fat diet intake modulates maternal intestinal adaptations to pregnancy and results in placental hypoxia, as well as altered fetal gut barrier proteins and immune markers

This chapter contains a published manuscript from The Journal of Physiology[1].

Host-microbe relationships mediate gut development, nutrient absorption, and immune function. The gut microbiota has surfaced as a potential candidate for

---

mediating the relationship between maternal obesity and offspring disease risk. Commensal bacteria and their metabolites are essential for the development and function of the immune system (16), maintenance of gut epithelial barrier integrity (17–19) and the breakdown of nutrients (14, 15) . As pregnancy progresses, gut microbial load increases (106), bacterial composition shifts (266), and the abundance of certain bacteria, including Proteobacteria, increases (93). It has been proposed that an interrelationship exists between bacterial and inflammatory triggers in pregnancy. Proinflammatory cytokines (interleukin-(IL)6, tumour necrosis factor (TNF)) are increased in 3rd compared to 1st trimester pregnant stool samples, and germ-free mice colonized with 3rd trimester microbiota show increased inflammation and greater adiposity (93); similar to results in germ-free mice inoculated with microbiota from obese individuals. Despite the fact that maternal obesity results in some shifts in the maternal gut microbiome (106–109), few data exist on the signalling molecules that relate microbial abundance to inflammatory and metabolic responses during pregnancy. short-chain fatty acids (SCFAs) are key fermentation products of gut commensal anaerobes and act as signalling molecules; SCFAs promote gut motility by binding receptors (G protein-coupled receptor (Gpr)41, Gpr43) on enteric neurons, influencing gut barrier function, and stimulating leptin production in adipose tissue.

SCFAs are believed to protect against obesity-induced metabolic syndrome via Gpr41 and Gpr43 (22, 23, 28, 29). The role of maternal SCFAs in mediating maternal metabolic outcomes and fetal development is unclear. Therefore, we aimed to determine the impact of high fat diet intake prior to and during

pregnancy on the maternal intestinal microbiota and its relationship with intestinal inflammation and barrier integrity, aiming to investigate whether maternal endotoxemia is associated with placental metabolic stress and inflammation, and also whether this adverse environment impairs fetal gut development. The study was completed equally by the candidate and by Wajiha Gohir, a former MSc Student of the Sloboda Lab. Wajiha Gohir completed the animal experiments, performed maternal in vivo permeability tests and maternal and placental inflammatory profiling, and processed fecal samples for bacterial sequencing, and participated in manuscript editing. The candidate processed cecal samples for SCFA quantification, contributed to gut microbiota analyses, assisted in lipopolysaccharide (LPS), TNF, and IL6 quantification in maternal serum, prepared placental for Nanostring analysis, performed all fetal gut analyses, and wrote the main manuscript. The following is the published manuscript resulting from this work. For the purpose of this thesis, the candidate's focus was on primarily on fetal intestinal gut barrier and ER stress markers and inflammatory activity.

High-fat diet intake modulates maternal intestinal adaptations to pregnancy and results in placental hypoxia, as well as altered fetal gut barrier proteins and immune markers

Wajiha Gohir[1,2,*], Katherine M. Kennedy[1,2,*] (iD), Jessica G. Wallace[1,2], Michelle Saoi[3], Christian J. Bellissimo[1,2], Philip Britz-McKibbin[3], Jim J. Petrik[7], Michael G. Surette[1,2,4] and Deborah M. Sloboda[1,2,5,6] (iD)

[1] *Department of Biochemistry and Biomedical Sciences*
[2] *Farncombe Family Digestive Health Research Institute*
[3] *Department of Chemistry and Chemical Biology*
[4] *Department of Medicine*
[5] *Department of Obstetrics and Gynecology*
[6] *Department of Pediatrics, McMaster University, Hamilton, ON, Canada*
[7] *Department of Biomedical Sciences, University of Guelph, Guelph, ON, Canada*

Edited by: Laura Bennet & Suzanne Miller

Key points

- Maternal obesity has been associated with shifts in intestinal microbiota, which may contribute to impaired barrier function
- Impaired barrier function may expose the placenta and fetus to pro-inflammatory mediators
- We investigated the impacts of diet-induced obesity in mice on maternal and fetal intestinal structure and placental vascularization
- Diet-induced obesity decreased maternal intestinal short chain fatty acids and their receptors, impaired gut barrier integrity and was associated with fetal intestinal inflammation.
- Placenta from obese mothers showed blood vessel immaturity, hypoxia, increased transcript levels of inflammation, autophagy and altered levels of endoplasmic reticulum stress markers.
- These data suggest that maternal intestinal changes probably contribute to adverse placental adaptations and also impart an increased risk of obesity in the offspring via alterations in fetal gut development.

Abstract Shifts in maternal intestinal microbiota have been implicated in metabolic adaptations to pregnancy. In the present study, we generated cohorts of female C57BL/6J mice fed a control

Wajiha Gohir completed her MSc under the supervision of Professor Deborah Sloboda at McMaster University. She investigated maternal intestinal adaptations to pregnancy and their influences on placental development. **Katherine Kennedy** is a PhD candidate at McMaster University under the supervision of Professor Deborah Sloboda. Previously, she completed her MSc in Biology at the University of Waterloo. Currently, her research is focused on the role of the gut microbiota in placental and fetal gut development.

---

*These authors contributed equally to this work.

(17% kcal fat, $n = 10–14$) or a high-fat diet (HFD 60% kcal from fat, $n = 10–14$; *ad libitum*) aiming to investigate the impact on the maternal gut microbiota, intestinal inflammation and gut barrier integrity, placental inflammation and fetal intestinal development at embryonic day 18.5. HFD was associated with decreased relative abundances of short-chain fatty acid (SCFA) producing genera during pregnancy. These diet-induced shifts paralleled decreased maternal intestinal mRNA levels of SCFA receptor *Gpr41*, modestly decreased cecal butyrate, and altered mRNA levels of inflammatory cytokines and immune cell markers in the maternal intestine. Maternal HFD resulted in impaired gut barrier integrity, with corresponding increases in circulating maternal levels of lipopolysaccharide (LPS) and tumour necrosis factor. Placentas from HFD dams demonstrated blood vessel immaturity and hypoxia; decreased free carnitine, acylcarnitine derivatives and trimethylamine-*N*-oxide; and altered mRNA levels of inflammation, autophagy, and ER stress markers. HFD exposed fetuses had increased activation of nuclear factor-kappa B and inhibition of the unfolded protein response in the developing intestine. Taken together, these data suggest that HFD intake prior to and during pregnancy shifts the composition of the maternal gut microbiota and impairs gut barrier integrity, resulting in increased maternal circulating LPS, which may ultimate contribute to changes in placental vascularization and fetal gut development.

Corresponding author D. M Sloboda: Department of Biochemistry and Biomedical Sciences, McMaster University, 1280 Main Street West HSC 4H30A, Hamilton, Ontario L8S 4K1, Canada.
Email: sloboda@mcmaster.ca

Introduction

Maternal obesity and excess gestational weight gain are key predictors of childhood obesity and metabolic complications in adulthood. The link between maternal and offspring obesity has been extensively investigated in both clinical and experimental settings (Gluckman & Hanson, 2004). Excess intake of saturated fats and obesity are associated with an increased risk of pregnancy complications, including pre-eclampsia (Triunfo and Lanzone 2014), and may result in altered placental development and fetal overgrowth (Wallace *et al.* 2012). Although animal studies have shown that maternal high-fat diet (HFD)-induced obesity is strongly associated with offspring metabolic disease (Elahi *et al.* 2009; Howie *et al.* 2009; Morris & Chen, 2009), the signalling pathways by which maternal HFD intake, obesity or excess gestational weight gain can confer offspring metabolic dysfunction are still unclear.

The relationship between intestinal microbes and host metabolism has become one of most studied factors mediating obesity risk (Holmes *et al.* 2012) and maternal HFD has been linked to an altered offspring microbiota (Ma *et al.* 2014; Chu *et al.* 2016; Steegenga *et al.* 2017). Pregnancy shifts the abundance and type of bacteria that colonize the maternal intestine (Koren *et al.* 2012) and these shifts have been suggested to contribute to maternal metabolic adaptations and pregnancy outcomes (Koren *et al.* 2012; Goltsman *et al.* 2018). Bacterial shifts were shown to be further modified by maternal HFD and obesity (Collado *et al.* 2008; Santacruz *et al.* 2010; Gohir *et al.* 2015), although the signalling molecules that relate microbial abundance to inflammatory and metabolic responses during pregnancy have not been thoroughly investigated.

Recent data show that maternal propionate is negatively associated with maternal leptin and measures of infant weight (Priyadarshini *et al.* 2014), suggesting that shifts in the pregnant gut microbiota could influence metabolism via alterations in short-chain fatty acid (SCFA) production. SCFAs influence gut barrier function (Burger-van Paassen *et al.* 2009). Changes in the gut microbiota of male HFD fed mice are associated with increased circulating bacterial lipopolysaccharide (LPS), inducing metabolic endotoxaemia (Cani *et al.* 2008).

In the context of pregnancy, maternal metabolic endotoxaemia probably leads to placental inflammation and impaired function, contributing to an adverse early-life environment. Early-life adversity has been linked to offspring metabolic dysfunction (Elahi *et al.* 2009; Howie *et al.* 2009; Morris & Chen, 2009). More recently, because intestinal microbial interactions with the host have been shown to modulate metabolism (Nicholson *et al.* 2012), several groups have shown that early adversity is associated with changes offspring gut bacterial composition (Guo *et al.* 2018; Robertson *et al.* 2018; Soderborg *et al.* 2018; Wankhade *et al.* 2018). Because intestinal bacteria interact with and modulate gut epithelial structure, mucosal thickness, barrier integrity and immune composition, we propose that changes in offspring metabolic × gut

interactions may be downstream of altered fetal intestinal structure and development. Thus, in the present study, investigated the impact of HFD intake prior to and during pregnancy on the maternal intestinal microbiota and its relationship with intestinal inflammation and barrier integrity, aiming to investigate whether maternal endotoxaemia is associated with placental metabolic stress and inflammation, and also whether this adverse environment impairs fetal gut development.

Methods

Ethical approval

All animal procedures for the present study were approved by the McMaster University Animal Research Ethics Board (Animal Utilization Protocol 12-10-38) in accordance with the guidelines of the Canadian Council of Animal Care and the ethical principles of the *Journal of Physiology* (Grundy, 2015).

Animal model

Following 1 week of acclimation to the McMaster Central Animal Facility, 4-week-old female C57BL/6J mice (RRID:IMSR_JAX:000664) were randomly assigned to a control diet (total $n = 30$; 17% fat, 29% protein, 54% carbohydrate, 3.40 kcal g^{-1}; HT8640 Teklad 22/5 Rodent Diet; Harlan, Indianapolis, IN, USA) or HFD diet (total $n = 24$; 60% fat, 20% protein, 20% carbohydrates, 5.24 kcal g^{-1}; D12492; Research Diets Inc., New Brunswick, NJ, USA). Females were housed two per cage with food and water available *ad libitum* at a constant temperature (25 °C) under a 12:12 light/dark cycle. Following 6 weeks of dietary intervention, a subset of control ($n = 24$) and HFD ($n = 24$) females were co-housed with a control-fed C57BL/6J male and mating was confirmed by visualization of a vaginal plug, whereas the remaining control females ($n = 6$) were not mated to serve as a control non-pregnant group for intestinal barrier integrity studies. A subset of control ($n = 14$) and HFD ($n = 14$) pregnant females, as well as control non-pregnant females ($n = 6$), were used exclusively to determine maternal intestinal permeability to fluorescein isothiocyanate (FITC)-dextran as described below. All other data were collected using the remaining control ($n = 10$) and HFD ($n = 10$) pregnant females. Maternal fecal samples were collected before mating and at embryonic day (E)0.5, E10.5, E15.5 and E18.5. On E18.5, maternal serum was collected via tail vein blood, and stored at −80°C for future analyses. Pregnant mice were killed by cervical dislocation. Maternal cecal contents and intestinal tissue from the duodenum, jejunum, ileum and colon were snap-frozen in liquid nitrogen and stored at −80°C. Fetuses and placental tissues were dissected free

and fetal weights were recorded, and whole placentas from one-half of each litter (randomly chosen) were snap-frozen in liquid nitrogen or fixed in 4% paraformaldehyde. Fetal intestinal tissues were dissected free and small and large intestines were snap-frozen in liquid nitrogen and stored at −80°C. All sample sizes in the study represent a litter or dam as a biological replicate, with one female and one male being randomly selected from each litter for each tissue of interest.

Maternal microbiota profiling

DNA extraction and 16S rRNA gene sequencing. Genomic DNA was extracted from fecal samples as described previously (Whelan *et al.* 2014) with some modifications: 0.2 g of fecal material was used and additional mechanical lysis step was included using 0.2 g of 2.8 mm ceramic beads. PCR amplification of the variable 3 region of the 16S rRNA gene was subsequently performed on the extracted DNA from each sample independently using methods described previously (Bartram *et al.* 2011; Whelan *et al.* 2014). Each reaction contained 5 pmol primer, 200 mm dNTPs, 1.5 μL of 50 mm MgCl$_2$, 2 μL of 10 mg mL^{-1} bovine serum albumin (irradiated with a transilluminator to eliminate contaminating DNA) and 0.25 μL of Taq polymerase (Life Technologies, Carlsbad, CA, USA) for a total reaction volume of 50 μL. 341F and 518R rRNA gene primers were modified to include adapter sequences specific to the Illumina technology and 6 bp barcodes were used to allow multiplexing of samples as described previously. 16S DNA products of the PCR amplification were subsequently sequenced using the Illumina MiSeq platform (2×150 bp) at the Farncombe Genomics Facility (McMaster University, Hamilton, ON, Canada).

Processing and analysis of sequencing. The resultant FASTQ files were processed using a custom in-house developed pipeline for the processing of 16S rRNA gene sequencing data, as described previously (Whelan *et al.* 2014). Briefly, reads exceeding the length of the 16S rRNA variable 3 region were trimmed (cutadapt; RRID:SCR_011841), paired-end reads were aligned (PANDAseq; RRID:SCR_002705) and operational taxonomic units (OTUs) were grouped based on 97% similarity (AbundantOTU+, SCR_016527). Taxonomy was assigned using the RDP Classifier (Ribosomal Database Project; RRID:SCR_006633) against the Feb 4, 2011 release of the Greengenes reference database (Greengenes; RRID:SCR_002830). Any OTU not assigned to the bacterial domain was culled, as was any OTU to which only one sequence was assigned. This processing resulted in a total of 11,027,452 reads (mean 137,843 reads per sample; range: 59,233–249,890) and 9237 OTUs.

Taxonomic summaries were created using Quantitative Insights Into Microbial Ecology (QIIME; RRID:SCR_008249). Alpha diversity measures were calculated using the Shannon diversity index (phyloseq; RRID:SCR_013080) in R (R Project for Statistical Computing; RRID:SCR_001905) and significance was assessed by repeated measures ANOVA with gestational day and diet as factors. Measures of beta diversity were computed using the Bray–Curtis dissimilarity metric in R software and tested for whole community differences across groups using permutational multivariate analysis of variance in the adonis command (vegan; RRID:SCR_011950). These results were visualized via principal co-ordinate analysis (PCoA) ordination (ggplot2; RRID:SCR_014601). Genera that differed significantly in abundance between groups (post-adjustment $\alpha = 0.01$) were calculated using the Benjamini–Hochberg multiple testing adjustment procedure (DESeq2; RRID:SCR_015687).

Quantification of maternal intestinal short-chain fatty acids

SCFA levels were measured in maternal cecal samples by the McMaster Regional Centre of Mass Spectrometry. A weight equivalent amount of 3.7% HCl, 10 μL of internal standard and 500 μL of diethyl ether was added to each cecal sample and vortexed for 15 min. After vortexing, 400 μL of diethyl ether fecal extract was transferred to a clean 1.5 mL Eppendorf tube. In a chromatographic vial containing an insert, 20 μL of N-tert-butyldimethylsilyl-N-methyltrifluoroacetamide was added, after which 60 μL of diethyl ether fecal extract was added. The mixture was incubated at room temperature for 1 h and analysed using gas chomatography-mass spectrometry (6890N GC, coupled to 5973N Mass Selective Detector; Agilent Technologies, Santa Clara, CA, USA).

RNA extraction and cDNA synthesis

Maternal intestinal, placental, and fetal small intestinal tissue was homogenized by bead beating in 900 μL of TRIzol (Life Technologies) and centrifuged at 12,000 g for 10 min at 4°C. Supernatant was removed and added to 300 μL of chloroform. The solution was thoroughly mixed and incubated at room temperature for 3 min. Samples were centrifuged for 10 min at 12,000 g at 4°C. Aqueous phase of the sample was removed and added to 500 μL of isopropanol. Samples were mixed thoroughly, incubated for 20 min at room temperature, after which they were centrifuged at 12,000 g for 10 min at 4°C. Supernatant was removed and the resulting pellet was

washed twice with 75% ethanol. RNA was reconstituted in 20 μL of ultrapure water. RNA was quantified using the NanoDrop 2000 spectrophotometer (Thermo Scientific, Waltham, MA, USA) with NanoDrop 2000/2000c software (Thermo Scientific). The A_{260}/A_{280} and A_{260}/A_{230} ratios for all samples were >2.0 and >1.5, respectively. All RNA samples were stored at –80°C until experimentation. As a result of the small amount of starting material, fetal small intestine RNA was extracted using the RNeasy Mini Kit (Qiagen, Valanecia, CA, USA) in accordance with the manufacturer's instructions. Following extraction, 2 μg of RNA was used for cDNA synthesis using the Super-script VILO^{TM} cDNA Synthesis Kit (Life Technologies) in accordance with the manufacturer's instructions. Each reaction consisted of 4 μL of 5 × VILO^{TM} Reaction Mix, 2 μL of 10 × SuperScript Enzyme Mix, 4 μL of RNA (concentration of 250 ng μL^{-1}) and 12 μL of ultrapure water for a total reaction volume of 20 μL. Tubes were incubated in a thermocycler (C1000 Touch; Bio-Rad, Hercules, CA, USA) at 25°C for 10 min, followed by 42°C for 1 h, and then 85°C for 5 min. Complementary DNA was stored at –20°C until quantitative PCR assays were performed.

Quantitative PCR

To quantify transcript levels, quantitative PCR was performed using the LightCycler 480 II (Roche, Basel, Switzerland) and LightCycler 480 SYBR Green I Master (catalogue no. 04887352001; Roche). Primers were designed using Primer-BLAST software (blast.ncbi.nlm.nih.gov) and manufactured by Life Technologies (Table 1).

The PCR cycling conditions used for each assay were enzyme activation at 95°C for 5 min; amplification of the gene product through 40 successive cycles of 95°C for 10 s, 60°C for 10 s and 72°C for 10 s. Specificity of primers was tested by dissociation analysis and only primer sets producing a single peak were used. Each plate for a gene of interest contained a standard curve (10-fold serial dilution) generated using pooled cDNA. Each sample and standard curve point was run in triplicate. The crossing point (Cp) of each well was determined via the second derivative maximum method using LightCycler 480 Software, version 1.5.1.62 (Roche). An arbitrary concentration was assigned to each well based on the standard curve Cp values by the software. The geometric mean of housekeeping genes was determined to use as reference gene value for each intestinal sample. B-actin, cyclophilin and hypoxanthine ribosyltransferase (HPRT) were used as housekeepers for maternal intestines; cyclophilin and HPRT for fetal intestines; and β-actin and UBC for placentae. Housekeeper mRNA levels did not differ significantly between groups. Relative mRNA levels for each sample were determined by dividing the

Table 1. Primer sequences

Function	Gene	Forward primer	Reverse primer	Accession number
Housekeeper	β-actin	ACGCAGCTCAGTAACAGTCC	AGATCAAGATCATTGCTCCCCT	NM_007393.5
	Cyclophilin	CTTCGAGCTGTTTGCAGA	TGGCGTGTAAAGTCACCAC	NM_008907.1
	Hprt	CAGTCCCAGCGTCGTGATTA	TCGAGCAAGTCTTTCAGTCCT	NM_013556.2
	Ubc	CAAAGCCCCTCAATCTCTGGA	AGATCTGCATCGTCTCTCTCAC	NM_019639.4
SCFA signalling	Gpr41	GTCCAATACTCTGCATCTGTGAC	AGTCCCACGAGGAACACCAA	NM_001033316.2
	Gpr43	ACTTGCCCAAGGAGTTCTGG	AGCTGTCTGCTCTTCACCAC	NM_146187.4
Gut barrier	Zo1	GAGAGACAAGATGTCCGCCA	CCATTGCTGTGCTCTTAGCG	NM_009386.2
	Occludin	ATGTCCGGCCGATGCTCTC	TTTGGCTGCTCTTGGGTCTGTAT	NM_001360538.1
	Muc2	GAAGCCAGATCCCGAAACCA	GAATCGGTAGACATCGCCGT	NM_023566.3
Inflammatory signalling	Tlr2	ATGTCGTTCAAGGAGGTGCG	ATTTGACGCTTTGTCTGAGGTTT	NM_011905.3
	Tlr4	TCTGGGGAGGCACATCTTCT	TGCTCAGGATTCGAGGCTT	NM_021297.3
	Nfkb1	CTGCTCAGGTCCACTGTC	TTGCGGAAGGATGTCTCCAC	NM_008689.2
	Tnf	GTAGCCCACGTCGTAGCAAA	TTGAGATCCATGCCGTTGGC	NM_013693.3
	Il6	GGGACTGATGCTGGTGACAA	ACAGGTCTGTTGGGAGTGGT	NM_031168.2
Immune cell marker	Cd4	CTCCTTCGGCTTTCTGGGTT	GCCTGGCGCTGTTGGT	NM_013488.3
	F4/80	TTGTGGTCCTAACTCAGTCTGC	AGACACTCATCAACATCTGCG	NM_010130.4
	Cd68	TGTTCAGCTCCAAGCCCAAA	GTACCGTCACAACCTCCCTG	NM_001291058.1
ER stress	Grp78	TTCAGCCAATTATCAGCAAACTCT	TTTTCTGATGTATCCTCTTCACCAGT	NM_001163434.1
	Atf4	GGGTTCTGTCTTCCACTCCA	AAGCAGCAGAGTCAGGCTTTC	NM_009716.3
	Chop	CCACCACACCTGAAAGCAGAA	AGGTGAAAGGCAGGGACTCA	NM_007837.4
	sXbp1	CTGAGTCCGAATCAGGTGCAG	GTCCATGGGAAGATGTTCTGG	NM_001271730.1

geometric mean of the triplicate for each sample by that sample's reference gene value.

Nuclear factor-kappa B (NF-κB) activity and western blot analysis

Maternal and fetal intestinal tissue was homogenized with ceramic beads using a Precellys 24 homogenizer (Bertin Technologies SAS, Montigny-le-Bretonneux, France) at 5 m s^{-1} for 60 s in buffer containing 50 mM KH$_2$PO$_4$, 5 mM EDTA, 0.5 mM dithiothreitol and 1.15% KCl with cOmplete protease inhibitor tablets (Roche). Protein concentrations were determined using the BCA method in the supernatant after homogenates were centrifuged for 10 min at 10,000 g at 4°C. NF-κB activity was measured in maternal and fetal intestinal homogenates using the TransAM^{TM} NF-κB p65 Transcription Factor Assay Kit in accordance with the manufacturer's instructions (catalogue no. 40096; Active Motif, Carlsbad, CA, USA). Western blot analyses were performed on 15 μg of protein using SDS-PAGE of varying percentage depending on the protein of interest. Each western blot analysis used a separate protein aliquot and membrane for each protein of interest. After transfer onto or polyvinylidene difluoride membrane, blots were blocked for 1 h at room temperature in 5% BSA Tris-Tween 20 and incubated with the following primary antibodies overnight: grp78 (dilution 1:2000; Abcam; catalogue no. ab21685; RRID:AB_2119834), phospho-PERK (dilution 1:500; Thermo Fisher Scientific;

catalogue no. MA5-15033; RRID:AB_10980432), PERK (dilution 1:1000; Cell Signaling Technology; catalogue no. 3192; RRID:AB_2095847), phospho-eIF2α (dilution 1:1000; Cell Signaling Technology; catalogue no. 9721; RRID:AB_330951), eIF2α (dilution 1:1000; Cell Signaling Technology; catalogue no. 9722; RRID:AB_2230924), occludin (dilution 1:1000; Abcam; catalogue no.168986; RRID: AB_2744671), phospho-JNK (dilution 1:500; Abcam; catalogue no. ab124956; RRID:AB_10973183), JNK (dilution 1:500; Abcam; catalogue no. ab179461; RRID: AB_2744672), β-actin (dilution 1:5000; Cell Signaling Technology; catalogue no. 5125; RRID:AB_1903890). Blots were washed in Tris-Tween 20 and incubated with HRP-conjugated goat anti-rabbit IgG secondary antibody (Abcam; catalogue no. ab6721; RRID: AB_955447) for 1 h at room temperature. Blots were developed using BioRad Clarity^{TM} Western enhanced chemiluminescence (ECL; Bio-Rad, 170–5061), images captured using a Bio-Rad ChemiDoc MP System and densitometric quantification was carried out using ImageLab software (Bio-Rad) relative to β-actin internal controls.

Maternal intestinal barrier integrity

A FITC-dextran assay was used to measure *in vivo* intestinal permeability, as described previously (Thevaranjan *et al*. 2017), to assess maternal intestinal barrier function prior to and during pregnancy. On

E18.5, a baseline blood sample was collected via tail vein bleed from dams. Plasma was isolated and stored at 4°C protected from direct light until analysis. Each dam was administered 150 μL of 80 mg mL^{-1} FITC labelled dextran (molecular mass 4 kDa; Sigma Aldrich, St Louis, MO, USA) by oral gavage. After 4 h, a second post-gavage blood sample was collected via tail vein bleed and plasma was isolated. Fluorescence intensity of maternal plasma was measured on a plate reader (BioTek, Oakville, ON, Canada) with an emission 530 nM and excitation at 485 nM. Intestinal barrier function was quantified by subtracting the baseline fluorescence values from the post-gavage fluorescence values in each dam and was expressed as relative fluorescence units.

Biochemical assays

LPS. An in-house colourimetric reporter bioassay was used for the quantification of NF-κB activation by the pattern recognition receptor Toll-like receptor (TLR)-4 in response to LPS. This assay was generated by the Bowdish lab at McMaster University (Verschoor *et al.* 2015). Briefly, an LPS-responsive reporter cell line was generated by transiently transfecting the pNifty2-SEAP plasmid, containing NF-κB transcription factor binding sites and a secreted alkaline phosphatase (SEAP) reporter gene, into a commercially available HEK293 cell line (RRID: CVCL_Y406) expressing TLR4, MD2 and CD14 (Invivogen, San Diego, CA, USA). Cells were seeded at 4×10^3 per well in a 96-well plate in Complete Dulbecco's modified Eagle's medium (DMEM) for 24 h. Serum samples were diluted 1:5 in PBS, then 1:1 in sterile water, and heat inactivated at 75°C for 5 min. Complete DMEM media was removed prior to the addition of heat-inactivated plasma in HEK Blue Detection media (Invivogen); 10 μL of sample and 190 μL of HEK Blue Detection media was added into the appropriate wells. Absorbance was measured at 630 nm, 72 h after stimulation, and background levels were subtracted from relative absorbance units. Standard curves generated using different doses of purified LPS were used to calculate the relative amount of LPS in serum.

Tumour necrosis factor receptor (TNF) and interleukin-6. Maternal serum TNF and interleukin-6 levels were measured using Milliplex Map Mouse Cytokine Magnetic Bead Panel (MCYTOMAG-70K; EMB Millipore, Darmstadt, Germany), which uses the Luminex xMAP (Luminex Corp., Austin, TX, USA) detection method. The protocol was followed in acordance with the manufacturer's instructions.

Immunohistochemistry

Paraformaldehyde (4%) fixed placentas were processed, embedded in paraffin and sectioned at 4 or 8 μm. To inhibit endogenous peroxidase activity, placental sections were immersed for 10 min in 30% aqueous hydrogen peroxide, except for F4/80 and activated caspase-3 (AC3), which were immersed for 25 min in 0.5% or 1.5% hydrogen peroxide in methanol, respectively. Antigen retrieval was performed by incubating tissues in 10 mM sodium citrate buffer with Tween, pH 6.0, at 90°C for 12 min, or by incubation with 1 mg mL^{-1} trypsin in ddH$_2$O (T7168; Sigma-Aldrich) for 12 min at 37°C for F4/80 staining. Non-specific binding was blocked with 5% bovine serum albumin for 10 min or 60 min (F4/80 and AC3) at room temperature and sections were incubated overnight at 4°C with the following primary antibodies: CD31 (dilution 1:200; Abcam; catalogue no. ab24590; RRID:AB_448167), α-smooth muscle actin (α-SMA) (dilution 1:400; Santa Cruz Biotechnology; catalogue no. sc-32251; RRID:AB_262054), vascular endothelial growth factor (VEGF) (dilution 1:400; Santa Cruz Biotechnology; catalogue no. sc-152; RRID:AB_2212984), VEGFR2 (dilution 1:400; Santa Cruz Biotechnology; catalogue no. sc-6251; RRID:AB_628431), carbonic anhydrase-IX (dilution 1:600; Abcam; catalogue no. ab15086; RRID:AB_2066533), F4/80 (dilution 1:100; Abcam; catalogue no. ab6640; RRID:AB_1140040), and AC3 (Cell Signaling Technology; catalogue no. 9661; RRID:AB_2341188). The following day, tissue sections were incubated at room temperature for 2 h with anti-mouse biotinylated secondary antibody (Sigma-Aldrich Canada Ltd) or for 1 h with anti-rat (BA-4001; Vector Laboratories, Burlingame, CA, USA) or anti-rabbit (PK6101; Vector Laboratories) secondary antibody. Biotinylated secondary antibodies were further incubated with ExtrAvidin (Sigma-Aldrich) or HRP conjugated streptavidin (PK6101; Vector Laboratories) for 1 h. Visualization of biotinylated antibody labelling was performed by chromogenic development using 3,3'-diaminobenzidine (D4293; Sigma-Aldrich), and all sections were counterstained with Gills 2 hematoxylin (GHS216; Sigma-Aldrich). For quantification of F4/80 and AC3 staining, whole tissue sections were scanned using an Eclipse Ni microscope (Nikon, Tokyo, Japan) at 10× magnification and a region of interest was defined around either the labyrinth compartment (F4/80) or total placenta (AC3). Chromogen detection was performed using an automated threshold function using NIS Image Analysis software, version 4.30.02 (Nikon; RRID:SCR_014329). For all other experiments, measurements were taken in six fields of view per section at 250× magnification and image analyses were performed using an BX-61 microscope (Olympus, Tokyo, Japan) and integrated morphometry software (MetaMorph Microscopy Automation and Image

Table 2. Genes in NanoString nCounter CodeSet

Metabolism	Inflammation and immune cell			ER stress, apoptosis and autophagy	EMT, angiogenesis and vascular remodelling		Other
Acc1	Arginase 1	Emr1	Mcp1	Akt	Acta2	Sfrp1	COll
Enpp1	Arginase 2	Foxp3	Myd88	Ap1	Angiopoeitin 1	Sfrp2	Fn1
Fas	B2M	Gp130	Ngf	Ask1	Angiopoeitin 2	Sfrp4	Gata4
Gapdh	Baff	Ido1	Nfkb1	Atf4	Bdnf	Snail1	Mmp1
Gk	C1Q-C	Ifn-γ	Nlrp3	Atf6	Bmp2	Snail2	Mmp14
Irs-1	Ccl20	Il-10	Nod1	Bad	Bmp4	Scf	Mmp2
Irs-2	Ccr3	Il-13	Nod2	Bak1	Bmp7	Tie	Mmp3
Pcsk9	Ccr4	Il-15	Stat-3	Bax	Bmpr1A	Timp1	Mmp7
Pgk1	Ccr5	Il-17A	Taok3	Bbc3	Bmprii	Timp3	Mmp9
Pparg	Ccr8	Il1α	Tgfb1	Bcl2	C-Myc	Trka	Polr2A
Ppia	Cd103	Il-1B	Tgfbr1	Bcl2L11	Collagen α (III)	Trkb	Rab-9
Srebp1-C	Cd11B	Il-2	Tlr2	Beclin-1	Dkk1	Trkc	RplpP2
	Cd11C	Il-21	Tlr4	Bid	E-Cadherin	Trp53	Tac1
	Cd23	Il-22	Tnf	Bif-1	Fzd1	Twist	Tacr1
	Cd25	Il-23	Traf2	Calnexin	Fzd3	Vegf	Tbp
	Cd4	Il-4	Traf6	Calreticulin	Gremlin	Vip	Trpv1
	Cd44	Il-6		Chop	Hmox1	Vpac1	
	Cd68	Il-6Rα		Edem1	Lgals1	Vpac2	
	Cd8	Inos		Faslg	Lgals3	Wnt1	
	Cgrp	Ip10		Fkbp13	Lgals9	Wnt10B	
	Csf2	Kcnn4		Fkbp65	Loxl2	Wnt11	
	Cxcl1	Lys6G		Grp78	Lrp5	Wnt2	
	Cxcl17	Cd206		Hsp27	Lrp6	Wnt3A	
	Cxcr3	Mapk14		Hsp47	Osm	Wnt4	
	Cxcr6	Mapk8		Ntf3	Osmr-β	Wnt5A	
				Xbp1	Pdi	Wnt7B	
				Vps-15	Phlda1	Wnt8A	
				Vps-34	Ror2		

Analysis Software; RRID:SCR_002368). All the image analyses were performed by an investigator who was blind to the study groups.

NanoString

In a subset of placental samples ($n = 4$ per sex per group), a custom nCounter Reporter CodeSet designed by Dr. Kjetil Ask (Department of Medicine, McMaster University) was used to analyse placental gene expression using NanoString nCounter gene expression system (Table 2). This CodeSet included 184 genes that were involved in inflammation, immunity, apoptosis and ER stress. Incubation of 100 ng of total RNA was performed overnight at 65°C with nCounter Reporter CodeSet, Capture ProbeSet and hybridization buffer. Post-hybridization, the samples were processed using the nCounter Prep-station and nSolver Analysis software, version 2.5, was used to normalized raw NanoString data to six housekeepers:

UBC, TUBA1A, HPRT, IPO8, GusB and β-actin. These analyses were performed in a subset of placenta to uncover novel signalling pathways affected by maternal HFD.

Placental metabolomics

A subset of frozen placental tissue samples ($n = 7–9$ per sex per group) was lyophilized, powdered and weighed (3–5 mg). A modified, two-step Bligh–Dyer extraction was employed to extract polar, hydrophilic metabolites from the placental tissue. The extraction procedure consisted of adding 64 μL of ice cold methanol: chloroform (1:1) followed by 26 μL of de-ionized water to enable phase separation. After vortexing for 10 min and centrifugation at 2000 *g* at 4°C for 20 min, the upper aqueous layer was obtained. A second extraction on the residual placental tissue was performed by adding another aliquot of 32 μL of methanol:deionized (1:1) water, followed by the same vortexing and centrifugation procedure described above.

The second upper aqueous layer was then transferred and combined with the first aliquot of aqueous layer from the first round of extraction for a total volume of ~80 μL of placental tissue extract. Prior to analysis, 5 μL of 3-chloro-L-tyrosine and 2-naphthalenesulphonic acid were added to 20 μL of placental tissue extract resulting in a final concentration of 25 μM for each internal standard when using both positive and negative mode multisegment injection-capillary electrophoresis-mass spectrometry (MSI-CE-MS) analysis, respectively (Macedo *et al.* 2017). Untargeted polar metabolite profiling of placental extracts was performed using MSI-CE-MS as a high throughput platform for metabolomics based on serial injection of seven or more samples within a single run (Kuehnbaum *et al.* 2013; Yamamoto *et al.* 2016). All MSI-CE-MS experiments were performed on an Agilent G7100A CE system (Agilent Technologies) equipped with a coaxial sheath liquid (Dual EJS) Jetstream electrospray ion source with heated nitrogen gas to an Agilent 6230 time-of-flight mass spectrometer. Separations were performed on a 120 cm long uncoated fused silica capillary (Polymicro Technologies, Phoenix, AZ, USA) with an inner diameter of 50 μm, using an applied voltage of 30 kV at 25°C. The background electrolyte consisted of 1 M formic acid with 15% *v/v* acetonitrile (pH 1.80) in positive ion mode and 50 mM ammonium bicarbonate (pH 8.50) in negative ion mode, for the separation and detection of cationic and anionic metabolites, respectively. Each experimental run consisted of six sequential injections of paired (i.e. from the same litter) male and female tissue extracts from control and HFD placentas in addition to a quality control (QC) consisting of a pooled placental extract sample ($n = 7$) to assess system drift and overall technical variance (DiBattista *et al.* 2017). Overall, fifty-one metabolites from placental extracts were consistently detected in the majority of specimens analysed ($>75\%$) at the same time as having adequate technical precision as determined by a relative standard deviation (RSD) of $<40\%$ based on repeated analysis of the pooled quality control throughout the study (Macedo *et al.* 2017). All experimental data were integrated and analysed using Agilent MassHunter Qualitative Analysis B.07.00 (RRID:SCR_015040). Integrated ion response ratios were measured for all placental metabolites relative to their corresponding internal standard and subsequently normalized to the dried mass of each placenta analysed (mg).

Statistical analysis

Maternal gestational weight gain was analysed using repeated measures two-way ANOVA, with maternal diet and gestational age as factors. Maternal intestinal mRNA levels and NF-κB activity were analysed by two-way ANOVA with maternal diet and intestinal section as factors. Maternal serum TNF and circulating LPS levels were analysed using unpaired *t* tests with Welch's correction. Intestinal permeability was analysed by the Mann–Whitney *U* test. SCFA concentrations were analysed by *t* tests with Holm–Sidak correction for multiple comparisons. Data used for all *t* tests passed the Kolmogorov–Smirnov test for normality. For all analyses of placentae and fetal intestines, the sample size represents the number of litters analysed where a representative male and female were analysed from each litter. Placental NanoString data, placental and fetal gut quantitative PCR data, fetal small intestinal NF-κB activity, and placental immunohistochemistry data were analysed using two-way ANOVA, with maternal diet and fetal sex as factors. Bonferroni *post hoc* analyses were used for multiple comparisons where appropriate. Supervised multivariate statistical analysis based on partial least square-discriminant analysis (PLS-DA) was applied for variable selection and ranking significant metabolites [variable importance in projection (VIP) score >1.0] associated with placental metabolomic changes as a function of diet and sex (Chong *et al.* 2018). Adding litter size to the statistical models as a covariate did not change the conclusions regarding effects of maternal diet. All data were also analysed using Prism, version 6.01 (GraphPad Software, San Diego, CA, USA).

Data availability

Data are available from the authors upon request.

Results

Maternal and fetal phenotype

HFD fed females were significantly heavier than controls throughout gestation (main effect of diet, $P = 0.011$): E0.5 mean difference = 2.59 (95% CI = –0.12 to 5.31); E10.5 mean difference = 3.35 (95% CI = 0.63–6.06); E15.5 mean difference = 2.66 (95% CI = –0.058 to 5.38); E18.5 mean difference = 2.53 (95% CI = –0.19 to 5.24; Control, $n = 9$; HFD, $n = 10$). At E18.5, maternal fasting blood glucose and serum insulin did not differ between groups ($P = 0.61$ and $P = 0.54$, respectively). Maternal HFD did not detectably alter litter size (Control, 95% CI = 6.28–8.60; HFD, 95% CI = 7.14–8.46; $P = 0.55$), fetal weight ($P = 0.73$) or fetal sex ratio (ANOVA, $P = 0.94$) (Fig. 1).

Pregnancy and HFD intake induce shifts in intestinal microbiota

Alpha diversity differed across gestation and between dams (Shannon index; $P = 0.01$ and $P = 0.008$, respectively) but

did not differ by diet (data not shown). At E18.5, the abundance of 29 microbial genera differed significantly between control and HFD dams (Fig. 2*A* and Table 3). Community composition of the maternal gut microbiota visualized by PCoA using the Bray–Curtis dissimilarity metric shows a distinct separation between control and HFD samples (Fig. 2*B*). Consistent with our previous study (Gohir *et al.* 2015), the gut microbiota of HFD fed females was significantly different from control females before pregnancy (adonis: $r^2 = 0.496$, $P = 0.002$) and at E0.5 ($r^2 = 0.517$, $P = 0.005$), E10.5 ($r^2 = 0.562$, $P = 0.004$), E15.5 ($r^2 = 0.550$, $P = 0.007$) and E18.5 ($r^2 = 0.532$, $P = 0.003$). Analysis of whole community differences across all samples found a significant effect of maternal diet ($r^2 = 0.447$, $P = 0.001$) and a small but significant effect of pregnancy timepoint (adonis: $r^2 = 0.0736$, $P = 0.025$). HFD dams had a higher relative abundance of *Akkermansia*, a mucin degrader and *Clostridium* (Family *Clostridiaceae*) (Fig 2*C*). The majority of genera within the order *Clostridiales* differing by HFD were decreased (Table 3), including butyrate-producing genera *Lachnospira* and *Ruminococcus* (Morrison and Preston 2016) (Fig. 2*C*). Consistent with a decrease in

Lachnospira and *Ruminococcus*, maternal cecal butyrate levels also tended to be lower in HFD dams compared to controls at E18.5 ($P = 0.061$) (Fig. 2*D*), as were intestinal transcript levels of SCFA receptor GPR41 (main effect of diet, $P = 0.001$) (Fig. 2*D*). Intestinal transcript levels of GPR43 were unchanged (data not shown).

HFD alters intestinal inflammatory and immune cell marker transcript levels

We found HFD fed dams had increased intestinal transcript levels of T-cell marker CD4 (main effect of diet, $P = 0.0013$) (Fig. 3*A*), predominantly in the duodenum and ileum ($P = 0.0363$ and $P = 0.0350$, respectively). HFD fed dams had increased transcript levels of monocyte lineage marker *Cd68* (main effect of diet, $P = 0.0008$), whereas levels of the macrophage maturity marker *F4/80* was increased in the ileum ($P = 0.05$) (Fig. 3*A*). To determine whether increases in immune cell markers were associated with intestinal inflammation, we measured transcripts of key pattern recognition receptors involved in immune-related inflammatory signalling. HFD fed
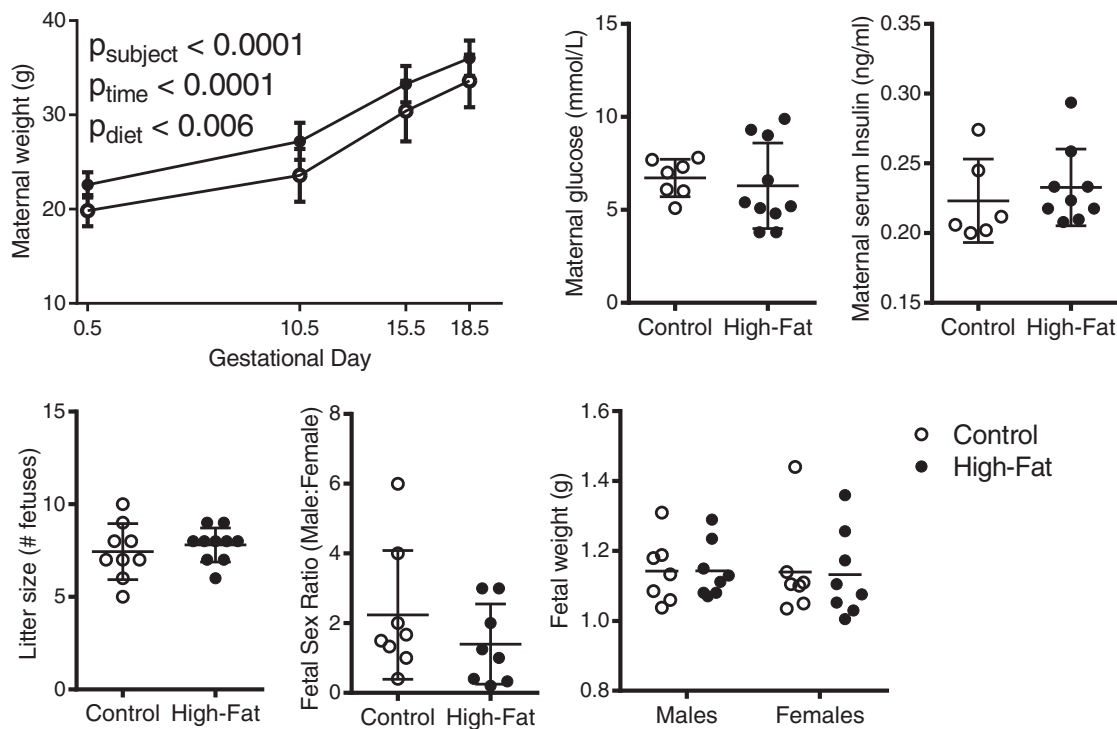
Figure 1. Maternal and pregnancy phenotype
High-fat dams were heavier than controls throughout pregnancy [ANOVA; main effect of diet, $P = 0.0061$; main effect of subject (matching), $P < 0.0001$, main effect of gestational day, $P < 0.0001$] but demonstrate that similar serum glucose and insulin levels and litter size, sex ratio and fetal weight are unaltered by a HFD. Data are the mean ± SD; individual data points are shown where appropriate. Control, $n = 6$–9; High-fat $n = 8$–10. *$P < 0.05$.

dams had increased intestinal mRNA levels of *Tlr2* (main effect of diet, $P = 0.006$) and *Il6* (main effect of diet, $P = 0.035$), particularly in the duodenum ($P = 0.0004$ and $P = 0.018$, respectively). *Tlr4* levels were increased in the colon ($P = 0.05$) (Fig. 3*B*). Intestinal NF-κB activation did not differ between HFD and control dams (main effect of diet, $P = 0.17$; data not shown).

HFD impairs maternal intestinal barrier integrity

To determine whether microbial shifts were associated with functional intestinal changes, we assessed intestinal barrier integrity. Pregnancy increased maternal gut permeability to FITC-dextran ($P = 0.0015$) compared to non-pregnant females and, although HFD fed dams had higher mean FITC dextran levels compared to control
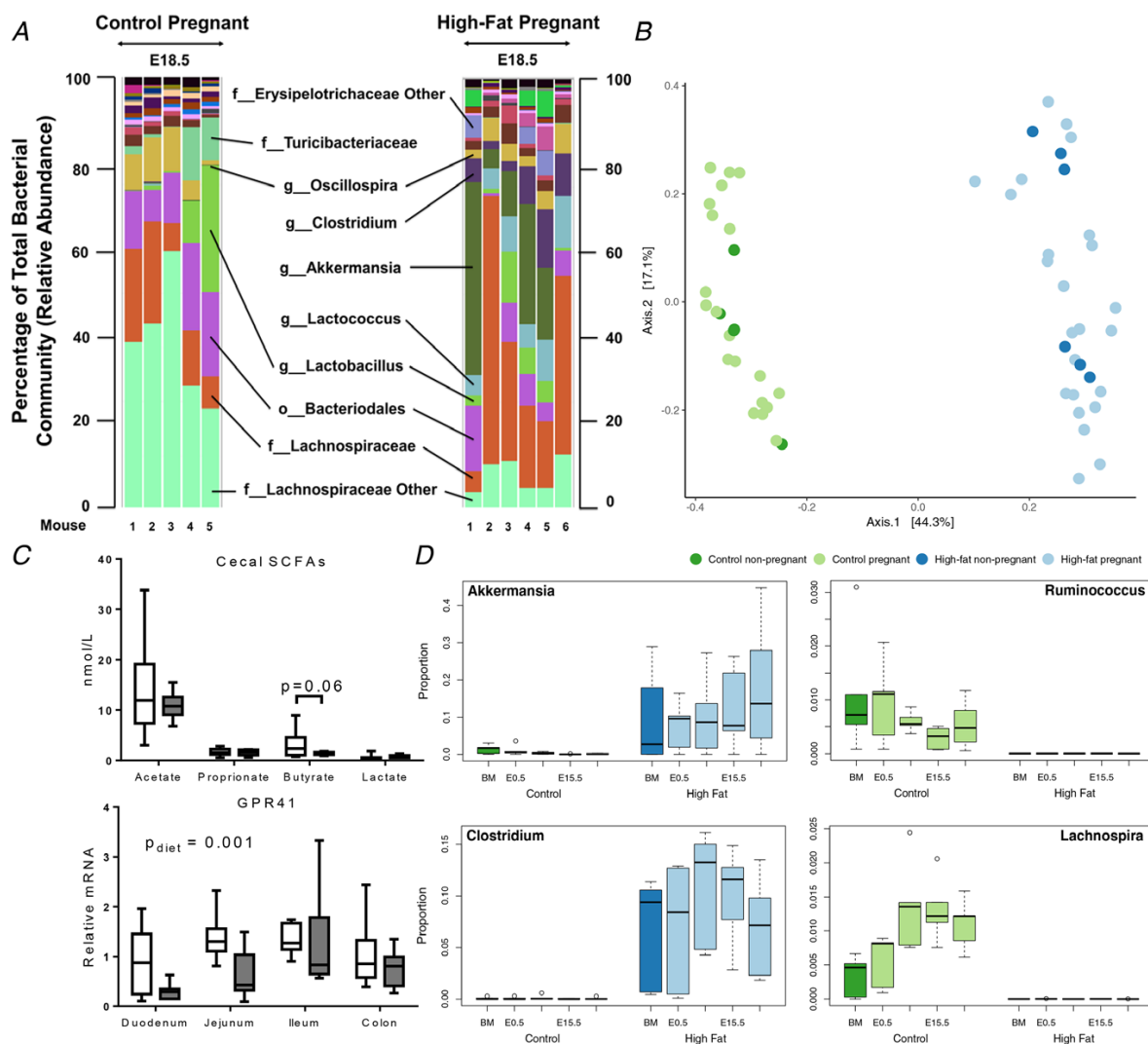
Figure 2. Maternal diet and pregnancy interact to promote shifts in the maternal gut microbiota
A, relative abundance of the top 25 most abundant taxa for each control ($n = 5$) and high-fat ($n = 6$) dam at E18.5 with significantly different taxa highlighted (f, family; o, order; g, genus). *B*, PCoA using the Bray–Curtis dissimilarity metric showed a distinct separation of gut microbial communities as a result of a maternal diet (adonis $P = 0.001$; $n = 5$; HF, $n = 6$). *C*, cecal SCFAs were measured by gas chomatography-mass spectrometry and relative mRNA levels of SCFA receptor *Gpr41* are shown in control (open bars, $n = 9$) and high-fat dams (grey bars, $n = 10$). Significance assessed by Bonferroni-adjusted *post hoc* test (*$P < 0.05$ compared to control). *D*, maternal HFD was associated with increased *Akkermansia* ($P = 0.0185$) and *Clostridium* ($P = 0.0014$) and decreased *Ruminococcus* ($P = 0.0018$) and *Lachnospira* ($P < 0.0001$) relative abundances across all pregnancy time points (two-way ANOVA; C, $n = 5$, HF $n = 6$).

Table 3. Microbial taxa differing in abundance between control and high-fat dams at E18.5 by DESeq2

Phylum	Class	Order	Family	Genus	log2 FC	*P* value
Actinobacteria	Actinobacteria	Bifidobacteriales	Bifidobacteriaceae	Bifidobacterium	−5.58	2.42×10^{-13}
Actinobacteria	Actinobacteria	Coriobacteriales	Coriobacteriaceae	Adlercreutzia	−1.71	0.00608
Actinobacteria	Actinobacteria	Coriobacteriales	Coriobacteriaceae	Olsenella	5.58	0.000139
Firmicutes	Bacilli	Bacillales	Staphylococcaceae	Staphylococcus	−1.71	0.000422
Firmicutes	Bacilli	Lactobacillales	Enterococcaceae	Enterococcus	3.56	2.74×10^{-18}
Firmicutes	Bacilli	Lactobacillales	Streptococcaceae	Lactococcus	8.14	1.74×10^{-88}
Firmicutes	Clostridia	Clostridiales	Clostridiaceae	Clostridium	6.09	7.66×10^{-35}
Firmicutes	Clostridia	Clostridiales	Clostridiales	Eubacterium	1.64	5.93×10^{-7}
Firmicutes	Clostridia	Clostridiales	Eubacteriaceae	Anaerofustis	−5.25	3.11×10^{-5}
Firmicutes	Clostridia	Clostridiales	Lachnospiraceae	Anaerostipes	−6.33	2.55×10^{-17}
Firmicutes	Clostridia	Clostridiales	Lachnospiraceae	Bacteroides	−2.02	0.00733
Firmicutes	Clostridia	Clostridiales	Lachnospiraceae	Blautia	−1.74	3.15×10^{-10}
Firmicutes	Clostridia	Clostridiales	Lachnospiraceae	Clostridium	−1.46	2.88×10^{-9}
Firmicutes	Clostridia	Clostridiales	Lachnospiraceae	Coprococcus	−8.26	1.27×10^{-28}
Firmicutes	Clostridia	Clostridiales	Lachnospiraceae	Dorea	2.85	0.000570
Firmicutes	Clostridia	Clostridiales	Lachnospiraceae	Lachnobacterium	−2.08	0.00139
Firmicutes	Clostridia	Clostridiales	Lachnospiraceae	Lachnospira	−10.44	2.01×10^{-137}
Firmicutes	Clostridia	Clostridiales	Lachnospiraceae	Moryella	−5.80	2.71×10^{-34}
Firmicutes	Clostridia	Clostridiales	Peptostreptococcaceae	Peptostreptococcus	−5.89	$1.31E \times 10^{-7}$
Firmicutes	Clostridia	Clostridiales	Ruminococcaceae	Clostridium	−1.32	0.000376
Firmicutes	Clostridia	Clostridiales	Ruminococcaceae	Ethanoligenens	−7.22	8.86×10^{-7}
Firmicutes	Clostridia	Clostridiales	Ruminococcaceae	Eubacterium	−9.81	9.01×10^{-36}
Firmicutes	Clostridia	Clostridiales	Ruminococcaceae	Oscillospira	−0.87	0.00274
Firmicutes	Clostridia	Clostridiales	Ruminococcaceae	Ruminococcus	−10.07	1.70×10^{-106}
Proteobacteria	Gammaproteobacteria	Pseudomonadales	Moraxellaceae	Moraxella	−2.62	3.59×10^{-8}
Tenericutes	Erysipelotrichi	Erysipelotrichales	Erysipelotrichaceae	Clostridium	5.55	7.87×10^{-19}
Tenericutes	Erysipelotrichi	Erysipelotrichales	Erysipelotrichaceae	Coprobacillus	2.69	2.07×10^{-9}
Tenericutes	Mollicutes	Anaeroplasmatales	Anaeroplasmataceae	Anaeroplasma	−10.46	$9.54E \times 10^{-75}$
Verrucomicrobia	Verrucomicrobiae	Verrucomicrobiales	Verrucomicrobiaceae	Akkermansia	4.16	1.33×10^{-10}

dams, this difference was not statistically significant ($P = 0.055$) (Fig. 4). HFD was also associated with decreased transcript levels of tight junction protein zonula occludens-1 (*Zo1*; main effect of diet, $P = 0.0003$). Occludin mRNA levels, however, were increased in the duodenum and ileum ($P = 0.035$ and $P = 0.0001$, respectively) (Fig. 4) in HFD dams compared to controls (main effect of diet × section interaction, $P < 0.0001$). Consistent with impaired gut barrier integrity, serum levels of LPS and TNF were higher in HFD dams compared to controls at E18.5 ($P = 0.0065$ and $P = 0.024$, respectively) (Fig. 4).

Maternal HFD results in placental hypoxia and altered placental vascularization

Increases in circulating inflammatory factors as a result of maternal HFD intake result in placental hypoxia (Fernandez-Twinn *et al.* 2017), which impacts placental vascularization (Hayes *et al.* 2012; Li *et al.* 2013), potentially by altering macrophage activation (Zhao *et al.* 2018). Consistent with these observations, we found increased immunostaining of carbonic anhydrase IX, a placental hypoxia marker, in male ($P < 0.0001$) and female ($P < 0.0001$) placentas derived from HFD fed dams (Fig. 5). This increase was associated with increased immunostaining of VEGF and its receptor

VEGFR2 (Fig. 5). Using immunostaining of an endothelial cell marker (CD31) as a measure of vessel density, we found increased CD31 in HFD placentas ($P < 0.0001$). A decrease in percentage of CD31+ve vessels associated with α-SMA+ve pericytes was used as an indicator of decreased blood vessel maturity ($P < 0.0001$) (Fig. 5). Although placental labyrinth immunostaining of macrophage maturity marker F4/80 was not significantly increased by maternal HFD (main effect of diet, $P = 0.089$; transcript levels were also not different, $P = 0.12$), we found increased placental immunostaining of apoptosis-marker AC3 with maternal HFD (main effect of diet, $P = 0.030$) (Fig. 5).

Maternal HFD intake alters markers of placental growth and development

We used the NanoString nCounter system to explore modulators of placental hypoxia in an untargeted manner. Shifts in placental macrophages, neutrophils and T cells have previously been associated with pregnancy complications, including preeclampsia (Wallace *et al.* 2014). Maternal HFD was associated with increased transcript levels of *Cd4* ($P = 0.018$) and *Il10* ($P = 0.017$) (Fig. 6A). *Arginase 1* mRNA levels were suppressed by maternal HFD, resulting in a decreased placental *Arg1:Nos2* ratio ($P = 0.046$) (Fig. 6A). Placental transcript

levels of inflammatory receptors were largely unaltered by maternal HFD, including Toll like receptors (*Tlr*2 and *Tlr4* (data not shown). Notably however, placental adapter protein transcript levels were significantly decreased by maternal HFD, including TNF receptor-associated factor 6 (*Traf6*), myeloid differentiation primary response 88 (*MyD88*), *Mapk8* and *Stat3* (Fig. 6*B*), without any changes to proinflammatory cytokine transcript levels (*Nfkb1*) (Fig. 6*B*). Immune cells (B and T lymphocytes and monocytes) express TrkC and it has been suggested that placental NT3 modulates inflammatory cell migration to the placenta (Casciaro *et al.* 2009). We found that maternal HFD intake was associated and a significant increase in levels of the NT3 receptor *TrkC* (diet, $P < 0.001$) (Fig. 7*A*). This is consistent with our observations that *Cd4* and *Cd25* transcripts were increased in HFD placentas.

Placental hypoxia is often associated with poor implantation and impairments in epithelial-mesenchymal transition (EMT) and maternal vessel remodelling early in pregnancy (Aplin, 2000; Davies *et al.* 2016). Transcript levels of factors associated with EMT, cell migration, invasion and vascular remodelling were decreased in placentas from HFD pregnancies, including bone morphogenetic protein receptor 2 (*Bmpr2*), *Wnt8a* and *Lrp5* (Fig. 7*A*). These decreases are consistent with our

observation of placental hypoxia and reduced αSMA immunostaining in high-fat placental tissue.

Transcript levels of ER stress factors X-box binding protein 1 (*Xbp1*) and activating transcription factor 4 (*Atf4*), as well as the molecular chaperone calnexin, were decreased with maternal HFD intake (Fig. 7*B*). Consistent with these reductions, mRNA levels of *Vps31* and *34*, which regulate the clearance of protein aggregates, were also decreased with maternal HFD, whereas levels of *Beclin1*, a central mediator in autophagy (Kang *et al.* 2011) were not statistically different (Fig. 7*B*). Transcript levels of pro-survival *Bcl2L1L* were decreased and pro-apoptotic and *Bcl2* was increased in placenta from HFD pregnancies (Fig. 7*B*), consistent with our observed increases in AC3 immunostaining in the placenta.

Maternal HFD alters placental metabolomics

The metabolomes of HFD and control placentas were well discriminated by PLS-DA 2D (8). We observed slightly more biological variation in metabolite levels in control placentas (median RSD = 57%; females = 78%, males = 35%) compared to HFD (median RSD = 42%; females: 59%, males = 26%), whereas technical precision was acceptable based on repeated analysis of a pooled
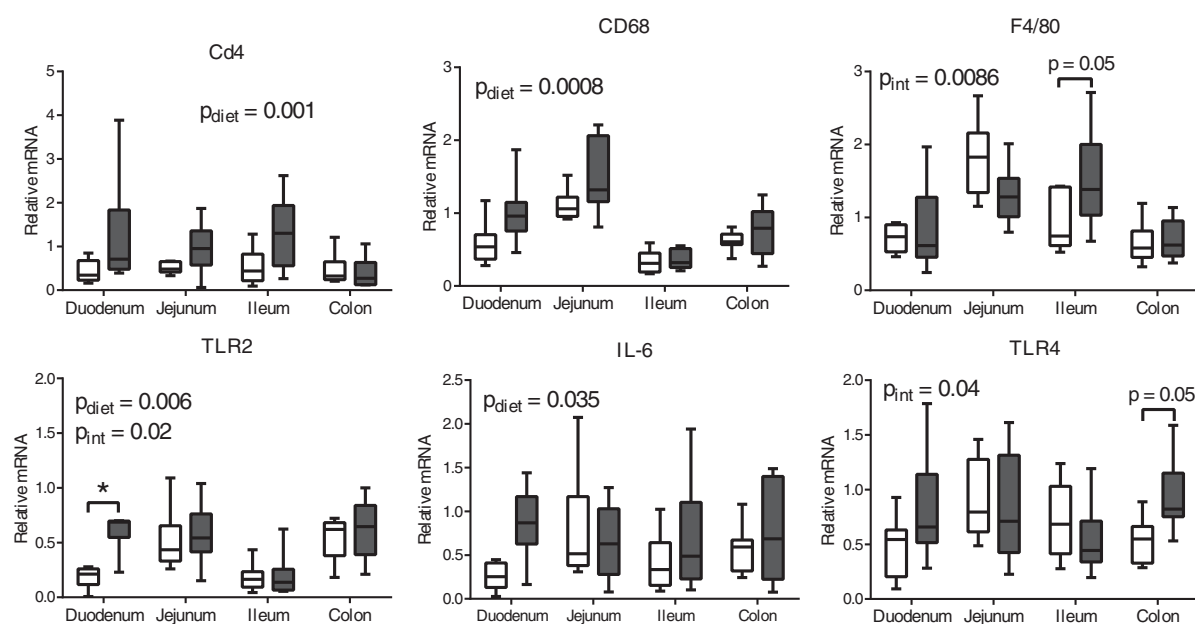
Figure 3. Maternal HFD is associated with elevated intestinal mRNA levels of immune cell markers and inflammatory signalling factors
Relative mRNA levels of Cluster of differentiation 4 (*Cd4*), *Cd68* and F4/80 immune cell markers, Toll-like receptor (*Tlr*)2 and *Tlr4*, and interleukin (*Il*)-6. Data are presented as box and whiskers plots (minimim to maximum), where the centre line represents the median. Control (open bars, $n = 9$) and high-fat fed dams (grey bars, $n = 10$). Significance was assessed by two-way ANOVA (main effect indicated as text) with the Bonferroni *post hoc* test, depicted as *$P < 0.05$ relative to control.

placental quality control extract (median RSD = 15%). The VIP scores plot (Fig. 8*B*) summarizes the top metabolites driving the separation between HFD and control placentas. Maternal HFD was associated with decreased levels of free carnitine (C0; main effect of diet, $P = 0.0006$), short-chain and medium-chain acylcarnitines (C2, C3, C8 and C10; main effect of diet, $P = 0.0007$, $P = 0.0013$, $P = 0.0026$ and $P = 0.0034$, respectively) and trimethylamine-*N*-oxide (TMAO; main effect of diet, $P = 0.0046$).

Maternal HFD impacts fetal intestinal cell stress pathways

We found that fetal intestinal NF-κB activation was increased by maternal HFD in the small intestine (main effect of diet, $P = 0.0007$). NF-κB activation was also increased in the large intestine of female ($P = 0.026$) but not male ($P > 0.99$) fetuses (Fig. 9*A*). This was not associated with increased mRNA levels of *Tnf*, *Il1β* and *Il10* in either the small or large intestine (data not shown).

Because NF-κB activation is influenced by ER stress, we explored ER-stress pathways in the fetal intestine. ER-chaperone 78 kDa glucose-regulated protein (*Grp78*) mRNA was decreased in the small (main effect of diet, $P = 0.0007$) but not the large intestine in fetuses exposed to maternal HFD (Fig. 9*A*), although protein levels were unchanged (data not shown). Maternal HFD was also associated with decreased *sXbp1* mRNA levels in the fetal small intestine but not large intestine (main effect of diet, $P = 0.0491$ and $P = 0.98$, respectively). Although no difference in PERK or eIF2α phosphorylation was detected by western blotting (main effect of diet, $P = 0.57$ and $P = 0.46$, respectively, data not shown), maternal HFD decreased transcript levels of *Atf4* ($p = 0.004$) and CCAAT/enhancer-binding protein homologous protein (*Chop*; $P = 0.01$) in the fetal large intestine (Fig. 9*B*).

To investigate whether maternal HFD was associated with altered fetal intestinal barrier development, we quantified mRNA levels of tight junction components. Maternal HFD increased occludin mRNA levels (main effect of diet, $P < 0.0001$), but not protein levels (main effect of diet, $P = 0.33$, data not shown) in the fetal small intestine. There was no detectable effect of maternal diet on *Zo1* mRNA levels in the fetal small or large intestine (main effect of diet, $P = 0.57$ and $P = 0.53$, respectively).
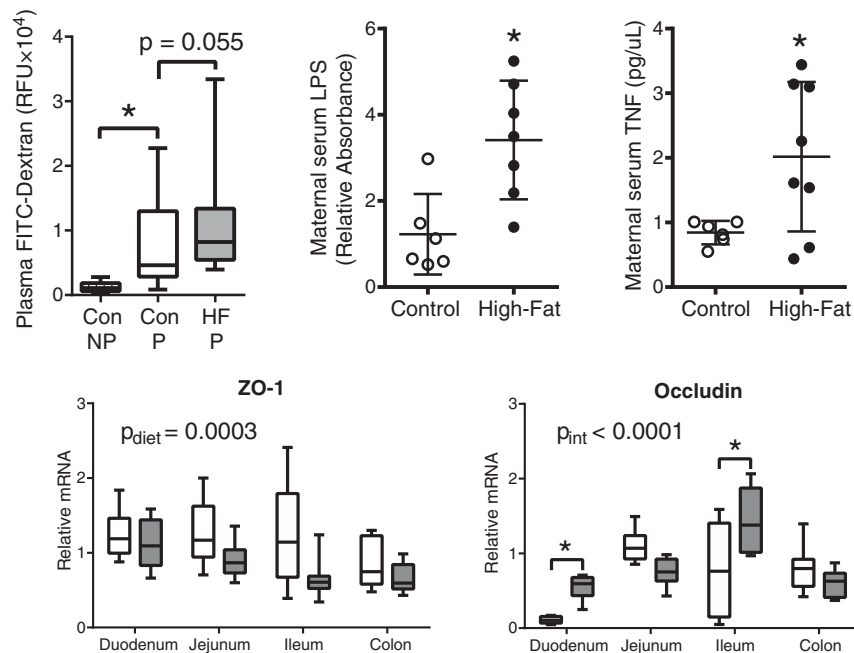
Figure 4. Maternal HFD impairs intestinal barrier integrity and elevates circulating inflammatory markers
FITC-dextran levels are shown in control non-pregnant (Con NP, *n* = 6), pregnant control (Con P, *n* = 14) and pregnant high-fat (HF P, *n* = 14) mice and are depicted as box and whiskers plots with the minimum – maximum and mean. Maternal serum LPS and TNF levels are shown in control (*n* = 5-6) high-fat dams (*n* = 7–8). Individual data points are shown with the mean ± SD. Relative mRNA levels of tight junction proteins *Zo1* and Occludin are shown in control (*n* = 9) and high-fat dams (*n* = 10). Data are presented as box and whiskers plots, minimum to maximum, where the centre line represents the median. Significance assessed by two-way ANOVA (main effect indicated as text) where appropriate with Bonferroni-adjusted multiple comparisons and *t* test analyses. *$P < 0.05$.

Maternal HFD also increased transcript levels of mucin 2 (*Muc2*), *Grp43* and *Tlr4* in the fetal small intestine ($P < 0.0001$, $P < 0.0001$ and $P = 0.032$, respectively) (Fig. 9*B*).

Discussion

Consistent with our previous work (Gohir *et al.* 2015), we found that HFD intake resulted in a decreased relative abundance of SCFA producing bacterial genera
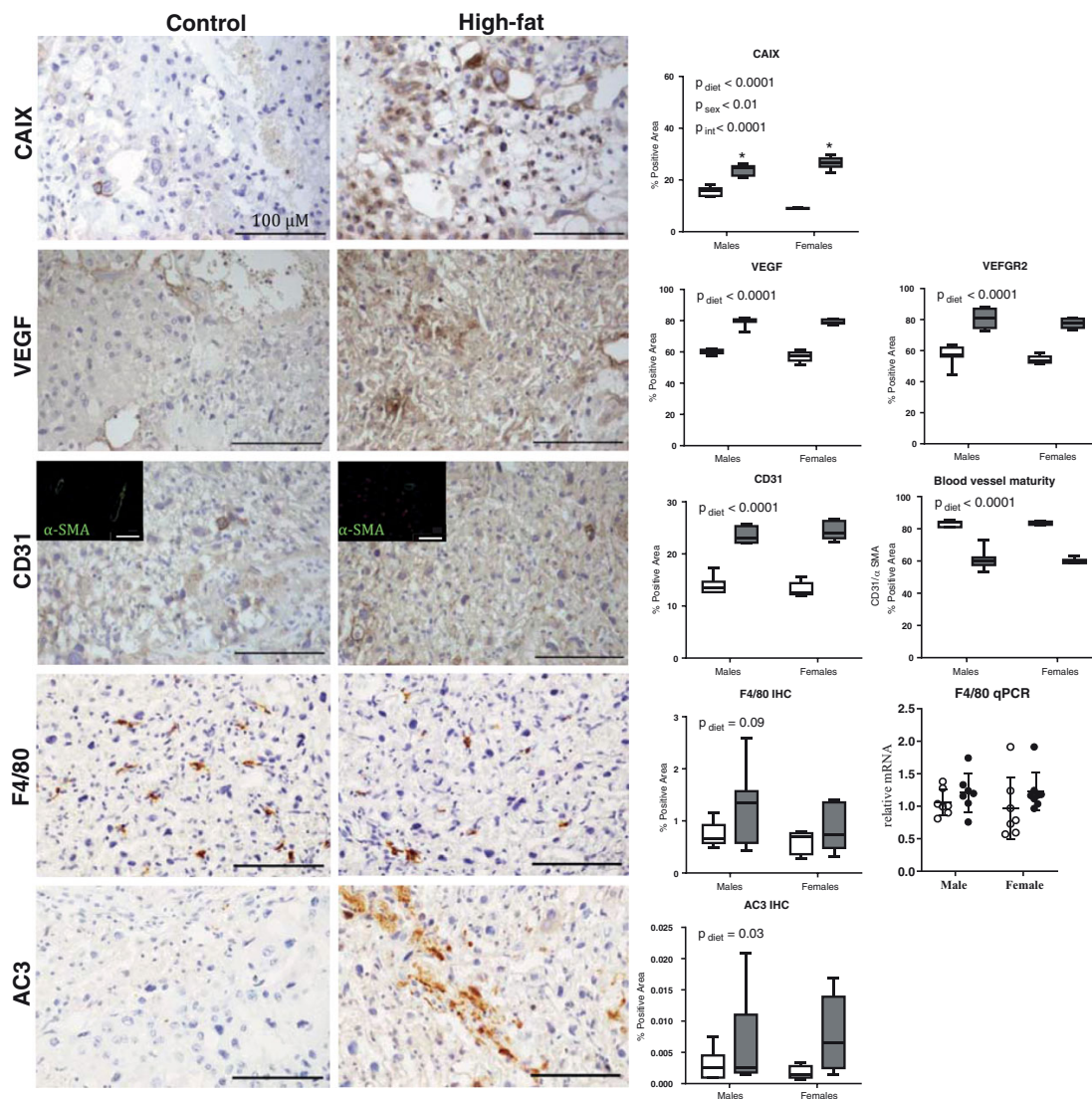
Figure 5. Maternal HFD is associated with placental hypoxia, altered angiogenesis and apoptosis
Immunostaining of female placental sections from control and high-fat dams. Males show similar staining patterns (images not shown). Scale bars = 100 μm. Image analyses of immunostaining show increased carbonic anhydrase (CAIX), VEGF, VEGFR2 and CD31 in placentas from high-fat dams (grey bars, $n = 5$) compared to controls (open bars, $n = 5$). Blood vessel maturity was assessed via the ratio of CD31 (endothelial cell marker) to α-SMA (pericyte marker) in green (inset: fluorescence staining image). Results of computerized image analyses of immunostaining of F4/80 and AC3 in placentas from control (open bars, $n = 5$–7) and high-fat dams (grey bars, $n = 6$–7). Data are presented as box and whiskers plots, minimum to maximum, where the centre line represents the median. Maternal HFD did not affect mRNA levels of F4/80 ($P = 0.12$; individual data points are shown with the mean ± SD). Significance assessed by Bonferroni-adjusted two-way ANOVA. *$P < 0.05$. All immunohistochemical assays were performed with negative controls (absence of primary antibodies) and showed no staining (data not shown).

at term pregnancy. We now show this decrease tended to be accompanied by lower maternal cecal butyrate levels, impaired maternal intestinal barrier integrity, and increased circulating LPS and TNF levels in HFD fed dams. We show maternal HFD induced placental hypoxia and impaired placental vascularization in both male and female fetuses, as well as changes in placental metabolomics strongly influenced by a decrease in carnitine levels. Finally, we extend previous observations showing maternal HFD disrupts offspring gut barrier function and inflammation (Xie *et al.* 2018) to include prenatal changes in key factors involved in the unfolded protein response (UPR) and increased NF-κB activation in the fetal intestine, particularly in female fetuses.

SCFAs produced by anaerobic bacteria play a key role in regulating intestinal immunity (Smith *et al.* 2013) but, despite the widespread interest in SCFAs and GPRs and their role in obesity and inflammation, our understanding of their function remains unclear. Data on GPR41 and 43 knockout models remain inconsistent, showing both inflammation promoting and inflammation resolving actions (Ang & Ding, 2016). In the present study, HFD dams had a decreased relative abundance of thirteen bacterial genera belonging to the butyrate-producing families *Lachnospiraceae* and *Ruminococcaceae*, although this was not accompanied by statistically significant lower

levels of cecal butyrate. We further found a decrease in relative abundance of *Bifidobacterium*, which promotes butyrate production through cross-feeding (Rivière *et al.* 2016), comprising decreases that have been associated with endotoxaemia in male HFD mice (Cani *et al.* 2008). Our observed microbial shifts were associated with decreased transcript levels of the SCFA receptor *Gpr41* in intestines of HFD dams, although the extent to which these changes result in specific receptor medicated changes in intestinal epithelial function is still unknown. Future studies employing Ussing chamber experiments are required to understand the relationship between microbial metabolites, GPR activity and intestinal epithelial function

The increase that we found with HFD in transcript levels of monocyte lineage marker *Cd68* is consistent with increased intestinal macrophage infiltration. Increased mRNA levels of *Cd4* can be attributed to T cells, monocytes, macrophages or dendritic cells and, although it is not possible to determine the specific cell type associated with this increase, it may be reflective of an increase in tissue resident macrophages (Shaw *et al.* 2018). Increased duodenal mRNA levels of *Tlr2* and *Il6* are consistent with intestinal inflammation in HFD dams (Hausmann *et al.* 2002). Future studies will investigate the maternal gut histologically, as well as to localize proteins, aiming to fully
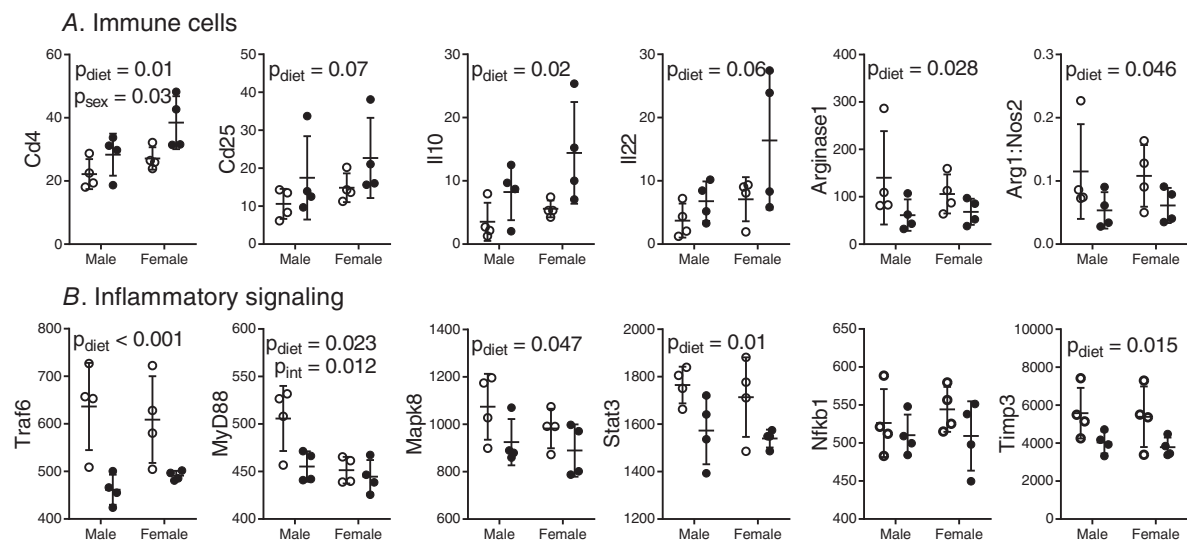
Figure 6. Maternal HFD alters placental mRNA levels of immune cell markers and inflammatory signalling molecules
A subset of placental samples was analysed using the NanoString nCounter gene expression system for key transcript levels of markers of (*A*) immune cells and (*B*) inflammatory signalling factors from control (open circles, $n = 4$) and high-fat dams (black circles, $n = 4$). Individual data points are shown with the mean ± SD. Significance assessed by Bonferroni-adjusted two-way ANOVA [main effect indicated as text; *post hoc* indicated by an asterisk (*); $P < 0.05$ compared to control]. CD: cluster of differentiation; IL, interleukin; Traf6, TNF receptor-associated factor; MyD88, myeloid differentiation primary response 88; MAPK8, mitogen-activated protein kinase 8; STAT3, signal transducer and activator of transcription 3; NF-κB, nuclear factor kappa-light-chain-enhancer of activated B cells; TIMP3, tissue inhibitor of metalloproteinase 3.

understand impacts on maternal intestinal inflammation. Unfortunately, this was beyond the scope of the present study.

The increased intestinal permeability that we observed with pregnancy in control mice suggests that decreased intestinal barrier integrity may be a normal adaptation to pregnancy, and also that maternal HFD may exacerbate this intestinal adaptation. Previous work suggests that increased paracellular permeability may be a result of decreased expression of tight junction proteins (Al-Sadi *et al.* 2011; Lee, 2015) and, consistent with this, we found decreased *Zo-1* transcript levels. However, our observation that occludin transcript levels were elevated highlights the need for future studies to co-localize tight junction proteins *in situ* in the maternal intestine in the context of pregnancy/high-fat intake because occludin

activity is highly dependent upon post-transcriptional and translational processing (Cummins, 2012).

We show that impaired maternal gut barrier integrity as a result of HFD intake corresponded to increased circulating maternal LPS and TNF levels and hypothesized that this low-grade systemic inflammation could alter placental function. However, we did not find altered pro-inflammatory cytokine transcript levels in our HFD placentas and, instead, we found a reduction in transcript levels of a number of adaptor proteins that participate in pro-inflammatory signalling, including *Traf6*, *MyD88*, *Mapk8* and *Stat3*. Because these data are limited to quantification of transcripts, we recognize that evidence of placental inflammation could be present at the protein level. We did observe increased transcript levels of *Cd4*, which is consistent with increased placental immune
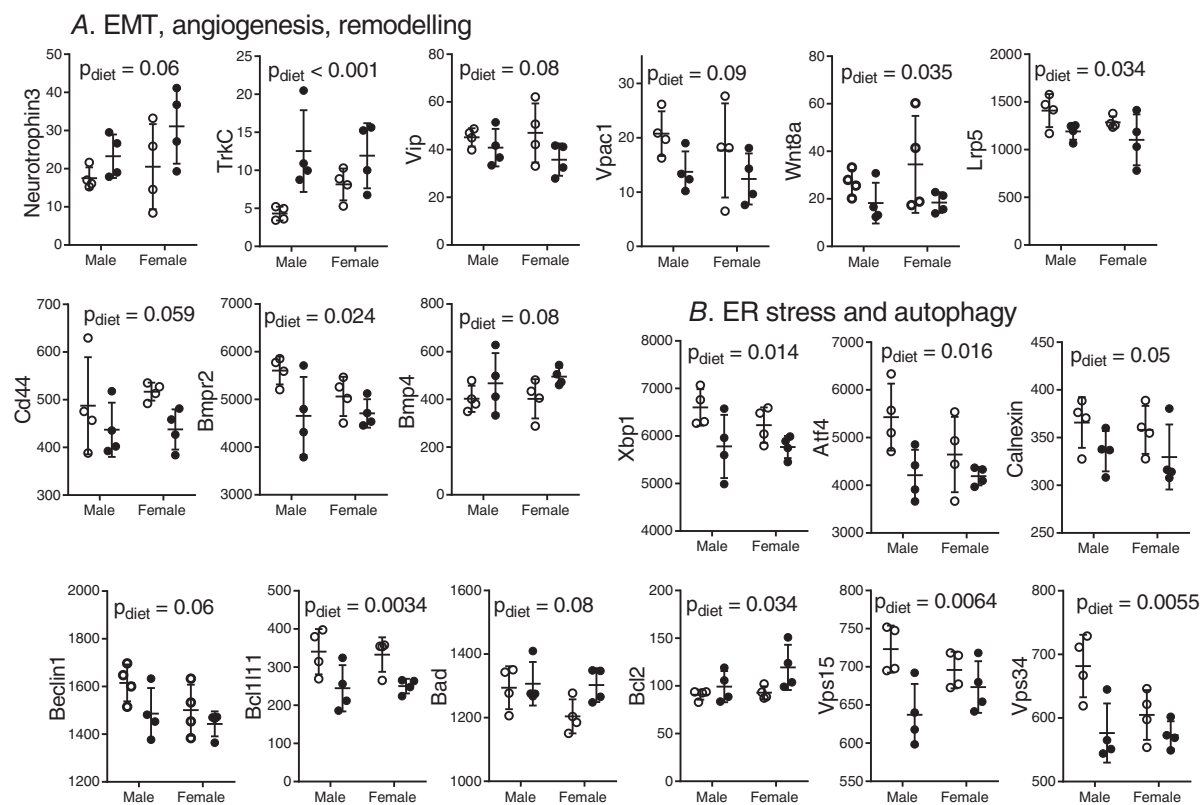
Figure 7. Maternal HFD alters placental mRNA levels of angiogenesis markers and ER stress factors
A subset of placental samples was analysed using the NanoString nCounter gene expression system for key transcript levels of markers of EMT, angiogenesis, ER stress, UPR and apoptosis from control (open circles, $n = 4$) and high-fat dams (black circles, $n = 4$). A, EMT, angiogenesis and tissue remodelling markers. B, ER stress, UPR and apoptosis and autophagy markers. Individual data points are shown with the mean ± SD. Main effect *P* values are indicated by as text. Significance was assessed by Bonferroni-adjusted two-way ANOVA. TrkC, tropomyosin receptor kinase C; CD, cluster of differentiation; VIP, vasoactive intestinal peptide; VPAC1, vasoactive intestinal polypeptide receptor 1; BMPR2, bone morphogenetic protein receptor type II; BMP4, bone morphogenetic protein 4; LRP5, low-density lipoprotein receptor-related protein 5; Wnt8a, Wnt family member 8a; XBP1, X-box binding protein 1; ATF4, activating transcription factor 4; VPS15/34, serine/threonine-protein kinase; Bcl2L1L, Bcl-2-like 1; Bcl2, B-cell lymphoma 2.

cell infiltration in humans (Challier *et al.* 2008; Saben *et al.* 2014) and in non-human primates (Farley *et al.* 2009). These observations, combined with increased *Il-10* and reduced *Arg1/Nos2* ratio, suggest that placental macrophage phenotype may be skewed by maternal HFD. Because alternatively activated macrophages are key regulators of placental angiogenesis (Zhao *et al.* 2018), a skewing of macrophage activation is consistent with the reductions that we observed in placental transcript levels of angiogenic factors, including Bmpr2, which is essential for uterine vascular development (Nagashima *et al.* 2013).

Hypoxia is a known stimulator of angiogenesis (Shweiki *et al.* 1992), which is consistent with our observed increase in VEGF and CD31 immunostaining. We hypothesize that the reduction we observed with HFD in placental smooth muscle actin may reflect impairments blood vessel maturation. This is supported by previous reports of HFD decreasing uteroplacental blood flow (Frias *et al.* 2011) and vascularization (Hayes *et al.* 2012) in rodents, although pathways in non-human primates and humans may be different (Farley *et al.* 2009; Lappas, 2014). Hypoxia also induces a metabolic switch from oxidative phosphorylation to glycolysis to
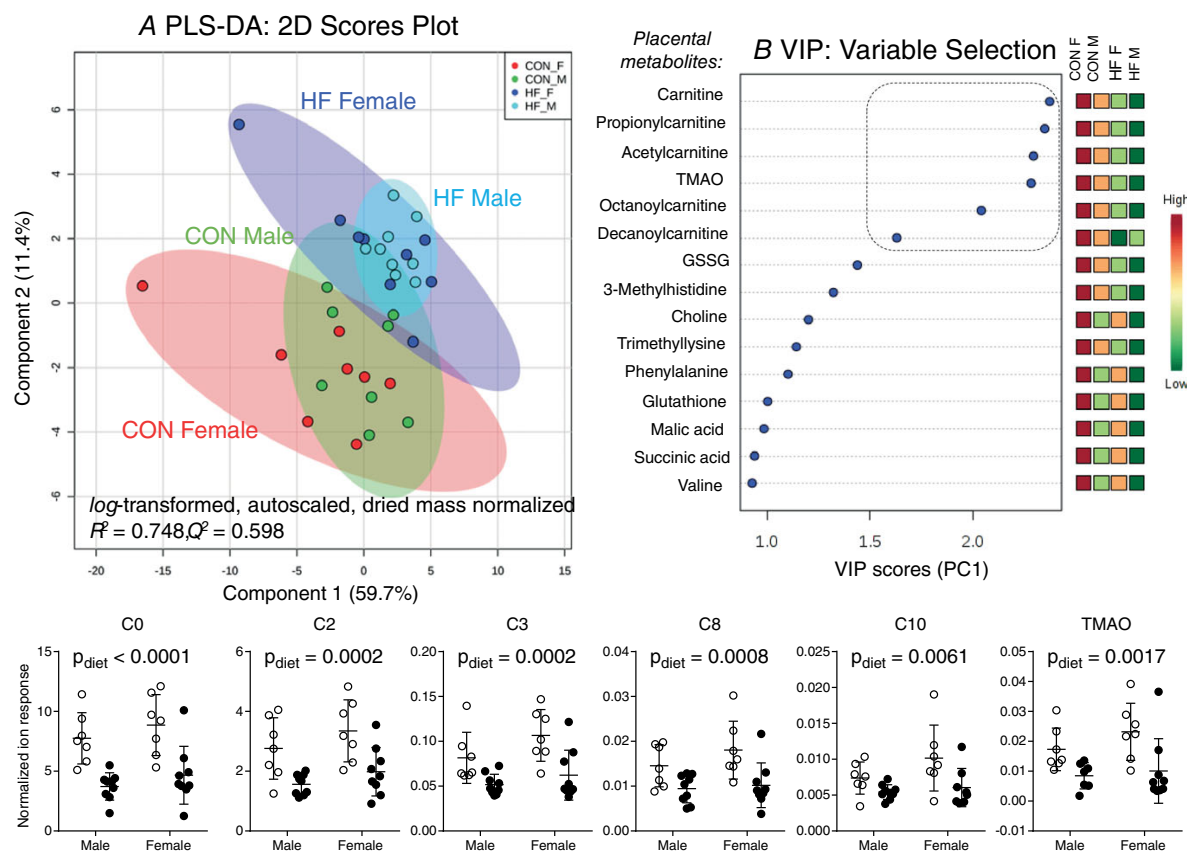
Figure 8. Maternal HFD is associated with decreased placental carnitine, as well as its related short/medium-chain acylcarnitine derivatives and TMAO
A, PLS-DA 2D scores plot illustrating diet and sex-dependent changes in the placental metabolome of control female (CON_F red, $n = 8$) and control male (CON_M green, $n = 8$) compared to placental extracts from high-fat female (HF_F, blue, $n = 9$) and high-fat male (HF_M, light blue, $n = 9$) groups. Supervised multivariate data analysis demonstrated good model accuracy ($r^2 = 0.75$) and robustness ($q^2 = 0.60$) when using leave one-out-at-a-time cross validation. *B*, a VIP along PC1 was used for variable selection, which summarizes the top 15-ranked placental metabolites primarily associated with high-fat maternal diet (VIP >1.0). The dashed box within the VIP plot highlights that six placental metabolites were found to be significantly lower in high-fat placentas when using an FDR adjustment ($q < 0.05$). Individual data points are shown with the mean ± SD (control open circles, HDF black circles). Significance assessed by Bonferroni-adjusted two-way ANOVA. C0, carnitine; C2, acetylcarnitine; C3, propionylcarnitine; C8, octanoylcarnitine; C10, decanoylcarnitine; TMAO, trimethylamine-*N*-oxide.

prevent ROS production (Weckmann *et al.* 2018) and has previously been associated with decreased placental carnitine uptake (Rytting & Audus, 2007; Chang *et al.* 2011). In humans, maternal HFD decreases levels of carnitine and short- and medium-chain acylcarnitines in the placenta (Calabuig-Navarro *et al.* 2017). We also show that maternal HFD significantly reduces placental carnitine (C0) and its acylcarnitine derivatives (C2, C3, C8 and C10). Carnitine is required for mitochondrial function, and its deficiency can suppress autophagy via
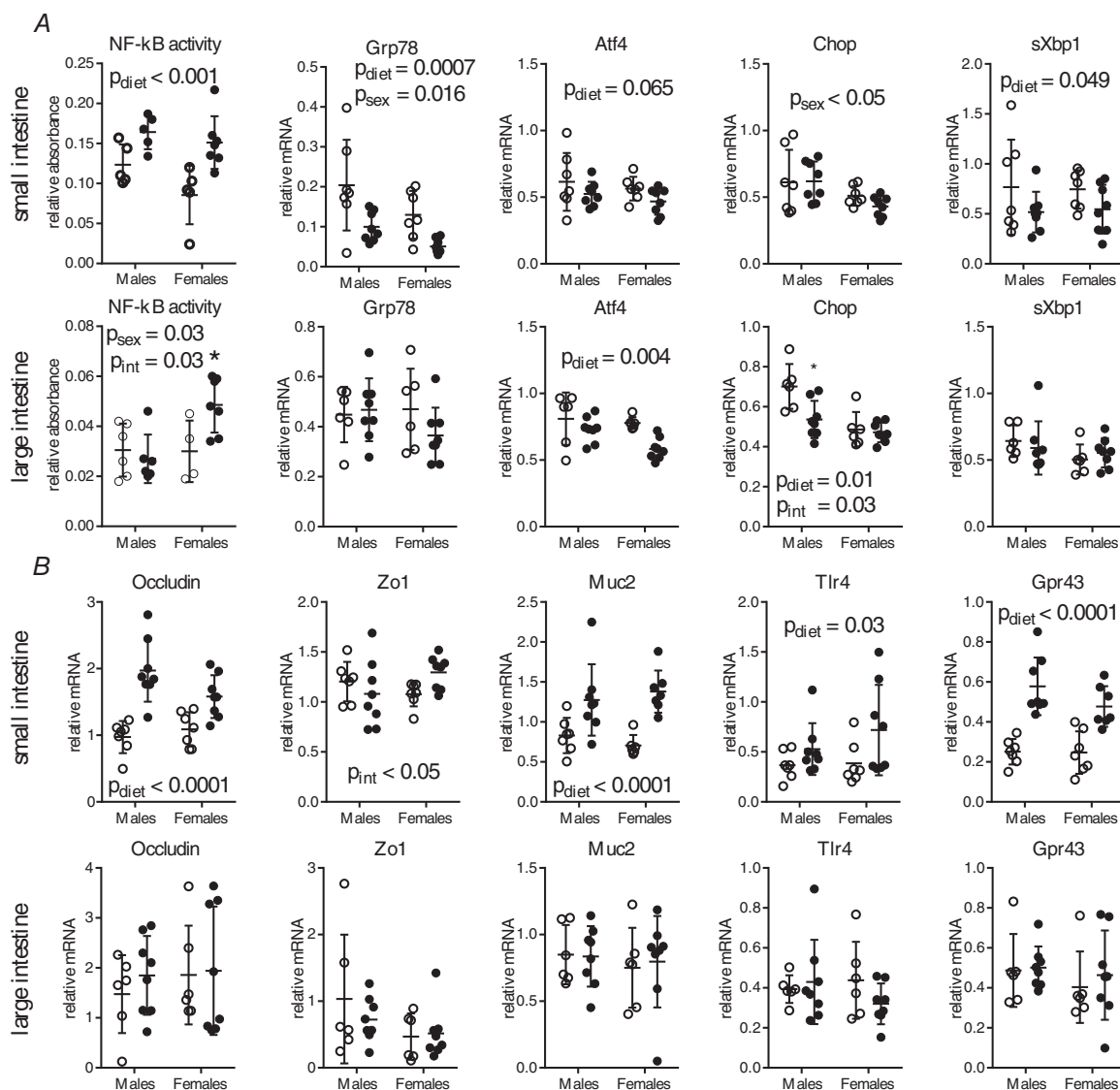
Figure 9. Transcript levels of factors regulating fetal gut barrier, UPR and NF-κB activity are altered by maternal HFD

A, in fetal small intestines, mRNA levels of *sXbp1* and *Grp78* were decreased in association with maternal HFD. In fetal large intestines, mRNA levels of *Atf4* and *Chop* were decreased in association with maternal HFD. *B*, in fetal small intestines, *Muc2*, occludin and *Tlr4* mRNA levels were increased in association with maternal HFD, whereas there was no significant effect of maternal HFD on mRNA levels of *Zo1*. NF-κB activation was increased with maternal HFD in fetal small intestines and female fetal large intestines. Individual data points are shown with the mean ± SD. Main effect *P* values are indicated as text. Small intestine ($n = 7–8$) and large intestine ($n = 6–8$) in control (open circles) and high-fat (black circles) female and male fetuses (small intestine, $n = 5–7$ and large intestine, $n = 4–7$ for NF-κB). Significance assessed by Bonferroni-adjusted two-way ANOVA. *$P < 0.05$.

increased levels of acetyl-CoA (Mariño *et al.* 2014). Decreased placental carnitine uptake may be responsible for our observed reductions in transcript levels of autophagy-regulators *Vsp15* and *Vps34*.

Reductions in these placental metabolites could impact fetal development. Carnitine is transported across the placenta to accumulate in fetal tissues over the course of gestation (Nakano *et al.* 1989) and carnitine deficiency has been associated with intestinal inflammation and apoptosis in neonatal mice (Sonne *et al.* 2012). Host–microbial interactions modulate metabolism (Nicholson *et al.* 2012), as well as gut epithelial cell structure, mucosal thickness, barrier integrity and immune composition, and thus we proposed that maternal HFD induced impairments in fetal intestinal development could be upstream of known offspring microbial dysbiosis and metabolic dysfunction. We found that NF-κB activity was increased in the fetal small and large intestine with maternal HFD, particularly in female fetuses, although this was not accompanied by increased transcription of pro-inflammatory cytokines. This may be a result of insufficient p38 MAPK activation, which has previously been shown to be essential for intestinal inflammation because of NF-κB activation (Guma *et al.* 2011), as well as intestinal epithelial cell differentiation (Houde *et al.* 2001). Canonical activation of NF-κB during development reduces TNF-induced apoptosis in fetal liver and lung (Espín-Palazón & Traver, 2016). Thus, increased NF-κB may represent a homeostatic response to HFD induced increases in maternal circulating TNF levels. Because amniotic fluid inhibits TLR signalling (Good *et al.* 2012), increased *Tlr4* transcripts in fetal intestines in association with maternal HFD may lead to increased gut inflammation postnatally upon microbial colonization. Although these data do not suggest that maternal HFD intake directly increased fetal gut inflammation, they suggest that previously reported increases in offspring intestinal inflammation may be a result of maternal HFD (Xie *et al.* 2018)

TLR4 signalling through MyD88-dependent pathways has previously been shown to be required for LPS-mediated increases in intestinal tight-junction permeability (Guo *et al.* 2015). We observed increased mRNA levels of tight junction proteins in fetuses of HFD fed dams but no change in protein levels. This may be related to the observed down-regulation of the IRE1-arm of the UPR. Down-regulation of the IRE1 arm may include decreased mRNA degradation via regulated IRE1-dependent decay, which could explain increased mRNA levels of ER-taxing proteins, including *Muc2*, *Gpr43* and occludin, as well as increased levels of *Grp78*, which is stabilized by regulated IRE1-dependent decay (Kimmig *et al.* 2012). The importance of the UPR in the differentiation of the intestinal epithelium has been demonstrated previously (Heijmans *et al.* 2013) and,

although our data do not support the hypothesis that maternal HFD induces fetal gut ER stress and decreased barrier function, they may indicate impaired intestinal differentiation. Future work will investigate the impact of maternal HFD on fetal intestinal proliferation and differentiation using histology and immunofluorescence. These investigations were beyond the scope of the present study.

We recognize that the present study is not without limitations. Despite employing a discovery-based NanoString platform to inform novel mediators of HFD effects on the placenta, our investigation was not exhaustive and future studies should focus on the relationship between ER stress and inflammation in a broader context, perhaps employing ER stress agonists/antagonists. Maternal immuno-phenotyping encompassing a broader immune cell investigation (using flow cytometry for example) would improve our understanding of HFD induced changes in maternal immunity and its relationship to intestinal and placental function. Future work should also include localization of immune cells, as well as tight junction proteins, because transcript and protein levels in intestinal and placental tissue are confounded by the heterogeneity of the tissue and thus this results in variability in the outcome measures. Localization via immuno-histochemistry or immunofluorescence combined with mRNA and protein levels will improve the resolution in our outcome measures. Finally, to fully understand the impact of pregnancy on maternal intestinal function, a full exploration of intestinal barrier integrity in non-pregnant and pregnant (control and HFD fed) animals is required.

Conclusions

In conclusion, we show significant changes in the maternal gut microbiota and intestinal adaptations during pregnancy in HFD-fed mice. HFD reduced maternal intestinal barrier function, possibly by impairing tight junction integrity, and increased mRNA levels of immune cell markers in the maternal intestine. Further work is required to understand the inflammatory signalling pathways that are initiated in response to altered microbiota and maternal intestinal barrier integrity. Maternal HFD was associated with increased placental hypoxia and apoptosis and reduced placental carnitine-derived metabolites, as well as increased NF-κB activation and decreased activation of the UPR in the fetal gut, particularly in female fetuses. Because of the significant role that gut microbiota and intestinal barrier function play in mediating HFD induced obesity, maternal intestinal changes could probably contribute to adverse maternal and placental adaptations and, via alterations in

fetal gut development, impart increased risk of obesity in the offspring.

References

Al-Sadi R, Khatib K, Guo S, Ye D, Youssef M & Ma T (2011). Occludin regulates macromolecule flux across the intestinal epithelial tight junction barrier. *Am J Physiol Gastrointest Liver Physiol* **300**, G1054–G1064.

Ang Z & Ding JL (2016). GPR41 and GPR43 in obesity and inflammation – protective or causative? *Front Immunol* **7**, 28.

Aplin JD (2000). Hypoxia and human placental development. *J Clin Invest* **105**, 559–560.

Bartram AK, Lynch MDJ, Stearns JC, Moreno-Hagelsieb G & Neufeld JD (2011). Generation of multimillion-sequence 16S rRNA gene libraries from complex microbial communities by assembling paired-end illumina reads. *Appl Environ Microbiol* **77**, 3846–3852.

Burger-van Paassen N, Vincent A, Puiman PJ, van der Sluis M, Bouma J, Boehm G, van Goudoever JB, van Seuningen I & Renes IB (2009). The regulation of intestinal mucin MUC2 expression by short-chain fatty acids: implications for epithelial protection. *Biochem J* **420**, 211–219.

Calabuig-Navarro V, Haghiac M, Minium J, Glazebrook P, Ranasinghe GC, Hoppel C, Hauguel de-Mouzon S, Catalano P & O'Tierney-Ginn P (2017). Effect of maternal obesity on placental lipid metabolism. *Endocrinology* **158**, 2543–2555.

Cani PD, Bibiloni R, Knauf C, Waget A, Neyrinck AM, Delzenne NM & Burcelin R (2008). Changes in gut microbiota control metabolic endotoxemia-induced inflammation in high-fat diet–induced obesity and diabetes in mice. *Diabetes* **57**, 1470–1481.

Casciaro A, Arcuri F, Occhini R, Toti MS, De Felice C & Toti P (2009). Expression of placental neurotrophin-3 (NT-3) in physiological pregnancy, preeclampsia and chorioamnionitis. *Clin Med Pathol* **2**, 9–15.

Challier JC, Basu S, Bintein T, Minium J, Hotmire K, Catalano PM & Hauguel-de Mouzon S (2008). Obesity in pregnancy stimulates macrophage accumulation and inflammation in the placenta. *Placenta* **29**, 274–281.

Chang T-T, Shyu M-K, Huang M-C, Hsu C-C, Yeh S-Y, Chen M-R & Lin C-J (2011). Hypoxia-mediated down-regulation of OCTN2 and PPARα expression in human placentas and in BeWo cells. *Mol Pharm* **8**, 117–125.

Chong J, Soufan O, Li C, Caraus I, Li S, Bourque G, Wishart DS & Xia J (2018). MetaboAnalyst 4.0: towards more transparent and integrative metabolomics analysis. *Nucleic Acids Res* **46**, W486–W494.

Chu DM, Antony KM, Ma J, Prince AL, Showalter L, Moller M & Aagaard KM (2016). The early infant gut microbiome varies in association with a maternal high-fat diet. *Genome Med* **8**, 77.

Collado MC, Isolauri E, Laitinen K & Salminen S (2008). Distinct composition of gut microbiota during pregnancy in overweight and normal-weight women. *Am J Clin Nutr* **88**, 894–899.

Cummins PM (2012). Occludin: one protein, many forms. *Mol Cell Biol* **32**, 242–250.

DiBattista A, McIntosh N, Lamoureux M, Al-Dirbashi OY, Chakraborty P & Britz-McKibbin P (2017). Temporal signal pattern recognition in mass spectrometry: a method for rapid identification and accurate quantification of biomarkers for inborn errors of metabolism with quality assurance. *Anal Chem* **89**, 8112–8121.

Davies JE, Pollheimer J, Yong HEJ, Kokkinos MI, Kalionis B, Knöfler M & Murthi P (2016). Epithelial-mesenchymal transition during extravillous trophoblast differentiation. *Cell Adh Migr* **10**, 310–321.

Elahi MM, Cagampang FR, Mukhtar D, Anthony FW, Ohri SK & Hanson MA (2009). Long-term maternal high-fat feeding from weaning through pregnancy and lactation predisposes offspring to hypertension, raised plasma lipids and fatty liver in mice. *Br J Nutr* **102**, 514–519.

Espín-Palazón R & Traver D (2016). The NF-κB family: Key players during embryonic development and HSC emergence. *Exp Hematol* **44**, 519–527.

Farley D, Tejero ME, Comuzzie AG, Higgins PB, Cox L, Werner SL, Jenkins SL, Li C, Choi J, Dick EJ Jr, Hubbard GB, Frost P, Dudley DJ, Ballesteros B, Wu G, Nathanielsz PW & Schlabritz-Loutsevitch NE (2009). Feto-placental adaptations to maternal obesity in the baboon. *Placenta* **30**, 752–760.

Fernandez-Twinn DS, Gascoin G, Musial B, Carr S, Duque-Guimaraes D, Blackmore HL, Alfaradhi MZ, Loche E, Sferruzzi-Perri AN, Fowden AL & Ozanne SE (2017). Exercise rescues obese mothers' insulin sensitivity, placental hypoxia and male offspring insulin sensitivity. *Sci Rep* **7**, 44650.

Frias AE, Morgan TK, Evans AE, Rasanen J, Oh KY, Thornburg KL & Grove KL (2011). Maternal high-fat diet disturbs uteroplacental hemodynamics and increases the frequency of stillbirth in a nonhuman primate model of excess nutrition. *Endocrinology* **152**, 2456–2464.

Gluckman PD & Hanson MA (2004). Living with the past: evolution, development, and patterns of disease. *Science* **305**, 1733–1736.

Gohir W, Whelan FJ, Surette MG, Moore C, Schertzer JD & Sloboda DM (2015). Pregnancy-related changes in the maternal gut microbiota are dependent upon the mother's periconceptional diet. *Gut Microbes* **6**, 310–320.

Goltsman DSA, Sun CL, Proctor DM, DiGiulio DB, Robaczewska A, Thomas BC, Shaw GM, Stevenson DK, Holmes SP, Banfield JF & Relman DA (2018). Metagenomic analysis with strain-level resolution reveals fine-scale variation in the human pregnancy microbiome. *Genome Res* **28**, 1467–1480.

Good M et al. (2012). Amniotic fluid inhibits Toll-like receptor 4 signalling in the fetal and neonatal intestinal epithelium. *Proc Natl Acad Sci U S A* **109**, 11330–11335.

Grundy D (2015). Principles and standards for reporting animal experiments in The Journal of Physiology and Experimental Physiology. *J Physiol* **593**, 2547–2549.

Guma M, Stepniak D, Shaked H, Spehlmann ME, Shenouda S, Cheroutre H, Vicente-Suarez I, Eckmann L, Kagnoff MF & Karin M (2011). Constitutive intestinal NF-κB does not trigger destructive inflammation unless accompanied by MAPK activation. *J Exp Med* **208**, 1889–1900.

Guo S, Nighot M, Al-Sadi R, Alhmoud T, Nighot P & Ma TY (2015). Lipopolysaccharide regulation of intestinal tight junction permeability is mediated by TLR4 signal transduction pathway activation of FAK and MyD88. *J Immunol* **195**, 4999–5010.

Guo Y, Wang Z, Chen L, Tang L, Wen S, Liu Y & Yuan J (2018). Diet induced maternal obesity affects offspring gut microbiota and persists into young adulthood. *Food Funct* **9**, 4317–4327.

Hausmann M, Kiessling S, Mestermann S, Webb G, Spöttl T, Andus T, Schölmerich J, Herfarth H, Ray K, Falk W & Rogler G (2002). Toll-like receptors 2 and 4 are up-regulated during intestinal inflammation. *Gastroenterology* **122**, 1987–2000.

Hayes EK, Lechowicz A, Petrik JJ, Storozhuk Y, Paez-Parent S, Dai Q, Samjoo IA, Mansell M, Gruslin A, Holloway AC & Raha S (2012). Adverse fetal and neonatal outcomes associated with a life-long high fat diet: role of altered development of the placental vasculature. *PLoS ONE* **7**, e33370.

Heijmans J, van Lidth de Jeude JF, Koo B-K, Rosekrans SL, Wielenga MCB, van de Wetering M, Ferrante M, Lee AS, Onderwater JJM, Paton JC, Paton AW, Mommaas AM, Kodach LL, Hardwick JC, Hommes DW, Clevers H, Muncan V & van den Brink GR (2013). ER stress causes rapid loss of intestinal epithelial stemness through activation of the unfolded protein response. *Cell Rep* **3**, 1128–1139.

Holmes E, Li JV, Marchesi JR & Nicholson JK (2012). Gut microbiota composition and activity in relation to host metabolic phenotype and disease risk. *Cell Metab* **16**, 559–564.

Houde M, Laprise P, Jean D, Blais M, Asselin C & Rivard N (2001). Intestinal epithelial cell differentiation involves activation of p38 mitogen-activated protein kinase that regulates the homeobox transcription factor CDX2. *J Biol Chem* **276**, 21885–21894.

Howie GJ, Sloboda DM, Kamal T & Vickers MH (2009). Maternal nutritional history predicts obesity in adult offspring independent of postnatal diet. *J Physiol* **587**, 905–915.

Kang R, Zeh HJ, Lotze MT & Tang D (2011). The Beclin 1 network regulates autophagy and apoptosis. *Cell Death Differ* **18**, 571–580.

Kimmig P, Diaz M, Zheng J, Williams CC, Lang A, Aragón T, Li H & Walter P (2012). The unfolded protein response in fission yeast modulates stability of select mRNAs to maintain protein homeostasis. *Elife* **1**, e00048.

Koren O, Goodrich JK, Cullender TC, Spor A, Laitinen K, Bäckhed HK, Gonzalez A, Werner JJ, Angenent LT, Knight R, Bäckhed F, Isolauri E, Salminen S & Ley RE (2012). Host remodelling of the gut microbiome and metabolic changes during pregnancy. *Cell* **150**, 470–480.

Kuehnbaum NL, Kormendi A & Britz-McKibbin P (2013). Multisegment injection-capillary electrophoresis-mass spectrometry: a high-throughput platform for metabolomics with high data fidelity. *Anal Chem* **85**, 10664–10669.

Lappas M (2014). Markers of endothelial cell dysfunction are increased in human omental adipose tissue from women with pre-existing maternal obesity and gestational diabetes. *Metabolism* **63**, 860–873.

Lee SH (2015). Intestinal permeability regulation by tight junction: implication on inflammatory bowel diseases. *Intest Res* **13**, 11–18.

Li H-P, Chen X & Li M-Q (2013). Gestational diabetes induces chronic hypoxia stress and excessive inflammatory response in murine placenta. *Int J Clin Exp Pathol* **6**, 650–659.

Ma J, Prince AL, Bader D, Hu M, Ganu R, Baquero K, Blundell P, Alan Harris R, Frias AE, Grove KL & Aagaard KM (2014). High-fat maternal diet during pregnancy persistently alters the offspring microbiome in a primate model. *Nat Commun* **5**, 3889.

Macedo AN, Mathiaparanam S, Brick L, Keenan K, Gonska T, Pedder L, Hill S & Britz-McKibbin P (2017). The sweat metabolome of screen-positive cystic fibrosis infants: revealing mechanisms beyond impaired chloride transport. *ACS Cent Sci* **3**, 904–913.

Mariño G et al. (2014). Regulation of autophagy by cytosolic acetyl-coenzyme A. *Mol Cell* **53**, 710–725.

Morris MJ & Chen H (2009). Established maternal obesity in the rat reprograms hypothalamic appetite regulators and leptin signalling at birth. *Int J Obes* **33**, 115–122.

Morrison DJ & Preston T (2016). Formation of short chain fatty acids by the gut microbiota and their impact on human metabolism. *Gut Microbes* **7**, 189–200.

Nagashima T, Li Q, Clementi C, Lydon JP, DeMayo FJ & Matzuk MM (2013). BMPR2 is required for postimplantation uterine function and pregnancy maintenance. *J Clin Invest* **123**, 2539–2550.

Nakano C, Takashima S & Takeshita K (1989). Carnitine concentration during the development of human tissues. *Early Hum Dev* **19**, 21–27.

Nicholson JK, Holmes E, Kinross J, Burcelin R, Gibson G, Jia W & Pettersson S (2012). Host-gut microbiota metabolic interactions. *Science* **336**, 1262–1267.

Priyadarshini M, Thomas A, Reisetter AC, Scholtens DM, Wolever TMS, Josefson JL & Layden BT (2014). Maternal short-chain fatty acids are associated with metabolic parameters in mothers and newborns. *Transl Res* **164**, 153–157.

Rivière A, Selak M, Lantin D, Leroy F & De Vuyst L (2016). Bifidobacteria and butyrate-producing colon bacteria: importance and strategies for their stimulation in the human gut. *Front Microbiol* **7**, 979.

Robertson RC, Kaliannan K, Strain CR, Ross RP, Stanton C & Kang JX (2018). Maternal omega-3 fatty acids regulate offspring obesity through persistent modulation of gut microbiota. *Microbiome* **6**, 95.

Rytting E & Audus KL (2007). Effects of low oxygen levels on the expression and function of transporter OCTN2 in BeWo cells. *J Pharm Pharmacol* **59**, 1095–1102.

Saben J, Lindsey F, Zhong Y, Thakali K, Badger TM, Andres A, Gomez-Acevedo H & Shankar K (2014). Maternal obesity is associated with a lipotoxic placental environment. *Placenta* **35**, 171–177.

Santacruz A, Collado MC, García-Valdés L, Segura MT, Martín-Lagos JA, Anjos T, Martí-Romero M, Lopez RM, Florido J, Campoy C & Sanz Y (2010). Gut microbiota composition is associated with body weight, weight gain and biochemical parameters in pregnant women. *Br J Nutr* **104**, 83–92.

Shaw TN, Houston SA, Wemyss K, Bridgeman HM, Barbera TA, Zangerle-Murray T, Strangward P, Ridley AJL, Wang P, Tamoutounour S, Allen JE, Konkel JE & Grainger JR (2018). Tissue-resident macrophages in the intestine are long lived and defined by Tim-4 and CD4 expression. *J Exp Med* **215**, 1507–1518.

Shweiki D, Itin A, Soffer D & Keshet E (1992). Vascular endothelial growth factor induced by hypoxia may mediate hypoxia-initiated angiogenesis. *Nature* **359**, 843–845.

Smith PM, Howitt MR, Panikov N, Michaud M, Gallini CA, Bohlooly-Y M, Glickman JN & Garrett WS (2013). The microbial metabolites, short-chain fatty acids, regulate colonic Treg cell homeostasis. *Science* **341**, 569–573.

Soderborg TK, Clark SE, Mulligan CE, Janssen RC, Babcock L, Ir D, Lemas DJ, Johnson LK, Weir T, Lenz LL, Frank DN, Hernandez TL, Kuhn KA, D'Alessandro A, Barbour LA, El Kasmi KC & Friedman JE (2018). The gut microbiota in infants of obese mothers increases inflammation and susceptibility to NAFLD. *Nat Commun* **9**, 4462.

Sonne S, Shekhawat PS, Matern D, Ganapathy V & Ignatowicz L (2012). Carnitine deficiency in OCTN2-/- newborn mice leads to a severe gut and immune phenotype with widespread atrophy, apoptosis and a pro-inflammatory response. *PLoS ONE* **7**, e47729.

Steegenga WT, Mischke M, Lute C, Boekschoten MV, Lendvai A, Pruis MGM, Verkade HJ, van de Heijning BJM, Boekhorst J, Timmerman HM, Plösch T, Müller M & Hooiveld GJEJ (2017). Maternal exposure to a Western-style diet causes differences in intestinal microbiota composition and gene expression of suckling mouse pups. *Mol Nutr Food Res* **61**, https://doi.org/10.1002/mnfr.201600141.

Thevaranjan N, Puchta A, Schulz C, Naidoo A, Szamosi JC, Verschoor CP, Loukov D, Schenck LP, Jury J, Foley KP, Schertzer JD, Larché MJ, Davidson DJ, Verdú EF, Surette MG & Bowdish DME (2017). Age-associated microbial dysbiosis promotes intestinal permeability, systemic inflammation, and macrophage dysfunction. *Cell Host Microbe* **21**, 455–466.

Triunfo S & Lanzone A (2014). Impact of overweight and obesity on obstetric outcomes. *J Endocrinol Invest* **37**, 323–329.

Verschoor CP, Naidoo A, Wallace JG, Johnstone J, Loeb M, Bramson JL & Bowdish DM (2015). Circulating muramyl dipeptide is negatively associated with interleukin-10 in the frail elderly. *Inflammation* **38**, 272–277.

Wallace JM, Horgan GW & Bhattacharya S (2012). Placental weight and efficiency in relation to maternal body mass index and the risk of pregnancy complications in women delivering singleton babies. *Placenta* **33**, 611–618.

Wallace K, Cornelius DC, Scott J, Heath J, Moseley J, Chatman K & LaMarca B (2014). CD4+ T cells are important mediators of oxidative stress that cause hypertension in response to placental ischemia. *Hypertension* **64**, 1151–1158.

Wankhade UD, Zhong Y, Kang P, Alfaro M, Chintapalli SV, Piccolo BD, Mercer KE, Andres A, Thakali KM & Shankar K (2018). Maternal high-fat diet programs offspring liver steatosis in a sexually dimorphic manner in association with changes in gut microbial ecology in mice. *Sci Rep* **8**, 16502.

Weckmann K, Diefenthäler P, Baeken MW, Yusifli K, Turck CW, Asara JM, Behl C & Hajieva P (2018). Metabolomics profiling reveals differential adaptation of major energy metabolism pathways associated with autophagy upon oxygen and glucose reduction. *Sci Rep* **8**, 2337.

Whelan FJ, Verschoor CP, Stearns JC, Rossi L, Luinstra K, Loeb M, Smieja M, Johnstone J, Surette MG & Bowdish DME (2014). The loss of topography in the microbial communities of the upper respiratory tract in the elderly. *Ann Am Thorac Soc* **11**, 513–521.

Xie R, Sun Y, Wu J, Huang S, Jin G, Guo Z, Zhang Y, Liu T, Liu X, Cao X, Wang B & Cao H (2018). Maternal high fat diet alters gut microbiota of offspring and exacerbates DSS-induced colitis in adulthood. *Front Immunol* **9**, 2608.

Yamamoto M, Ly R, Gill B, Zhu Y, Moran-Mirabal J & Britz-McKibbin P (2016). Robust and high-throughput method for anionic metabolite profiling: preventing polyimide aminolysis and capillary breakages under alkaline conditions in capillary electrophoresis-mass spectrometry. *Anal Chem* **88**, 10710–10719.

Zhao H, Kalish FS, Wong RJ & Stevenson DK (2018). Hypoxia regulates placental angiogenesis via alternatively activated macrophages. *Am J Reprod Immunole* **88**, e12989.

Additional information

Competing interests

The authors declare that they have no competing interests.

Author contributions

DMS designed the experiments. WG performed the animal experiments. WG, KMK, MS, CB, JGW, CJB, and JJP contributed to the acquisition of data. WG, KMK, MS, CJB, JGW, PBM, JJP and DMS contributed to the analysis of data. WG, KMK and DMS contributed to the interpretation of data. MGS assisted in the analysis of bacterial sequencing data. KMK, WG, and DMS wrote the manuscript. JGW, MS, CJB, PBM, JJP and MGS edited the manuscript. All authors have approved the final version of the manuscript and agree to be accountable for all aspects of the work. All persons listed as authors qualify for authorship, and all those who qualify are listed.

Chapter 6

The impact of diet-induced obesity on maternal gut microbiota and maternal and fetal intestinal development: the role of TNF

6.1 Introduction

There is no doubt that the early life environment shapes long-term health (267). Many clinical (268–271) and experimental (272–274) studies have shown that one such environment, maternal obesity (or fetal exposure to an obesogenic diet), is associated with increased risk of glucose intolerance and increased adiposity in

offspring (275). One potential mechanism driving this "programming" of offspring by maternal obesity is fetal exposure to chronic low-grade inflammation (276–278); where circulating levels of pro-inflammatory cytokines, including tumour necrosis factor (TNF) and interleukin- (IL)6, are associated with increased offspring adiposity (279, 280) and metabolic dysfunction (281–283). More recent data suggest a clear relationship between maternal obesity, inflammation, the microbiota and offspring gut function (146, 147, 284–286). The mechanistic signalling pathways governing these associations are still unclear, and under intense investigation in both clinical and experimental models.

One potential signalling pathway is the induction of endoplasmic reticulum (ER) stress. In experimental models, maternal obesity is associated with increased transcription of ER stress-associated genes in the hypothalamus (287, 288), adipose tissue (289), and pancreas (290), but whether similar impacts occur in intestinal tissue is still unclear.

Within the gut, ER stress induces apoptosis of intestinal epithelial cells (IECs) and causes under-glycosylation of secreted mucins, decreasing barrier integrity (180). We previously showed that diet-induced obesity (DIO) during pregnancy increases maternal gut permeability, and is associated with increased levels of serum lipopolysaccharide (LPS) (p=0.0065) and TNF in maternal serum (p=0.024; Chapter 5, (265)). Downregulation of TNF receptor-associated factor 2 (TRAF2) during ER stress blocks nuclear factor kappa B (NF-κB) activation by TNF, thereby increasing activation of its apoptotic pathways (291). TNF can induce transcription and hypersecretion of mucin (Muc)2 (292), however, this is through the NF-κB pathway, and c-Jun N-terminal kinase (JNK) pathway

activation inhibits Muc2 expression (38). It is possible that ER stress similarly blocks the NF-κB pathway, resulting in increased JNK activation and inhibition of mucin production.

Maternal gut ER stress combined with a shift in maternal gut microbes may increase intestinal permeability and contribute to fetal (and placental) exposure to systemic inflammation. In conventional, but not germ-free mice, up-regulation of TNF expression and NF-κB activation in the gut precedes obesity, and this has been proposed to lead to the systemic inflammation associated with obesity (293). This interaction between the gut microbiota, ER stress, and intestinal inflammation may underlie the signals that alter fetal intestinal development (Chapter 5). ER stress within the developing fetal gut may alter gut development, resulting in altered selective pressures on the gut microbiota that may perpetuate dysbiosis, which has been correlated to offspring metabolic syndrome (294, 295). As elevated levels of TNF have previously been shown to be causal in intestinal permeability increases through the dysregulation of tight junction proteins and increased epithelial cell apoptosis (296), in this study, we aimed to investigate the role of TNF in inducing ER stress in maternal intestinal adaptations to pregnancy as well as fetal intestinal development in the context of diet-induced obesity.

We hypothesized that the interaction between ER stress and increased TNF in gut of high-fat (HF)-fed dams drives decreased barrier function contributes to impaired fetal gut development.

6.2 Results

6.2.1 Maternal and fetal phenotype

To assess whether our previously shown effects of DIO on maternal intestinal adaptations to pregnancy (Chapter 5 (265)) are modulated by increased TNF-mediated systemic inflammation we used a TNF knockout (TNF$^{-/-}$) model of DIO during pregnancy. Mice investigated in this study were not littermates. A pilot study of wildtype (Wt) and TNF$^{-/-}$ littermates is included in Appendix C. Female Wt and TNF$^{-/-}$ mice were fed a standard chow diet (control; 17% kcal fat, 29% kcal protein, 54% kcal carbohydrate, 3.40 kcal/g) or a high-fat diet (HF; 60% kcal fat, 20% kcal protein, 20% kcal carbohydrates, 5.24 kcal/g) for 6 weeks prior to mating and throughout gestation until endpoint at embryonic day (E)18.5. HF-fed Wt and TNF$^{-/-}$ mice were significantly heavier than controls (main effect of diet, p<0.0001) at 2 weeks (Wt p=0.042) and 1 week (TNF p=0.032) of dietary intervention, respectively, onward (Fig. 6.1). Overall, Wt dams were heavier than TNF$^{-/-}$ dams (main effect of genotype, p=0.012) and gained more weight before mating (main effect of genotype, p=0.00068), particularly on HF diet (HF Wt vs. HF TNF$^{-/-}$, p=0.0001).

Throughout pregnancy, HF-fed Wt dams were heavier than Wt controls (main effect of diet, p=0.0001). HF-fed TNF$^{-/-}$, however, were of similar weights to TNF$^{-/-}$ controls (main effect of diet, p=0.06), except at E10.5 (p=0.028; Fig. 6.2). Correspondingly HF Wt dams were heavier than HF TNF$^{-/-}$ dams throughout pregnancy, while weights of Wt and TNF$^{-/-}$ controls were similar. There was no significant effect of diet (p=0.11) or genotype (p=0.24) on

111
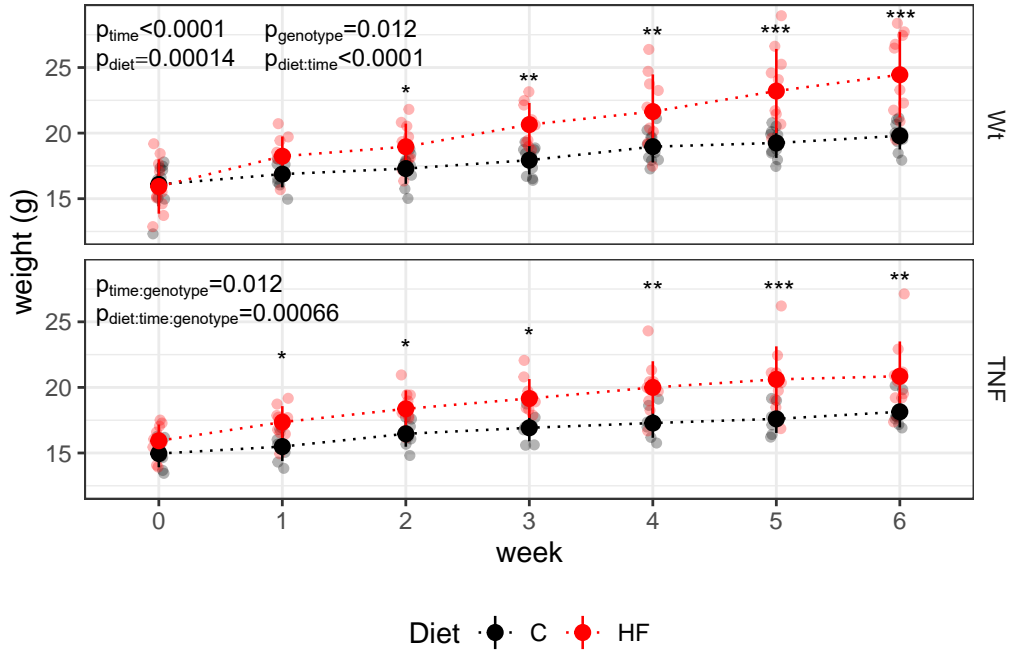
Figure 6.1. Pre-pregnancy weight gain by genotype and diet.
Female Wt and TNF$^{-/-}$ mice were placed on a standard chow diet (control; C, black) or 60% HF diet (red) for 6 weeks and body weight
was measured weekly. HF diet increased body weight in both Wt and
TNF$^{-/-}$ mice (main effect of diet, $p<0.0001$). Individual data points
are shown as well as the mean and standard deviation. Significance
was assessed by mixed linear model with time, diet, and genotype as
interacting fixed effects and individual mouse ID as a random effect
($n=8-10$ per group).* indicates $p<0.05$; ** $p<0.01$, *** $p<0.001$ compared to control-fed counterparts.

gestational weight gain. These data suggest that the absence of TNF somewhat
protected dams from HF diet-induced weight gain.

We next investigated whether similar protection could also be observed in
measures of maternal glucose metabolism. At term gestation (E18.5), maternal
fasted whole blood glucose (WBG) and serum insulin levels were similar across
all groups (Wt: WBG $p=0.16$, insulin $p=0.083$; TNF$^{-/-}$: WBG $p=0.42$, insulin
$p=0.83$; Fig. 6.3). This is consistent with our previously published Wt cohort
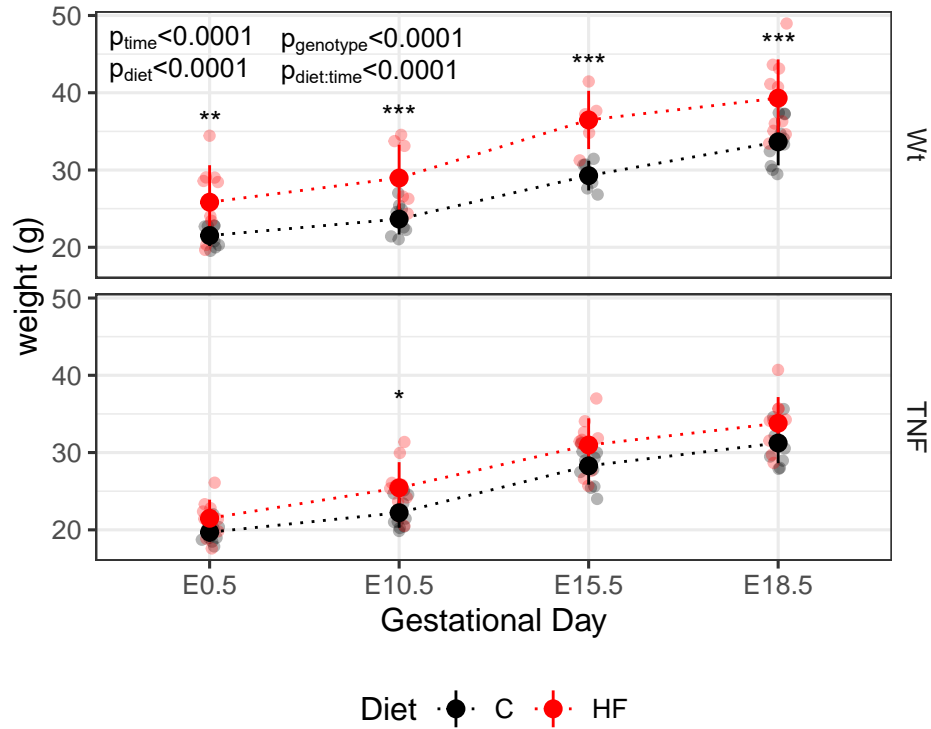
Figure 6.2. Pregnancy weight gain by genotype and diet. After 6-weeks of dietary intervention, Wt and TNF dams were mated with control-fed male mice of the same genotype, and dam body weight was recorded at gestational/embryonic day (E)0.5, E10.5, E15.5, and E18.5. In Wt mice, HF dams (red) were heavier than Wt controls (black) throughout pregnancy (main effect of diet, p<0.0001), but HF TNF$^{-/-}$ dams were only heavier than control TNF$^{-/-}$ at E10.5 (p=0.028). Individual data points are shown as well as the mean and standard deviation. Significance was assessed by mixed linear model with time, diet, and genotype as interacting fixed effects and individual mouse ID as a random effect (n=8-10 per group).* indicates p<0.05; ** p<0.01, *** p<0.001 compared to control-fed counterparts.

(Chapter 5, (265)), where we did not observe any changes in term gestation glucose levels in dams fed a HF diet. In Wt dams, HF diet was associated with increased absolute liver weight (p=0.039), but no difference in relative liver weight (grams (g) per g body weight, p=0.40; Fig.6.4A). Both absolute (p=0.91) and relative (p=0.20) liver weights were similar across diets in TNF$^{-/-}$ dams (Fig. 6.4a).
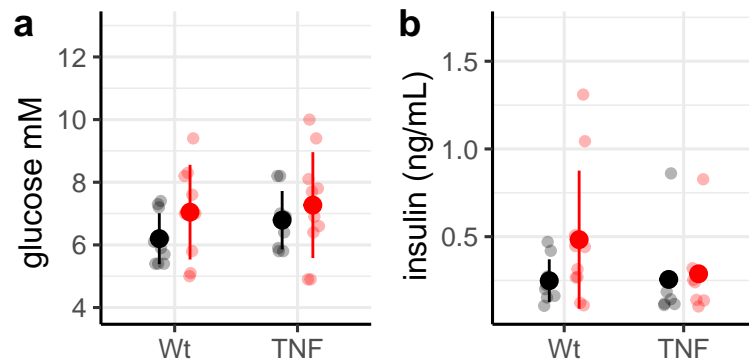
Figure 6.3. Maternal whole-blood glucose and serum insulin not affected by diet or genotype. Individual data points are shown as well as the mean and standard deviation. Significance was assessed by linear model with diet and genotype as interacting fixed effects (TNF$^{-/-}$, n=7-10 per group; Wt, n=9-10 per group).

We next investigated whether HF diet impacted maternal adipose depots. Absolute and relative mesenteric fat mass did not differ with HF diet in either Wt and TNF$^{-/-}$ dams, but both were significantly lower in TNF$^{-/-}$ dams than in Wt dams (main effect of genotype p<0.0001; Fig. 6.4b). In Wt dams, HF diet was associated with increased absolute (p=0.00016) and relative (p=0.00045) gonadal fat mass (Fig. 6.4c). This HF diet-induced increase in adiposity was absent in TNF$^{-/-}$ dams; both absolute (p=0.28) and relative (p=0.083) gonadal fat mass were similar across diets in TNF$^{-/-}$ dams.
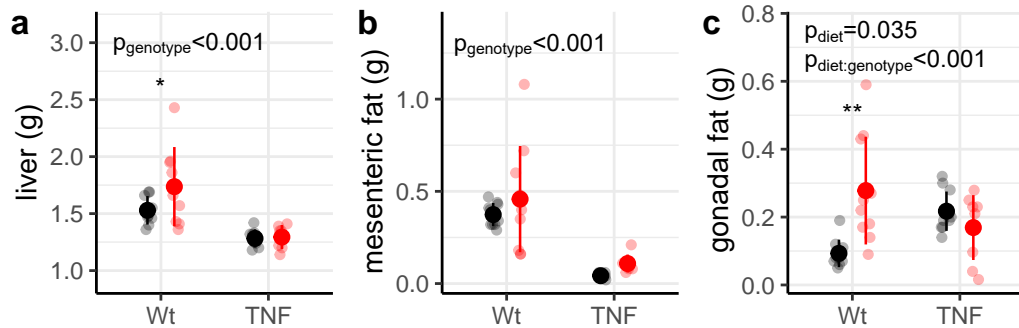
Figure 6.4. Effect of diet and genotype on weights of maternal liver and fat depots. Individual data points are shown as well as the mean and standard deviation. Significance was assessed by linear model with diet and genotype as interacting fixed effects ($TNF^{-/-}$, n=7-11 per group; Wt, n=9-10 per group).* indicates p<0.05; ** p<0.01, *** p<0.001 compared to control-fed counterparts.

Although neither diet nor genotype significantly affected litter size or sex ratio (Fig. 6.5a and d), both female (p=0.014) and male (p=0.0015) fetal weights were decreased by HF diet in Wt litters (main effect of diet in Wt, p=0.00072) but not in $TNF^{-/-}$ litters (main effect of diet in $TNF^{-/-}$, p=0.45; Fig. 6.5b). Among $TNF^{-/-}$ fetuses, males were heavier than females (main effect of sex, p=0.0025), but weights of male and female Wt fetuses were similar (main effect of sex, p=0.17). In Wt, but not $TNF^{-/-}$ mice, male placentas were heavier than female placentas (main effect of sex, p<0.0001) in both control (p=0.00016) and HF litters (p=0.044; Fig. 6.5c). This corresponded to greater fetal weight:placental weight ratio in Wt females compared to Wt males (main effect of diet, p=0.00002) in both control (p=0.0064) and maternal HF diet groups (p=0.013; Fig. 6.5e). Using the ratio as a marker of placental efficiency, these data suggest that female placenta may be more efficient than males in Wt litters. Fetal WBG was higher in male Wt fetuses than in female Wt fetuses (main effect of sex, p=0.022) but this was not significant among $TNF^{-/-}$ fetuses (main effect of sex,

p=0.069; Fig. 6.5f). These data suggest that fetal-placental growth patterns, and
their response to maternal HF diet, differ in the absence of TNF.
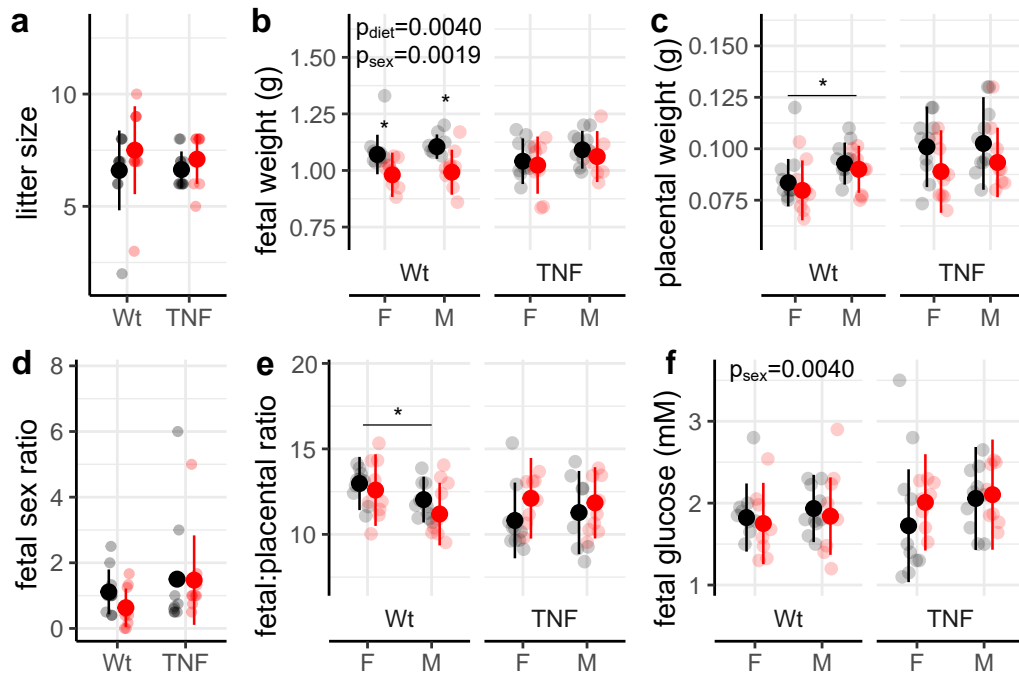
Figure 6.5. Fetal phenotype by sex and genotype. Individual
data points are shown as well as the mean and standard deviation.
Significance was assessed by linear model with diet, sex, and genotype
as interacting fixed effects (TNF$^{-/-}$, n=7-11 per group; Wt, n=9-10
per group). * indicates p<0.05; ** p<0.01, *** p<0.001 compared to
control-fed counterparts.

6.2.2 Impacts on the maternal gut microbiome

Maternal fecal samples were collected prior to dietary randomization at week 0
(W0), before mating (E0), and at term gestation (E18.5). Bacterial DNA present
in fecal samples was assessed by 16S rRNA gene sequencing of the combined
variable 3 and 4 (V3-V4) region amplicons from 30 cycles of PCR amplification
(see Methods 2.4 for details).

To evaluate differences in within-sample alpha diversity, the Shannon Index was used as a measure of richness and evenness (234) (Fig. 6.6). The impacts of diet, genotype, and sample time on alpha diversity were assessed by a mixed linear model, with those factors as interacting fixed effects and individual mouse ID as a random effect. Alpha diversity was similar between Wt and TNF$^{-/-}$ dams (main effect of genotype, p=0.44), and was decreased by HF diet in both Wt and TNF$^{-/-}$ dams after 6 weeks of dietary intervention (E0; Wt, p=0.010; TNF$^{-/-}$, p=0.033) and this decrease persisted to term gestation (E18.5; Wt, p<0.0001; TNF$^{-/-}$, p<0.0001). In Wt dams, this was mediated by increased alpha diversity in controls at E18.5 compared to E0 (p=0.044), suggesting an effect of pregnancy on alpha diversity that was absent in Wt HF dams (p=0.71). In TNF$^{-/-}$ dams, however, alpha diversity did not change with pregnancy in controls (p=0.56) but decreased with pregnancy in HF dams (p=0.026). These data suggest that, at least in control-fed dams, TNF may influence a pregnancy-induced shift in the microbiota.

We next evaluated overall community composition between samples (beta diversity) using Bray-Curtis dissimilarity and visualized these data by principal coordinate analysis (PCoA) across the 4 axes that explained the greatest amount of variation (Fig. 6.7). When all samples were analyzed together, the majority of variation between samples was explained by genotype (R^2 =0.21, p=0.001) and individual mouse (R^2 =0.30, p=0.001) with significant effects of diet (R^2 =0.08, p=0.001) and sample time (R^2 =0.09, p=0.001; PERMANOVA, Fig. 6.7).

Within genotypes, HF shifted microbiota community composition before pregnancy (E0) and at term gestation (E18.5) in both Wt (E0, R^2 =0.37,
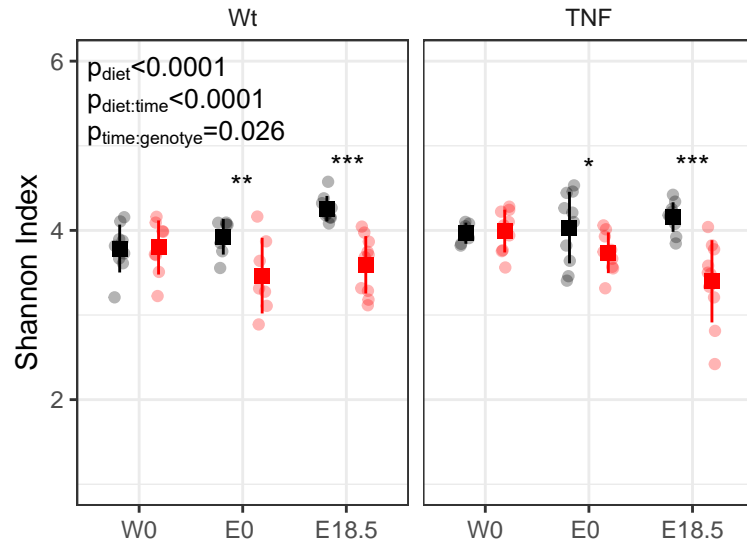
Figure 6.6. Alpha diversity by genotype and diet across sample times. HF diet (red) decreased alpha diversity compared to controls (black) in both Wt and TNF$^{-/-}$ dams. Individual data points are shown as well as the mean and standard deviation. Significance was assessed by linear model with diet and genotype as interacting fixed effects (Wt, n=7-9 per group; TNF$^{-/-}$, n=6-10 per group). * indicates p<0.05; ** p<0.01, *** p<0.001 compared to control-fed counterparts.

p=0.001; E18.5, R^2 =0.41, p=0.001) and TNF$^{-/-}$ dams (E0, R^2 =0.35, p=0.001; E18.5, R^2 =0.35, p=0.001). Additionally, pregnancy shifted microbiota community composition (E18.5 vs. E0) in both Wt (control (C), R^2 =0.11, p=0.001; HF, R^2=0.13, p=0.003) and TNF$^{-/-}$ dams (C, R^2 =0.10, p=0.013; HF, R^2=0.26, p=0.001). Together these data suggest that both diet and pregnancy drive shifts in microbiota community composition and these effects are not TNF dependent.

We next investigated which specific taxa contribute to these overall shifts in community composition using differential abundance testing (DESeq2, RRID: SCR_015687; Fig. 6.9 and see taxa summaries in Fig. 6.8). Overall, 62 genera
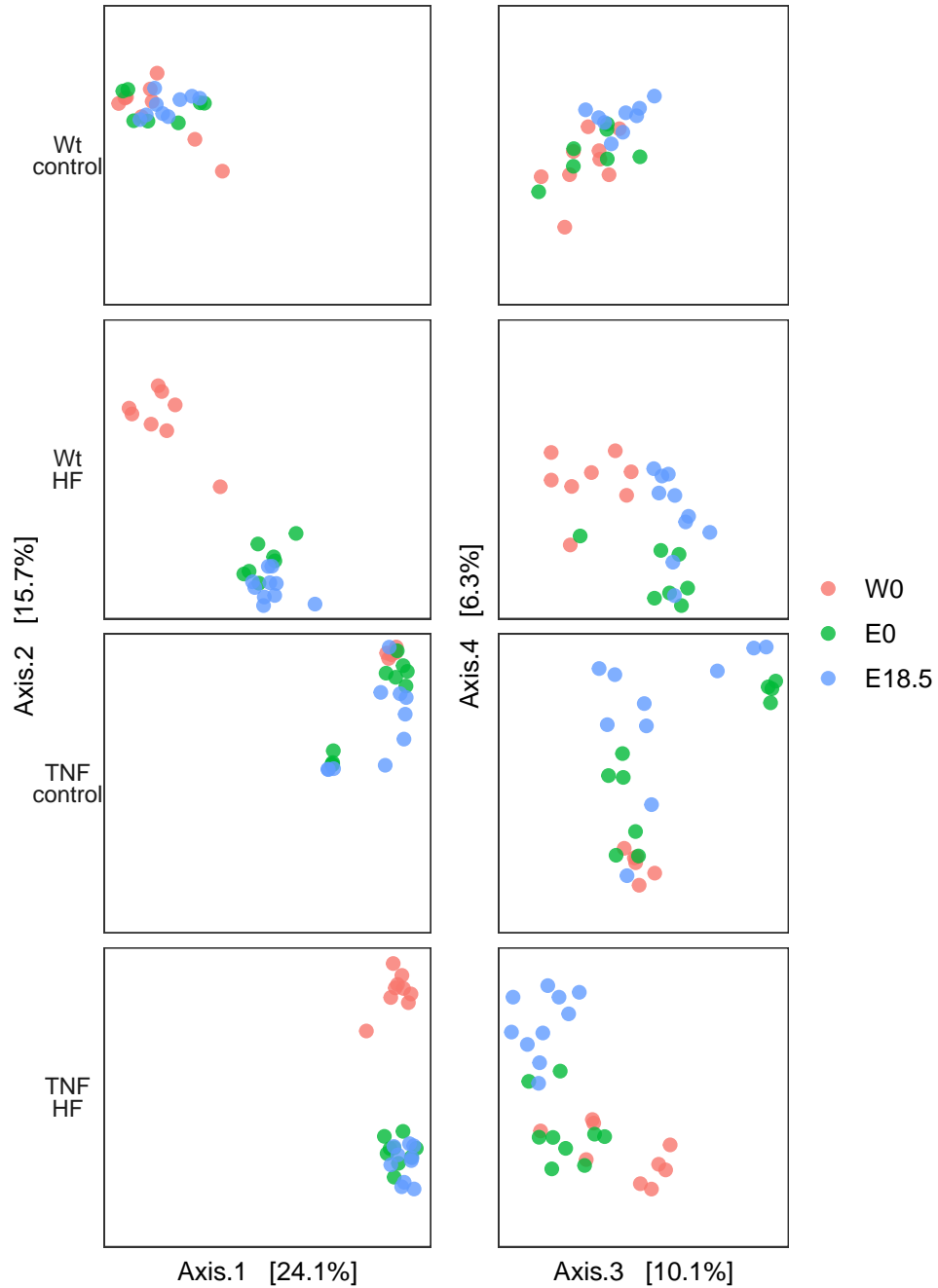
Figure 6.7. PCoA of Bray-Curtis Dissimilarity beta diversity by genotype and diet across sample times. Points represent individual samples and are coloured by sample time (W0, red; E0, green; E18.5 blue). The first four axes, explaining the largest percentages of variation, are shown, faceted by genotype and diet.

differed significantly with HF diet: 33 genera in both Wt and TNF$^{-/-}$ dams, 19 genera in only TNF$^{-/-}$ dams, and 10 genera in only Wt dams (Fig. 6.9). HF diet was associated with decreased relative abundances of an unknown member of the family *Muribaculaceae* in both Wt and TNF$^{-/-}$ dams, and additionally associated with decreased *Muribaculum* in Wt dams only. *Muribaculaceae* species can degrade a variety of complex carbohydrates (297), and are key mucin degraders (298) linked to short-chain fatty acid (SCFA) production (299). The relative abundances of *Bacteroides* and *Parabacteroides*, the second and fifth most abundant genera overall, were increased by HF diet in both Wt and TNF$^{-/-}$ dams at term gestation (E18.5). *Bacteroides* (300) and *Parabacteroides* (301) species also metabolize host-mucins, and *Bacteroides* can induce colitis in genetically-susceptible mice (302). Together, these shifts indicate HF diet and pregnancy may interact to alter microbe-host mucin metabolism in both Wt and TNF$^{-/-}$ dams.

Despite this, some shifts in key mucin degraders were genotype-dependent. Akkermansia was significantly decreased with HF diet in Wt at E18.5 but increased with HF diet in TNF$^{-/-}$ dams at both E0 and E18.5. This genotype-effect was replicated in our littermate cohort (Appendix C) but is in contrast to our previous Wt cohort (Chapter 5 (265)) where *Akkermansia* was increased with HF diet, so the difference observed here between Wt and TNF$^{-/-}$ in response to HF diet may not be due to the absence of TNF. A similar pattern was seen for the genus *Parasutterella*, which was decreased by HF diet in Wt dams but increased by HF diet in TNF$^{-/-}$ dams at E18.5. The abundance of *Parasutterella* has previously been found to be reduced by HF diet (303, 304)
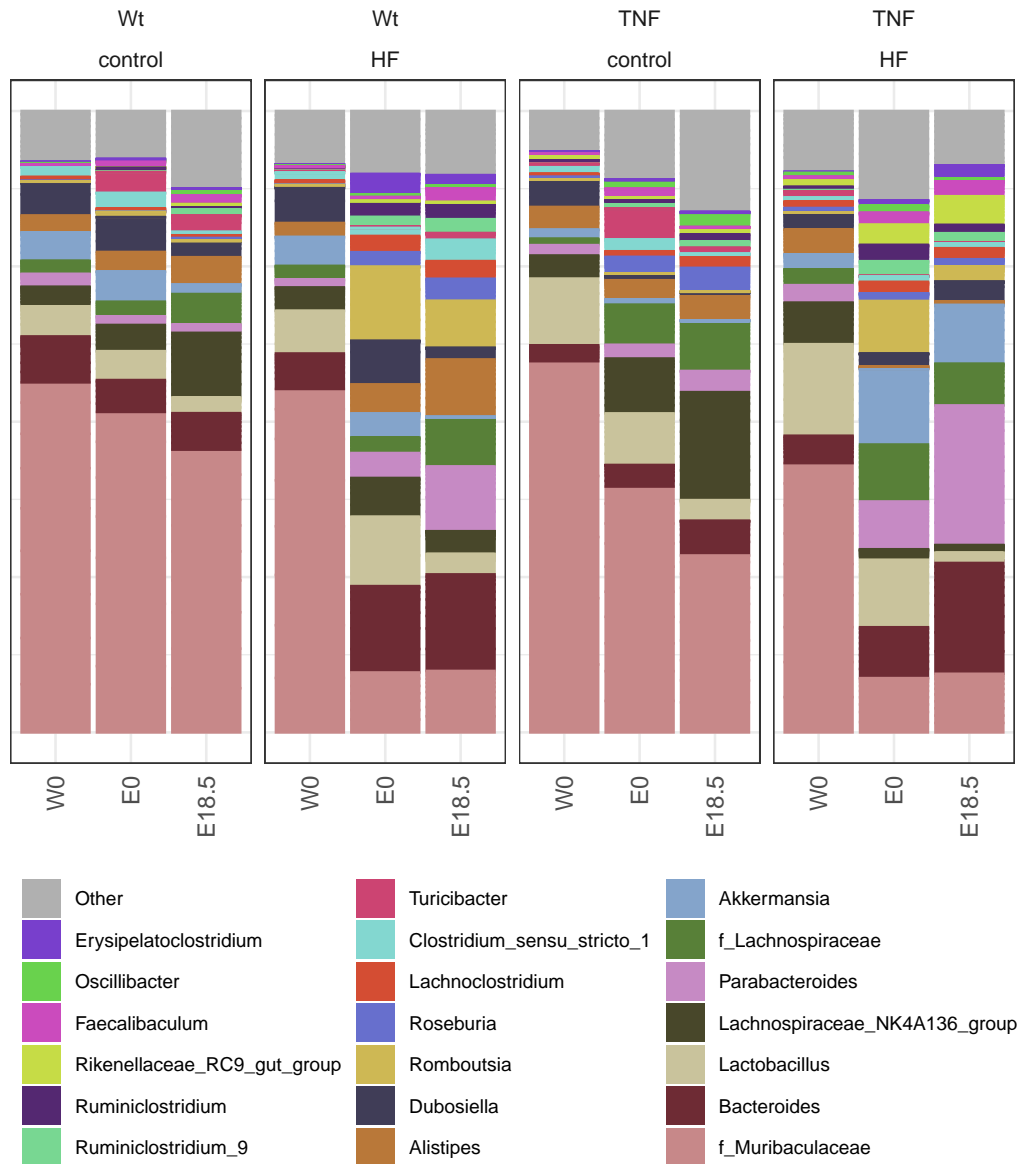
Figure 6.8. Relative abundance of the 20 most abundant genera. Mean relative abundances were calculated for each sample time (W0, E0, and E18.5) within genotype (Wt and TNF$^{-/-}$) and diet group (control and HF) and plotted as stacked bar plots.
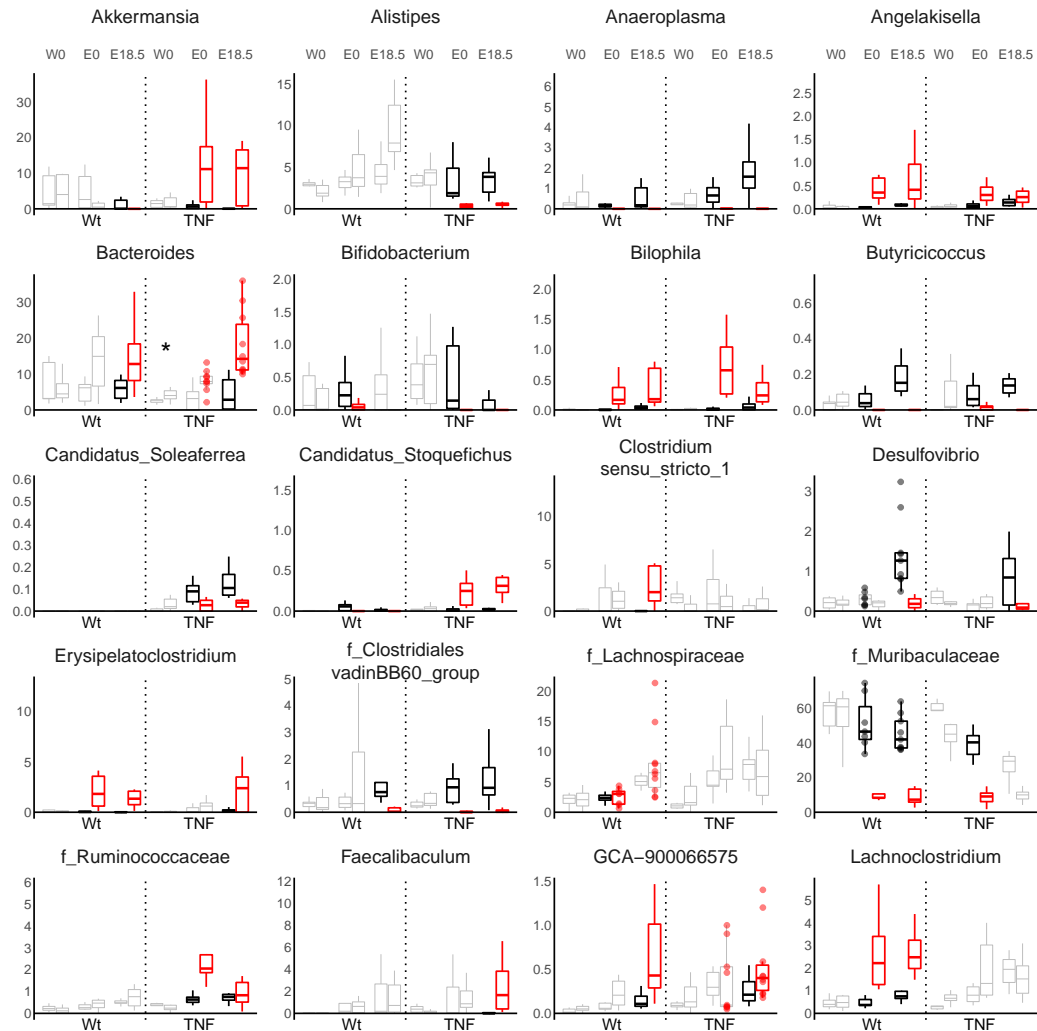
Figure 6.9. Bacterial genera significantly enriched or depleted by diet or pregnancy. Box plots of the relative abundance of each genus at each sample time point (baseline at week 0, W0; before mating, E0; term gestation, E18.5) for control (black) and HF (red) wildtype (Wt) and TNF$^{-/-}$ (TNF) dams and are shown for genera significantly affected by diet (coloured box plot indicates significance relative to control within that genotype and sample time point) or pregnancy (coloured points indicate significant difference at E18.5 relative to E0 within that genotype and diet). Genera that differed significantly by genotype at baseline (W0) are indicated by an asterisk. Significance was assessed by DESeq2.The box plot centre line represents the median; the box limits represent the upper and lower quartiles; the whiskers represent the 1.5x interquartile range.

Figure 6.9. continued. Bacterial genera significantly enriched or depleted by diet or pregnancy.
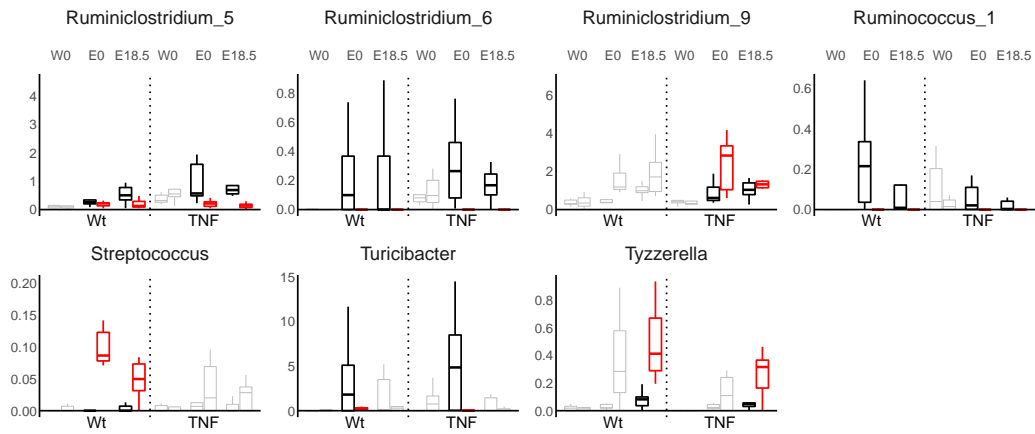
Figure 6.9. continued. Bacterial genera significantly enriched or depleted by diet or pregnancy.

and linked to mucin O-glycan fucosylation (305). These differences between genotypes suggest the absence of TNF may alter the effect of HF diet on host mucin synthesis and bacterial mucin degradation.

Overall, 10 genera were significantly affected in the same direction by HF diet in both Wt and TNF$^{-/-}$ dams at both E0 and E18.5. Although 6 of these 10 genera belonged to the SCFA producing family *Ruminococcaceae* (4 decreased and 2 increased by HF diet) the overall abundance of this family was unchanged by HF diet. *Lactococcus* was increased by HF diet in both genotypes at both time points, but this is likely a non-viable dietary contaminant as non-viable *Lactococcus* contamination was recently shown to be widespread in casein-containing high-fat research diets (306), such as the one used in this study.

Additionally, 2 genera were significantly affected by HF diet in opposite directions in Wt and TNF$^{-/-}$ dams at both E0 and E18.5: *Candidatus Stoquefichus* was decreased by HF in Wt dams but increased by HF in TNF$^{-/-}$

dams and *Roseburia* was increased by HF diet in Wt dams but decreased by HF diet in TNF$^{-/-}$ dams. *Candidatus Stoquefichus* is an uncultured member of the family *Erysipelotrichaceae*, which was increased overall at E18.5 in TNF$^{-/-}$ but not Wt dams (log2 fold change = 2.59, p<0.0001). TNF is a negative regulator of bile acid synthesis (307), and its inhibition enhances bile acid excretion in response to HF diet (308). As bile salt hydrolase genes are abundant in *Roseburia* and *Erysipelotrichaceae* species (309), these differential effects of HF diet by genotype may be due to differences in host bile acid metabolism. Together these data suggest that many, but not all, of the impacts of HF on specific genera are independent of host TNF, and the absence of TNF may specifically impact genera involved in mucin and bile acid metabolism.

We next investigated which specific genera contribute to the shift in microbiota community composition seen with pregnancy. The only genus that was consistently differentially abundant with pregnancy in both Wt and TNF$^{-/-}$ control dams was a member of the order *Rhodospirillales* of the *Alphaproteobacteria*, which was decreased at E18.5 compared to E0 (Fig. 6.9). The unknown genera of the family *Muribaculaceae* that was decreased by HF diet in both Wt and TNF$^{-/-}$ dams was also decreased by pregnancy in Wt control dams, but this decrease was not significant in TNF$^{-/-}$ control dams. This suggests that both pregnancy and HF diet may impact the abundance of this genus through a shared mechanism, potentially involving host-mucin production (298). The relative abundances of *Bacteroides* and *Parabacteroides*, which were increased by HF diet in both Wt and TNF$^{-/-}$ dams, were also increased with pregnancy in HF TNF$^{-/-}$ dams, but these increases were not significant in control

TNF$^{-/-}$, control Wt, or HF Wt dams. Together, these data suggest that many of the impacts of pregnancy on specific genera interact with the impacts of HF diet in genotype-specific ways, potentially due to differences in mucin metabolism.

To investigate differences in functional products of microbial metabolism due to these differences in gut microbiota composition, we measured SCFA concentrations by gas chromatography-mass spectroscopy (GC/MS) in cecal contents collected from pregnant dams at E18.5 by (Fig. 6.10). We found HF diet-induced elevated levels of cecal lactate (main effect of diet, p=0.00014) in both Wt (p=0.023) and TNF$^{-/-}$ dams (p=0.00086; Fig 6.10). In contrast, HF diet-induced decreased levels of cecal butyrate (main effect of diet, p=0.0056), particularly in TNF$^{-/-}$ dams (p=0.0056). These data are consistent with our previous observations in Wt dams (Chapter 5 (265)) and with our observed decrease in the relative abundances of butyrate producers including *Lachnospiraceae NK4A136* (Figs. 6.8 and 6.9). As butyrate is the main energy source of intestinal colonocytes and is important in maintaining gut barrier function [52], these data may suggest that HF diet impacts on intestinal structure and function are likely due to indirect contributions of a changing microbial environment and downstream production of metabolites. While propionate concentrations were below the limit of detection, its levels have previously been correlated with *Muribaculaceae* abundance (310), which was one of the genera most decreased in relative abundance by HF diet in this study.

Overall, these data indicate that the majority of differentially abundant genera due to HF diet alone are independent of TNF, while differentially abundant genera due to pregnancy, or the interaction of HF diet and pregnancy,
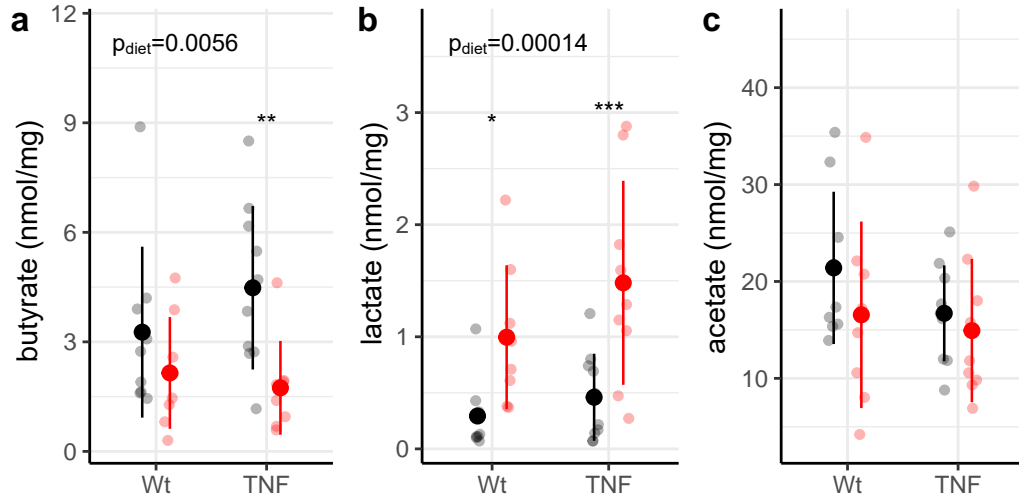
Figure 6.10. HF-diet is associated with decreased butyrate and increased lactate in cecal contents. SCFA concentrations were measured by GC/MS and significance assessed by linear model with genotype and diet as fixed effects. * indicates $p<0.05$; ** $p<0.01$, *** $p<0.001$ compared to control-fed counterparts.

were more variable between Wt and TNF$^{-/-}$ dams. This suggests that the changes in cecal SCFA levels observed at term gestation with HF diet may be differentially mediated by microbial shifts due to pregnancy, diet, and the interaction between pregnancy and diet in Wt and TNF$^{-/-}$ dams. As many of the genera that were differentially affected by HF or pregnancy in Wt and TNF$^{-/-}$ dams are involved in mucin degradation, these differences may be driven in part by TNF-mediated differences in host mucin production.

6.2.3 Maternal intestinal structure and function: role of ER Stress

Given the extensive changes that we observed in maternal phenotype and microbiota community composition, we next evaluated the impact of diet on

maternal intestinal structure and function at E18.5, and whether TNF impacted the relationship between diet, microbes, and the maternal intestine. HF diet decreased intestinal villus goblet cell (GC) density (GC count per 100 μM villus length) in both Wt (p=0.0083) and TNF$^{-/-}$ (p=0.016) dams (main effect of diet, p=0.0012; Fig. 6.11a). In Wt dams, this change was due both to a decrease in goblet cell count (p=0.049, Fig. 6.11b) and an increase in villus length (main effect of diet, p=0.031; Fig. 6.11c).

We observed no changes due to HF diet in crypt goblet cell density, goblet cell counts, or crypt length in ileums or colons (Fig. 6.11d-i). Although generally, TNF$^{-/-}$ dams had fewer goblet cells (main effect of genotype, p=0.023) and shorter crypt depths in their colons (main effect of genotype, p=0.012) than Wt dams, suggesting that TNF plays a role in host-mucin production in the colon of pregnant mice.

To investigate the mechanisms driving these HF diet-induced changes to maternal intestinal morphology, we measured transcript levels of key factors that regulate intestinal structure via quantitative polymerase chain reaction (qPCR). Previous work suggests that increased paracellular permeability in the intestine may be due to decreased expression of tight junction proteins (311, 312). However, despite showing changes in intestinal morphology (crypt depth and goblet cell number) and previously reporting increased intestinal permeability (Chapter 5 (265)) we did not observe significant changes in transcript levels of a key intercellular *tight junction protein 1 (Tjp1)* in dams fed a HF diet (main effect of diet: ileum p=0.093, colon p=0.35, Fig. 6.12a,b). Tjp1 is a key scaffold protein that binds to several proteins to form a junction between intestinal
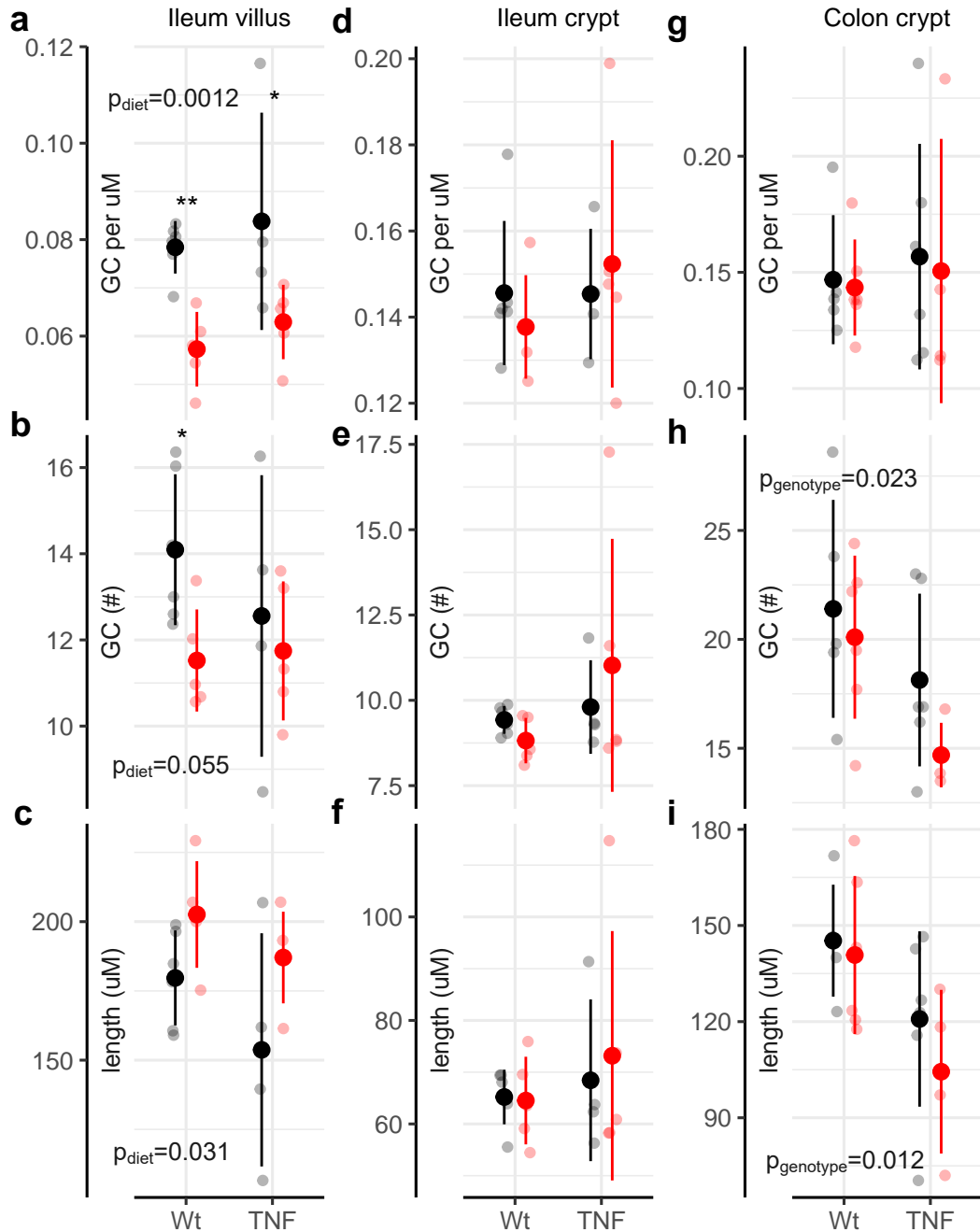
Figure 6.11. Maternal intestinal morphology is impacted by HF diet. Individual data points are shown as well as the mean and standard deviation for control (black) and HF dams (red). Significance was assessed by linear model with genotype and diet as interacting fixed effects (n=4-6 per group). * indicates $p < 0.05$; ** $p < 0.01$, *** $p < 0.001$ compared to control-fed counterparts.

epithelial cells. A lack of difference in *Tjp1* transcripts is in contrast to our previous report (Chapter 5 (265)) of a decrease in *Tjp1* mRNA levels in the ileum of pregnant dams fed a HF diet.

We also did not find any differences between groups in transcript levels of SCFA receptors *G protein-coupled receptor (Gpr)*41 or *Gpr*43 in the ileum or colon of Wt or TNF$^{-/-}$ dams (Fig. 6.12g-j). However, in Wt dams HF diet decreased ileum transcript levels of *Cldn2* (p=0.037) and *Muc*2 (p=0.036; main effect of diet, p=0.0068). Claudin-2 protein forms actively gated channels that are selective for water and small cations including sodium (Na+) (313), and mucin-2 is the principal structural component of the mucus membrane, which is densely packed in goblet cells and its expansion upon secretion is partially mediated by lumenal sodium ions (314). These data suggest that HF diet may impair the intestinal mucus barrier through an interaction of decreased *Muc*2 and *Cldn2* in Wt but not TNF$^{-/-}$ dams.

As previous work has shown that Muc2 secretion is triggered LPS signalling through toll-like receptor (Tlr)4 (315), our observation of decreased *Muc*2 messenger RNA (mRNA) levels is consistent with observed decreases in *Tlr*4 mRNA levels in the ileum of Wt dams (p=0.0.039; main effect of diet, p=0.022; Fig. 6.13a). This decrease in ileum *Tlr*4 mRNA levels differs from our previous cohort, where we found HF diet to be associated with increased mRNA levels of *Tlr*4 in colons of Wt dams (Chapter 5). As the dams from our previous cohort were not bred in-house, this difference between cohorts may be related to differences in the composition of the gut microbiome in the current in-bred mice that comprised this study. One of the most notable differences in the gut
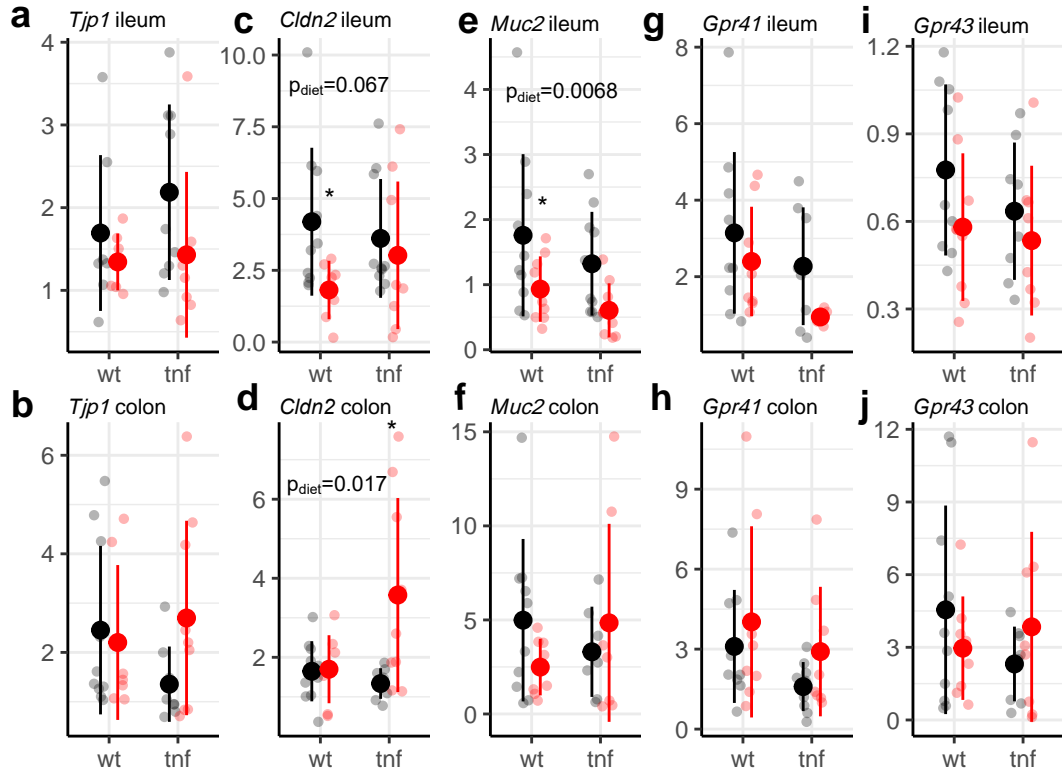
**Figure 6.12. HF diet altered maternal transcript levels of
gut barrier markers** in Wt and TNF$^{-/-}$ dams. Individual values
for mRNA levels are plotted with the mean and standard deviation
within genotype for control (black) and HF (red) ileums and colons.
Significance was assessed by linear model with diet and genotype as
fixed effects, and pairwise post-hoc comparison within genotypes.(n=8-
10 per group). * indicates $p<0.05$; ** $p<0.01$, *** $p<0.001$ compared
to control-fed counterparts.

microbiome of Wt dams in this cohort compared to our previous cohort (Chapter
5) is the increase in *Bacteroides* with HF diet, in both Wt and TNF dams,
whereas *Bacteroides* was decreased with HF diet in our previous cohort (Chapter
5 (265)). The tetra- and penta-acylated lipid A domains of *Bacteroides* LPS have
previously been shown to inhibit Tlr4 activation and endotoxin tolerance (84).
Therefore, the increase in *Bacteroides* abundance with HF diet in this cohort
may have inhibited the upregulation of Tlr4.
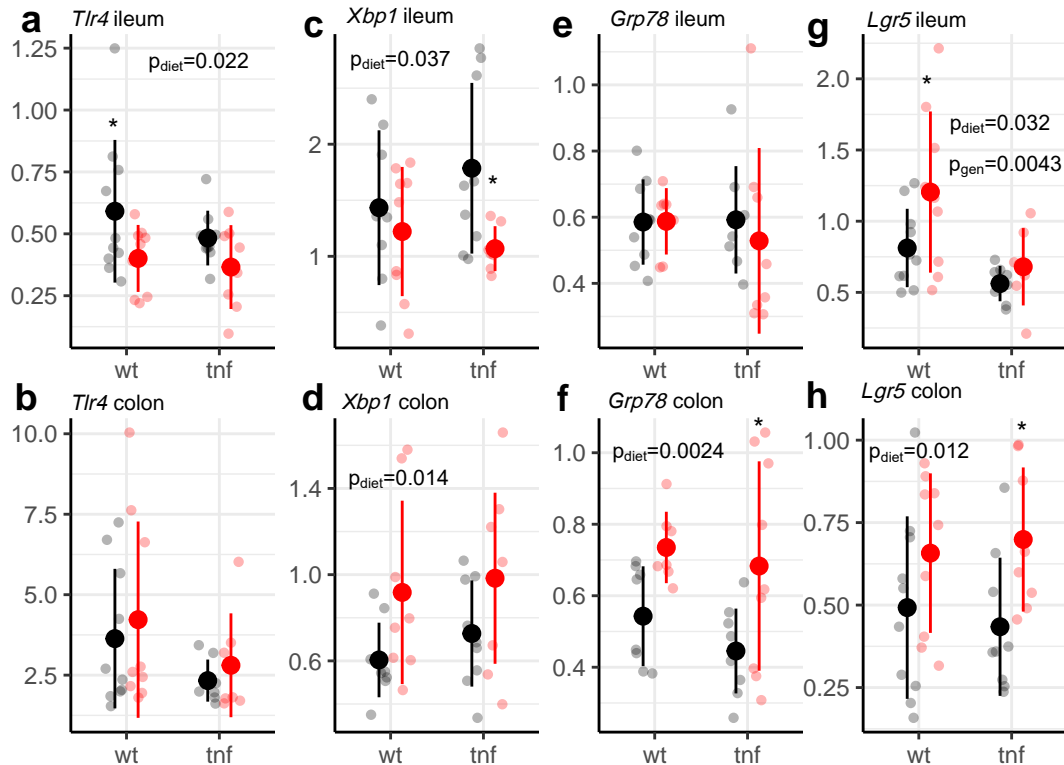
Figure 6.13. HF diet altered maternal transcript levels of ER stress markers in Wt and TNF$^{-/-}$ dams. Individual values for mRNA levels are plotted with the mean and standard deviation within genotype for control (black) and HF (red) ileums and colons. Significance was assessed by linear model with diet and genotype as fixed effects, and pairwise post-hoc comparison within genotypes.(n=8-10 per group). * indicates p<0.05; ** p<0.01, *** p<0.001 compared to control-fed counterparts.

Translation of secreted and membrane-bound proteins such as Muc2 requires ER homeostasis, and HF diet-intake has previously been shown to induce ER stress in Wt mice (316). HF diet decreased colonic mRNA levels of the unfolded protein response (UPR) signalling molecule *X-box binding protein 1 (Xbp1)* (main effect of diet, p=0.014) and ER chaperone *Gpr*78 (main effect of diet, p=0.0024) independent of genotype (Fig. 6.13c-f). HF diet has previously been shown to enhance the number and regenerative capacity of leucine-rich repeat-containing

G protein-coupled receptor 5 (Lgr5)+ intestinal stem cells (ISCs) (317) through increased Wnt signalling (318). This is consistent with increased mRNA levels of *Lgr5* with HF diet in the ileum (main effect of diet, p=0.032) and colon (main effect of diet, p=0.012). However, in non-pregnant animals, this effect is dependent on TNF (318), while we observed it in both Wt and TNF$^{-/-}$ dams at E18.5. As HF diet did not impact colon goblet cell number or crypt length, these increases in ISC and ER stress markers may be in response to increased colonic inflammation driven by IL-1β (316) but we did not test this directly.

Together, these data indicate that HF diet may impair the production of the intestinal mucus barrier in the ileum and that the absence of TNF may be somewhat protective. This is consistent with our microbiota data, where many of the genera that were differentially affected by HF or pregnancy in Wt and TNF$^{-/-}$ dams are involved in mucin degradation. Additionally, these data suggest HF diet increases some markers of ER stress in the colons of both Wt and TNF$^{-/-}$ dams at term gestation, but this was not associated with altered colonic transcript levels of gut barrier markers. These data highlight the need to perform a more detailed evaluation of the ultrastructure of the maternal gut during pregnancy, to localize tight junction proteins and observe whether at the protein level these key mediators of paracellular permeability are structurally altered.

6.2.4 Fetal intestinal cell stress pathways

Maternal obesity results in offspring metabolic dysfunction (319) that has been associated with shifts in offspring gut microbial populations (236). Shifts in the offspring microbiome may be predicated on altered fetal gut development prior to

colonization. Part of our aim was to investigate the role of TNF in mediating the impact of maternal high-fat diet or obesity on offspring outcomes. We hypothesized that maternal inflammation would induce ER stress in the fetal gut and change fetal gut development and structure. Indeed, the gut is a key metabolic and immune organ, and its development in utero is sensitive to programming effects that can impact offspring health (168). So far, we have conducted pilot analyses of in the fetal gut via qPCR but complete analysis including fetal gut histology has been delayed by the pandemic.

Contrary to our hypothesis, maternal HF diet did not increase ER stress in the Wt fetal gut, and transcript levels of markers of the UPR were decreased. Maternal HF diet was also associated with increased mRNA levels intestinal barrier markers including *Muc*2, the principle component of the epithelial mucus barrier, and the tight-junction adhesion components *Ocln* ($p < 0.0001$) and *Tjp1* ($p < 0.05$ in females only; Chapter 5 (265)). Unlike in Wt mice, in the TNF$^{-/-}$ fetal small intestine, maternal HF diet was not associated with any significant change in mRNA levels of *Muc*2 or UPR markers *78-kDa glucose-regulated protein (Grp78), activating transcription factor (Atf)4, CCAAT-enhancer-binding protein homologous protein (Chop)*, or *Xbp1*. As the UPR is necessary for intestinal epithelial differentiation (320), these data suggest that TNF may contribute to impaired intestinal development with maternal HF diet.

Despite the observed decrease in UPR activation in Wt fetal small intestines, NF-κB activity was increased (Chapter 5 (265)). In TNF$^{-/-}$ fetuses, this maternal HF diet-induced increase was absent both in small intestines (main effect of diet, $p=0.90$) and large intestines (main effect of diet, $p=0.98$; (Fig. 6.15). Our
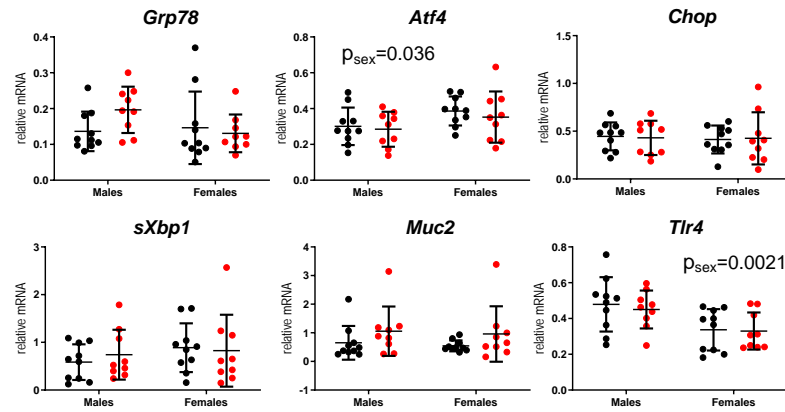
Figure 6.14. UPR and gut barrier markers are not impacted by maternal HF diet in TNF$^{-/-}$ fetal small intestine. Individual values for mRNA levels are plotted with the mean and standard deviation within genotype for control (black) and HF (red) fetal small intestine. Significance was assessed by Bonferroni-adjusted two-way ANOVA.(n=9-10 per group). * indicates p<0.05; ** p<0.01, *** p<0.001 compared to control counterparts.

hypothesis that maternal HF diet influences fetal intestinal development is supported by increased protein levels of active β-catenin in Wt fetuses (p=0.021; Fig. 6.16), indicating increased Wnt signalling, which has been linked to precocious Paneth cell differentiation at E18.5 (128). This increase was absent in TNF$^{-/-}$ fetuses (main effect of diet, p=0.59). Together, these data support the hypothesis that TNF is a key mediator of the effects of maternal HF diet on fetal gut development and future experiments will evaluate which signalling pathways are central to this relationship.
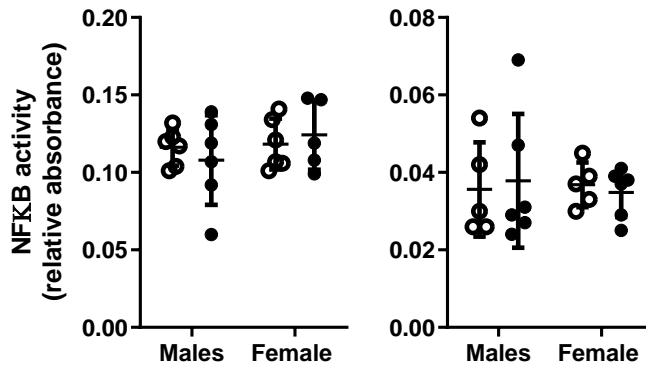
Figure 6.15. Maternal HF diet does not increase NF-κB activation in fetal small or large intestine in TNF$^{-/-}$ mice. Individual values for mRNA levels are plotted with the mean and standard deviation within genotype for control (white) and HF (black) fetal small intestine. Significance was assessed by Bonferroni-adjusted two-way ANOVA.(n=5-6 per group).
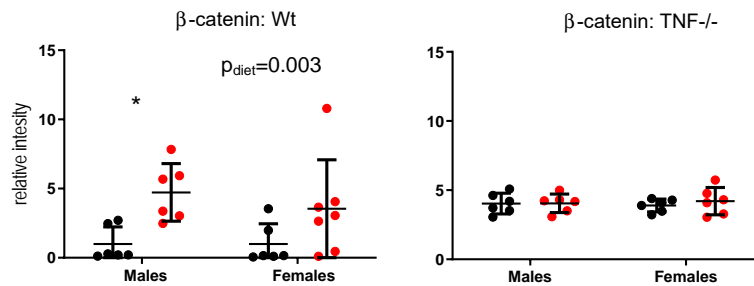
Figure 6.16. Maternal HF diet increases Wnt activity in Wt but not TNF$^{-/-}$ fetal small intestine Individual values for mRNA levels are plotted with the mean and standard deviation within genotype for control (black) and HF (red) fetal small intestine. Significance was assessed by Bonferroni-adjusted two-way ANOVA.(n=6-7 per group). * indicates p<0.05; ** p<0.01, *** p<0.001 compared to control counterparts.

6.3   Discussion

In our previous Wt cohort (Chapter 5 (265)) we found that a maternal high-fat diet was associated with a proinflammatory maternal milieu, characterized by increased serum levels of TNF, decreased maternal gut barrier function, and altered fetal gut development. This study investigated whether TNF-mediated systemic inflammation was a key player in maternal intestinal and microbial adaptations to HF diet in pregnancy using a TNF$^{-/-}$ model. We found that Wt HF females gained more weight prior to pregnancy compared to TNF$^{-/-}$ HF females and that this persisted throughout pregnancy. We also found the relative abundances of specific genera involved in mucin degradation were differentially affected by HF diet or pregnancy in Wt and TNF$^{-/-}$ dams, and these microbial shifts were accompanied by genotype-specific changes in intestinal mucus-producing goblet cells. Finally, we extended our previous observation that maternal HF diet impaired fetal intestinal development in Wt mice by finding that these changes appear to be TNF dependent. Together these data suggest that maternal TNF-mediated proinflammatory signalling regulates some of the impacts of HF diet on maternal intestinal and microbial adaptations to pregnancy, and on fetal gut development.

While the inflammatory effects of HF feeding are best characterized in male mice, a recent study demonstrated that like their male counterparts, non-pregnant female HF-fed TNF$^{-/-}$ mice weighed less than their HF-fed Wt littermates (321), though the effect was less pronounced than the effect we observed this study. This suggests that TNF signalling plays a role in adipose accumulation in response to HF diet in non-pregnant and pregnant female mice.

We show that HF diet in Wt, but not TNF$^{-/-}$ pregnancies, reduces birth weight – particularly in female fetuses (Fig. 6.5). Traditionally, maternal HF diet and obesity have been associated with fetal macrosomia (322, 323); maternal obesity and hyperglycemia results in increased transplacental transfer of nutrients (324), increased placental and fetal-growth-stimulating insulin-like-growth factors (325) and placental inflammation (277) all of which drive fetal growth. There are, however, reports of intrauterine growth restriction, where increasing maternal body mass index (BMI) correlated with significantly smaller ultrasound fetal measures than expected (326–328). A recent study suggests that this discrepancy is also sex-specific where female embryos grew more slowly in pregnancies complicated by obesity (329). Recent work in mice, also suggests that maternal obesity was associated with fetal growth restriction at mid and late pregnancy, where females appear more vulnerable (330). We and others have shown that maternal obesity is associated with placental hypoxia (Chapter 5 (265)) which is consistent with data showing that maternal high-fat diet is associated with a reduction in placental genes that are required for appropriate development of placental vasculature (330). Reduced blood flow and hypoxia have been suggested to drive this reduction in fetal growth. However, whether these changes arise because of, or are in parallel with drivers of, inflammation has not been conclusively established.

Other data suggest that maternal obesity-related inflammation is associated with changes in maternal intestinal microbial profiles. Data from our lab (284) and others (93) show that as pregnancy progresses, gut microbial load increases, bacterial composition shifts and the abundance of certain bacteria, including

Proteobacteria, increases (106). Intriguingly, high Proteobacteria abundance is associated with gut dysbiosis in inflammatory gut disorders (94), and it has been suggested that a similar gut dysbiosis occurs during late pregnancy. It has previously been shown that TNF contributes to microbial dysbiosis and that TNF$^{-/-}$ mice are protected from age-related increases in intestinal permeability (331). Our data suggest TNF also contributes to HF diet-induced shifts in the maternal gut microbiota. Although microbial alpha-diversity was similar between Wt and TNF dams, pregnancy was associated with increased alpha diversity in control Wt dams but not in control TNF$^{-/-}$ dams. Conversely, pregnancy was associated with decreased alpha diversity in HF TNF$^{-/-}$ dams, but not in HF Wt dams. This indicates that TNF may mediate microbial shifts that occur over the course of pregnancy.

The impact of TNF in pregnancy-related microbiota composition shifts and the additive effect of HF diet was assessed by permutational multivariate analysis of variance (PERMANOVA) analysis of Bray-Curtis dissimilarities. Individual differences between mice explained the largest percentage of variation between samples ($R^2 =0.30$). Within genotypes, pregnancy was associated with a shift in microbial community composition in both Wt and TNF$^{-/-}$ dams. We have previously shown that diet and pregnancy are independently associated with changes in the maternal microbiota (Chapter 5 (265)). Data from this cohort corroborate and extend these observations to suggest that some of these changes may be mediated by TNF.

Consistent with our previous work, HF dams showed significant decreases in the relative abundance of the *Lachnospiraceae* family (Fig. 6.9), which

139

corresponded to decreased cecal butyrate levels (Fig. 6.10). Interestingly, despite its attenuated impact on TNF$^{-/-}$ dam weight, HF diet induced many of the same microbial changes in TNF$^{-/-}$ dams, suggesting TNF may not be a key player in mediating HF diet-induced changes in SCFA producers during pregnancy.

Despite this, Wt and TNF$^{-/-}$ dams differed significantly in their HF diet-induced shifts in mucin-degrading genera. Whereas HF diet decreased *Akkermansia* and in Wt dams, the opposite occured in TNF$^{-/-}$ dams where *Akkermansia* was increased with HF diet. This is in contrast to our previous observations of HF diet-induced increases in *Akkermansia* in pregnant dams (Chapter 5 (265)), but consistent with our littermate cohort (Appendix C), as well as previous studies investigating the impact of obesity and HF diet in male mice (332) and pregnant women (107). TNF dams had a decreased relative abundance of *Akkermansia*, which was increased by HF diet in our previous Wt cohort (Chapter 5). *Akkermansia* has been suggested to be a biomarker of intestinal health (333), but more research is required on its impact on host physiology during pregnancy (91), and if and how TNF regulates its abundance.

A similar interaction was found for *Parasutteralla*, a recently characterized member of the core gut microbiota in humans and mice that has previously been found to be reduced by HF diet (303, 304) and linked to mucin O-glycan fucosylation (305). In this study, the relative abundance of *Parasutterella* was decreased by HF diet in Wt dams but increased by HF diet in TNF$^{-/-}$ dams. We also observed additive increases in mucus-degrading genera *Bacteroides* (300) and *Parabacteroides* (301) with HF diet and pregnancy, particularly in TNF$^{-/-}$ dams. As previous work has shown pregnancy and HF diet independently alter

mucin glycosylation (334, 335), these differences between genotypes suggest the absence of TNF may alter the effect of HF diet on host mucin synthesis and bacterial mucin degradation.

This hypothesis is consistent with HF diet-induced decreased goblet cell counts and *Muc*2 mRNA levels in Wt ileums. As Tlr4 signalling through myeloid differentiation primary response 88 (Myd88) can upregulate *Muc*2 expression (336), these decreases may be related to increases in the relative abundance of the Tlr4 inhibiting genus *Bacteroides* (84). Alternatively, expression of *Muc*2 may be down-regulated to protect against ER stress (337) due to HF diet-induced intestinal epithelial proliferation (317).

The intestinal epithelium requires tight regulation of ER homeostasis to maintain translation of secreted and membrane-bound proteins such as mucins and tight junction proteins. Unlike the genotype-specific effects of HF diet on the ileum, HF diet increased transcript levels of key ER stress markers in both Wt and TNF$^{-/-}$ colons. Long-term HF diet has previously been shown to induce ER stress in Wt mice (316), and our data indicate that this appears independent of TNF. This may impair translation, modification, and assembly of tight junction proteins and mucins, but remains to be investigated. Future work will localize and quantify tight junction proteins in Wt and TNF$^{-/-}$ dams to investigate the role TNF plays in maternal intestinal barrier function.

Despite the known association between maternal obesity and offspring gut dysbiosis (294, 338, 339), the mechanisms driving this relationship remain unclear. Some have hypothesized that the relationship is governed by in utero

141

colonization (either in the fetus or the placenta), but we show that the prenatal fetus is devoid of bacteria (Chapter 3, (222)). A more plausible explanation is the influence of the maternal environment (be it bacterial metabolites such as SCFAs, or in utero inflammation (277)) on fetal gut development. In our previous study (Chapter 5 (265)), maternal HF diet was associated with inhibition of the UPR and activation of NF-κB and in the small intestine of Wt fetuses at E18.5. We hypothesized that these increases may be a homeostatic response to protect the fetal intestine from TNF-induced apoptosis (340). In this study, we found no effect of maternal HF diet on NF-κB activity in TNF$^{-/-}$ fetal intestines, consistent with this hypothesis (Fig. 6.15). Correspondingly, mRNA levels of *Muc*2, *Tlr*4, *Atf*4, *Chop*, and *Grp78* were not increased by maternal HF diet.

In conclusion, our data suggest that maternal TNF-mediated proinflammatory signalling regulates some of the impacts of HF diet on maternal intestinal and microbial adaptations to pregnancy, and on fetal gut development. It is possible that the absence of TNF-mediated intestinal inflammation prevents HF diet-induced increases to maternal gut permeability, and that this prevents fetal exposure to pro-inflammatory microbial components including LPS. Previous studies have found fetal exposure to LPS induced gut inflammation (341), impaired gut barrier development (342), and postnatal intestinal injury (343). Our data show that maternal HF diet-induced fetal intestinal inflammation and altered markers of intestinal development, and that this was dependent on TNF. Future work will investigate whether these effects are associated with altered fetal intestinal tight-junction assembly.

Chapter 7

The impact of maternal diet-induced obesity on offspring gut structure and function

7.1   Introduction

The postnatal effects of in utero adaptation are often modulated by environmental exposures including changes in diet, (344), stress (345) or chemical exposures (346). Many experimental studies have shown additive effects of a postnatal high-fat (HF) diet in offspring born after in utero adversity (347–353). The mechanisms by which this "second hit" creates cumulative risk impacts on offspring are unclear. One understudied driver may be early life gut development.

Normal gut development is key to ensuring a barrier to pathogens (32), appropriate nutrient handling, effective immune development (16) and a niche for

commensal bacteria (10). Our preliminary data suggest that maternal HF diet induces structural/morphological changes to the fetal gut (Chapters 5 and 6, (265)). The early-postnatal period between birth and weaning is a critical "window of opportunity" in establishing host-microbe interactions. "Immune imprinting" has been suggested to occur during this window, when exposure to colonizing microbiota and their metabolites impact gut health (354), and gut barrier integrity (355). "Pathological imprinting" (356) may result due to colonization by a dysbiotic microbiota during this "window of opportunity" (357).

Postnatal gut colonization occurs in predictable patterns (358–360), and although recent reports suggest this may occur in utero (203, 361), it remains controversial (206, 224), and our data suggest that colonization occurs during and after birth (Chapter 3 (222)). The infant gut is colonized by maternal microbiota, initially dominated by facultative anaerobes including *Proteobacteria* (e.g *Enterobacteriaceae*) and *Firmicutes* (e.g. *Streptococcus*) and shifting towards anaerobic communities dominated by *Bifidobacterium*, *Bacteroides*, and *Clostridia* in breastfed infants (358, 360, 362–365). Dietary and immunological components of breast milk shape neonatal gut microbial community structure (88) which is dominated by *Gammaproteobacteria* (e.g. *Enterobacteriaceae*) (366). During this neonatal temporal window, microbial exposure is crucial for immune development (356, 357). Innate immune factors, including toll-like receptor (Tlr)s and Tlr/interleukin- (IL)1R adaptor protein myeloid differentiation primary response 88 (Myd88), maintain homeostatic host-microbe interactions (367) and in normal neonatal mice *Proteobacteria* facilitate immunoglobulin (Ig)A production by B cells. Deficiency in IgA results in

144

predisposition to colonic inflammation and the persistence of an "immature" microbiota (366).

In this "window of opportunity" – between birth and weaning – exposure to microbes is critical for the development of effective immunity and if impaired, has long-term pathological consequences (78, 356, 368). Indeed, "immune imprinting" has been suggested to occur during this window, when exposure to colonizing microbiota and their metabolites (e.g. short-chain fatty acids (SCFAs)), impact lymphoid and myeloid cells (357, 369, 370), maintain gut health (354) and gut barrier integrity (355). "Pathological imprinting" (i.e. susceptibility to inflammatory pathologies (356)) may result due to exposure to a dysbiotic microbiota during this "window of opportunity" (357). In support of this, the disruption of normal gut colonization (with antibiotics or in germ-free mice) results in immunopathology (356), as well as increased susceptibility to allergy (371), and neurodevelopmental (372, 373) and metabolic impairments (374). Indeed, the rate of acquisition of certain microbiota in neonates predicts adiposity at 18 mos of age (375), and gut dysbiosis in neonates due to antibiotics is associated with childhood weight gain and obesity (83, 376, 377). Early life adversity (fetal exposure to high maternal pre-pregnancy body mass index (BMI)) is also associated with neonatal gut dysbiosis (156, 158, 236), and this dysbiosis appears to confer metabolic disease risk in children that is driven by changes in immunity (285).

Previous studies have found that maternal HF diet consumption increased offspring susceptibility to Dextran sulphate sodium (DSS)-induced colitis (169), and induced offspring gut dysbiosis at 8 weeks of age (147), however, the

underlying mechanisms are not well defined. In our previous study (Chapter 5 (265)) we found that maternal HF diet was associated with fetal gut unfolded protein response (UPR) inhibition and increased *Tlr*4 transcript levels and we hypothesized that this may predispose offspring to increased intestinal inflammation postnatally upon microbial colonization. In the present study, we investigated the relationship between early-life exposure to maternal HF diet and the offspring gut microbiota, as well as offspring gut permeability and susceptibility to postnatal HF challenge.

7.2   Chapter-specific methods

After some initial animal model validation (see Appendix D), female C57Bl/6J dams were generated from the Sloboda Lab breeding colony and randomly assigned to a control (C; n=40; 17% kcal fat) or HF diet (n=55; 60% kcal fat) at 11 weeks of age. Females were housed two per cage with *ad libitum* food and water. Following 2 weeks of dietary intervention, females were co-housed with a control-fed male. Mating was confirmed by visualization of a vaginal plug (embryonic day (E)0.5). Pregnant females (dams; C, n=30; HF, n=42) were housed individually, and weights were recorded throughout pregnancy and lactation. Dams were allowed to deliver and surviving litters (C, n=20; HF, n=16) were normalized to 6 offspring at postnatal day 3 (P3) with equal numbers of female and male offspring where possible, to ensure standardized nutrition during lactation.

Offspring weights were recorded at postnatal day (P)3, P7, P14, and P21 prior to weaning. At P28 offspring were weaned onto a control diet and were

housed in same-sex pairs with *ad libitum* food and water. Body weights and food intake were recorded weekly from weaning until the end of the experiment, when tissues were collected from a maximum of one male and one female offspring per dam at P3, P14, and P120. A subset of adult offspring at P120 were challenged with a HF-diet (60% kcal fat) for 6 weeks and sacrificed for tissue collection at P165 (post-HF diet challenge (pHFD)).

Offspring were sacrificed by either decapitation (P3 and P14) or cervical dislocation (P120 and pHFD). Offspring serum was collected and stored at -80℃ for future analysis. Offspring cecal contents and intestinal tissue from the duodenum, jejunum, ileum, and colon were fixed in Carnoy's fixative and stored in 70% ethanol or snap-frozen in liquid nitrogen and stored at -80℃.

7.3 Results

7.3.1 Offspring phenotype

Unlike previous reports (378) we found no effect of maternal diet on offspring weight at sacrifice at any time point (main effect of maternal diet: overall, p=0.155; males, p=0.06; female, p=0.77) and males were heavier than females (age:sex interaction, p<0.0001) at P120 (p<0.0001) and pHFD (p<0.0001; Fig. 7.1). Offspring non-fasted whole blood glucose (WBG) levels were not affected by maternal diet (main effect of maternal diet, p=0.86; Fig. 7.2).

Small intestine length was decreased with maternal HF diet in females (main effect of maternal diet, p=0.01) but not males (main effect of maternal diet, p=0.94; Fig. 7.3). Postnatal HF-challenge did not alter small intestine length in
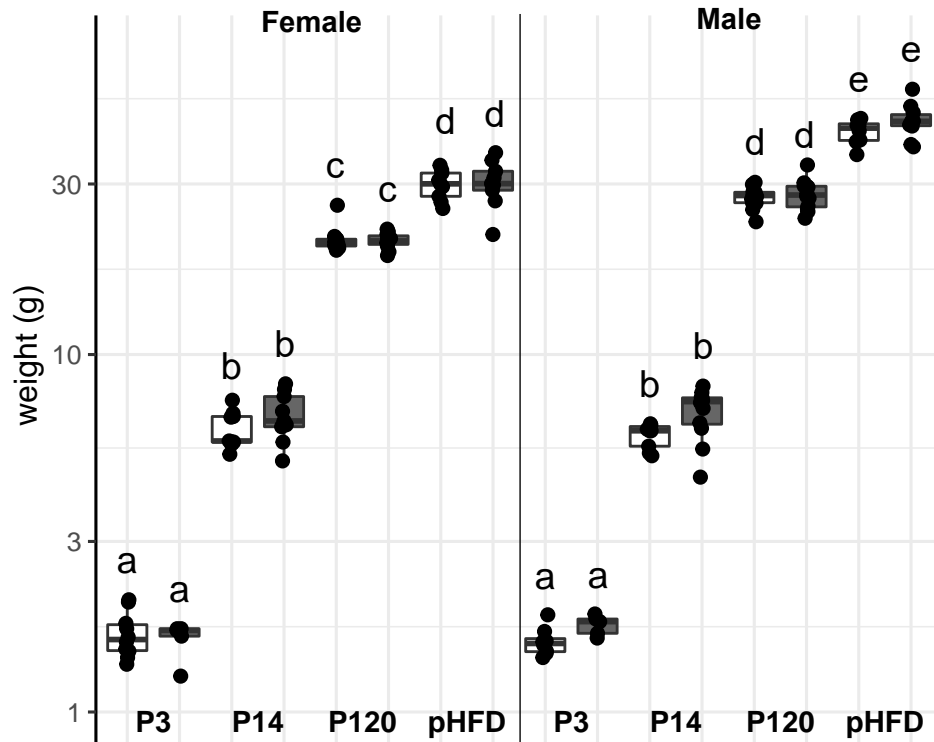
Figure 7.1. Offspring weight at sacrifice does not differ by maternal diet

offspring of either control-fed or HF-fed mothers (Fig. 7.3). Large intestine length did not differ by maternal diet at any age, but the interaction effect of maternal diet and age was significant (p=0.048; 7.4). This interaction was mediated by postnatal HF-challenge induced decreases in large intestine length in female (p=0.0050) and male offspring (p=0.040) of HF dams, indicating that both maternal and postnatal HF diet are required to reduce large intestine length. Cecal weight was decreased by maternal HF diet (main effect, p=0.017), and this was driven by cecal weights at P120 in both females (p=0.00035) and males (p<0.0001; Fig. 7.5). These data suggest that maternal HF diet impacts offspring gut structure early in life (P3, P14), while microbially-mediated

Figure 7.1. Offspring weight at sacrifice does not differ by maternal diet (main effect of maternal diet, p=0.155) in males (p=0.06) or females (p=0.77). Offspring weights increased with age (main effect of age, p<0.0001) and males weighed more than females (main effect of sex, p<0.0001). Significance was assessed by mixed linear model with age, sex, and maternal diet as fixed effects and litter as a random effect. Different letters indicate groups differ by multiple comparison (p<0.05). F=female; M=male. Offspring from control mothers are open boxes and offspring from HF-fed mothers are grey boxes.

structural changes (i.e. decreased cecal weight) occur in adulthood. There was no effect of maternal diet on absolute (p=0.93) or relative (% of body weight, p=0.10) liver weight. Liver weight increased with postnatal HF-challenge in males but not in females (Fig. 7.6).

Male and female offspring born to HF-fed mothers had increased relative gonadal (main effect of maternal diet, p=0.00044) and mesenteric fat mass (main effect of maternal diet, p=0.0036) (Fig. 7.7). This increase was particularly evident in HF male offspring, who gained considerably more relative gonadal mass after HF-challenge (pHFD; p=0.0001) compared to offspring of control fed mothers. Despite this increase in tissue mass, % body fat assessed by quantitative magnetic resonance (ECHO-MRI™) was not different in male offspring, and was lower in female HF offspring compared to control offspring after HF-challenge (p=0.033; age:maternal-diet interaction, p=0.0015; age:maternal-diet:sex interaction, p=0.024; Fig. 7.8). These data suggest that either ratios of body fat to other tissues (lean, water %) may hinder the MRI calculations – or that other adipose depots in offspring were differentially affected.
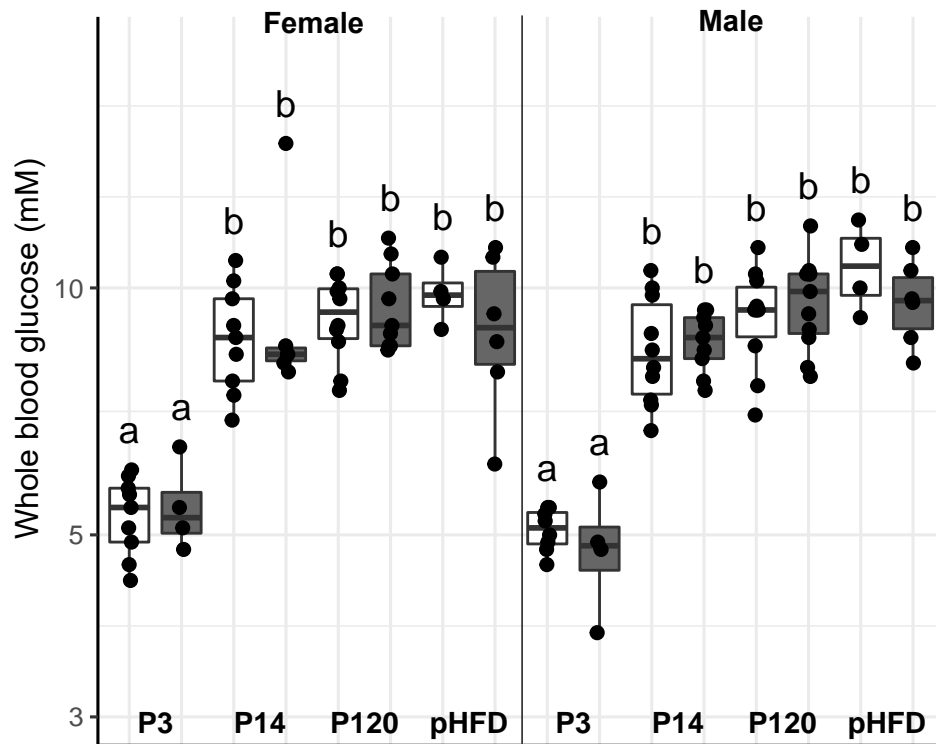
Figure 7.2. Offspring WBG at sacrifice does not differ by maternal diet. Significance was assessed by mixed linear model with age, sex, and maternal diet as fixed effects and litter as a random effect. Different letters indicate groups differ by multiple comparison (p<0.05). Offspring from control mothers are open boxes and offspring from HF-fed mothers are grey boxes.

Figure 7.3. Offspring small intestine length is decreased by maternal HF diet in females (main effect of maternal diet, p=0.01) but not males (main effect of maternal diet, p=0.94). Small intestine length increased with age (main effect of age, p<0.001), and was greater in males than females at P120 and pHFD (main effect of sex, p<0.001). Significance was assessed by mixed linear model with age, sex, and maternal diet as fixed effects and litter as a random effect. Different letters indicate groups differ by multiple comparison (p<0.05). Offspring from control mothers are open boxes and offspring from HF-fed mothers are grey boxes.
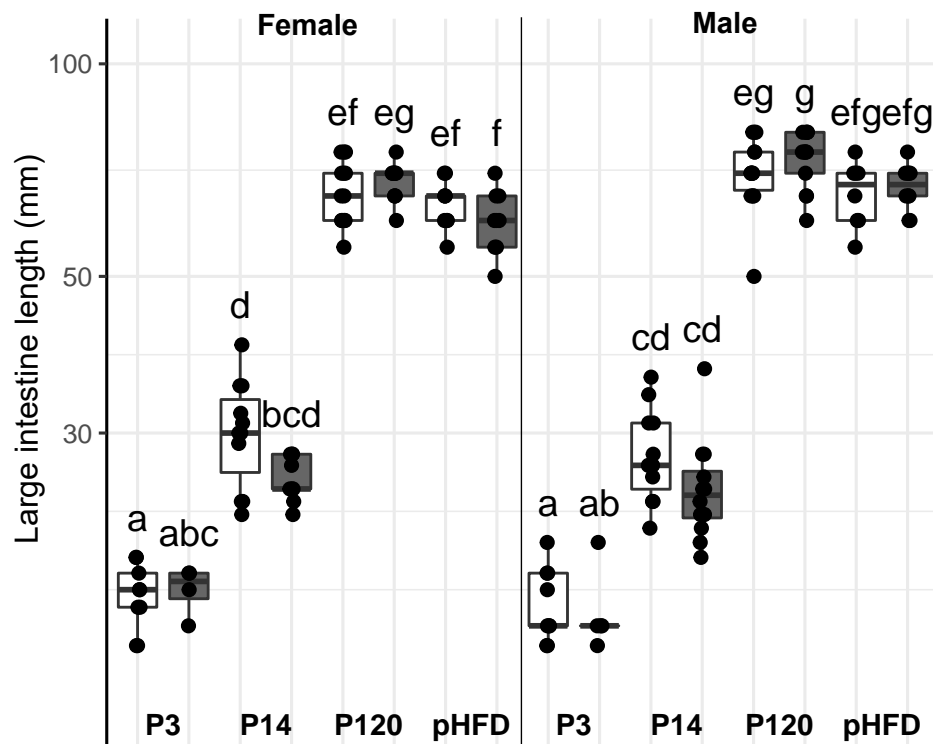
Figure 7.4. Offspring large intestine length is significantly impacted by the interaction of age and maternal diet (main effect of interaction, p=0.048). Large intestine length increased with age (main effect of age, p<0.001). Significance was assessed by mixed linear model with age, sex, and maternal diet as fixed effects and litter as a random effect. Different letters indicate groups differ by multiple comparison (p<0.05). Offspring from control mothers are open boxes and offspring from HF-fed mothers are grey boxes.
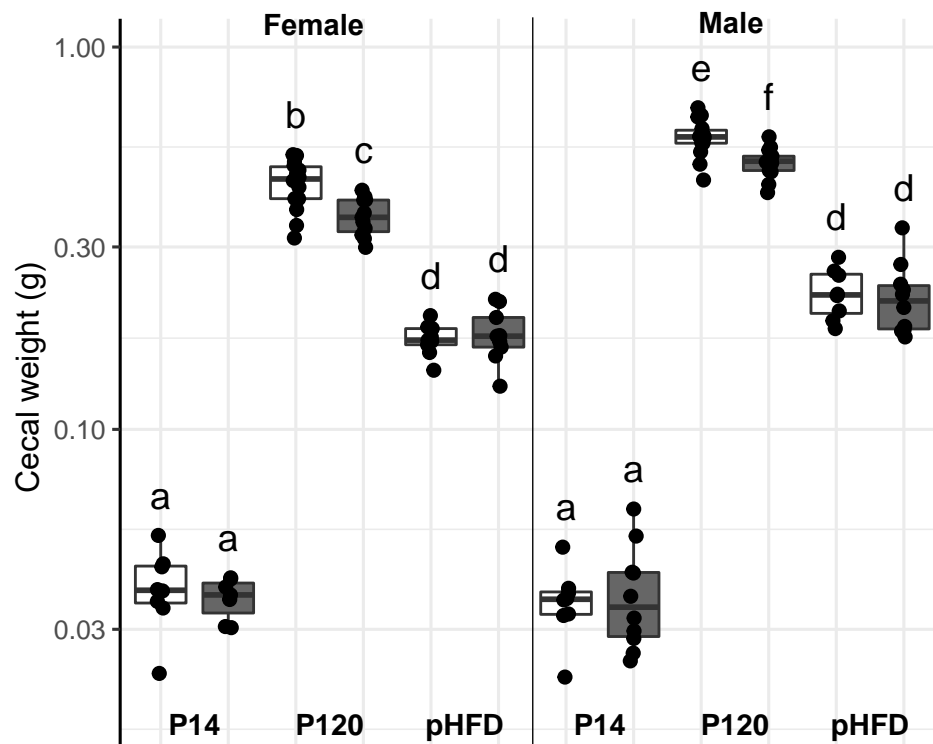
Figure 7.5. Offspring cecal weight is decreased by maternal HF diet (main effect of maternal diet, p=0.0056), particularly at P120 (p<0.001). Significance was assessed by mixed linear model with age, sex, and maternal diet as fixed effects and litter as a random effect. Different letters indicate groups differ by multiple comparison (p<0.05). Offspring from control mothers are open boxes and offspring from HF-fed mothers are grey boxes.
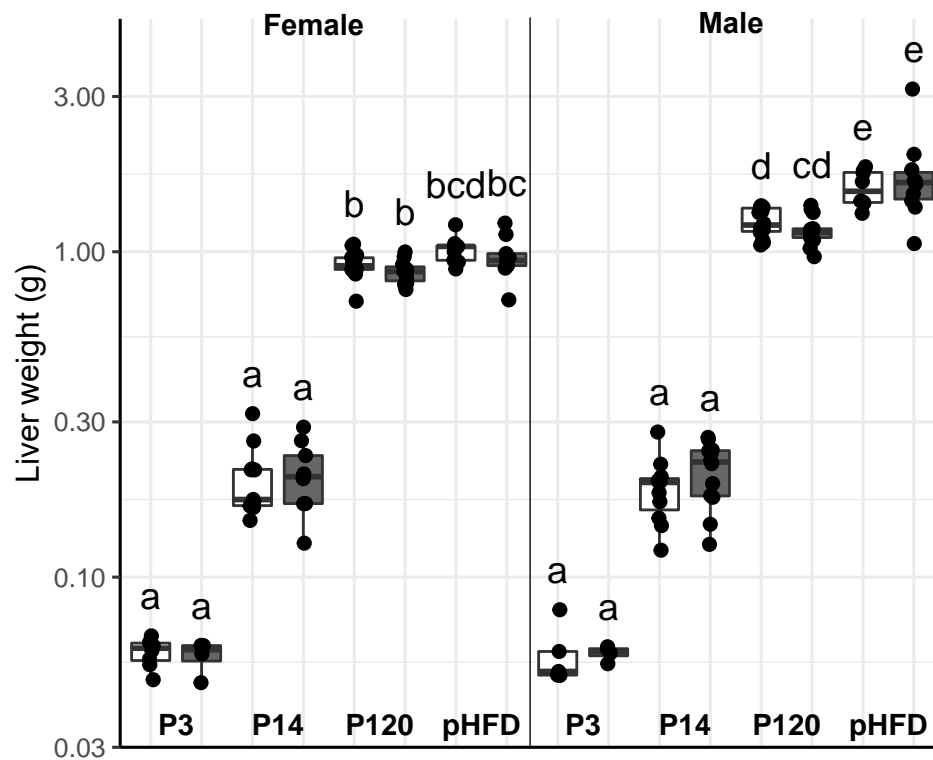
Figure 7.6. Offspring liver weight is increased by postnatal HF challenge in males but not in females. Significance was assessed by mixed linear model with age, sex, and maternal diet as fixed effects and litter as a random effect. Different letters indicate groups differ by multiple comparison (p<0.05). Offspring from control mothers are open boxes and offspring from HF-fed mothers are grey boxes.
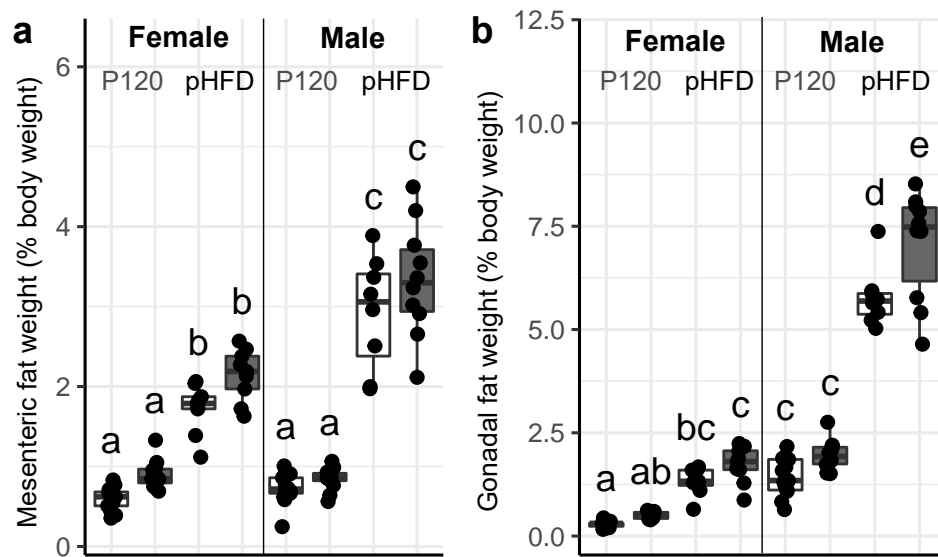
Figure 7.7. Maternal HF diet increases offspring relative fat mass (% body weight). Maternal HF diet was associated with increases to both relative gonadal (main effect of maternal diet, p=0.00044) and relative mesenteric (main effect of maternal diet, p=0.0036) in offspring. Significance was assessed by mixed linear model with age, sex, and maternal diet as fixed effects and litter as a random effect. Different letters indicate groups differ by multiple comparison (p<0.05). Offspring from control mothers are open boxes and offspring from HF-fed mothers are grey boxes.
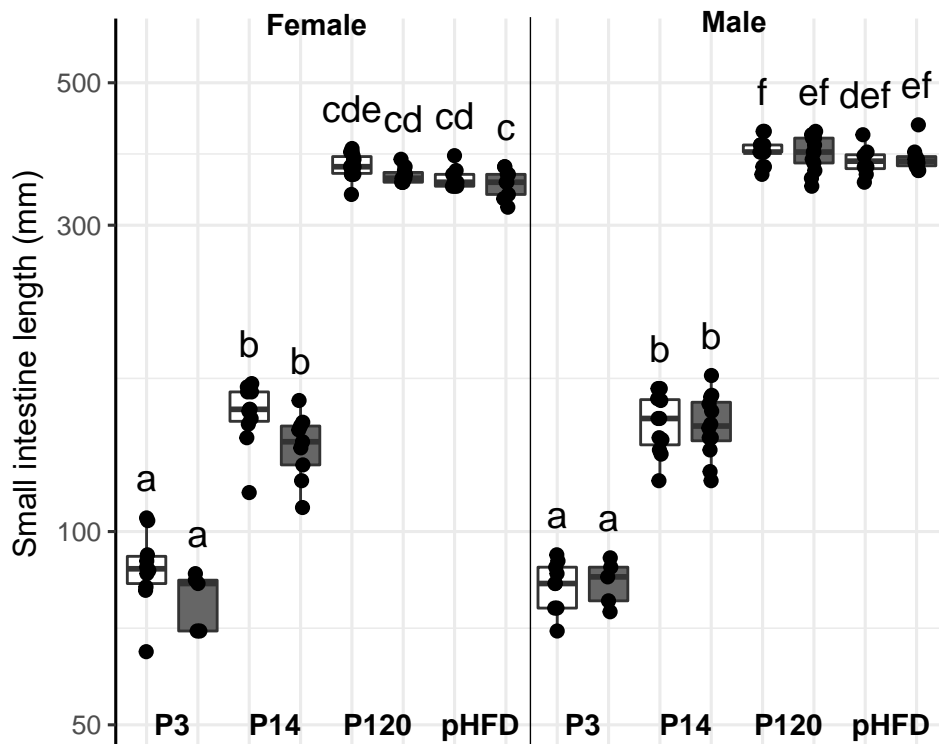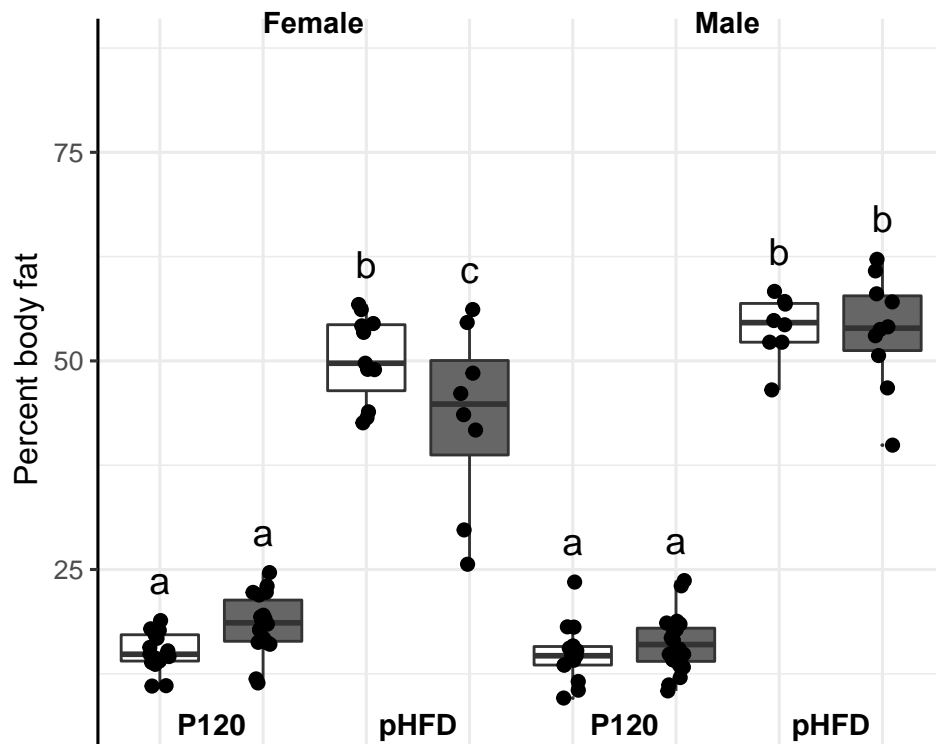
Figure 7.8. **Maternal HF diet decreased offspring percent body fat after HF-challenge** in females (p=0.033) but not males (p=1). Percent body fat was significantly increased by HF-challenge (P120 vs. pHFD: main effect of age, p<0.0001). Significance was assessed by mixed linear model with age, sex, and maternal diet as fixed effects and litter as a random effect. Different letters indicate groups differ by multiple comparison (p<0.05). Offspring from control mothers are open boxes and offspring from HF-fed mothers are grey boxes.

7.3.2   Offspring microbiome

Many experimental studies have shown a relationship between maternal high fat diet and offspring intestinal dysbiosis (147, 160, 338, 379). Therefore we next investigated whether the phenotypic changes we observed in offspring from HF-fed dams were associated with shifts in the offspring microbiota. Offspring cecal contents were collected during sacrifice at P3 and P14 and fecal pellets were collected at P120 and pHFD. Fecal pellets were also collected from dams at P3, P14, and P28 for a pilot study assessing the maternal microbiome during lactation (see Appendix D). Bacterial DNA was assessed by 16S rRNA gene sequencing of the combined variable 3 and 4 (V3-V4) region amplicons from 30 cycles of PCR amplification (see Methods 2.4).

To evaluate differences in within-sample alpha diversity, the Shannon Index was used as a measure of richness and evenness (234), and the number of observed amplicon sequence variants (ASVs) was used as a measure of species richness to capture neonatal microbiota maturation (380) (Fig. 7.9). The impacts of offspring age, sex, and maternal diet on alpha diversity were assessed by a mixed linear model, with those factors as interacting fixed effects and litter as a random effect. Alpha diversity increased with increasing offspring age (main effect of age: Shannon Index, $p < 0.0001$; Observed ASVs, $p < 0.0001$) and the effect of maternal diet varied by age (age:maternal diet effect: Shannon Index, $p = 0.0007$; Observed ASVs, $p = 0.0039$). At P3, alpha diversity was increased by maternal HF diet (Shannon Index, $p < 0.0001$), particularly in males ($p < 0.0001$). This may indicate that maternal HF diet accelerates the maturation of the offspring gut microbiota. Alpha diversity was decreased by maternal high-fat diet

at P14 (Observed ASVs, p=0.0026; female, p=0.032; male, p=0.021) and P120 (Observed ASVs, p<0.0001; female, p=0.0003; male, p=0.0022). This may be due to vertical transfer of a less diverse microbiota from HF-fed dams, as maternal alpha diversity was also decreased by HF diet (main effect of diet: Shannon, p=0.0031; Observed ASVs, p<0.0001) during lactation (see Appendix D).

Consistent with previous reports (303, 381, 382), a postnatal HF-challenge decreased offspring alpha diversity (pHFD vs. P120; Shannon Index main effect, p=0.040; Observed ASVs, p<0.0001), but showed a sex-specific effect: combined richness and evenness (Shannon Index) was decreased by postnatal HF-challenge in male offspring (p=0.011) but not in female offspring (p=0.74) born to either control or HF mothers. Species richness (Observed ASVs) was decreased by postnatal HF-challenge in offspring of control-fed dams (female, p=0.0003; male, p=0.0001) but not was further decreased by postnatal HF-challenge in offspring of HF-fed dams (female, p=0.20; male, p=0.12). It is possible that the species that are absent after postnatal HF-challenge were already absent in offspring of HF-fed dams at P120.

To determine whether these changes in alpha diversity were accompanied by overall shifts in microbial community composition, we assessed between-sample diversity (beta diversity) using Bray-Curtis dissimilarity and visualized these data by principal coordinate analysis (PCoA) (Fig. 7.10). Across all offspring samples, maternal diet had a small effect on offspring beta diversity (PERMANOVA; R^2=0.022, p<0.0001), and beta diversity was more strongly affected by offspring age (R^2=0.40, p<0.0001) and litter (R^2=0.19, p<0.0001).
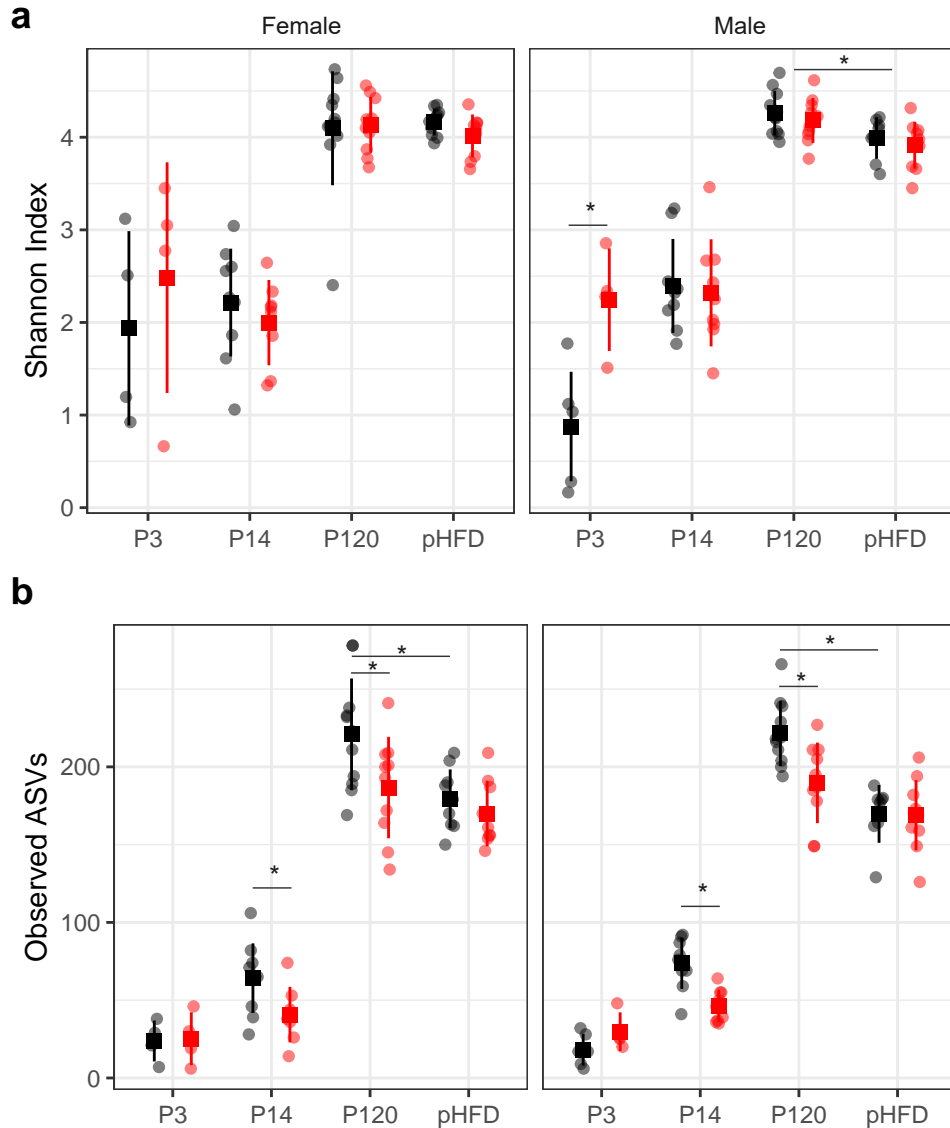
Figure 7.9. Offspring alpha diversity by age and maternal diet. Offspring alpha diversity is increased by maternal HF diet (red circles; control diet, black circles) at P3 (Shannon Index, p<0.0001) but decreased by maternal HF diet at P14 (Observed ASVs, p=0.0026; female, p=0.032; male, p=0.021) and P120 (Observed ASVs, p<0.0001; female, p=0.0003; male, p=0.0022). Individual values are shown with the mean and standard deviation for each group. Significance was assessed by mixed linear model with age, sex, and maternal diet as fixed effects and litter as a random effect (* p<0.05).

Offspring beta diversity was not significantly affected by maternal diet at P3 (p=0.15), but was at P14 (R^2=0.11, p<0.0001), and was significantly affected by both sex and maternal diet at P120 (sex: R^2=0.027, p=0.039; maternal diet: R^2=0.13, p<0.0001) and pHFD (sex: R^2=0.033, p=0.024; maternal diet: R^2=0.062, p<0.0001). Within sexes, the effect of maternal HF-diet after postnatal HF-challenge (pHFD) was significant in male (R^2=0.13, p=0.0015), but not in female offspring (R^2=0.056, p=0.42). These data indicate that the effects of maternal HF-diet on microbial community composition persist until adulthood (P120) in offspring despite being fed a control diet from weaning, and persist even after HF-challenge in male offspring.
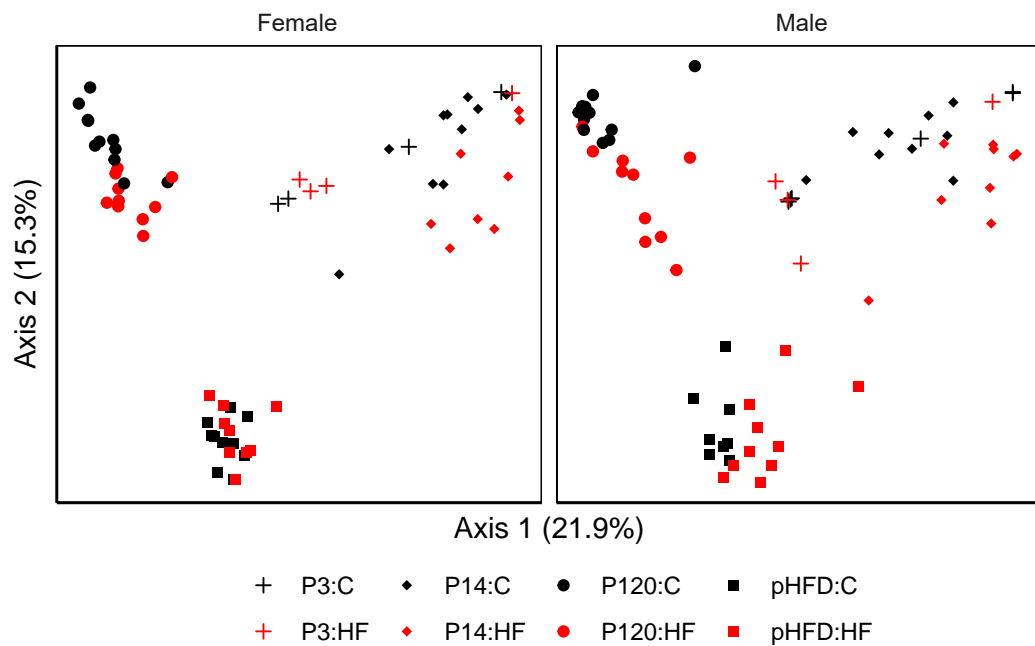
Figure 7.10. Offspring beta diversity differs by age and maternal diet. PCoA of Bray-Curtis distances shows that the microbiota of offspring clusters by age (P3, cross; P14, diamond; P120, circle; pHFD, square) and maternal diet (control, C, black; HF, red).

We next investigated which specific taxa contribute to these overall shifts in community composition using differential abundance testing (DESeq2, RRID: SCR_015687; see taxa summaries in Fig. 7.11, Table 7.1). Offspring P3 samples were excluded from differential abundance testing due to the high heterogeneity of ASVs present (see Appendix D.3). Overall maternal HF diet decreased the relative abundance of the genus *Akkermansia*, consistent with decreases in HF wildtype (Wt) dams at term gestation (Chapter 6) and during lactation (Appendix D). As expected, within each age group maternal HF diet impacted the greatest number of genera before weaning, at P14 (9 genera), when offspring were still directly exposed to their dams. At P14, maternal HF-diet was associated with an increased relative abundance of *Lachnospiraceae* genera *Roseburia* and *Lachnoclostridium*, and *Ruminococcaceae* genus *Angelakisella*. These increases are likely directly due to vertical transfer from the maternal gut microbiota, as they were also increased by HF diet in the maternal gut microbiota (see Appendix D).
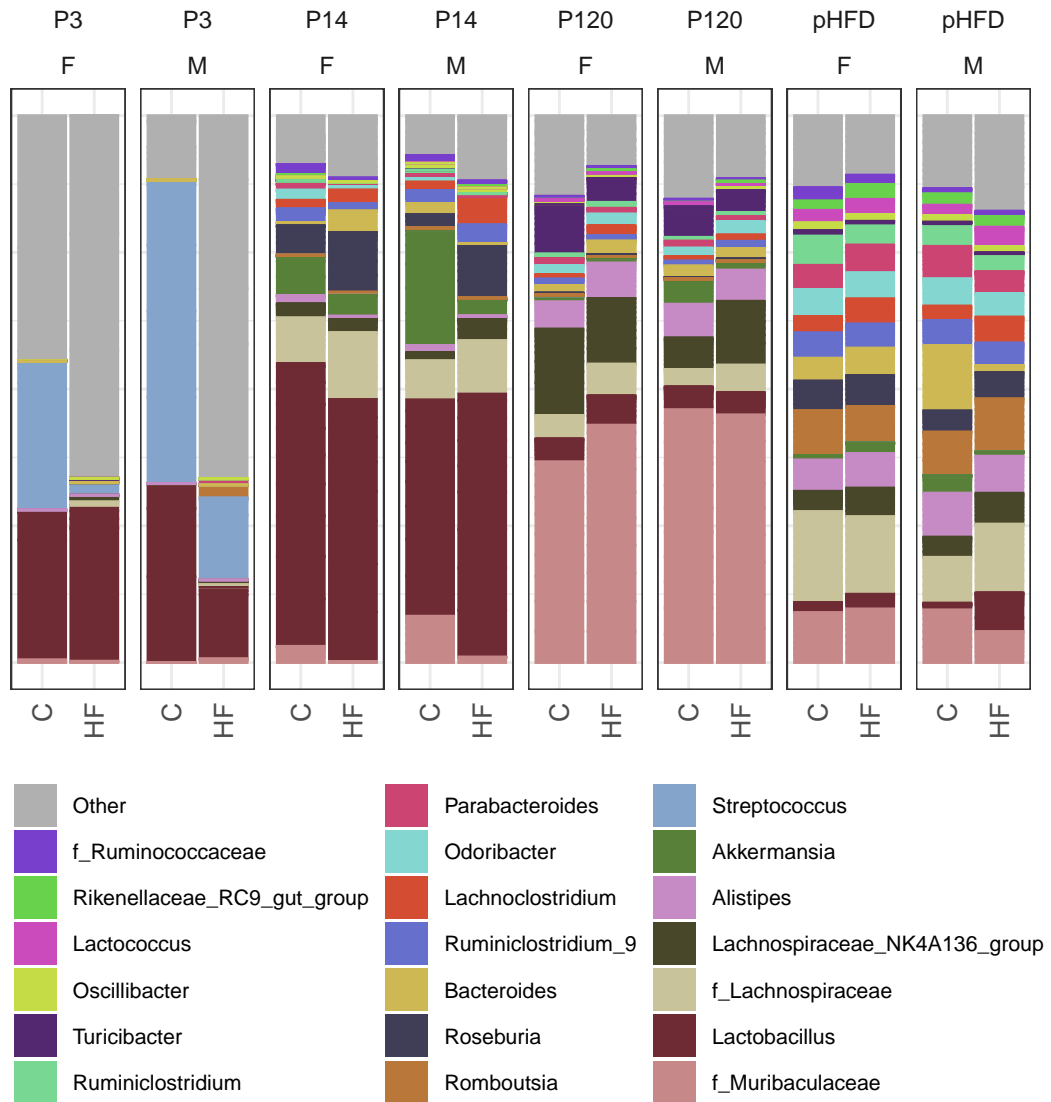
Figure 7.11. Taxonomic summary of top 20 genera in offspring by age and maternal diet. The mean relative abundance of the top 20 most abundant bacterial genera was calculated within age, sex (M, male; F, female) and maternal diet (C, control; HF, high-fat) and is shown in a stacked bar plot coloured by genus.

Despite being fed a control diet from weaning onward, in utero and lactational exposure to maternal HF diet decreased the relative abundances of 5 genera in offspring at P120. Within the family *Ruminococcacceae*, maternal HF diet was associated with a decrease in *UCG-014* and *Ruminococcus 1* at P120. These genera were both further decreased by postnatal HF-challenge in offspring from both control and HF-fed mothers. At P120, the relative abundances of genera *Faecalibaculum* and *Dubosiella* of the family *Erysipelotrichaceae* and the genus *Parasutterella* were also lower in offspring of HF-fed dams. Some of these decreases may be due to vertical transfer of an altered gut microbiota from dams to their offspring, as HF-fed dams also had a decreased relative abundance of *Ruminococcus 1* and *Parasutterella*, but *Faecalibaculum* and *Dubosiella* were increased with HF diet in dams.

Male offspring born to HF-fed mothers showed an increased relative abundance of *Lactobacillus* after post-natal HF-challenge (pHFD). This increase in offspring may be due to altered seeding of specific *Lactobacillus* species or strains as the relative abundance of this genus did not differ in offspring by maternal diet prior to postnatal HF-challenge, but was increased in HF-fed dams at P3. These data suggest that maternal HF diet decreases diversity within individuals and shifts the overall microbial community composition of the offspring microbiota and that these changes persist into adulthood (P120). Changes in specific taxa are not consistent between P14 and P120, likely due to the impact of offspring diet transitioning from maternal milk to control chow diet.

Table 7.1. Differentially abundant genera in offspring microbiota. Genera shown were increased or decreased in offspring of HF mothers compared to offspring of control mothers. Taxa with a mean abundance less than 40 were excluded. Mean, base mean abundance, log2FC, log2 fold change; SE, standard error.

age	Order	Family	Genus	Mean	log2FC	SE	p adjusted
overall	Bacteroidales	Muribaculaceae	unknown	32,119	−1.89	0.35	8.20E-07
overall	Clostridiales	Lachnospiraceae	NK4A136 group	12,768	−0.86	0.32	0.02064464
overall	Clostridiales	Peptostreptococcaceae	Romboutsia	5,314	2.17	0.63	0.002672175
overall	Verrucomicrobiales	Akkermansiaceae	Akkermansia	3,209	−2.41	0.83	0.012616897
overall	Erysipelotrichales	Erysipelotrichaceae	Turicibacter	2,521	−1.42	0.48	0.011140305
overall	Clostridiales	Ruminococcaceae	Oscillibacter	1,897	−0.9	0.33	0.020658986
overall	Lactobacillales	Streptococcaceae	Lactococcus	1,464	1.76	0.59	0.010466907
overall	Clostridiales	Ruminococcaceae	unknown	1,450	−1.14	0.34	0.003528839
overall	Clostridiales	Lachnospiraceae	GCA-900066575	881	−1.38	0.34	0.000212167
overall	Clostridiales	Ruminococcaceae	Ruminiclostridium$_5$	603	−1.84	0.37	6.75E-06
overall	Bacteroidales	Muribaculaceae	Muribaculum	531	−3.67	0.54	1.61E-10
overall	Clostridiales	Ruminococcaceae	UCG-014	501	−1.97	0.47	0.000202552
overall	Clostridiales	Lachnospiraceae	A2	430	−3.54	0.65	5.58E-07
overall	Clostridiales	Lachnospiraceae	FCS020 group	408	−2.11	0.39	7.77E-07
overall	Betaproteobacteriales	Burkholderiaceae	Parasutterella	372	−2.02	0.55	0.001113889
overall	Clostridiales	Lachnospiraceae	UCG-006	362	−2.69	0.46	8.29E-08
overall	Erysipelotrichales	Erysipelotrichaceae	Dubosiella	282	−6.81	1.41	1.18E-05
overall	Clostridiales	Ruminococcaceae	Ruminococcus$_1$	241	−8.31	0.75	1.25E-26
overall	Clostridiales	Ruminococcaceae	Butyricicoccus	237	−2.78	0.6	2.83E-05

Table 7.1. cont. Differentially abundant genera in offspring microbiota.

age	Order	Family	Genus	Mean	log2FC	SE	p adjusted
overall	Erysipelotrichales	Erysipelotrichaceae	Ileibacterium	163	5.55	1.36	0.00024442
overall	Clostridiales	Lachnospiraceae	UCG-001	155	−6.63	0.71	2.92E-19
overall	Clostridiales	Peptococcaceae	unknown	147	−1.11	0.33	0.002991734
overall	Clostridiales	Ruminococcaceae	Ruminiclostridium$_6$	142	−7.76	1.1	2.78E-11
overall	Clostridiales	Ruminococcaceae	UCG-009	139	−1.6	0.39	0.000255034
overall	Clostridiales	Lachnospiraceae	ASF356	88	−1.87	0.78	0.043356793
overall	Clostridiales	Ruminococcaceae	NK4A214$_{group}$	74	−2.38	0.57	0.00019428
overall	Mollicutes RF39	unknown	unknown	74	−1.75	0.73	0.043356793
overall	Saccharimonadales	Saccharimonadaceae	Candidatus Saccharimonas	73	−1.75	0.65	0.020864464
overall	Bacteroidales	Prevotellaceae	UCG-001	54	−4.3	1.05	0.000229449
overall	Clostridiales	Lachnospiraceae	Anaerostipes	45	−26.03	2.21	6.10E-30
P14	Clostridiales	Lachnospiraceae	Roseburia	2,686	2.23	0.86	0.042138743
P14	Clostridiales	Lachnospiraceae	Lachnoclostridium	1,793	1.7	0.66	0.042138743
P14	Clostridiales	Ruminococcaceae	Angelakisella	1,165	4.41	0.93	2.43E-05
P14	Clostridiales	Lachnospiraceae	GCA-900066575	336	−3.1	0.89	0.003291793
P14	Clostridiales	Lachnospiraceae	Tyzzerella	178	−5.05	1.38	0.002312962
P14	Bacteroidales	Marinifilaceae	Odoribacter	89	−5.61	1.94	0.022070077
P14	Bacteroidales	Bacteroidaceae	Bacteroides	84	−10.07	2.05	1.38E-05
P14	Clostridiales	Peptostreptococcaceae	Romboutsia	59	8.05	1	1.99E-14
P14	Bacteroidales	Tannerellaceae	Parabacteroides	58	−25.61	2.87	1.85E-17
pHFD	Lactobacillales	Lactobacillaceae	Lactobacillus	2,080	2.2	0.48	0.000491885

7.3.3   Offspring intestinal structure and function

Gut microbes and their metabolites impact gut barrier function and immunity through SCFA receptors (383). Given the shift in offspring microbial community composition with maternal HF diet, we assessed messenger RNA (mRNA) levels of the SCFA receptors G protein-coupled receptor (Gpr)41 and Gpr43 to assess functional changes that may be associated with these microbial changes (Fig. 7.12). In male offspring of HF-fed mothers, mRNA levels of *Gpr*41 (p=0.0014; main effect of maternal diet, p=0.00064) and *Gpr*43 (p=0.014; sex:maternal diet p=0.0063) were increased in the colon at P14. However, at P120, offspring of HF-fed mothers had decreased mRNA levels of *Gpr*41 (main effect of maternal diet, p=0.0011) and *Gpr*43 (main effect of maternal diet, p=0.0063) in the ileum of both females (*Gpr*41 p=0.0052; *Gpr*43 p=0.0035) and males (*Gpr*41 p=0.040). Together with the decrease we found in cecal weights at P120 (Fig. 7.5) and decreases in the relative abundance of SCFA producers (Fig. 7.11), these decreases point to the possibility that these offspring have a decrease in SCFA levels in the small intestine at P120. Future work will assess offspring intestinal SCFA levels directly.

An altered offspring gut microbiota may have an altered capacity for pro-inflammatory signalling through the lipopolysaccharide (LPS) receptor Tlr4. In the offspring ileum, *Tlr*4 mRNA levels were decreased with maternal HF diet at P14 (p=0.023), and increased by postnatal HF-challenge in offspring from control dams (pHFD vs. P120, p=0.0011) but not HF dams (p=0.51), suggesting an interaction between early-life exposure and post-natal HF-challenge. In the offspring colon, maternal HF diet decreased *Tlr*4 levels at P120 (main effect of

166

maternal diet, p=0.040; male p=0.045) and at P14 in females only (p=0.026; diet:sex p=0.017; main effect of sex p=0.037). Colon *Tlr*4 mRNA levels were also increased by postnatal HF-challenge in male offspring of HF-fed but not control dams. These data suggest the impact of postnatal HF-challenge on Tlr4 expression is modulated by maternal diet, and that maternal HF diet may result in increased LPS tolerance in offspring.

To determine whether these changes in the gut microbiota were associated with altered intestinal structure and function, we next assessed offspring intestinal barrier function by fluorescein isothiocyanate (FITC)-dextran assay at P120 as well as after postnatal HF-challenge (pHFD). Offspring were fasted for 4-hours (water-fasted 1 hour) prior to gavage with 4kDa FITC-dextran dose-adjusted to body weight (50 mg/kg body weight, 8 mg/mL in sterile PBS). Plasma levels of 4kDA-FITC were measured over a 4-hour time course (at minutes 0, 30, 60, 120, and 240) after gavage to capture peak serum fluorescence and account for differences in transit time (Fig. 7.14). Offspring from high-fat dams were assessed on the same day as control dams to minimize bias due to FITC dilution. Due to high variability between days and no significant effect of offspring sex, data from males and females were grouped and analyzed together.

There was a significant interaction between maternal diet and offspring high-fat challenge on intestinal permeability (age:maternal-diet interaction, p=0.0087; main effect of maternal diet, p=0.060; main effect of age, p=0.0015). Offspring of mothers fed a HF diet showed increased gut permeability (increased plasma fluorescence) compared to offspring born to control mothers after postnatal HF-challenge (pHFD; main effect of maternal diet, p=0.038), but not

before HF-challenge (P120; main effect of maternal diet, p=0.60). This suggests that maternal HF diet may increase offspring susceptibility to postnatal dietary challenges and may have lasting impacts on intestinal permeability. HF-challenge also increased fluorescence at 4 hours post-gavage (time = 240 min) in offspring from both control (p=0.035) and HF (p=0.013) dams. This is likely due to increased gastrointestinal transit time with HF challenge (384). The total response to the FITC challenge (area under the curve (AUC) for fluorescence) was not significantly affected by maternal HF diet (p=0.15) or offspring HF challenge (p=0.065). This may be due to decreased rates of FITC clearance in control offspring after HF-challenge as fluorescence decreased from 60 minutes to 240 minutes in maternal HF diet pHFD offspring (p=0.038) but not in control pHFD offspring (p=0.99).

We next assessed whether this increase in permeability was associated with altered mRNA levels intestinal tight junction proteins, and used these as gut barrier markers (Fig. 7.15). Prior to HF-challenge (at P120), maternal HF diet was associated with a decrease in mRNA levels of tight junction protein 1 (Tjp1) in the colon (main effect of maternal diet, p<0.0001; Fig. 7.15a). Tjp1 mRNA levels did not significantly differ by maternal diet after postnatal HF-challenge (pHFD) in the ileum or colon.

Occludin mRNA levels (*Ocln*) were increased in the offspring ileum at P14 (main effect of maternal diet, p=0.0059; female p=0.015) and pHFD (main effect of maternal diet, p=0.018; male p=0.048), and decreased at P120 (main effect of maternal diet, p=0.0019; male p=0.0030; Fig. 7.15). Postnatal HF-challenge decreased *Ocln* mRNA levels in offspring from control dams (female p=0.0007,

male p<0.0001), but not in offspring from HF-fed dams. *Ocln* mRNA levels were below the limit of detection in the offspring colon. The pore-forming claudin *Cldn2* was decreased by maternal HF diet in the ileum of female offspring at P120 (p=0.019) and in the colon of female offspring at P14 (p=0.0004; diet:sex p=0.0030; sex p=0.048; Fig. 7.15). Together, these data show that decreased mRNA levels of gut barrier markers with maternal HF diet at P120 precede and may contribute to impaired barrier function after postnatal HF-challenge (pHFD, see Fig. 7.14).

Previous studies suggest that intestinal endoplasmic reticulum (ER) stress is associated with changes in gut permeability (385)). We next investigated whether maternal HF diet or postnatal HF challenge were associated with markers of intestinal ER stress (Fig. 7.16). Postnatal HF challenge increased mRNA levels of ER chaperone protein *78-kDa glucose-regulated protein (Grp78)* in the ileum of female offspring from both control (p=0.0026) and HF mothers (p=0.036). After postnatal HF challenge, male offspring from HF-fed mothers had increased ileum mRNA levels of the UPR marker spliced *X-box binding protein 1 (Xbp1)* compared males before HF challenge (p=0.0018) and also compared to male offspring from control mothers after HF challenge (p=0.018; Fig. 7.16). Postnatal HF-challenge also increased spliced *Xbp1* in the ileum of female offspring from HF (p=0.040) but not control mothers (Fig. 7.16). In offspring from control but not HF mothers, postnatal HF-challenge also increased mRNA levels of *Atf4* (female p=0.038; male p=0.036) and Chop (female p=0.011; male p=0.0002) in the ileum. In offspring from both control and HF mothers, postnatal HF-challenge increased colon mRNA levels of *Grp78* (control

p=0.032; HF p<0.0001), *Xbp1* (control p=0.0007; HF p=0.039) in males, as well as *Chop* in both females (control p=0.0001; HF p<0.043) and males (control p<0.0001; HF p=0.0004; Fig. 7.16). Together these data suggest that postnatal HF-challenge induces some markers of ER stress in the offspring colon, particularly in males, and that maternal HF diet and postnatal HF-challenge interact to affect ER stress markers in the ileum.

Previous studies have shown intestinal ER stress is associated with aberrant mucin production (386). In the ileum, female offspring of HF-fed mothers had decreased *mucin (Muc)*2 mRNA levels compared to offspring of control mothers. Ileum *Muc*2 mRNA levels were increased by postnatal HF-challenge in male offspring of control mothers (p=0.0051), but HF mothers. Future work will investigate Muc2 protein levels and localization to determine whether there are post-transcriptional associations with the observed increases in markers of ER stress.

To investigate whether these changes in mRNA levels of gut barrier markers ER stress were associated with structural changes, we next performed a pilot analysis of intestinal morphology in offspring ileums. The lengths and number of goblet cells were recorded for 5 villi and/or crypts and the mean values were calculated. Significance was assessed by linear model with age, sex, and maternal diet as fixed effects.

In the villi of the ileum, maternal HF diet was associated with a decrease in goblet cells (GCs) per μM in female offspring at P120 (p=0.011; Fig. 7.18a). Ileum villus GCs per μM (p=0.0044) and GC number (p=0.013) were decreased

by postnatal HF-challenge in female offspring of control mothers, but were not further reduced in female offspring of HF mothers. After postnatal HF-challenge, ileum villus length (p=0.025) and GC number (p=0.015), and ileum crypt length (p=0.014) were increased in male offspring of HF mothers. At P14, female offspring of HF mothers had increased GCs per μM (p=0.0009) and GC numbers (p=0.026) in ileum crypts. These data suggest that female intestinal morphology is more vulnerable to maternal HF diet early on (P14) and in adulthood (P120), while males are more affected by the combination of maternal HF diet and postnatal HF challenge.

We next assessed whether these changes were associated with altered mRNA levels of intestinal stem cell (ISC) and proliferation marker leucine-rich repeat-containing G protein-coupled receptor 5 (Lgr5) and differentiated cell marker Kruppel like factor 4 (Klf4) (Fig. 7.19). In the ileum, *Klf4* was significantly increased in offspring of HF mothers P120 (p=0.0080) and also by postnatal HF-challenge in female offspring of control but not HF mothers (pHFD vs P120, p=0.033). There was also a significant interaction of maternal HF diet and postnatal HF-challenge in offspring ileums (p=0.035; Fig. 7.19a). In the colon, *Klf4* was significantly increased by postnatal HF-challenge in both female (p=0.0009) and male (p=0.0005) offspring of control mothers, as well as in male offspring of HF mothers (p<0.0001). These data suggest that postnatal HF-challenge increases transcript levels of key markers of epithelial proliferation in the colon, and that both maternal HF diet and postnatal HF-challenge may impact epithelial differentiation in the offspring ileum.
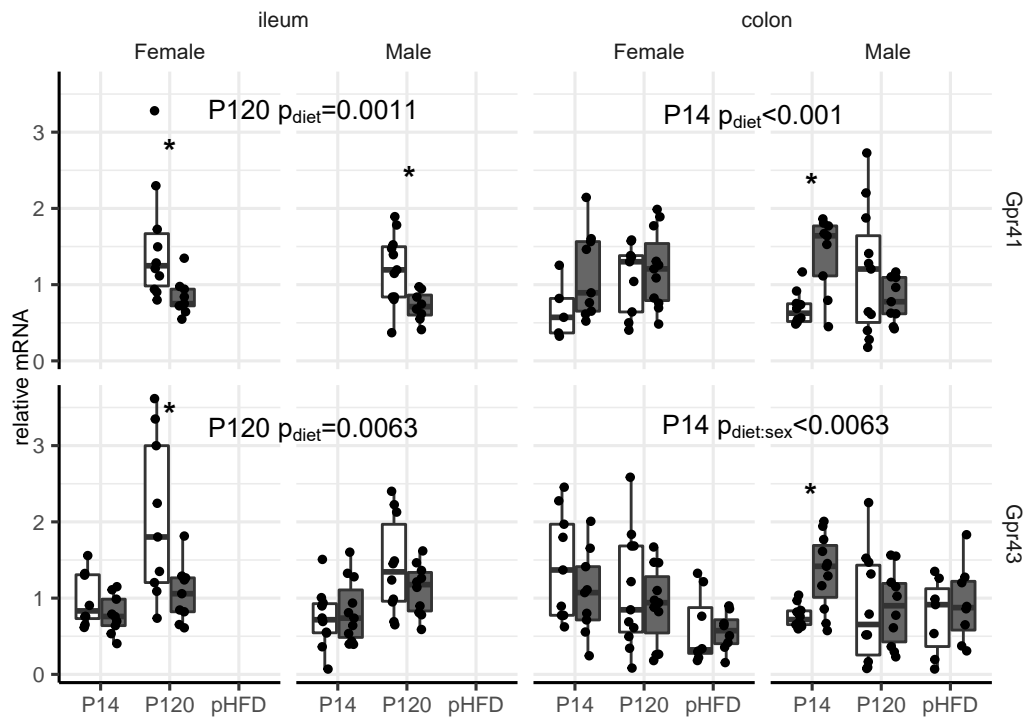
Figure 7.12. SCFA receptor transcript levels decreased in offspring ileum by maternal HF diet. Relative mRNA levels of Gpr41 and Gpr43 are shown in the ileum and colon of female (F) and male (M) offspring from control (white) and HF (grey) dams. Significance was assessed within each age group and intestinal section by linear model with age, sex, and maternal diet as interacting fixed effects. The box plot centre line represents the median; the box limits represent the upper and lower quartiles; the whiskers represent the 1.5x interquartile range. P14 n=8-11; P120 n=9-11; pHFD n=7-8; * p<0.05, control vs. HF.
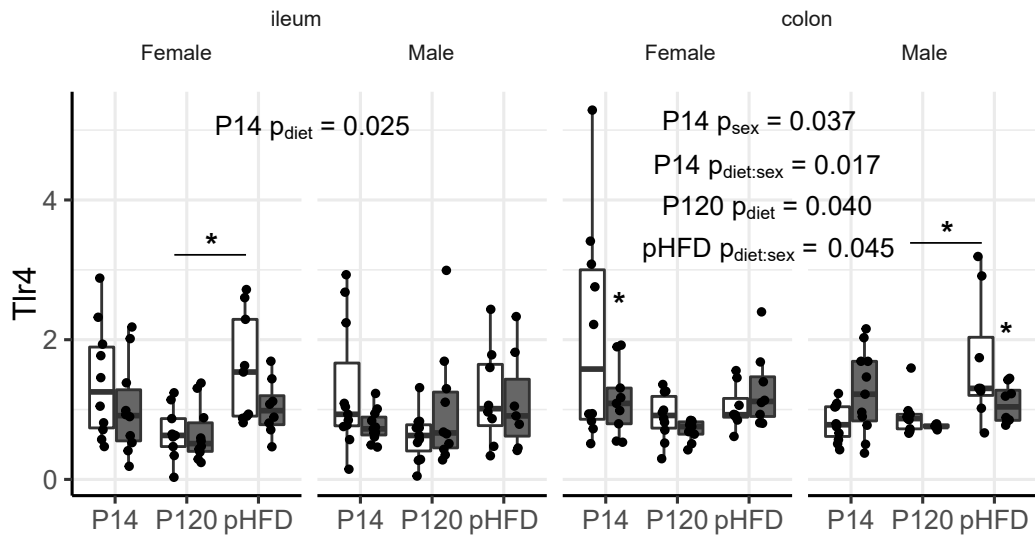
Figure 7.13. Maternal and postnatal HF diet interact to impact Tlr4 transcript levels. Relative mRNA levels of Tlr4 are shown in the ileum and colon of female (F) and male (M) offspring from control (white) and HF (grey) dams. Significance was assessed within each intestinal section by linear model with age, sex, and maternal diet as interacting fixed effects. The box plot centre line represents the median; the box limits represent the upper and lower quartiles; the whiskers represent the 1.5x interquartile range. P14 n=9-11; P120 n=6-11; pHFD n=7-9; * p<0.05.
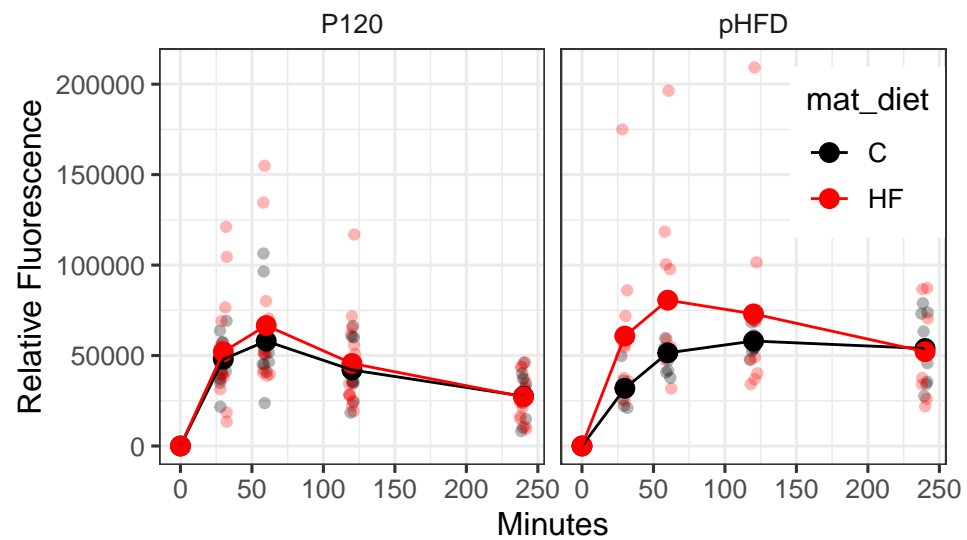
**Figure 7.14. Offspring intestinal permeability is increased by
maternal HF diet after HF-challenge** (maternal-diet:age interaction, p=0.033). Significance was assessed by mixed linear model with
time, age, and maternal diet as fixed effects and litter as a random effect
(P120: C n=12, HF n=15; pHFD: C n=10, HF n=10).
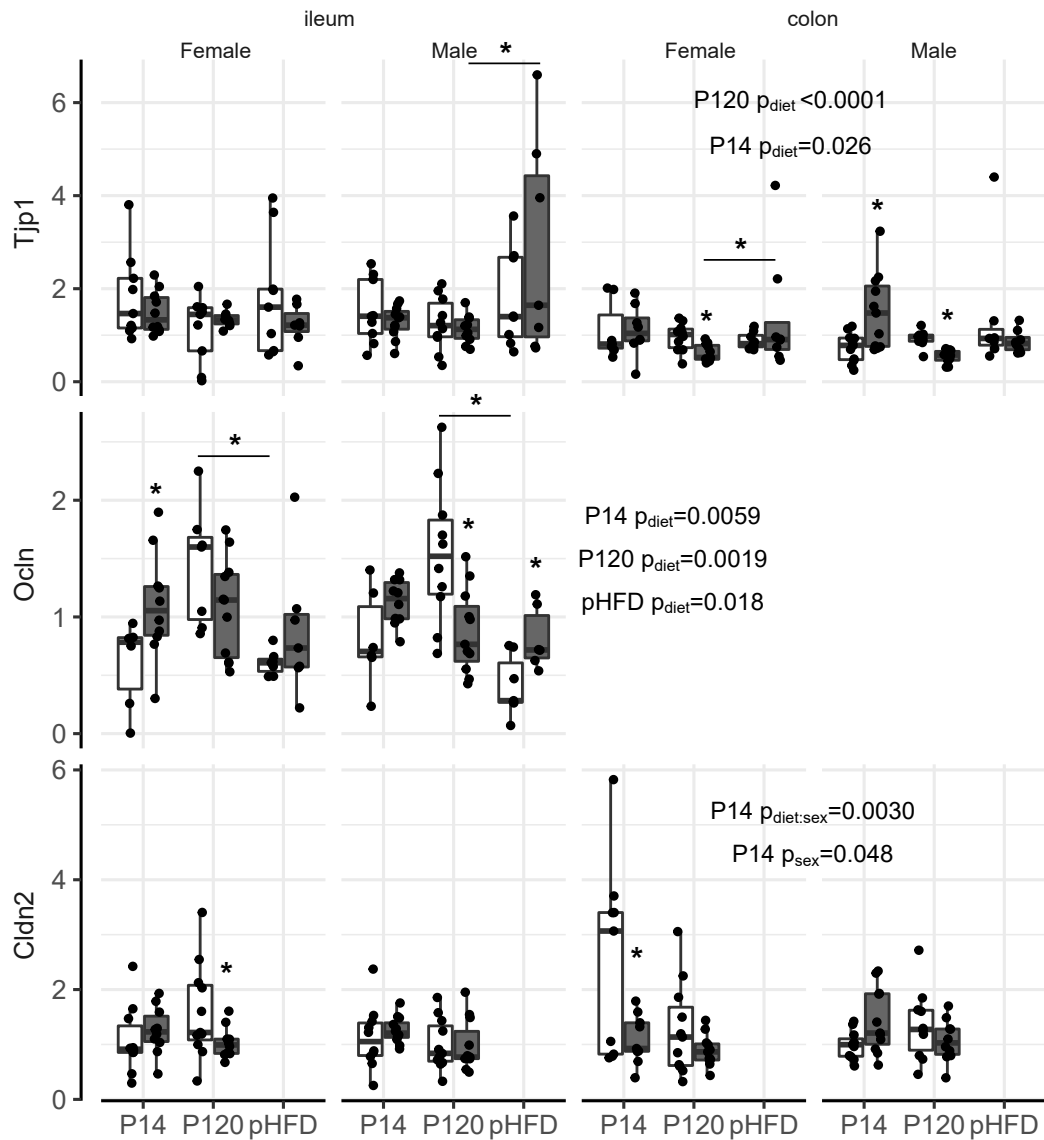
Figure 7.15. Offspring markers of intestinal barrier function are decreased by maternal HF diet. Relative mRNA levels of *Tjp1*, *Ocln*, and *Cldn2* are shown in the ileum and colon of female (F) and male (M) offspring from control (white) and HF (grey) dams. Significance was assessed within each intestinal section by linear model with age, sex, and maternal diet as fixed effects. The box plot centre line represents the median; the box limits represent the upper and lower quartiles; the whiskers represent the 1.5x interquartile range. P14 n=7-11; P120 n=8-11; pHFD n=7-9; * p<0.05.

Figure 7.16. Maternal and postnatal HF diet interact to impact offspring intestinal ER stress markers.

Figure 7.16. Maternal and postnatal HF diet interact to impact offspring intestinal ER stress markers. Relative mRNA levels of activating transcription factor (Atf)4, CCAAT-enhancer-binding protein homologous protein (Chop), and Grp78 are shown in the ileum and colon of female (F) and male (M) offspring from control (white) and HF (grey) dams. Significance was assessed within each intestinal section by linear model with age, sex, and maternal diet as fixed effects. The box plot centre line represents the median; the box limits represent the upper and lower quartiles; the whiskers represent the 1.5x interquartile range. P120 n=8-11; pHFD n=7-9; * p<0.05.
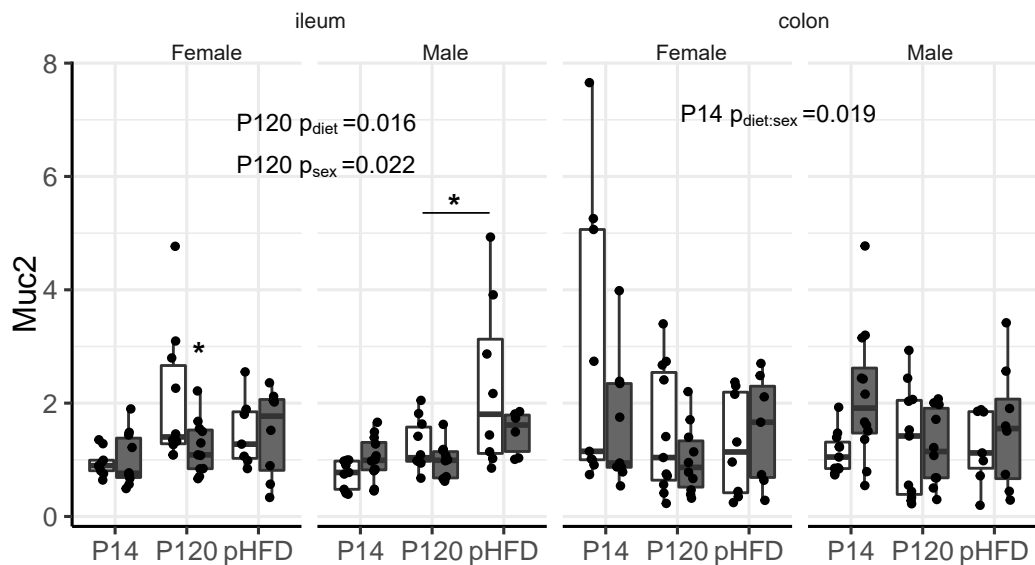
Figure 7.17. Maternal and postnatal HF diet interact to impact offspring intestinal ER stress markers. Relative mRNA levels of Atf4, Chop, and Grp78 are shown in the ileum and colon of female (F) and male (M) offspring from control (white) and HF (grey) dams. Significance was assessed within each intestinal section by linear model with age, sex, and maternal diet as fixed effects. The box plot centre line represents the median; the box limits represent the upper and lower quartiles; the whiskers represent the 1.5x interquartile range. P14 n=7-11; P120 n=8-11; pHFD n=7-9; * p<0.05.

**Figure 7.18. Offspring intestinal morphology is impacted by maternal and postnatal HF diet.**

Figure 7.18. Offspring intestinal morphology is impacted by maternal and postnatal HF diet. GC per μM, GC number, and villus or crypt length are shown for villi and crypts of the ileum in offspring of control (black) and HF (red) dams. Mean values are shown for individual animals, as well as group means and standard deviations. Significance was assessed by linear model with age, sex, and maternal diet as fixed effects. * p<0.05 control vs. HF unless otherwise indicated.
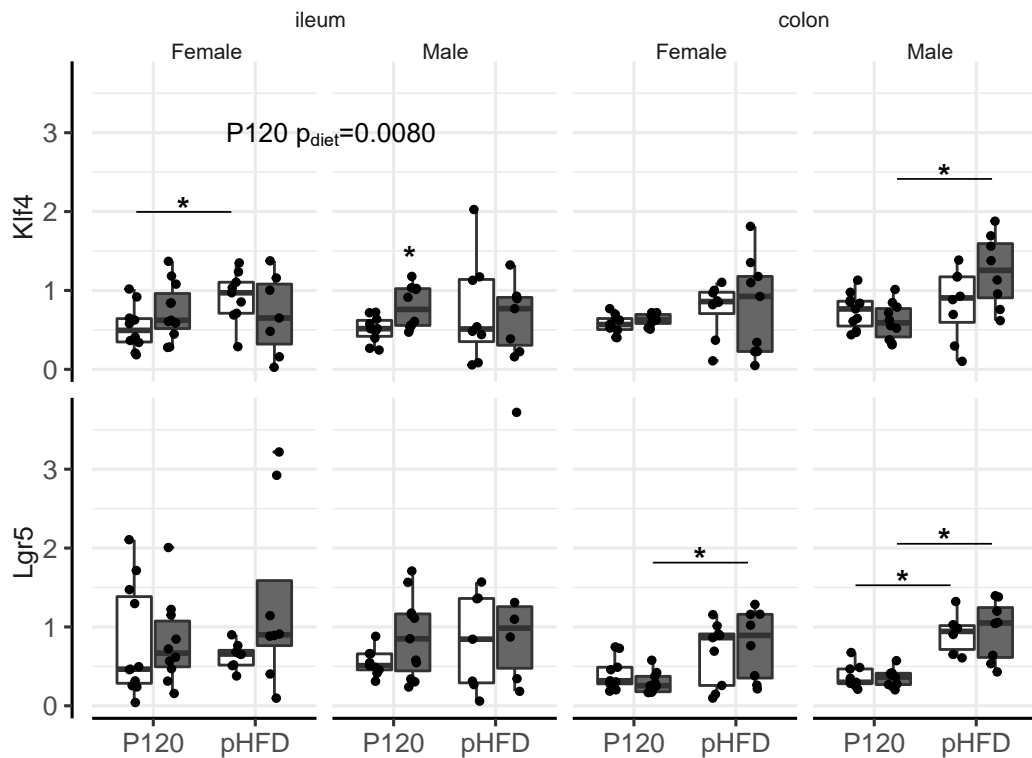
Figure 7.19. Maternal and postnatal HF diet interact to impact offspring intestinal proliferation and differentiation markers. Relative mRNA levels of Klf4 and Lgr5 are shown in the ileum and colon of female (F) and male (M) offspring from control (white) and HF (grey) dams. Significance was assessed within each intestinal section by linear model with age, sex, and maternal diet as fixed effects. The box plot centre line represents the median; the box limits represent the upper and lower quartiles; the whiskers represent the 1.5x interquartile range. P120 n=8-11; pHFD n=7-9; * p<0.05.
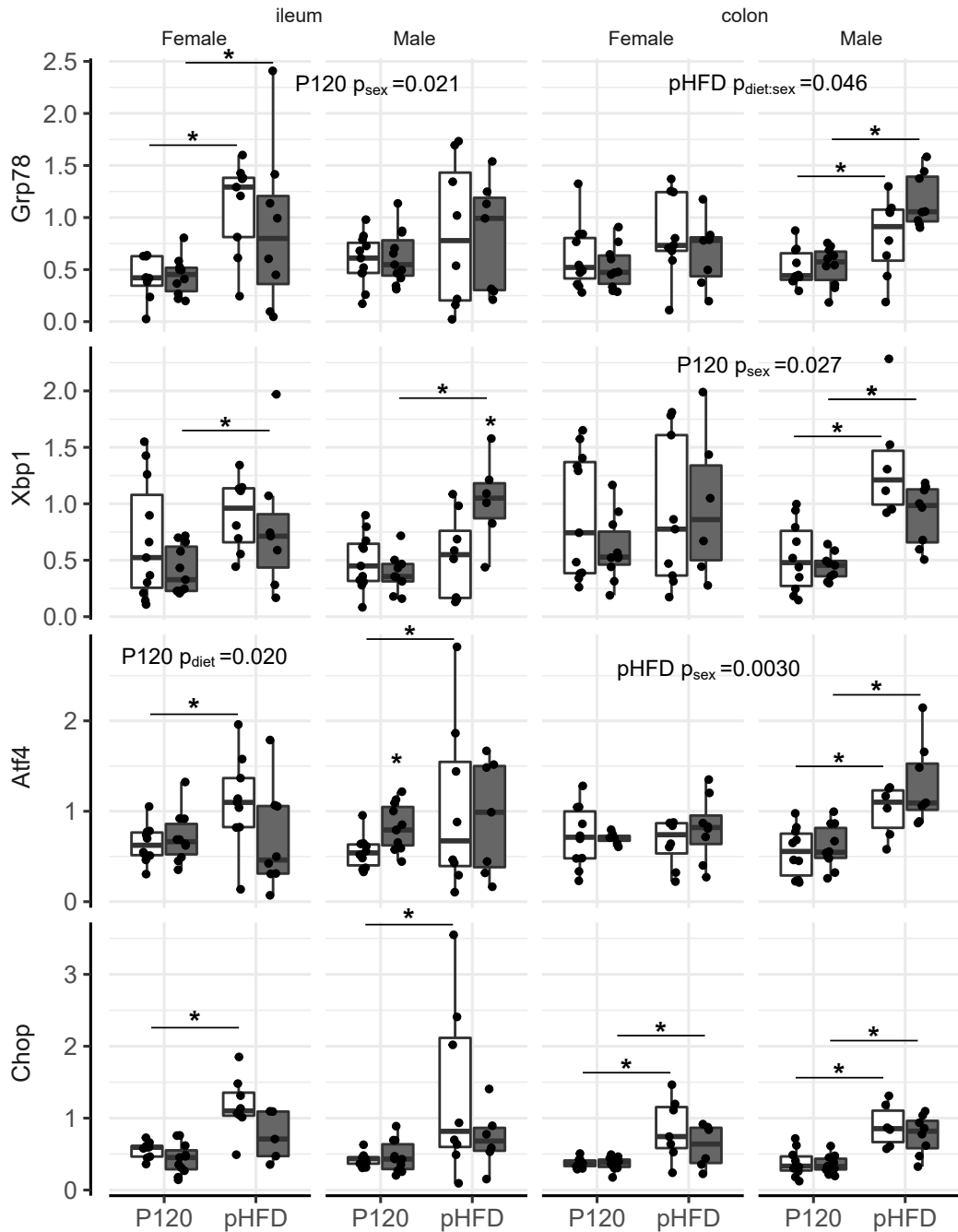
7.4   Discussion

Recently, studies have shown maternal HF diet to predispose offspring to intestinal inflammation induced by DSS (147, 169) or in mice genetically predisposed to inflammation (166, 168), however, the underlying mechanisms are not well defined.

As we previously found that maternal HF diet shifted gut microbiota community composition and was associated with UPR inhibition and increased *Tlr*4 mRNA levels in the fetal gut (see Chapter 5, (265)), we hypothesized that early-life exposure to maternal HF diet would impair offspring gut barrier function, persistently shift gut microbiota composition, and increase offspring susceptibility to intestinal ER stress.

We found that maternal HF diet shifted offspring microbiota community composition and decreased alpha diversity not only prior to weaning (P14) but also into adulthood (P120). In general, maternal HF diet had a greater impact on females at P14 and P120, but males were more affected by maternal HF diet combined with postnatal HF challenge (pHFD).

Maternal HF diet has previously been shown to alter the offspring microbiome in early-life (387) and adolescence (147) in mice, including decreased alpha diversity and changes in overall community composition. In our study, we found alpha diversity (Shannon Index) was decreased with maternal HF diet in both males and females, and further decreased by postnatal HF-challenge but only in male offspring. A decrease in alpha diversity in females, but not males, has previously been reported with postnatal HF diet in the absence of maternal HF

diet (381), suggesting our observed sex-specific effect may be driven by differences in the gut microbiota prior to postnatal HF challenge.

In humans, a recent study found sex-specific associations between the gut microbiota and fat distribution (388). In our study, we found a sex-specific decrease in whole-body adiposity (percent body fat) in females and increases in gonadal fat mass in male offspring of HF dams compared to offspring of control dams after postnatal HF-challenge.

The only bacterial genus significantly affected by maternal HF diet after postnatal HF-challenge was *Lactobacillus*, which was increased in male offspring. As lactobacilli have a diverse repertoire of bile salt hydrolases (389), this increase may be due to their ability to cleave and detoxify bile acids, which are increased in response to HF diet (390). Sex differences in bile-acid metabolism in response to HF diet have previously been reported in humans (391, 392) and mice (393–396) and in response to maternal HF diet, where male offspring had higher levels of serum bile acids than female offspring in response to combined maternal and postnatal HF diet (338). It is possible that similar sex-differences in bile acids are responsible for our observed sex-specific increases in *Lactobacillus*.

This would be consistent with our observed sex-specific increases in markers of ER stress with postnatal HF diet. Elevated bile acids due to HF diet have previously been associated with intestinal ER stress and decreased goblet cell differentiation (397). We found increased markers of ER stress in the ileum and colon and decreased GC numbers in the ileum of pHFD offspring compared to P120 offspring. These outcomes had sex-specific associations between the impact

of postnatal HF-challenge and maternal diet, with additive effects of maternal HF-diet and postnatal HF-challenge on ER stress and intestinal morphology in male offspring.

We additionally found additive effects of maternal and postnatal HF diet on offspring intestinal permeability in pHFD offspring, preceded by decreased mRNA levels of gut barrier markers Tjp1, *Ocln*, and Muc2 with maternal HF diet in P120 offspring. These decreases at P120 were accompanied by decreases in genera of the SCFA producing family *Ruminococcaceae*, decreased mRNA levels of the SCFA receptors Gpr41 and Gpr43, and decreased cecal weight. As we have previously found intestinal SCFA levels to be decreased by HF diet (Chapter 5 (265)) and SCFAs are key modulators of intestinal barrier function (398), this decrease in barrier function may be due to decreased SCFA levels. Future work will quantify cecal levels of SCFA.

In conclusion, we show significant and sex-specific changes to the offspring microbiome and markers of intestinal structure and function with maternal HF diet. We have previously shown that maternal HF diet-induced impairments to fetal gut development are tumour necrosis factor (TNF)-dependent, and further work is required to investigate whether this is also true in neonatal and adult offspring.

Chapter 8

General Discussion

8.1 Summary of findings

The prenatal period represents a critical developmental window, during which adverse environmental stimuli, including maternal obesity or high-fat (HF) diet intake, can trigger in utero adaptive responses that increase the risk of offspring obesity (399). Obesity is associated with shifts in the composition of the gut microbiota in humans (10, 15), and microbiota-dependent gut inflammation precedes HF diet-induced obesity in mice (293). Indeed, the gut microbiota has been suggested to be a central driver of the relationship between maternal obesity and offspring metabolic dysfunction. The pathways that govern this inter-relationship, however, are not clear. The central aim of this thesis was to investigate host-microbe relationships in the context of excess adiposity during pregnancy and their impact on fetal gut development and offspring gut dysbiosis (Fig. 8.1).

offspring gut
dysbiosis

no fetal
microbiota

microbially mediated

fetal gut
development

Maternal metabolic
adaptations to pregnancy

intestinal
permeability

proinflammatory
signalling

Figure 8.1. Updated central thesis

Recent studies have reported human microbial colonization prior to birth (224, 225), but we (Appendix A) and others (400) have noted batch effects and inadequate use of negative controls in studies that report an in utero microbiome. In healthy term infants (Chapter 3), we found that gut colonization does not occur before birth. In light of this new evidence, therefore in the absence of fetal colonization, the maternal gut microbiota likely impacts fetal gut development via microbial antigens or metabolites (88, 110), which then modulates postnatal infant gut colonization. We explored the relationship between the maternal gut microbiota and infant colonization in Chapter 4, and also investigated whether maternal body mass index (BMI)/obesity changed the nature of this relationship. In humans (Chapter 4), we found the maternal gut microbiota composition changed less over the course of pregnancy in participants with higher pre-pregnancy BMI, and that a combination of high pre-pregnancy BMI and excess gestational weight gain (GWG) was associated with decreased

microbiota diversity within infants at 6 months of age. Pre-pregnancy overweight or obesity was also associated with a decreased relative abundance of short-chain fatty acid (SCFA) producers, suggesting that changes in maternal microbial community composition, fueled by maternal BMI, likely have functional outcomes either on the mother or on the developing fetus.

Our in vivo data in mice support this notion. We found that HF diet intake before and during pregnancy increased maternal intestinal permeability and increased levels of maternal circulating proinflammatory factors at term gestation (Chapter 5). Both pregnancy and HF diet shifted maternal gut microbiota composition, and this was modestly modulated by tumour necrosis factor (TNF) (Chapter 6). Maternal HF diet-induced fetal intestinal inflammation (Chapter 5) dependent on TNF (Chapter 6). Whether a proinflammatory milieu in utero impacts offspring gut structure and function was investigated next. In offspring, maternal HF diet intake resulted in changes in gut microbiota community composition that persisted to adulthood. Offspring born to HF mothers were predisposed to increased gut barrier permeability. The changes that we observed in offspring were exacerbated by a metabolic challenge (HF diet challenge in adulthood) which induced intestinal endoplasmic reticulum (ER) stress in a sex-specific manner.

8.2   In utero sterility

Our gut microbes affect our health and wellbeing throughout our lives. Recent data suggest that our relationship with our intestinal passengers is greatest in early life, during critical stages of immunological and physiological development

(285, 401, 402). However, how our gut microbes participate in shaping our earliest development is still unclear. If we want to understand how microbes influence our early-life development, first we must know how and when we are colonized.
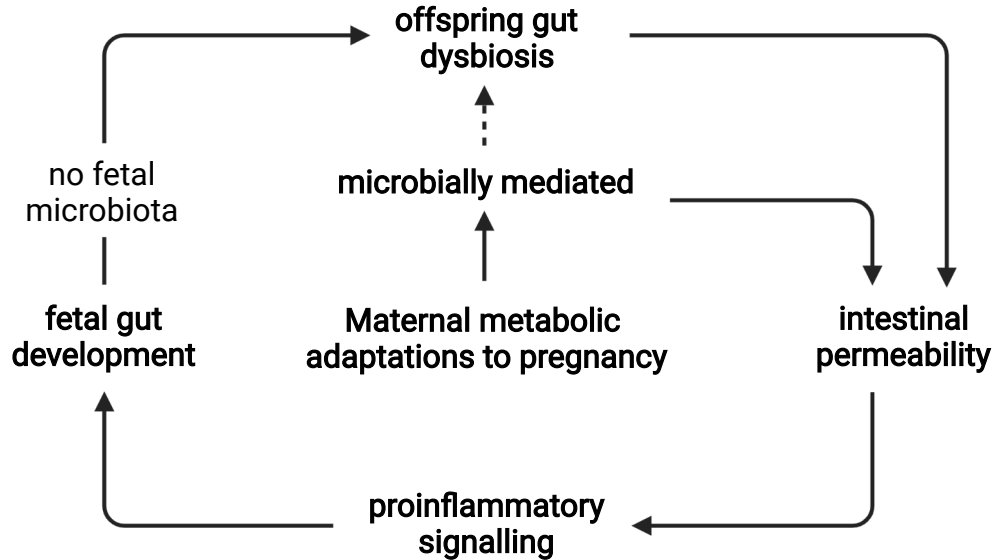
Recent studies have reported human microbial colonization prior to birth (224, 225), but we (Appendix A) and others (400) have noted batch effects and inadequate use of negative controls. Therefore, we embarked on a study that developed new stringent collection methods and expanded our suite of controls to thoroughly test whether the fetus is, in fact, colonized. In healthy term infants (Chapter 3), we found that gut colonization does not occur before birth. Our study demonstrates that stringent experimental methods with robust controls are critical in producing highly reliable, reproducible robust data when investigating low-biomass microbial communities. It also shows that we are not normally colonized before birth. Rather, our relationship with our microbiota emerges during and after birth, which makes it not only vulnerable to early environmental influences, but also offers a window of potential intervention.

8.3 Maternal microbial composition in pregnancy and impacts of adiposity: human studies

Since we have shown that colonization occurs during and after birth, the maternal gut microbiota likely impacts offspring health both directly, through differential colonization during birth, and indirectly, through maternal gut

function and/or fetal exposure to maternally derived microbial components and metabolites. If direct, then changes to the normal composition of the maternal microbiota could influence offspring health. Previous studies have shown inconsistent results of whether pregnancy itself is associated with shifts in the maternal gut microbiota (93, 98, 99, 229). Few studies have investigated the relationship between maternal BMI or GWG and the gut microbiota during pregnancy (106–109).

In humans (Chapter 4), we found the maternal gut microbiota composition changed less over the course of pregnancy in participants with higher pre-pregnancy BMI and was less diverse in participants with excess or insufficient GWG. If the maternal gut microbiota directly impacts colonization in infants, then babies born to participants with excess *GWG* should show lower diversity. This hypothesis is consistent with our observation that infant microbiota diversity was decreased by insufficient GWG, but inconsistent with the association of excess GWG and increased infant microbiota diversity. Microbial diversity has been previously associated with indicators of health (8) and a loss of diversity with indicators of poor health in adults (403–405) and infants (406, 407).

We found that pre-pregnancy overweight or obesity was also associated with a decreased relative abundance of SCFA producers. It has recently been suggested that maternal bacterial components and/or metabolites, rather than microbes *per se*, mediate the link between maternal and offspring health (408). Thus it is possible that amongst the indirect factors that mediate the relationship between maternal adiposity and offspring disease risk (e.g. poor placental function,

inflammation, nutrient transfer) changes in early-life gut development via the transfer of maternal microbiota-derived bacterial components and metabolites (i.e. SCFAs) are likely another contributing factor.

Our observed decrease in beta-dispersion over the course of pregnancy within individuals with higher pre-pregnancy BMIs may reflect differences in maternal metabolic adaptations to pregnancy. Pregnancy is associated with metabolic shifts that mirror characteristics often seen in metabolic syndrome, including hyperglycemia and hyperinsulinemia in addition to increased adiposity (409). Previous studies have found that pre-pregnancy obesity is associated with reduced gains in adiposity over the course of pregnancy (410), while others have reported high pre-pregnancy BMI to be associated with increased GWG (411). Pre-pregnancy obesity has also been associated with increased metabolic rates during pregnancy compared to non-obese individuals (412, 413). These data suggest that individuals with lower pre-pregnancy BMI make greater metabolic adaptations to pregnancy compared to individuals that are already in a "heightened" metabolic state. Consistent with this, we found an increase in microbial shifts over the course of pregnancy in participants with lower pre-pregnancy BMI. It is unknown whether these individuals have to make greater metabolic adaptations during the course of pregnancy, but it would be interesting to determine the microbial community composition in underweight individuals and how this changes over the course of pregnancy.

8.4   Pregnancy and the microbiota and the role of TNF

To gain insights into the signalling pathways that govern the relationship between the pregnant gut microbiota, excess adiposity, and inflammatory and metabolic responses, we performed animal studies using a HF diet-induced obesity model in both wildtype (Wt) and TNF knockout (TNF$^{-/-}$) mice. We hypothesized that HF diet intake prior to and during pregnancy would induce maternal intestinal ER stress and lead to impaired gut barrier function and increased circulating inflammatory factors, which would impair fetal gut development. Consistent with previous studies (308, 321, 414), we showed that the absence of TNF protected female mice from HF diet-induced weight gain prior to pregnancy and from increased adiposity at term gestation. This inhibition of diet-induced weight gain could be due to differences in maternal intestinal lipid absorption, as the absence of TNF signalling has been shown to increase fecal bile acid and lipid content excretion (308). The rate-limiting enzyme in classical bile acid synthesis, cholesterol 7α-hydroxylase (CYP7A1), is inhibited by TNF (307) and its overexpression prevents HF diet-induced obesity (415). The prevention of HF diet-induced obesity by TNF knockout may be mediated in part by altered bile acid synthesis, and although this was not directly measured in this thesis, future work will assess hepatic bile acid synthesis pathways.

Modulation of dietary lipid absorption may also impact intestinal permeability as lipid micelles and chylomicrons mediate the transfer of lipopolysaccharide (LPS) across the intestinal barrier during dietary fat

absorption (416, 417). Our data show that HF diet intake increased circulating TNF and LPS at term gestation in Wt mice, and decreased messenger RNA (mRNA) levels of tight junction proteins (Chapter 5). This is consistent with previous studies in male mice, showing high-fat diet increases intestinal permeability, and that this effect was dependent on the intestinal microbiota rather than due to a direct effect of lipids (418).

Indeed, specific bacteria including *Akkermansia*, *Roseburia*, and *Bacteroides* have been repeatedly linked to increased or decreased levels of circulating LPS (reviewed in (419)). We found that HF diet intake had opposing effects on the relative abundance of these genera in Wt and TNF$^{-/-}$ mice, suggesting that a relationship may exist between these genera, TNF, and intestinal barrier function. Although we found members of the butyrate-producing family *Lachnospiraceae* were generally decreased by HF diet in both Wt and TNF$^{-/-}$ mice, the genus *Roseburia* was increased in Wt but decreased in TNF$^{-/-}$ mice. Interestingly, *Roseburia* can metabolize mucin-derived oligosaccharides, but cannot initiate mucin degradation (420). Only a few species have the enzymatic capacity to initiate mucin degradation, including *Akkermansia*, *Bacteroides*, and *Ruminoccoccus* (421). Our data show both *Akkermansia* and an unknown member of the family *Ruminococcaceae* were increased by HF diet in TNF$^{-/-}$ mice at embryonic day (E)0 and E18.5, but decreased or unchanged in Wt mice. This TNF-dependent differential effect of HF diet on these specific genera may be due to differences in mucin degradation or production between Wt and TNF$^{-/-}$ mice, where Wt mice may have impaired mucin production. This hypothesis is consistent with our observed HF diet-induced decreases in *mucin (Muc)*2

transcript levels and goblet cell (GC) numbers in HF-fed Wt dams. Together, these shifts in community composition indicate that pregnancy likely alters microbe-host mucin metabolism in both Wt and TNF$^{-/-}$ dams, but the absence of TNF further alters the effect of HF diet on host mucin synthesis and bacterial mucin degradation.

Many beneficial genera that specifically colonize and adhere to intestinal mucins are butyrate-producers (422). We found that HF diet decreased relative abundances of butyrate-producing genera, and decreased cecal levels of butyrate in both Wt and TNF$^{-/-}$ mice. As butyrate is the main energy source of intestinal colonocytes and is important in maintaining gut barrier function (20), these data may suggest that the impact of HF diet on intestinal structure and function are due to indirect contributions of a changing microbial environment and downstream production of metabolites. Indeed, butyrate supplementation alone has been shown to restore HF-diet impaired gut barrier function in association with reduced inflammation (423). As we found HF diet to reduce cecal butyrate levels in both Wt and TNF$^{-/-}$ mice, it is possible that the absence of TNF-mediated inflammation prevents some of the negative effects of decreased butyrate on intestinal barrier function. This would be consistent with the ability of TNF to impair tight junction assembly in the absence of decreased tight-junction protein levels (424). Intestinal permeability was not measured in TNF$^{-/-}$ mice in the current study, but would be of interest to test this hypothesis.

If the absence of TNF-mediated inflammation prevents HF diet-induced increases to maternal gut permeability, it could also prevent fetal exposure to pro-inflammatory microbial components including LPS. Previous studies have

found fetal exposure to LPS induced gut inflammation (341), impaired gut barrier development (342), and postnatal intestinal injury (343). Our data show that maternal HF diet-induced fetal intestinal inflammation and altered markers of intestinal development, and that this was dependent on TNF. Future work will investigate whether these effects are associated with altered fetal intestinal tight-junction assembly.

8.5 Maternal obesity impacts offspring gut structure, function, and microbial colonization

Previous studies have found that maternal HF diet consumption induced offspring gut dysbiosis at 8 weeks of age (147) and increased offspring susceptibility to Dextran sulphate sodium (DSS)-induced colitis (169). The underlying mechanisms are not well defined. Therefore, we employed a HF diet-induced pregnancy mouse model to investigate impacts on fetal and postnatal offspring gut structure and function. In Chapter 5 (265), we found that maternal HF diet was associated with down-regulation of the unfolded protein response (UPR) in the fetal intestine, as well as increases in markers of inflammation, and we hypothesized that these changes may predispose offspring to altered host-microbe relationships postnatally. We next investigated the relationship between early-life exposure to maternal HF diet and the offspring gut microbiota, and evaluated offspring gut permeability and susceptibility to postnatal HF challenge. We found that maternal HF diet intake persistently

shifted gut microbiota community composition in offspring into adulthood and predisposed offspring to increased gut barrier permeability and gut ER stress induced by HF-challenge in a sex-specific manner.

We found that maternal HF diet-induced sex-specific structural changes in the offspring small intestine: in females, but not males, maternal HF diet decreased offspring small intestine length as well as goblet cell numbers and *Muc*2 transcript levels in the ileum. In contrast, in males, but not females, maternal HF diet combined with postnatal HF challenge increased offspring villus and crypt length in the ileum, and postnatal HF diet-induced markers of ER stress in the colon (independent of maternal diet). These sex-specific effects are consistent with the hypothesis that under adverse conditions female offspring make more early-life physiological adaptations, whereas males trade-off immediate growth and survival, making fewer early-life adaptations, but then are more prone to adverse outcomes later (425).

We found sex had a small impact on offspring gut microbiota beta-diversity in adult (postnatal day (P)120, post-HF diet challenge (pHFD)), but not neonatal mice (P3, P14). This sex effect was more subtle than the impact of maternal diet, which persistently impacted offspring gut microbiota beta diversity into adulthood, and even after postnatal HF-challenge in males but not in females. Despite this overall effect of maternal HF-diet on offspring gut microbiota community composition, changes in the abundances of specific bacteria at P120 were subtle, which is consistent with the known large effect of postnatal diet (426).

193

Although HF diet decreased the relative abundance of genera within the butyrate-producing family *Lachnospiraceae* in the maternal gut microbiota during pregnancy (Chapter 6) and lactation (Appendix D), only *Anaerostipes* remained decreased at P120 in offspring, and were in fact not detected in offspring from HF mothers. This suggests that the majority of genera that are decreased in offspring born to mothers fed a HF diet are likely vertically transferred to the offspring, or are otherwise acquired from the environment postnatally, and that differences in the offspring gut microbiota are not due to a lack of exposure to specific taxa.

Offspring born to mothers fed a HF diet showed a persistently decreased abundance of SCFA producing *Ruminococcaceae* genera and *Parasutterella*, a regulator of bile acid metabolism, despite offspring being weaned onto control diet. This suggests it is highly likely that maternal diet-induced changes in the structure and function of the developing fetal intestine and offspring gut, resulting in an altered intestinal niche for colonizing microbes postnatally. As *Ruminococcaceae* and *Parasutterella* species are known mucin degraders with preferences for specific post-translational modifications (305, 427), maternal HF diet-induced changes to offspring mucin production may shift the mucous layer microbial niche. Decreases in these "healthy" mucin degraders may open a niche for pathobionts such as *Bacteroides*, which can penetrate the mucus layer and reside deep within intestinal crypts (428) and induce colitis in genetically susceptible hosts (302). Future work will further characterize the intestinal mucus of the offspring ileum and colon.

8.6 Limitations

We recognize that the experiments presented herein are not without limitations. In our study of human fetal meconium (Chapter 3 (222)), although we used both culture- and sequencing-based techniques there remains a possibility, however unlikely (Appendix A), that bacteria are present below the limits of detection or in a location within the fetal intestine that we were unable to sample, such as these found within immune cells as suggested by Rackaityte et al. (224).

As in previous studies of the human gut microbiota in pregnancy (93, 106–109, 158), our human studies are limited by sample size (Chapter 4, Appendix B). This limitation is particularly evident in the low number of participants with high pre-pregnancy BMI and within the recommended range for GWG. This is consistent with previous studies reporting pre-pregnancy overweight and obesity are associated with an increased risk of excess GWG (429–431). Low sample sizes also limited our ability to assess the effect of sex or delivery mode on the infant gut microbiota.

As our experimental studies (Chapters 5, 6, 7) were conducted using mice some of the results may not be directly translatable to humans. As mice are polytocous, producing multiple offspring per pregnancy, individuals within the same litter may have variable fetal and neonatal nutrient supply, and variation in litter size can impact maternal adaptations to pregnancy (432). Furthermore, although approximately 90% of genera are shared between the gut microbiota of humans and mice (433), the selective pressures of the host intestine vary by species (155) and thus our data on microbial community composition in mice

likely does not reflect what is found in humans. The human and mouse intestine also have important immunological (434) and developmental differences (114) that limit translatability.

Finally, to investigate the role of TNF in inducing ER stress in maternal intestinal adaptations to pregnancy as well as fetal intestinal development due to HF diet we used a whole-body knockout model, which presents key confounders when interpreting these data. Although we conducted pilot analyses in littermates (Appendix C) our TNF experiments were conducted in non-littermates (Chapter 6) and thus differences in TNF-mediated changes in other pregnancy adaptations that might influence our measures cannot be accounted for in our analyses.

8.7   Future directions

This thesis has presented new and exciting data in the field of perinatal biology and host-microbe relationships during pregnancy. However, there are key experiments that still need to be undertaken to thoroughly test the central hypothesis. Given our data showing that colonization does not occur prior to birth in healthy pregnancies, future work should focus on the impact of maternal microbiota-derived microbial components and metabolites on fetal gut development, and on the role that maternal diet and health status plays in modulating these factors.

To further investigate the relationship between maternal pre-pregnancy BMI, GWG, shifts in the maternal gut microbiota over the course of pregnancy, and

the infant gut microbiota future work is needed to quantify SCFA levels in maternal and infant stool as well as maternal and cord blood. To test the hypothesis that the effects of maternal obesity are mediated by increased pro-inflammatory signalling future work is also needed to measure circulating pro-inflammatory cytokines and chemokines in maternal and cord blood serum.

Future work should also explore the role of the placenta in mediating the impacts of excess maternal adiposity, including untargeted metabolomics, gene, and protein expression analyses to thoroughly evaluate all three arms of the UPR and markers of ER stress and pro-inflammatory signalling in the fetal and offspring gut. Future work is needed to quantify and localize tight junction proteins in the maternal, fetal, and offspring intestine of Wt and TNF$^{-/-}$ mice, and further assess the relationship between mucin-degrading microbial taxa, host mucin production, and intestinal ER stress.

8.8   Concluding remarks

Fetal intestinal and immune development prepares the neonate for life in a microbial world, and the environment within which this development occurs has implications for lifelong health and the prevention of chronic diseases. Largely overlooked until recently, the gut microbiome has emerged in perinatal biology to be a central factor in the correspondence between the mother and the developing offspring. However, our understanding of how the microbiome governs maternal-fetal-neonatal communication and, ultimately, long-term health continues to be rudimentary. In this thesis, we explored this relationship and showed that excess maternal adiposity (obesity, excess GWG, or high-fat diet)

shifts the offspring gut microbiota and increases offspring susceptibility to HF diet-induced increases in intestinal permeability. These outcomes are likely mediated by impaired fetal gut development resulting from exposure to pro-inflammatory factors in maternal circulation due impaired maternal gut barrier function, likely due to TNF-mediated inflammation and degradation of the mucus barrier. Collectively, our data provide new insights host-microbe relationships and their impact on the mother and offspring.

Appendix A

Chapter 3 Supplement: Letter to the Editor

This chapter contains a Letter to the Editor in response to a recent Cell publication entitled "Microbial exposure during early human development primes fetal immune cells" by Mishra et al. (225).

Over-Celling Fetal Microbial Exposure

Katherine M. Kennedy[1,2], Christian J. Bellissimo[1,2], Jessica A. Breznik[3,4,5], Jon Barrett[6], Thorsten Braun[7], Frederic D. Bushman, Marcus De Goffau[9], Michal Elovitz[10, 11], Markus Heimesaat[7], Liza Konnikova[12], Omry Koren[13], Samuel Parry[11], Laura Rossi[2,5], Nicola Segata[14], Rebecca A. Simmons[15,16,17], Michael G. Surette[1,2,5], Jens Walter[18], Deborah M. Sloboda[1,2,6,19]

[1]Department of Biochemistry and Biomedical Sciences, McMaster University, Hamilton, Canada
[2]Farncombe Family Digestive Health Research Institute, McMaster University, Hamilton, Canada
[3]McMaster Immunology Research Centre, McMaster University, Hamilton, Canada
[4]Michael G. DeGroote Institute for Infectious Disease Research, McMaster University, Hamilton, Canada
[5]Department of Medicine, McMaster University, Hamilton, Canada
[6]Department of Obstetrics and Gynecology, McMaster University, Hamilton, Canada
[7]Charité – Universitätsmedizin Berlin, corporate member of Freie Universität Berlin and Humboldt-Universität zu Berlin, Department of Obstetrics and 'Experimental Obstetrics', Berlin, Germany
[8]Department of Microbiology, Perelman School of Medicine, University of Pennsylvania, Philadelphia, USA
[9]Department of Veterinary Medicine, University of Cambridge, Cambridge, UK
[10]Department of Obstetrics and Gynecology, Perelman School of Medicine, University of Pennsylvania, Philadelphia, USA
[11]Maternal and Child Health Research Center, Perelman School of Medicine, University of Pennsylvania, Philadelphia, USA
[12]Department of Pediatrics, Department of Obstetrics, Gynecology and Reproductive Sciences, Human and Translational Immunology, Yale Medical School, New Haven, USA.
[13]The Azrieli Faculty of Medicine, Bar Ilan University, Safed, Israel
[14]Department CIBIO, University of Trento, Povo, Italy
[15]Center for Research on Reproduction and Women's Health, Perelman School of Medicine, University of Pennsylvania, Pennsylvania
[16]Center of Excellence in Environmental Toxicology, Perelman School of Medicine, University of Pennsylvania, Philadelphia, USA
[17]Division of Neonatology, Children's Hospital of Philadelphia, Philadelphia, USA
[18]APC Microbiome Ireland, School of Microbiology and Department of Medicine, University College Cork – National University of Ireland, Cork, Ireland
[19]Department of Pediatrics, McMaster University, Hamilton, Canada

The *in-utero* environment shapes health beyond fetal life and influences long term health trajectories. Early-life colonization with specific microbes has been suggested to predict later health outcomes including asthma[1], allergy[2], and obesity[3]. The possible colonization of humans prior to birth has been controversial. Measurements are technically challenging because low microbial biomass samples, with little or no authentic signal, can be dominated by contamination introduced during sampling, DNA isolation, PCR amplification and sequencing. Sequencing of appropriate negative controls is essential to account for contamination and to ensure reproducibility. Multiple sequencing runs of the same samples can account for stochastic sequencing noise. To date, none of the studies that reported human microbial colonization prior to birth have accounted for all of these sources of bias, including the recent paper by Mishra et al.[4]. This is in contrast to the increasing number of studies which account for sources of bias and contamination[5–8], and report no microbial colonization before birth in the absence of infection with well-known ecologically capable pathogens[8].

Mishra et al.[4] set out to test the hypothesis that in utero microbes result in fetal-immune priming before birth, studying "live microbes in fetal organs during the 2nd trimester of gestation" and immune responses to these microbes. Despite emphasizing the use of negative controls, they lack controls for maternal vaginal and skin microbiota, which are the greatest sources of contamination. In this study, terminations of 2nd trimester pregnancies were initiated by prostaglandin treatment, followed by vaginal delivery. This clinical procedure typically requires many hours of labour and rupture of fetal

membranes—during which ascending colonization is common[9]—followed by passage through the vaginal canal assuring contamination. Procedural swab controls could have accounted for this but were not included, so the maternal skin and vaginal microbiota cannot be discounted as a source of contamination. We therefore conclude that the experimental approach applied by Mishra et al.'s[4] was inherently flawed to test the actual hypotheses of the study.

Contamination by vaginal microbes is clearly evident in the heterogenous distribution of fetal-enriched genera reported in the study (see Fig. 2G and S3D in Mishra et al.[4]): *Lactobacillus* and *Gardnerella* are the most abundant genera—and most heterogeneously distributed— particularly in placental and fetal skin samples. These sites are directly exposed to the vaginal canal during delivery, and the findings are consistent with those of De Goffau et al. in that vaginal lactobacilli are more commonly detected in vaginally delivered placentas as compared to those delivered by C-section[10]. Other fetal-enriched genera in this paper are present at similar abundances in gut samples as in thymus internal controls—consistent with operator or environmental contamination—and thus, are unlikely to represent fetal organ colonization. The most obvious case of environmental contamination reported by Mishra et al.[4] is *Bradyrhizobium*, which is a soil bacterium and one of the most dominant and consistent contaminants in sequencing studies[11,12].

These contamination issues can be mitigated with appropriate use of multiple controls. Mishra et al.[4] compared most of their samples to DNA isolated from PBS. In our recent study[5], we found no differences in alpha- or beta-diversity between term fetal meconium

and negative controls. Mishra et al. similarly found no difference in alpha-diversity (Mishra Fig. S2F, S2G) but present this as a statistically significant difference in the fraction of samples below the 95th percentile Shannon index in PBS negative controls (Mishra Fig. 2D), which is not a genuine test of their hypothesis. Mishra et al. further report a difference in beta diversity (Fig. 2E and S2H). However, since controls and samples were sequenced in different batches, an analysis to account for batch effects is required but was omitted. Using the sequencing data that was publicly provided with their paper, we reanalyzed these data and found the difference in beta-diversity to be driven by a batch effect (PERMANOVA, $R^2 = 0.27$, $p = 0.001$). Within batches that included environmental or operator negative controls (batches MUX7225/7, MUX9413, and MUX9414) only fetal skin, placenta, and operator controls were more dissimilar from PBS controls than PBS controls were from themselves (Fig. 1). These findings are again consistent with surface contamination during sample collection.

Surface contamination of the fetuses was also evident in the culture data reported by Mishra et al.[4]. The authors cultured live bacteria in increasing abundance from internal organs (spleen, thymus) to exposed organs (gut, lung) and external tissue (skin, placenta). As the species that were cultured (e.g. *L. iners* and *L. jensenii*, but also *Gardnerella vaginalis*; Table S5), are dominant inhabitants of the human vagina, the vaginal microbiota is almost certainly a source of contamination. The only genera cultured from fetal lung or gut (but not from fetal skin or placenta) were *Propionimicrobium* and *Propionibacterium*/*Cutibacterium* (Mishra Fig. 3D). As these genera were present in the sequencing data from the same donor's thymus, spleen, skin, placenta, and PBS control

(Table S3), they are likely procedural contaminants. Mishra et al.'s positive culture results from internal controls (spleen and thymus) additionally support the presence of procedural contamination. This conclusion is supported by the Scanning Electron Microscopy (SEMs) analysis. The micrographs clearly show pockets of largely singular coccoid structures. This cell morphology is inconsistent with their sequencing data, where all but one of the genera enriched in fetal gut tissues were rod-shaped bacilli. As the samples were washed and stored in PBS, which the authors report to be enriched in *Micrococcus*, the coccoid structures in the SEM images are likely to have been contamination acquired during sample processing, rather than *in situ* fetal bacteria.

Despite the susceptibility of the experimental approach applied by Mishra et al.[4]. to contamination, and the clear evidence that it did in fact occur, the microbial signals as determined by qPCR (CT of >30 cycles) and culture analysis (<100 colonies per fetus on average) were extremely low. The approaches used by Mishra et al. did not constitute genuine tests of their hypothesis[13], and an increasing number of studies with more robust experimental designs support the absence of viable bacterial colonization *in-utero* under normal circumstances[5–8]. Independent evidence for our conclusion comes from the field of gnotobiology. Animals entirely free of microbes can be generated by delivery of neonates via sterile Cesarean section, followed by transfer to a sterile isolator. This method is used routinely at many sites to derive novel strains of germ-free mice. In rare cases, human neonates have also been delivered in a sterile fashion, sequestered in a sterile environment afterwards, and shown to remain sterile; providing strong functional evidence of in utero sterility[14]. Despite this, the absence of a fetal microbiota does not

preclude potential education of the fetal immune system by microbial antigens since microbial components and metabolites[15] can cross the placenta from maternal circulation and prime fetal immune development[16].

Growing appreciation of how perinatal exposures and microbes independently shape our health trajectories, coupled with increased accessibility to sequencing technologies, has created a wealth of research on the microbial world during pregnancy. While scientific advancements in maternal-fetal health are urgently needed, microbiome studies *must* consider biological processes—such as parturition— and biological plausibility in experimental design, and data interpretation. Without this consideration findings due to systemic experimental errors appear reproducible when these systemic errors are repeated/replicated. The interpretation of such research has to remain sceptical, and researcher have to be willing to reject their hypothesis[13] and to accept limitations in their experimental design otherwise resulting in confirmation bias. Only robust research with a critical mindset will allow us to establish solid scientific foundations, research, and funding priorities, and ultimately achieve progress in this important field of study.

References

1. Fujimura, K. E. *et al.* Neonatal gut microbiota associates with childhood multisensitized atopy and T cell differentiation. *Nat. Med.* **22**, 1187–1191 (2016).
2. Ruohtula, T. *et al.* Maturation of gut Microbiota and circulating regulatory T cells and development of IgE sensitization in early life. *Front. Immunol.* **10**, 2494 (2019).
3. Soderborg, T. K. *et al.* The gut microbiota in infants of obese mothers increases inflammation and susceptibility to NAFLD. *Nat. Commun.* **9**, 4462 (2018).
4. Mishra, A. *et al.* Microbial exposure during early human development primes fetal immune cells. *Cell* (2021) doi:10.1016/j.cell.2021.04.039.
5. Kennedy, K. M. *et al.* Fetal meconium does not have a detectable microbiota before birth. *Nature Microbiology* 1–9 (2021).
6. Lauder, A. P. *et al.* Comparison of placenta samples with contamination controls does not provide evidence for a distinct placenta microbiota. *Microbiome* **4**, 29 (2016).
7. de Goffau, M. C., Charnock-Jones, D. S., Smith, G. C. S. & Parkhill, J. Batch effects account for the main findings of an in utero human intestinal bacterial colonization study. *Microbiome* **9**, 6 (2021).
8. Kuperman, A. A. *et al.* Deep microbial analysis of multiple placentas shows no evidence for a placental microbiome. *BJOG* **127**, 159–169 (2020).
9. DiGiulio, D. B. *et al.* Prevalence and diversity of microbes in the amniotic fluid, the fetal inflammatory response, and pregnancy outcome in women with preterm pre-labor rupture of membranes. *Am. J. Reprod. Immunol.* **64**, 38–57 (2010).
10. de Goffau, M. C. *et al.* Human placenta has no microbiome but can contain potential pathogens. *Nature* **572**, 329–334 (2019).
11. Laurence, M., Hatzis, C. & Brash, D. E. Common contaminants in next-generation sequencing that hinder discovery of low-abundance microbes. *PLoS One* **9**, e97876 (2014).
12. Salter, S. J. *et al.* Reagent and laboratory contamination can critically impact sequence-based microbiome analyses. *BMC Biol.* **12**, 87 (2014).
13. Walter, J. & Hornef, M. W. A philosophical perspective on the prenatal in utero microbiome debate. *Microbiome* **9**, 5 (2021).
14. Perez-Muñoz, M. E., Arrieta, M.-C., Ramer-Tait, A. E. & Walter, J. A critical assessment of the "sterile womb" and "in utero colonization" hypotheses: implications for research on the pioneer infant microbiome. *Microbiome* **5**, 48 (2017).
15. Li, Y. *et al.* In utero human intestine harbors unique metabolome, including bacterial metabolites. *JCI Insight* **5**, (2020).
16. Gomez de Agüero, M. *et al.* The maternal microbiota drives early postnatal innate immune development. *Science* **351**, 1296–1302 (2016).

Figure 1.
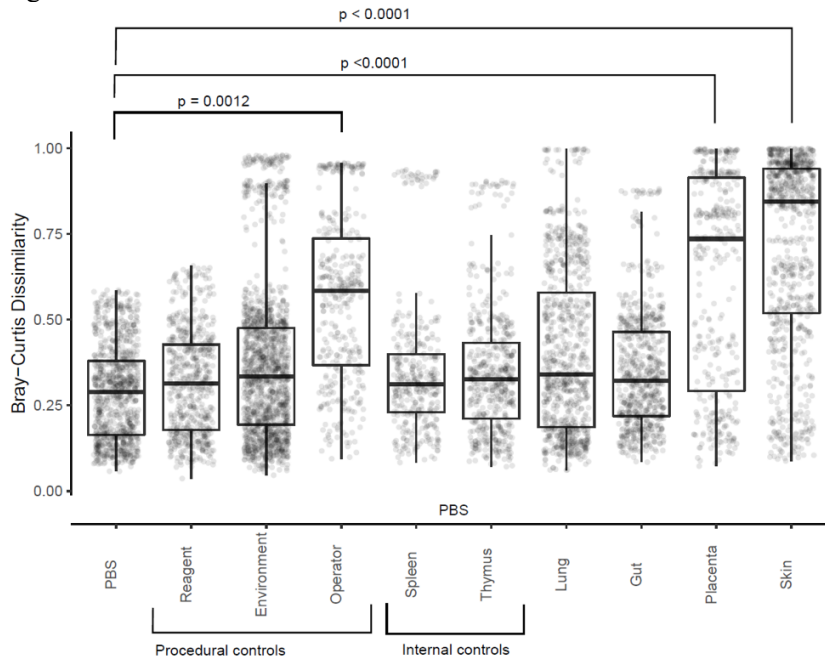
Fig. 1| Fetal gut beta diversity does not differ from that of negative controls for batches that included procedural controls. Box plots of Bray-Curtis dissimilarities between each sample type and PBS show that fetal lung and gut microbial communities are no more dissimilar to PBS negative controls than PBS negative controls are to each other. Fetal skin and placental microbial communities were more dissimilar to PBS negative controls than PBS negative controls were to each other, consistent with surface contamination during sample collection. Samples from batches MUX3180, MUX4197, MUX4811, and MUC5612 were excluded (67 of 294 samples excluded) due to absence of procedural controls within those batches. Sample-to-sample dissimilarities are grouped by sample type-to-PBS comparisons. Significance was assessed by a linear mixed model with sample type as a fixed effect and sample ID as a random effect.

Appendix B

Maternal and infant gut microbiota in humans and the impact of excess adiposity during pregnancy: cohort 2 pilot analyses

B.1   Introduction

Gut microbiome studies have shown that environmental factors, including diet, significantly impact the composition of the intestinal microbiota (185, 186), but inter-individual/participant differences have also been shown to be important confounders in evaluating intestinal microbiota (7, 8). Inter-individual differences

between participants account for a large percentage of the variation observed in cohorts of humans (228) and even in experimental studies, where cage effects are often seen (435). Therefore, in order to investigate whether pregnancy-associated and BMI/adiposity-associated changes in maternal and infant microbiota can be replicated in a different geographically located cohort of pregnant women; we replicated our microbiome studies in Chapter 4, in a second cohort of women located in Hamilton, Ontario.

In collaboration with the Atkinson Lab at McMaster University, we collected stool samples from a subset of participants that were enrolled in their Randomized Clinical Trial (Atkinson, Be Healthy in Pregnancy (BHIP– Clinical Trials registration – NCT01689961) at McMaster University. The objective of the RCT was to test the effectiveness of a novel structured and monitored Nutrition + Exercise intervention on management of gestational weight gain in pregnancy.

Our objective was to evaluate the relationship between pre-pregnancy body mass index (BMI), gestational weight gain (GWG), and the maternal gut microbiota and to compare data from this cohort of pregnant women to those collected from women in Berlin Germany. Unfortunately, due to constraints in recruitment and acquiring metadata data from the RCT cohort, only a pilot analysis was performed to date. Recruitment, participant follow-up, collection of participant information was all performed by the Atkinson Lab. Stool sample preparation and processing and the analysis of bacterial sequencing was performed by the candidate.

Participants that consented to enter the BHIP study were approached to enter

the BUGS in BHIP study. Inclusion criteria for participants include: within the first 17 weeks of pregnancy; BMI < 40; over 18 years of age; no diabetes or other known medical conditions; no contraindications to exercise; not opposed to consuming all food groups; and being a non-smoker. BMI of participants was measured at the time of recruitment and participants were categorized as healthy (18.5-24.9), overweight (25-29.9), or obese (30-40). Participants were evaluated at the end of the first (10-17 weeks), second (26-28 weeks), and third (>36 weeks) trimesters, and again at 6 months postpartum. At each evaluation (4 in total), participants completed a standard 3-day food and supplement intake record, and maternal serum and stool samples were collected. At 6 months postpartum maternal and infant stool was collected. Antenatal data was collected by BHIP from clinical charts, including mode of delivery, birth weight, gestational age. At the time of delivery, cord blood was collected, and 3 discrete biopsies of placental tissue were collected and placed in Allprotect Tissue Reagent at 4º C for 48 hours before being stored at -80ºC. One full-thickness placental sample including decidua and amnion and a 1 cm length of umbilical cord were fixed in 4% paraformaldehyde for morphological analysis and localization of immune cells.

B.2 Results

B.2.1 Participant characteristics

Stool samples were collected from participants enrolled in the Be Health in Pregnancy randomized controlled trial (RCT) (NCT01689961) (436). Randomization to either an intervention group (high-dairy nutrition and structured exercise) or a control group (standard care as per National Health

Canada recommendations) was stratified by pre-pregnancy BMI category. As GWG was the primary outcome measure of the BHIP RCT these data were not yet available to the candidate for analysis and therefore preliminary microbiota analysis to date has focused on the impact of pre-pregnancy BMI.

Sample time points were the same as in the Berlin cohort (see Chapters 2 (methods) 4), with the exception that maternal and infant samples were not collected at delivery. Maternal fecal samples from 31 participants in the Control arm and 32 participants in the Intervention arm were sequenced and analyzed. Pre-pregnancy BMI was used as a continuous variable or by BMI category: optimal (18.5-24.9: Control, n=19; Intervention, n=22), overweight (>30: Control, n=9); Intervention n=6) or obese (25-29.9: Control, n=3; Intervention, n=3). Of the 58 participants with a recorded delivery mode, the majority of participants delivered vaginally (41/58; 71%). Within the Control arm, the majority of participants delivered vaginally overall (21/26; 81%), and within each pre-pregnancy BMI category: optimal (13/17; 76%), overweight (5/6; 83%), obese (3/3; 100%).

B.2.2   Pre-pregnancy BMI impacts the maternal microbiota

In this cohort, we assessed the gut microbiota using 16S ribosomal RNA (rRNA) gene sequencing of the variable 3 region (V3) as sequencing was performed in 2017 prior to combined V3V4 sequencing becoming available within the Farncombe Metagenomic Facility at McMaster University. After removing host-associated sequences and taxa present in less than 5% of samples, the

median read count was 72,854 (minimum 7,405; maximum, 145,629). As GWG data were not available, the impact of pre-pregnancy BMI on maternal alpha diversity was assessed by a mixed linear model with pre-pregnancy BMI and sample time point as fixed effects and participant ID as a random effect. Sample alpha diversity (Shannon Index) was not significantly different between sample time points (p=0.90) or by pre-pregnancy BMI (p=0.86). This differed from the Berlin cohort, potentially due to a smaller sample of participants with pre-pregnancy overweight or obesity. Within only control arm participants and only pregnancy sample time points the effects of pre-pregnancy BMI (p=0.66) and sample time point (p=0.29) were also not significant (Fig. B.1.

Beta diversity was assessed by Bray-Curtis dissimilarity and visualized by principal coordinate analysis (PCoA) (Fig. B.2). Group allocation (Intervention vs. Control) had a small but significant effect on beta diversity (R^2=0.015, p=0.0001), and samples from participants in the Intervention arm were excluded from further analysis. Across all sample time points, pre-pregnancy BMI category (R^2=0.042, p=0.0001) and sample time point (R^2=0.024, p=0.016) had small but significant effects on beta diversity. The effect of pre-pregnancy BMI was not significant within any individual sample time point. As in the Berlin cohort (Chapter 4), individual variation between participants explained the majority of variation between samples (R^2=0.62, p=0.0001).

To investigate whether pre-pregnancy BMI impacts beta diversity within participants, we grouped samples by participant and calculated the mean distance to the centroid within each group (beta dispersion) using Bray-Curtis dissimilarity. Pre-pregnancy BMI was not significantly correlated with mean beta
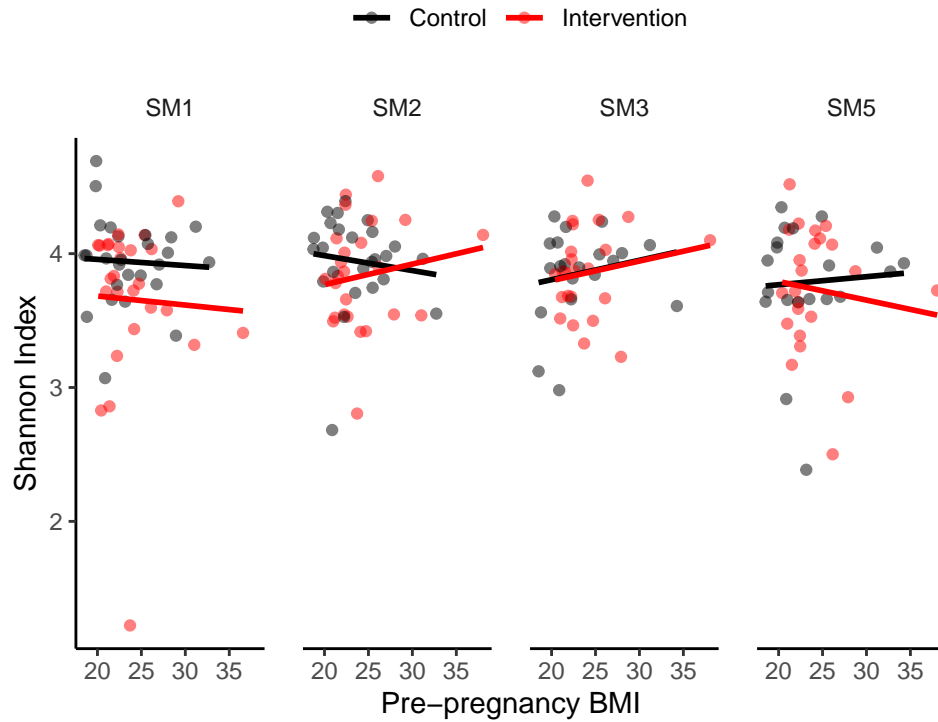
Figure B.1. Alpha diversity is similar across sample time points. Scatter plots of alpha diversity (Shannon Index) measures by sample time point. Alpha diversity did not vary significantly by pre-pregnancy BMI overall or within sample time points. Significance was assessed by mixed linear model with pre-pregnancy BMI and sample time point as interacting fixed effects, and individual participant ID as a random effect.

dispersion across all sample time points (p=0.082; Fig. B.3). As this correlation was driven by increased dissimilarity of samples from the end of pregnancy (delivery; sample: maternal (SM)4) in the Berlin cohort, the lack of significance in the BHIP cohort may be due to the absence of this sample time point.

To investigate specific taxa affected by pre-pregnancy BMI category, differential abundance testing was performed using DESeq2 (RRID: SCR_015687). As there were only 3 control-arm participants with pre-pregnancy
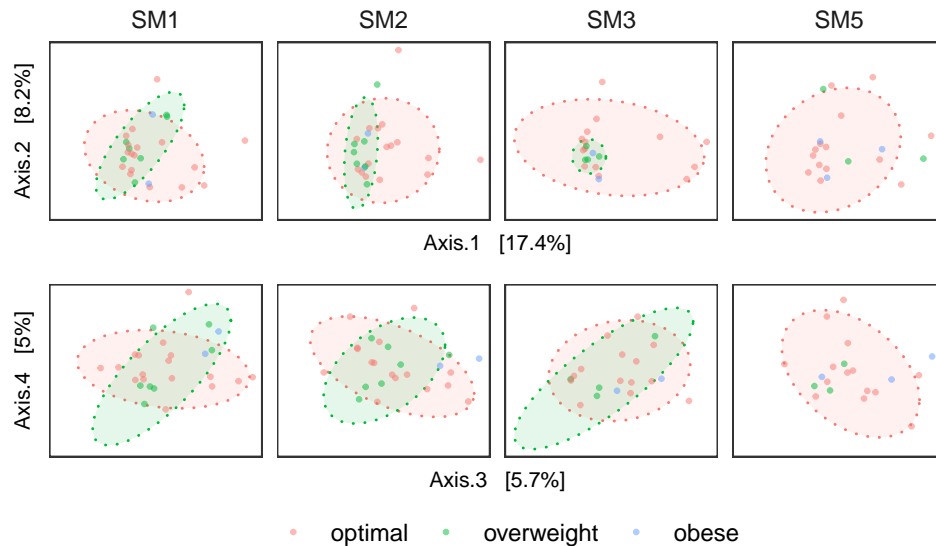
Figure B.2. Beta diversity varies with pre-pregnancy BMI category. Principle coordinate analysis plots of Bray-Curtis dissimilarities show samples from participants with a pre-pregnancy BMI 18.5-24.9 (optimal; red), 25-29.9 (overweight; green) or greater than 30 (obese; blue). Significance was assessed by permutational multivariate analysis (adonis; vegan) with pre-pregnancy BMI category, GWG category, and sample time point as interacting fixed effects and participant ID as an additive fixed effect. Ellipses are shown for 90% confidence level.

obesity, their samples were grouped with those from participants with pre-pregnancy overweight. Across all sample time points, pre-pregnancy overweight or obesity was associated with a decreased relative abundance of *Bacteroidales* genera *Prevotella* and *Porphyromonas*, as well as *Clostridiales* genera *Ezakiella* and *Anaerococcus* (Fig. B.5; Table B.1).

Table B.1. Differentially abundant families in maternal microbiota with pre-pregnancy overweight or obesity compared to a pre-pregnancy BMI within the optimal range (18.5-24.9). Taxa with a mean abundance of less than 40 were excluded. Mean, base mean abundance, log2FC, log2 fold change; SE, standard error.

Phylum	Order	Family	Genus	Mean	log2FC	SE	stat	padj
Firmicutes	Clostridiales	Family XI	Ezakiella	3,648.87	-2	0.38	5.28	$5.79 \cdot 10^{-6}$
Bacteroidetes	Bacteroidales	Prevotellaceae	Prevotella	2,231.33	-1.64	0.44	3.69	$3.37 \cdot 10^{-3}$
Bacteroidetes	Bacteroidales	Porphyromonadaceae	Porphyromonas	2,086.91	-1.25	0.39	3.24	$1.18 \cdot 10^{-2}$
Firmicutes	Selenomonadales	Veillonellaceae	Dialister	1,248.03	-0.81	0.3	2.73	$4.32 \cdot 10^{-2}$
Firmicutes	Clostridiales	Family XI	Anaerococcus	1,097.25	-1.54	0.38	4.03	$1.12 \cdot 10^{-3}$
Firmicutes	Clostridiales	Family XI	Peptoniphilus	1,028.42	-1.07	0.4	2.7	$4.58 \cdot 10^{-2}$
Firmicutes	Lactobacillales	Lactobacillaceae	Lactobacillus	442.65	-1.44	0.34	4.21	$5.67 \cdot 10^{-4}$
Epsilonbacteraeota	Campylobacterales	Campylobacteraceae	Campylobacter	424.5	-1.5	0.45	3.36	$8.23 \cdot 10^{-3}$
Firmicutes	Clostridiales	Family XIII	S5-A14a	312.08	-2.25	0.49	4.63	$9.24 \cdot 10^{-5}$
Firmicutes	Clostridiales	Ruminococcaceae	UCG-013	183.29	-0.34	0.12	2.76	$4.17 \cdot 10^{-2}$
Firmicutes	Clostridiales	Family XIII	f Family XIII	158.61	-2.1	0.39	5.35	$5.1 \cdot 10^{-6}$
Firmicutes	Clostridiales	Ruminococcaceae	Butyricicoccus	149.19	-0.44	0.14	3.21	$1.18 \cdot 10^{-2}$
Firmicutes	Clostridiales	Peptococcaceae	Peptococcus	97.53	-1.1	0.35	3.18	$1.26 \cdot 10^{-2}$
Actinobacteria	Bifidobacteriales	Bifidobacteriaceae	Gardnerella	88.17	-5.52	1.12	4.91	$2.72 \cdot 10^{-5}$
Actinobacteria	Actinomycetales	Actinomycetaceae	Varibaculum	72.46	-2.89	0.74	3.89	$1.63 \cdot 10^{-3}$
Tenericutes	RF39	unknown	unknown	65.42	-2.5	0.5	5.04	$1.66 \cdot 10^{-5}$
Fusobacteria	Fusobacteriales	Fusobacteriaceae	Fusobacterium	62.94	-3.1	0.79	3.91	$1.61 \cdot 10^{-3}$
Bacteroidetes	Bacteroidales	Prevotellaceae	Paraprevotella	38.17	-13.65	0.98	13.87	$1.63 \cdot 10^{-41}$
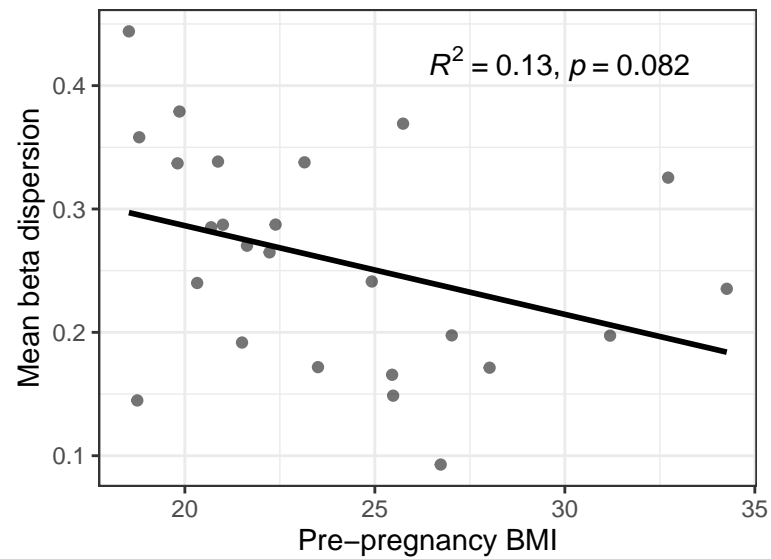
Figure B.3. Beta dispersion within participants across pre-pregnancy BMI. Scatter plot of the mean distance to the centroid of each participants samples (beta dispersion) by pre-pregnancy BMI show no significant correlation across all sample time points.

Figure B.4. Taxonomic summary of top 20 families by pre-pregnancy BMI category and sample time point. The mean relative abundance of the 20 most abundant bacterial families was calculated within each combination of sample time point and pre-pregnancy BMI category is shown in a stacked bar plot coloured by family.

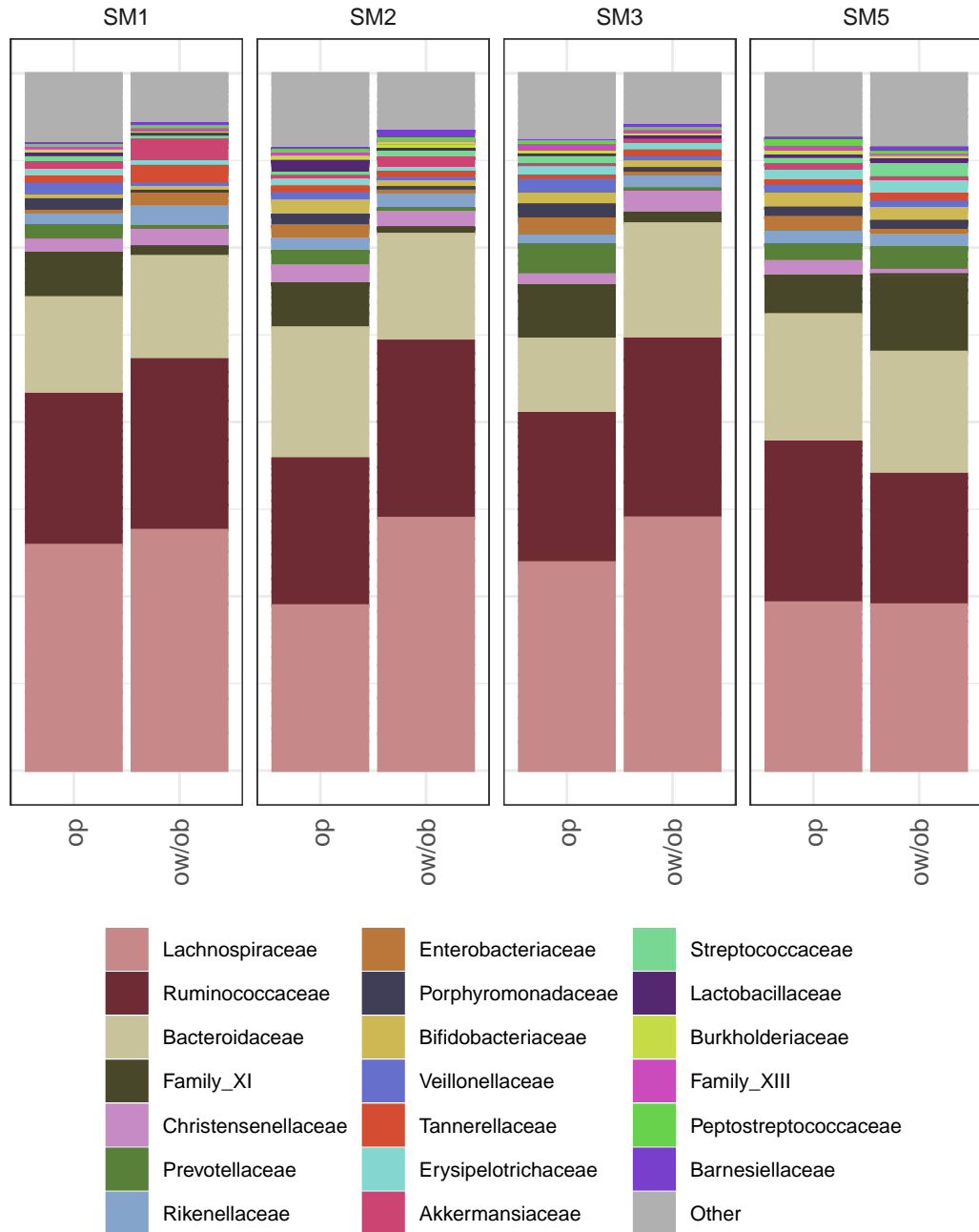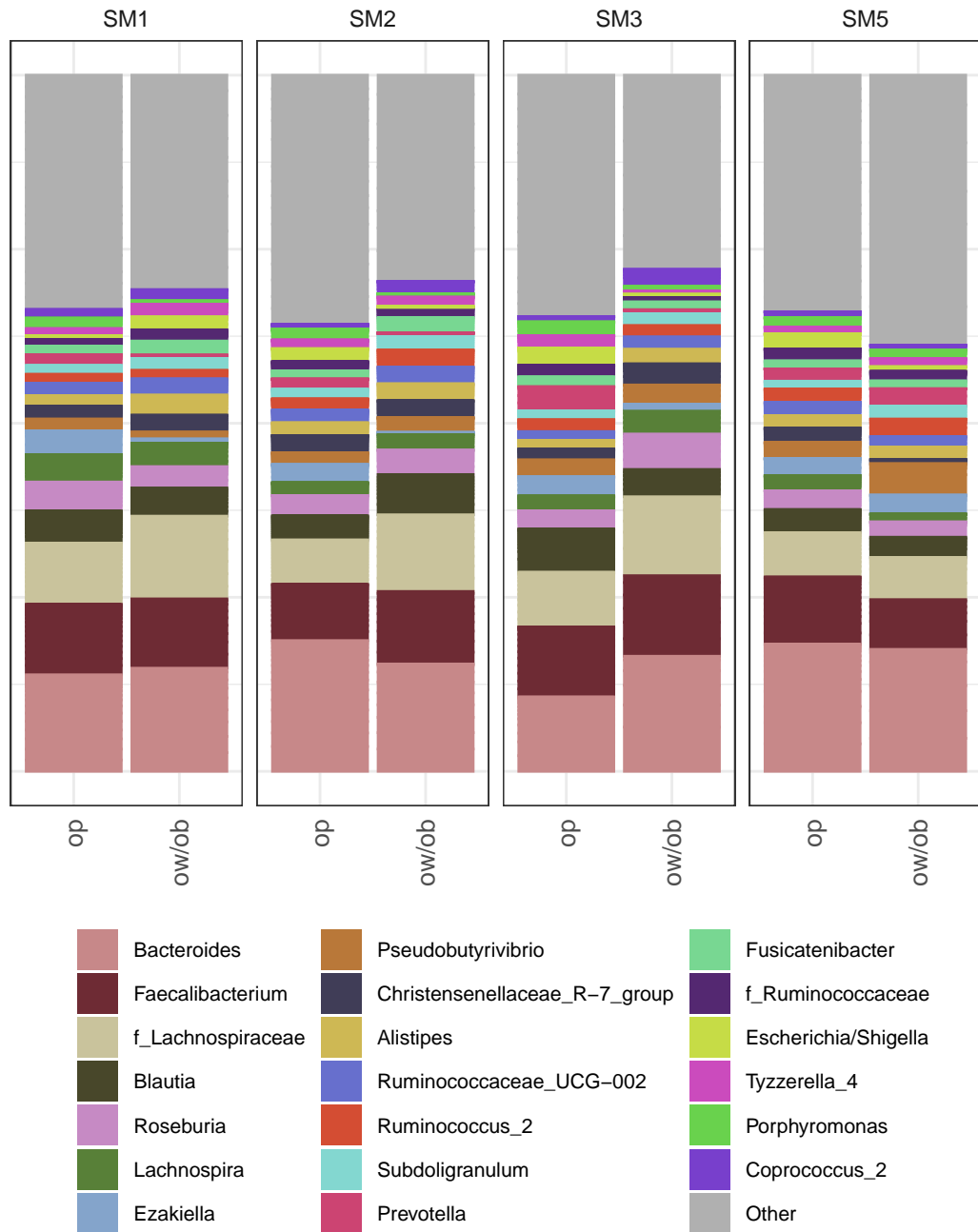**Figure B.5. Taxonomic summary of top 20 genera by pre-pregnancy BMI category and sample time point.** The mean relative abundance of the 20 most abundant bacterial genera was calculated within each combination of sample time point and pre-pregnancy BMI category is shown in a stacked bar plot coloured by family.

B.3   Discussion

In this study, we investigated the impact of maternal pre-pregnancy BMI on the
maternal gut microbiota over the course of pregnancy and during lactation. We
found maternal microbiota beta diversity differed significantly by pre-pregnancy
BMI and across sample time points.

Previous studies of the gut microbiota during pregnancy have found alpha
diversity to decrease (93) or remain stable (98, 99, 229) over the course of
pregnancy. In this study, consistent with the Berlin cohort (Chapter 4), alpha
diversity was similar between sample time points. In the Berlin cohort, we found
an interaction between pre-pregnancy BMI and GWG on alpha diversity. It is
possible that this relationship exists in this cohort as well, but this has not been
tested yet. We found sample time point and maternal pre-pregnancy BMI
category had modest effects on beta diversity, consistent with our Berlin cohort
(Chapter 4). In contrast to our Berlin cohort, in this cohort we found maternal
overweight/obesity was associated with a decreased relative abundance of
Prevotella, although *Paraprevotella* was decreased in both groups.

The detected effects of pre-pregnancy BMI on the maternal gut microbiota
likely differed between this cohort and the Berlin cohort (Chapter 4) for a
number of reasons. Firstly, sample collection methods varied between cohorts. In
the Berlin cohort, whole stool was collected and sample volumes obtained were
larger than in this cohort, where stool was collected on toilet paper. This could
explain the higher abundance of potential vaginal microbes in this cohort,
including *Ezakiella* (437), which we found to be decreased with pre-pregnancy

overweight/obesity in this cohort. Sequencing methods also differed between cohorts, as in this cohort the V3 region was amplified and sequenced and in the Berlin cohort the combined V3-V4 region was amplified and sequenced. The reduced variability in the V3 region alone compared to the combined V3-V4 region means that there is less information available to differentiate taxa, and the use of different variable regions is known to influence relative abundances of taxa (438). There are likely also population-level differences in the gut microbiota between participants in Hamilton, Ontario and participants in Berlin, Germany (73). Finally, differences in our detected effects of pre-pregnancy overweight/obesity on the gut microbiota may be explained by sample characteristics including the number of participants with pre-pregnancy overweight/obesity or excess GWG. This cohort will be further analyzed once GWG data are available.

Appendix C

Chapter 6 Supplement: Littermate experiments

C.1 Introduction

Wildtype (Wt) and TNF knockout (TNF$^{-/-}$) dams used to generate data in Chapter 6 were generated from separate breeding colonies and Wt dams were housed under specific-pathogen-free (SPF) conditions while TNF$^{-/-}$ dams were housed in clean rooms. Differences in maternal intestinal, placental, and fetal intestinal measures could be due to maternal genotype alone or confounded by housing conditions and colony-specific microbiota. To control for these potential confounders, I generated a cohort of littermate Wt and TNF$^{-/-}$ dams following the same maternal high-fat (HF) diet pregnancy model as non-littermate Wt and TNF$^{-/-}$ dams, resulting in 4 additional groups (Wt control, Wt HF, TNF$^{-/-}$ control, TNF$^{-/-}$ HF; n=3-5 per group).

C.2 Results

C.2.1 Littermate phenotype

During gestation, there was no significant effect of diet or genotype on maternal weight (Fig. C.1). This differs from non-littermates, where HF diet increased dam weight in both Wt and TNF$^{-/-}$ prior to and throughout gestation (Chapter 6; Fig. 6.1, Fig. 6.2). Absolute and relative (% bodyweight) liver, gonadal fat and mesenteric fat mass did not differ by diet or genotype (Fig. C.3). Maternal fasting blood glucose was higher in Wt than TNF$^{-/-}$ littermates, and serum insulin did not differ by diet or genotype (main effect of genotype, p=0.010; Fig. C.2). HF diet was associated with decreased maternal large intestine length (main effect of diet, p<0.0001) and cecal weight (p<0.0001) in both Wt and TNF$^{-/-}$ littermate dams (Fig. C.4).
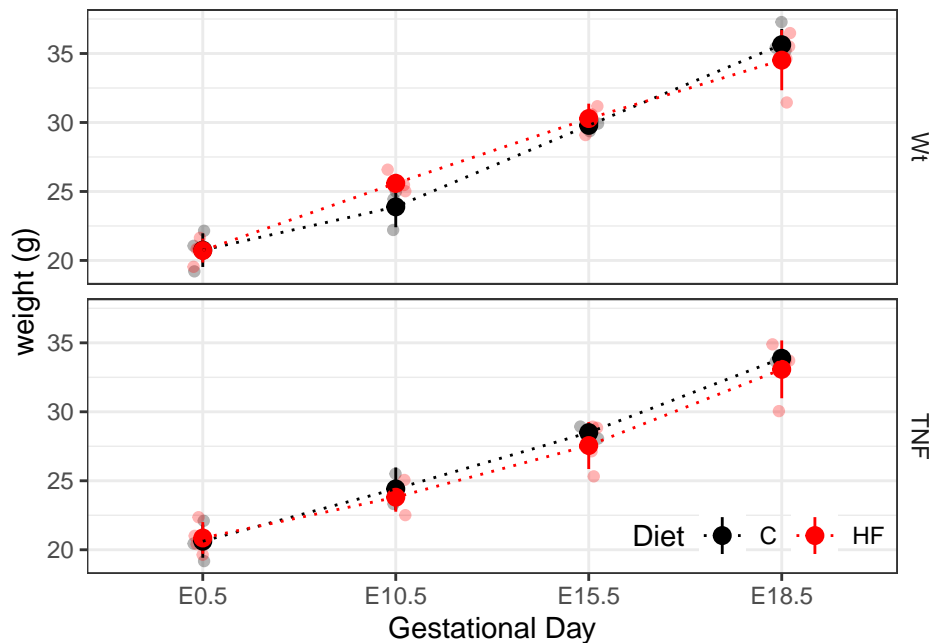

Figure C.1. Pregnancy weight gain by genotype and diet.

Figure C.1. Pregnancy weight gain by genotype and diet.
After 6-weeks of dietary intervention, Wt and tumour necrosis factor
(TNF) dams were mated with control-fed male mice of the same geno-
type, and dam body weight was recorded at gestational/embryonic day
(E)0.5, embryonic day (E)10.5, E15.5, and E18.5. In Wt and TNF$^{-/-}$
littermates, HF dam weights (red) were were similar to control weights
(black) throughout pregnancy. Individual data points are shown as well
as the mean and standard deviation. Significance was assessed by mixed
linear model with time, diet, and genotype as interacting fixed effects
and individual mouse ID as a random effect (n=3-5 per group).
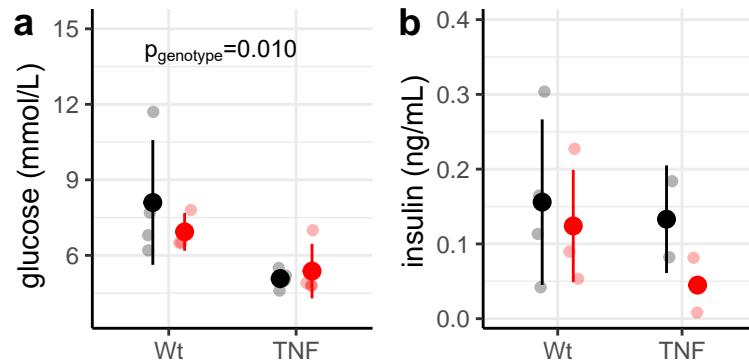
**Figure C.2. Maternal whole blood glucose (WBG) is de-
creased in TNF$^{-/-}$ compared to Wt littermates.** Individual data
points are shown as well as the mean and standard deviation. Signifi-
cance was assessed by linear model with diet and genotype as interacting
fixed effects (n=3-5 per group).

There was no significant effect of genotype, fetal sex, or maternal diet on litter
size (Fig. C.5a), fetal sex ratio (male:female; Fig. C.5d), or fetal whole blood
glucose (Fig. C.5f). Wt control male and female fetuses weighed more than
TNF$^{-/-}$ male (p<0.0001) and female (p=0.031) fetuses respectively, and Wt
males weighed more than Wt females (p=0.0013; Fig. C.5b). Overall, male
placentas weighed more than female placentas (main effect of sex, p=0.013).
There was a significant diet:genotype interaction for fetal-placental ratio
(p=0.0077), which is an indicator of placental efficiency, and control males had a
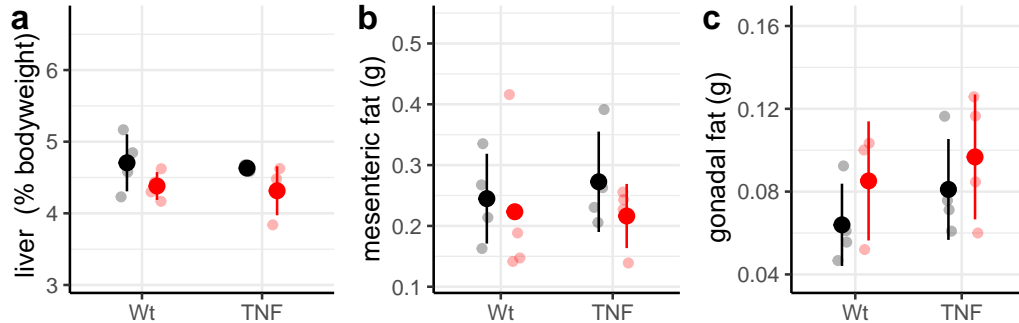
**Figure C.3. Effect of diet and genotype on weights of maternal
liver and fat depots.** Individual data points are shown as well as the
mean and standard deviation. Significance was assessed by linear model
with diet and genotype as interacting fixed effects (n=3-5 per group).

lower ratio than HF males (p=0.044; Fig. C.5e). There was no significant effect
of genotype, fetal sex, or maternal diet on fetal whole blood glucose (Fig. C.5f).
These data differ from those of our non-littermate cohort, where Wt fetal weight
was decreased by maternal HF diet but not different between males and females,
and TNF$^{-/-}$ fetal weight was greater in males than females (Fig. 6.5a).
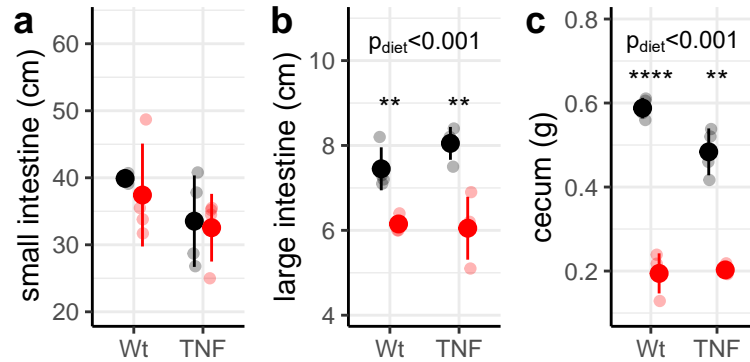
Figure C.4. Maternal cecal weight and large intestine length decreased by HF diet in littermate dams. Individual data points are shown as well as the mean and standard deviation. Significance was assessed by linear model with diet and genotype as interacting fixed effects (n=3-5 per group).
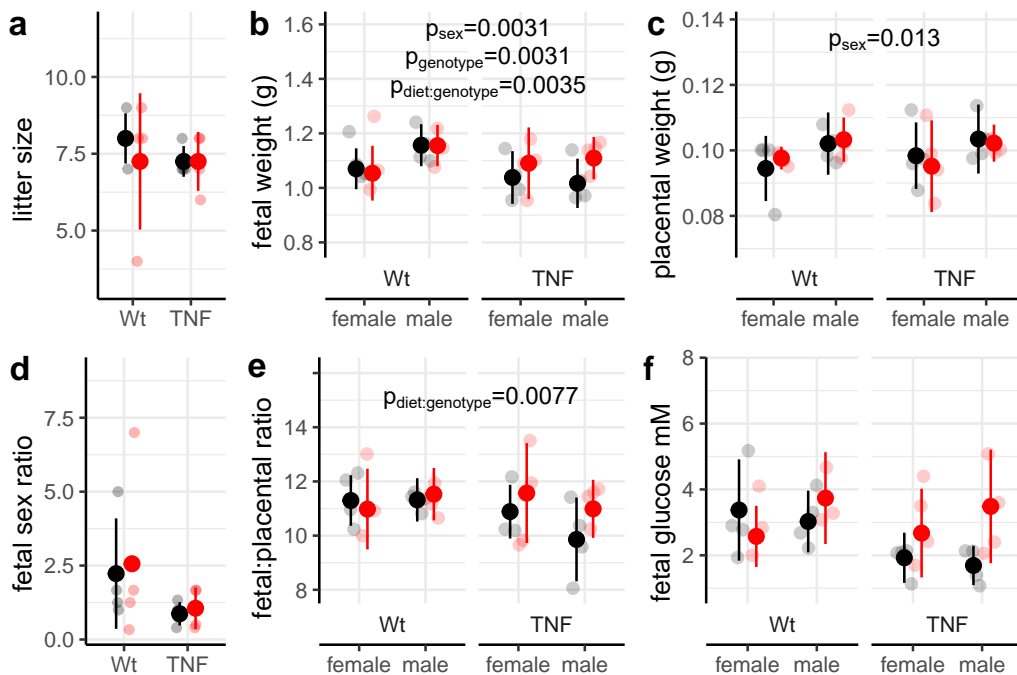
Figure C.5. Fetal phenotype by sex and genotype. Individual data points are shown as well as the mean and standard deviation. Significance was assessed by linear model with diet, sex, and genotype as interacting fixed effects (n=3-5 per group).

C.2.2   Littermate gut microbiome

Maternal fecal samples were collected prior to dietary randomization at week 0 (W0), before mating (E0), and at term gestation (E18.5). Bacterial DNA present in fecal samples was assessed by 16S rRNA gene sequencing of the combined variable 3 and 4 (V3-V4) region amplicons from 30 cycles of PCR amplification (see Methods 2.4 for details).

To evaluate differences in within-sample alpha diversity, the Shannon Index was used as a measure of richness and evenness (234) (Fig. C.6). The impacts of diet, genotype, and sample time on alpha diversity were assessed by a mixed linear model, with those factors as interacting fixed effects and individual mouse ID as a random effect. Alpha diversity was similar between Wt and TNF$^{-/-}$ littermates (main effect of genotype, p=0.92), and was decreased by HF diet in both Wt and TNF$^{-/-}$ dams at term gestation (E18.5; Wt p=0.0002; TNF$^{-/-}$ p=0.0008). Unexpectedly, alpha diversity was also decreased in littermates assigned to HF diet prior to dietary intervention (W0; Wt p=0.0003; TNF$^{-/-}$ p=0.0067). This is likely due to differences in age at baseline (W0), as littermates were obtained at different ages and younger mice were assigned to receive HF diet to ensure consistency in age at initiation of HF diet between cohorts.

We next evaluated overall community composition between samples (beta diversity) using Bray-Curtis dissimilarity and visualized these data by principal coordinate analysis (PCoA) across the 4 axes that explained the greatest amount of variation (Fig. 6.7). When all samples were analyzed together, the majority of variation between samples was explained by individual mouse (R^2 =0.27, p=0.001) and genotype explained a small amount of variation (R^2 =0.022,
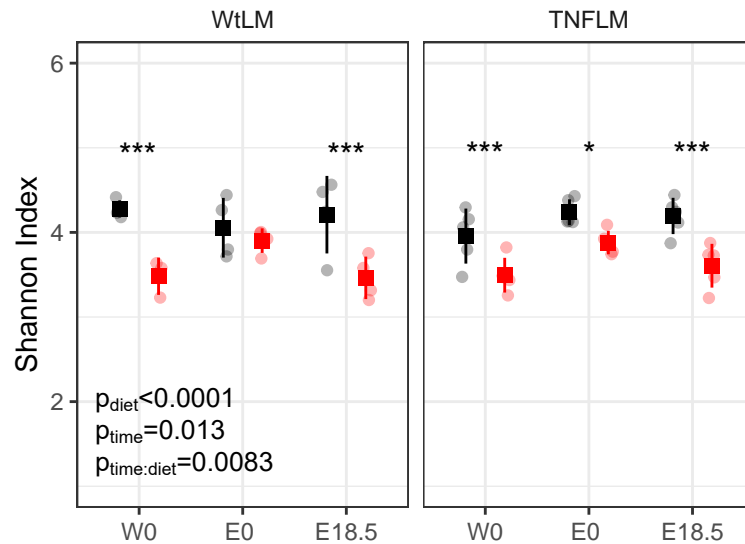
Figure C.6. Alpha diversity by genotype and diet across sample time in littermates HF diet (red) decreased alpha diversity compared to controls (black) in both Wt and TNF-/- littermate dams. Individual data points are shown as well as the mean and standard deviation. Significance was assessed by linear model with diet and genotype as interacting fixed effects (n=4-5 per group). * indicates p<0.05; ** p<0.01, *** p<0.001.

p=0.021), though this was not significant when only control-fed littermates were analyzed (R^2 =0.056, p=0.058). This contrasts our data in non-littermates (Chapter 6), where genotype had a larger effect than diet or sample time, and indicates that that effect was likely due to room effects. There were also significant effect of diet (R^2 =0.16, p=0.001) and sample time point (R^2 =0.16, p=0.001). effects of diet (R^2 =0.08, p=0.001; PERMANOVA, Fig. C.7).

Within genotypes, HF shifted microbiota community composition before pregnancy (E0) and at term gestation (E18.5) in both Wt (E0, R^2 =0.36, p=0.031; E18.5, R^2 =0.46, p=0.022) and TNF$^{-/-}$ dams (E0, R^2 =0.42, p=0.011; E18.5, R^2 =0.40, p=0.007). Additionally, pregnancy shifted microbiota

Figure C.7. PCoA of Bray-Curtis Dissimilarity beta diversity by genotype and diet across sample time. Points represent individual samples and are coloured by sample time (W0, red; E0, green; E18.5 blue). The first four axes, explaining the largest percentages of variation, are shown, faceted by genotype and diet (n=4-5 per group).
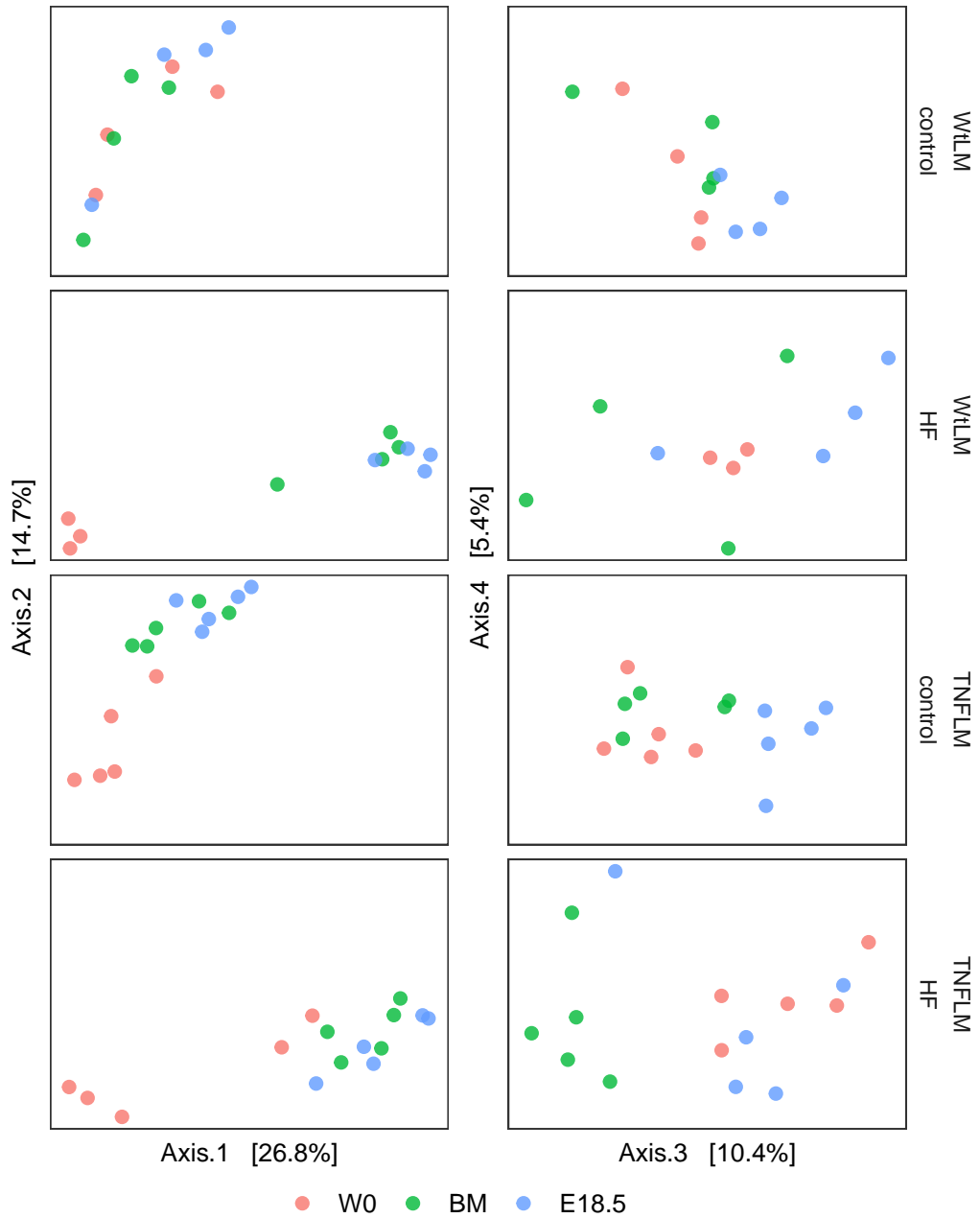
community composition (E18.5 vs. E0) in both Wt (control (C), R^2 =0.17,
p=0.037; HF, R^2=0.27, p=0.045) and TNF$^{-/-}$ dams (C, R^2 =0.17, p=0.002; HF,
R^2=0.20, p=0.001). Together these data suggest that both diet and pregnancy
drive shifts in microbiota community composition, and these effects are not TNF
dependent.

We next investigated which specific taxa contribute to these overall shifts in
community composition using differential abundance testing (DESeq2, RRID:
SCR_015687; Fig. 6.9 and see taxa summaries in Fig. 6.8). Overall, 50 genera
differed significantly with HF diet: 20 genera in both Wt and TNF$^{-/-}$ dams, 21
genera in only TNF$^{-/-}$ dams, and 12 genera in only Wt dams (Fig. 6.9). HF diet
was associated with decreased relative abundances of *Muribaculum* and of an
unknown member of the family *Muribaculaceae* in both Wt and TNF$^{-/-}$ dams.
Muribaculaceae species can degrade a variety of complex carbohydrates (297),
and are key mucin degraders (298) linked to short-chain fatty acid (SCFA)
production (299). *Bacteroides* was less abundant in littermates than in
non-littermates (Chapter 6), and unlike in non-littermates its abundance did not
differ significantly with HF diet. The relative abundances of *Parabacteroides*, the
seventh most abundant genus overall, was increased by HF diet in both Wt at
term gestation (E18.5).

Some of the genotype-specific impacts of HF diet on the gut microbiota
differed between littermates and non-littermates. *Alistipes*, which was decreased
by HF-diet in non-littermates TNF$^{-/-}$ dams and not in non-littermate Wt dams
was decreased by HF diet in both Wt and TNF$^{-/-}$ littermates, though only before
pregnancy in Wt littermates (Fig. C.9). *Roseburia*, which was increased by HF
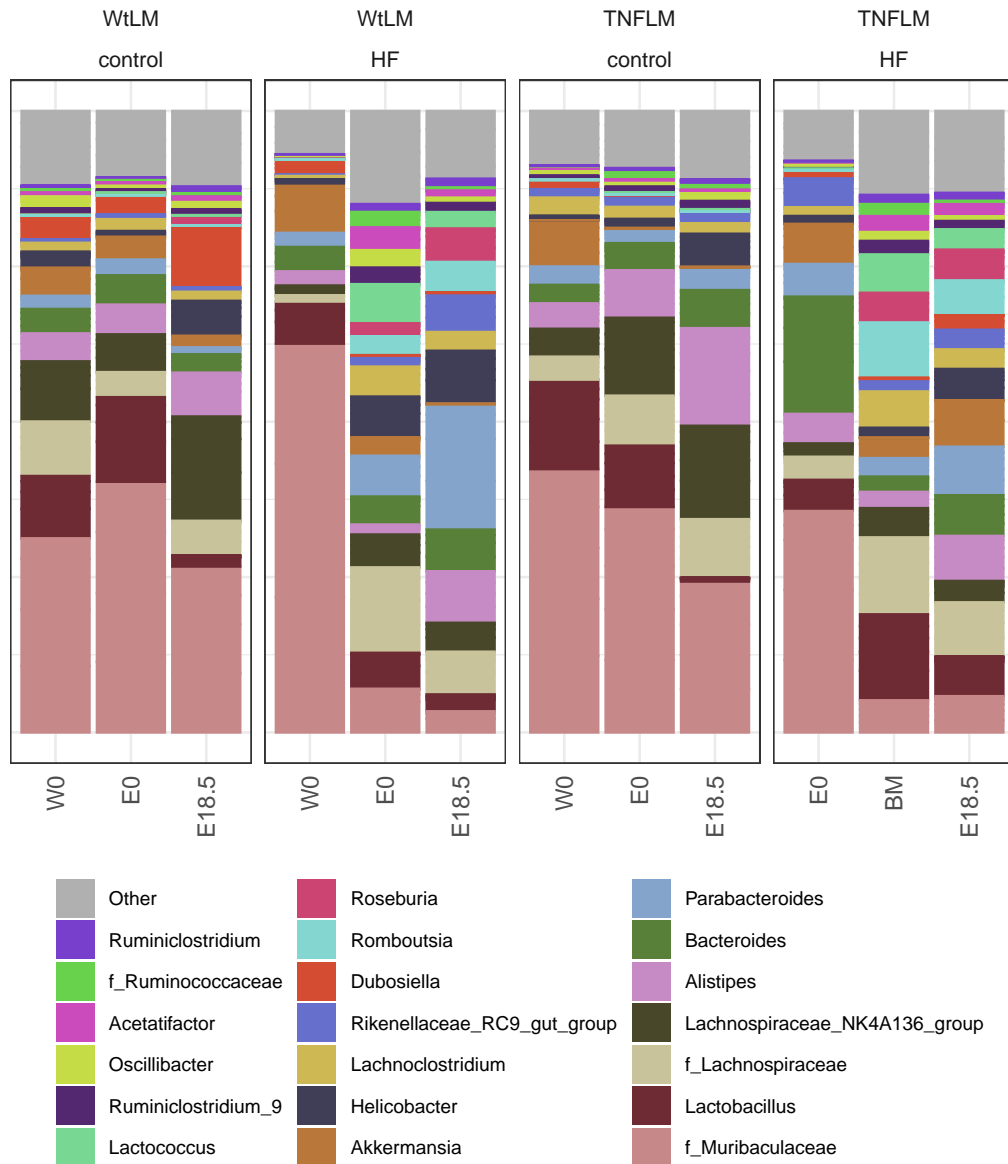
Figure C.8. Relative abundance of the 20 most abundant genera. Mean relative abundances were calculated for each sample time (W0, E0, and E18.5) within genotype (Wt and TNF$^{-/-}$) and diet group (control and HF) and plotted as stacked bar plots.
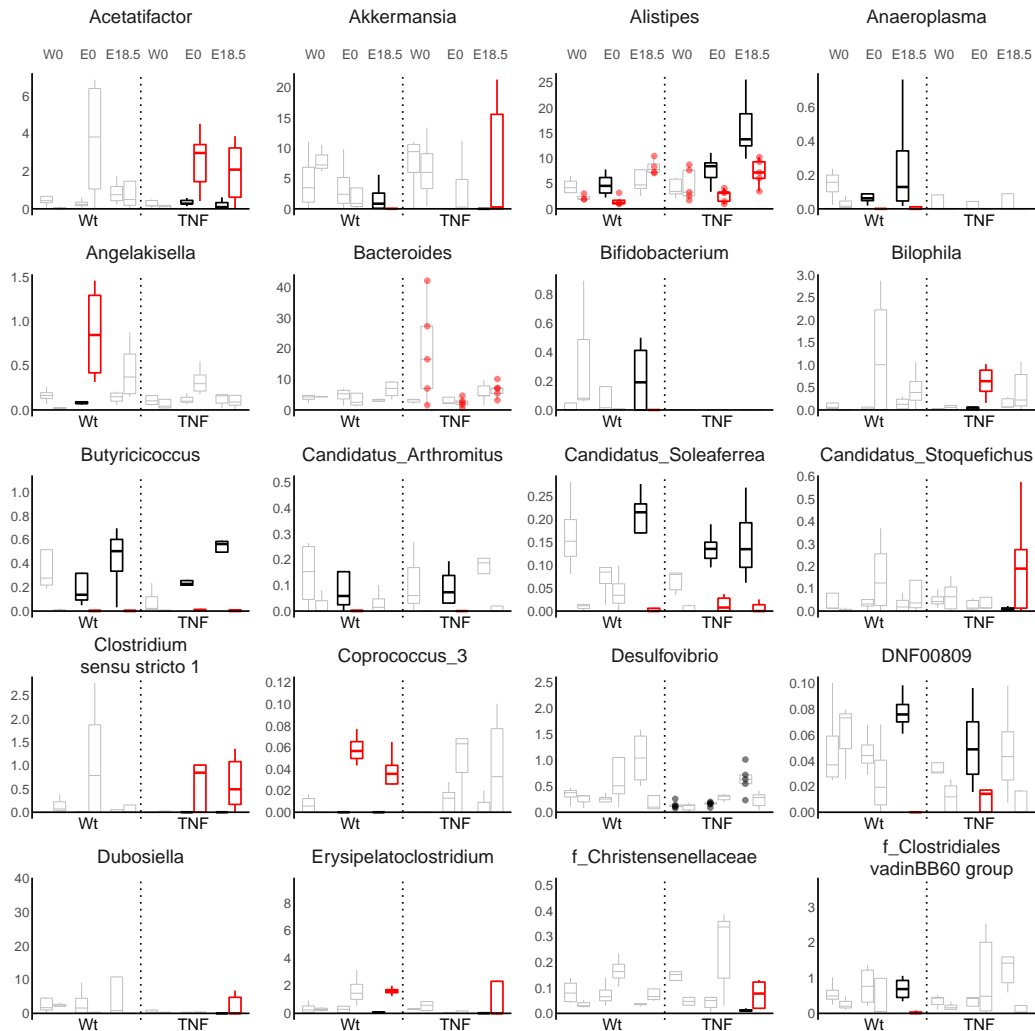
Figure C.9. Bacterial genera significantly enriched or depleted by diet or pregnancy. Box plots of the relative abundance of each genus at each sample time points (baseline at week 0, W0; before mating, E0; term gestation, E18.5) for control (black) and HF (red) wild-type (Wt) TNF$^{-/-}$ (TNF) dams and are shown for genera significantly affected by diet (coloured box plot indicates significance relative to control within that genotype and sample time point) or pregnancy (coloured points indicate significant difference at E18.5 relative to E0 within that genotype and diet). Genera that differed significantly by genotype at baseline (W0) are indicated by an asterisk. Significance was assessed by DESeq2.The box plot centre line represents the median; the box limits represent the upper and lower quartiles; the whiskers represent the 1.5x interquartile range.
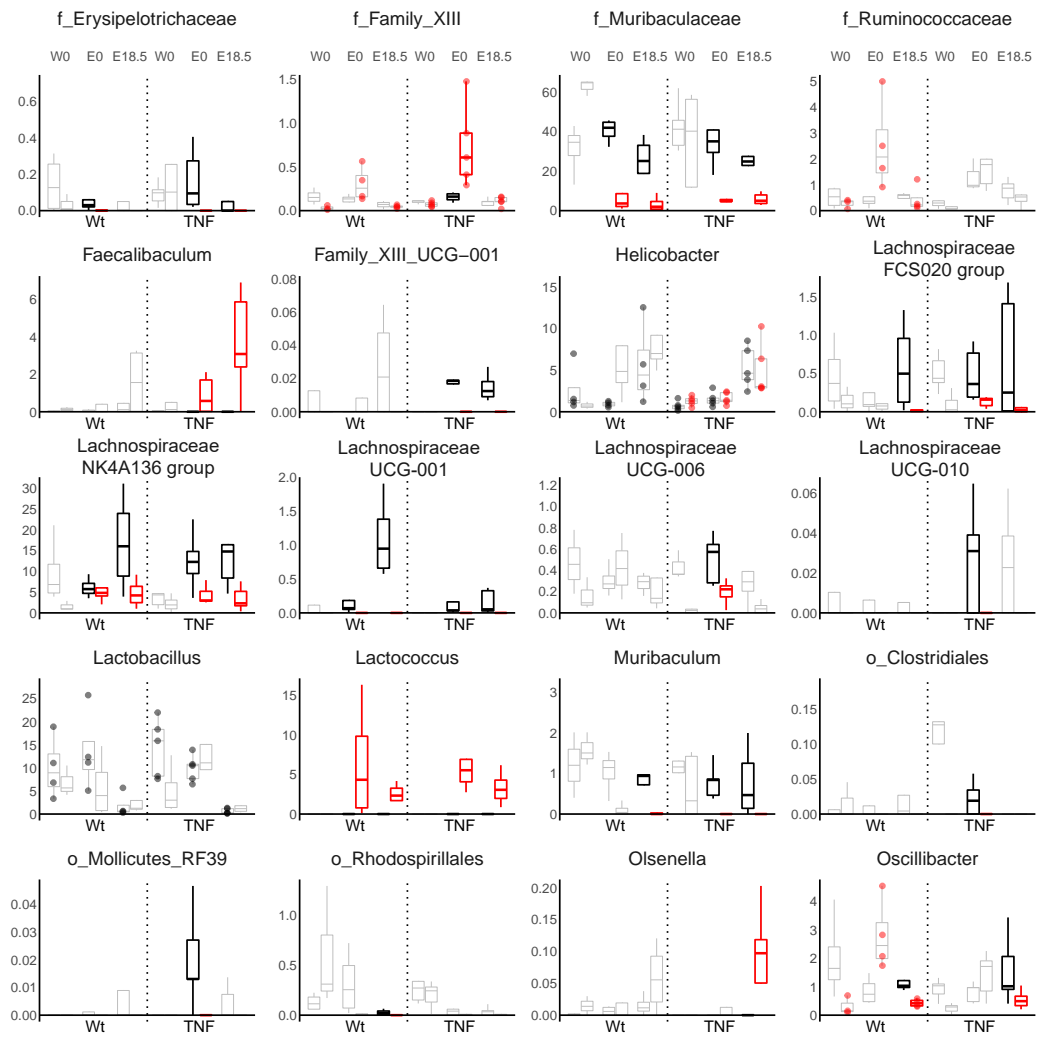
Figure C.9. **Bacterial genera significantly enriched or depleted by diet or pregnancy cont.**
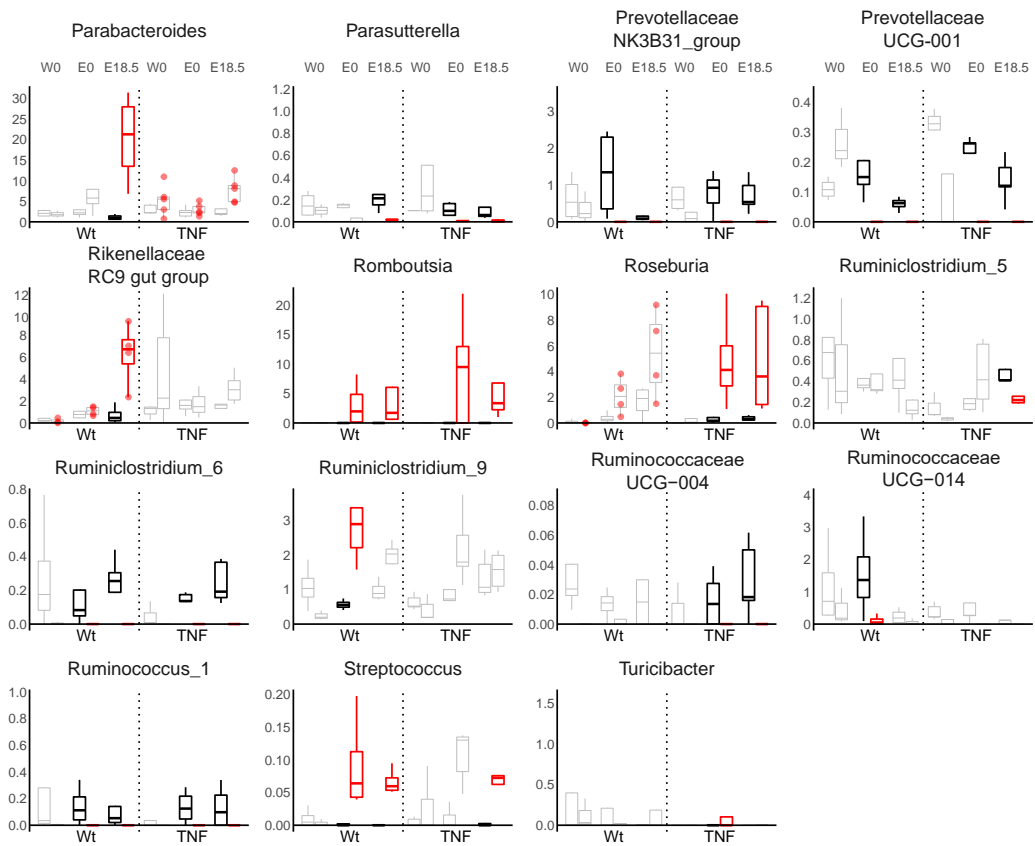
Figure C.9. Bacterial genera significantly enriched or depleted by diet or pregnancy cont.

diet in Wt non-littermates but decreased by HF diet in TNF$^{-/-}$ non-littermates was increased by HF diet in TNF$^{-/-}$ littermates. *Parasutterella*, which was decreased by HF diet in Wt non-littermates but increased by HF diet in TNF$^{-/-}$ non-littermates, was decreased by HF diet in both Wt and TNF$^{-/-}$ littermates. This indicates that some of the genotype-specific responses observed in non-littermates (Chapter 6) were not due to the presence or absence of TNF, and were more likely due to differences in microbial composition prior to dietary intervention.

Our littermate data did, however, replicate our previous finding of genotype-specific effects of HF diet on the abundance of *Akkermansia*, which we found to be decreased by HF diet in Wt littermates and increased by HF diet in TNF$^{-/-}$ littermates at term gestation (Fig. C.9). As we have observed an increase of *Akkermansia* with HF diet in our previous Wt cohort (Chapter 5 (265)), we cannot say that this effect of genotype is due to TNF alone.

Of the 20 genera that varied due to HF diet in both Wt and TNF$^{-/-}$ littermates, 12 were also increased or decreased in both Wt and TNF$^{-/-}$ non-littermates. In addition to the genotype-specific effects observed for *Akkermansia*, this reproducible effects of HF diet also included decreased *DNF00809*, *Erysipelatoclostridium*, *f Muribaculaceae*, *Oscillibacter*, *Ruminoclostridium 6*, and *Lachnospiraceae* members *FCS020 group*, *NK4A136 group*, and *UCG-001*, as well as increased *Lactococcus* and *Romboutsia*.

234

C.3   Discussion

In our non-littermate cohort, we found that Wt females gained more weight prior to pregnancy compared to TNF$^{-/-}$ females, and that this persisted throughout pregnancy. In this cohort, neither Wt nor TNF$^{-/-}$ dams gained more weight on HF diet than dams on control diet. We found that many of the genera impacted by HF diet in our non-littermate cohort were similarly affected in this littermate cohort, including decreases in SCFA producers, and genotype-specific shifts in *Akkermansia* abundance were present in both cohorts. Together these data demonstrate that the many, but not all, of the effects observed in our non-littermate cohort (Chapter 6) were also observed in littermates and, therefore, are attributable to genotype.

We show an interaction between genotype and diet on fetal weight that differs from our non-littermate data, where HF diet in Wt, but not TNF$^{-/-}$ pregnancies reduces birth weight. In this cohort, HF diet did not reduce fetal weight in either Wt or TNF$^{-/-}$ pregnancies. It is possible that the reduction observed in our non-littermate Wt pregnancies was due to maternal obesity, rather than HF diet *per se*.

The impact of TNF in pregnancy-related microbiota composition shifts and the additive effect of HF diet was assessed by permutational multivariate analysis of variance (PERMANOVA) analysis of Bray-Curtis dissimilarities. In our non-littermate cohort, we found that genotype explained a large percentage of variation (R^2 =0.21). In this cohort, we found that genotype explained a small but significant percentage of variation (R^2 =0.022, p=0.021). This suggests that

the large percentage of variation explained by genotype in non-littermates was due to inherited microbial communities (i.e. colony and room effects), but that genotype *per se* does have an impact of microbial community composition.

Overall shifts in specific genera due to HF diet intake were similar between this cohort and our non-littermate cohort (Chapter 6). Some genotype-specific effects of HF diet were not reproduced in littermates. It is possible that this is due to a smaller sample size in littermates reducing our power to detect significant differences, but it is also possible that this reflects effects due to differences in initial microbial communities rather than genotype-specific effects. Interestingly, our littermate data did reproduce our non-littermate observation that *Akkermansia* abundance was differentially affected by HF diet in Wt and TNF$^{-/-}$ mice. Whereas HF diet decreased *Akkermansia* and in Wt dams, the opposite occured in TNF$^{-/-}$ dams where *Akkermansia* was increased with HF diet. It is possible that this TNF-dependent differential effect of HF diet on *Akkermansia* is due to differences in mucin degradation or production between Wt and TNF$^{-/-}$ mice, where Wt mice may have impaired mucin production in response to HF diet intake.

Appendix D

Chapter 7 Supplement: Offspring behaviour and dam gut microbiota during lactation

D.1 Offspring generation

The diet-induced obesity model previously used for tissue collection during pregnancy (Chapter 6) was not successful in generating offspring (Fig. D.1). As first litters are commonly thought to have higher mortality rates (439) I attempted a second cohort with generation of offspring from second pregnancies: 5-week-old dams were randomized to receive a control or 60% Cal high-fat (HF) diet for 2 weeks prior to mating for first litters. First litters were sacrificed, and dams were mated again after one week of recovery to produce second-pregnancy offspring. Although mating success rates were similar between groups for first

pregnancy (control 14/22 dams; high-fat 13/22 dams), only 4/13 high-fat first litters survived until sacrifice at postnatal day 3 (P3), while 12/14 control first litters survived to P3. Of the 13 HF dams that delivered a first litter only 5 were successfully mated a second time, with only 2 litters surviving (pups n=2 and n=8). In this cohort, the variable length of time spent mating increased the duration of exposure to HF diet which could contribute to litter mortality. To control for this, I generated a third cohort with diet randomization occurring after successful generation of a first litter. After 6-weeks of control or HF diet, dams were mated again to generate second pregnancies. Although a large proportion of first pregnancies had litters surviving to sacrifice at p3, only 6/11 HF dams generated second pregnancies and only 2 had litters survive to p3. Both HF litters were reared by the same dam from postnatal day 7 weaning due to maternal death one week postpartum, and both female offspring from this litter died shortly after weaning.

As first litter survival rates after 2 weeks of HF diet were acceptable, a forth cohort was started on diet at 11-weeks of age to match age-at-mating and total length of dietary exposure to that from embryonic day (E)18.5 collections (9 weeks total: 2 weeks before mating, 3 weeks during pregnancy, 4 weeks during lactation).
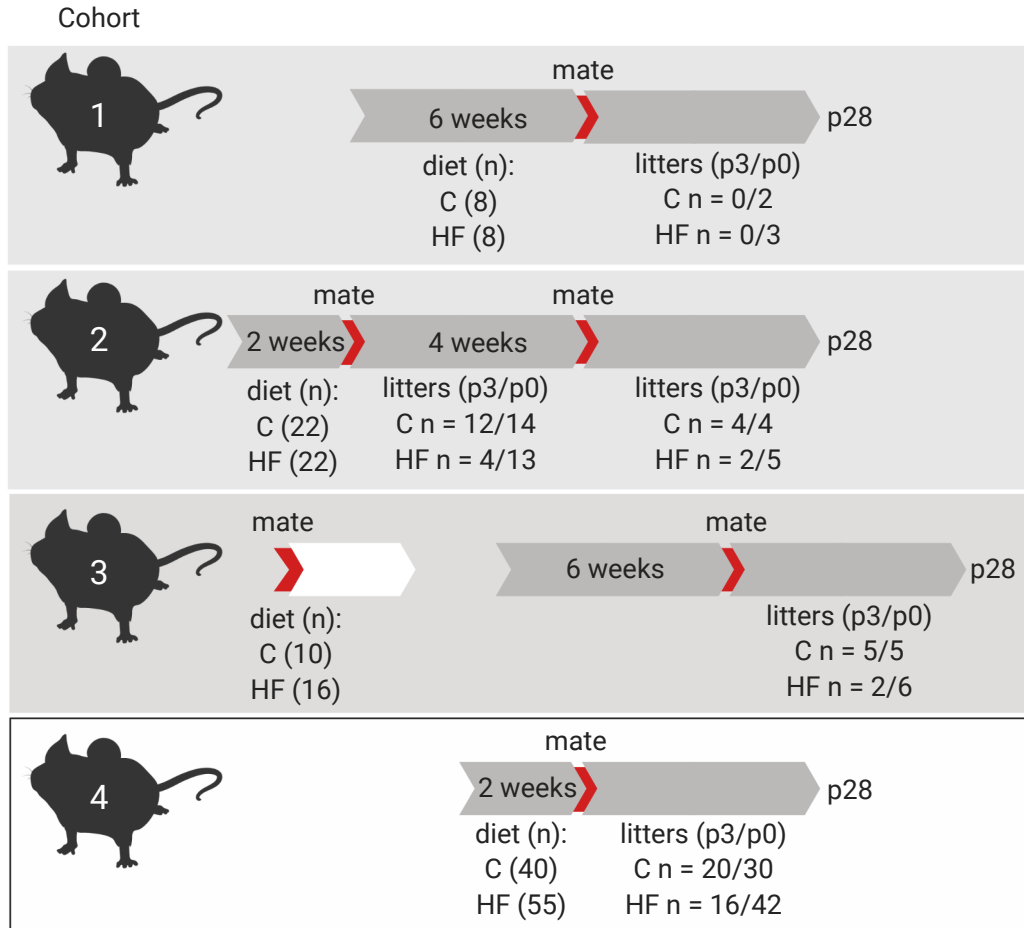
Figure D.1. Generation of offspring from control and HF-fed mothers (C = control; HF = high-fat).

D.2   Offspring behaviour

Prior to P120 experiments and collections (postnatal day 113), offspring were video recorded in their home cages as a pilot experiment to assess any effect of maternal diet on offspring behaviour and response to a novel object. Offspring were video recorded for 1 minute prior to introduction of a novel object (marble), and 3 minutes afterwards. Cages were changed 1-week prior to assessment. Video recording was conducted in their home room. Videos were analyzed by a

blinded assessor who recorded instances of digging, grooming, supported rearing, unsupported rearing, and interactions with the marble. Maternal HF diet increased the frequency of digging in females (p=0.011) but not in males (maternal-diet:sex interaction, p=0.037; main effect of maternal diet, p=0.056), and increased the frequency of interactions with the marble (main effect of maternal diet, p=0.025), particularly in females (p=0.039; Fig. D.2).
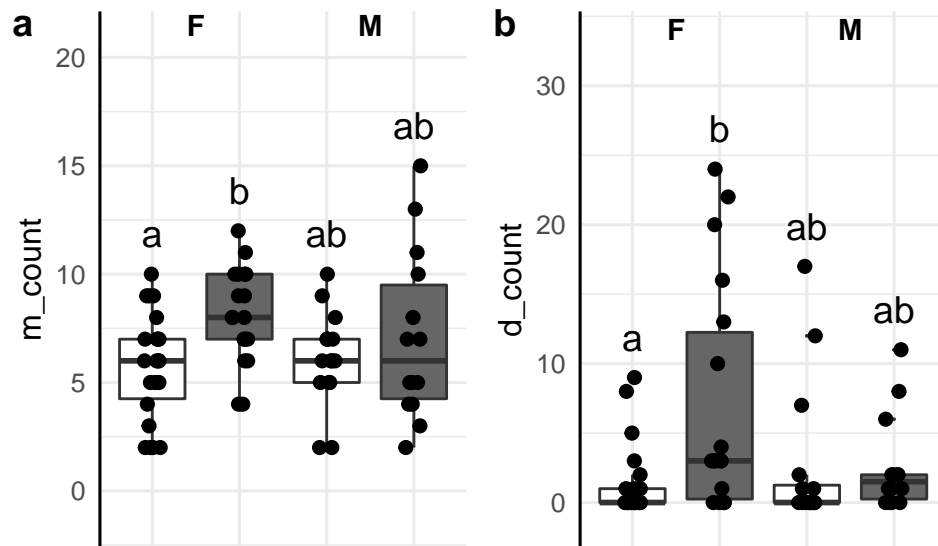
Figure D.2. Maternal HF diet increases offspring digging and novel object interactions. Maternal HF diet increased the frequency of digging (d_count) in females (p=0.011) but not in males (maternal-diet:sex interaction, p=0.037) and increased the frequency of interactions with the marble novel object (m_count; main effect of maternal diet, p=0.025), particularly in females (p=0.039). Significance was assessed by mixed linear model with sex, and maternal diet as fixed effects and litter as a random effect. Different letters indicate groups differ by multiple comparison (p<0.05).

D.3   Offspring microbiota at P3

The most abundant genera in the offspring gut microbiota at postnatal day (P)3 were *Streptococcus*, *Lactobacillus*, and *Corynebacterium*, consistent with previous reports (440), however, no genus was universally detected in individual offspring. Contamination was also abundant and prevalent, including *Stenotrophomonas*, *Halomonas*, *Massilia*, and *Rhizobium*, likely due to low microbial biomass in pups at this time point. Of the 56 genera detected at P3, only 16 were present in at least half of the offspring assessed.
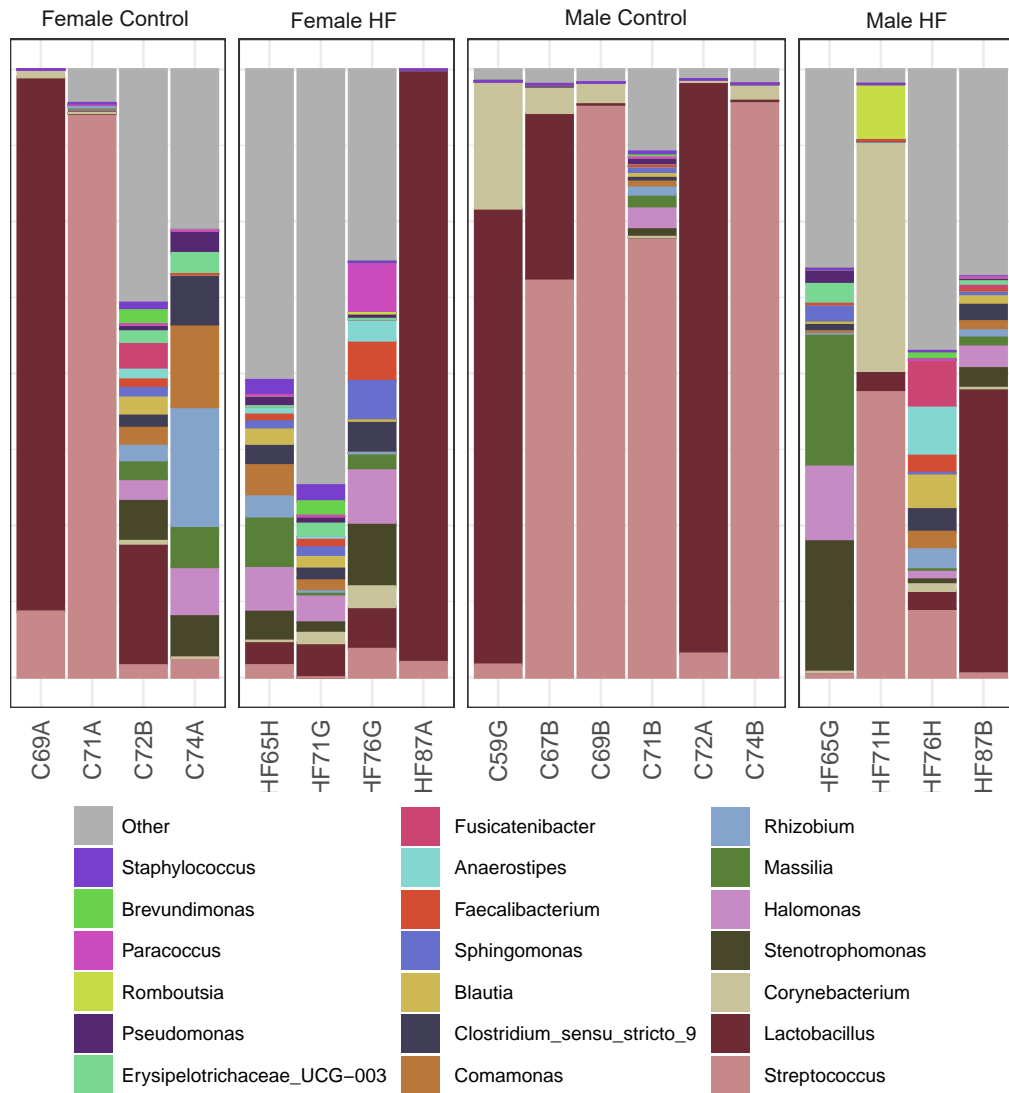
Figure D.3. Taxonomic summary of top 20 genera in offspring at P3 by sex and maternal diet. The relative abundance of the top 20 most abundant bacterial genera is shown for individual offspring at P3 (M, male; F, female) by maternal diet (C, control; HF, high-fat).

D.4 Maternal lactation microbiota

To evaluate differences in within-sample alpha diversity, the Shannon Index was used as a measure of richness and evenness (234) in addition to the number of observed species as a measure of richness (Fig. D.4). The impacts of diet and sample time on alpha diversity were assessed by a mixed linear model, with those factors as interacting fixed effects and individual mouse ID as a random effect. Alpha diversity as measured by the Shannon Index was decreased by HF diet at postnatal/lactational day 3 (P3; p=0.0005; main effect of diet, p=0.0092) but not at P14 or P28 (weaning). The number of observed species was decreased by HF diet at P3 (p=0.0006; main effect of diet, p=0.00031) and at P28 (p=0.0041), but not at P14. This corresponded to a decrease in the number of observed species in control dams at P14 compared to P3 (p=0.041).

We next evaluated overall community composition between samples (beta diversity) using Bray-Curtis dissimilarity and visualized these data by principal coordinate analysis (PCoA) (Fig. D.5). HF shifted maternal microbiota community composition at lactational/postnatal day 3 (P3; R^2 =0.34, p=0.0001), P14 (R^2 =0.40, p=0.0019), and at P28 (R^2 =0.46, p=0.0001). Beta-diversity was significantly different between lactation time points in HF-fed dams (R^2 =0.22, p=0.0005) but did was not significantly different in control dams.
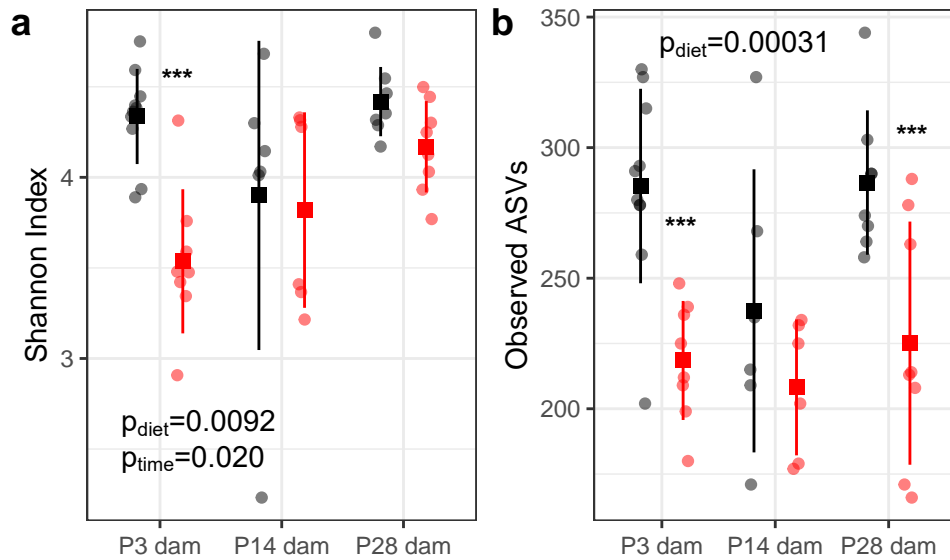
Figure D.4. Alpha diversity by diet across sample times. HF
diet (red) decreased alpha diversity compared to controls (black) in
dams during lactation. Individual data points are shown as well as the
mean and standard deviation. Significance was assessed by mixed linear
model with diet and sample time point as interacting fixed effects, and
individual dam ID as a random effect. * indicates $p<0.05$; ** $p<0.01$,
*** $p<0.001$ compared to control-fed counterparts.
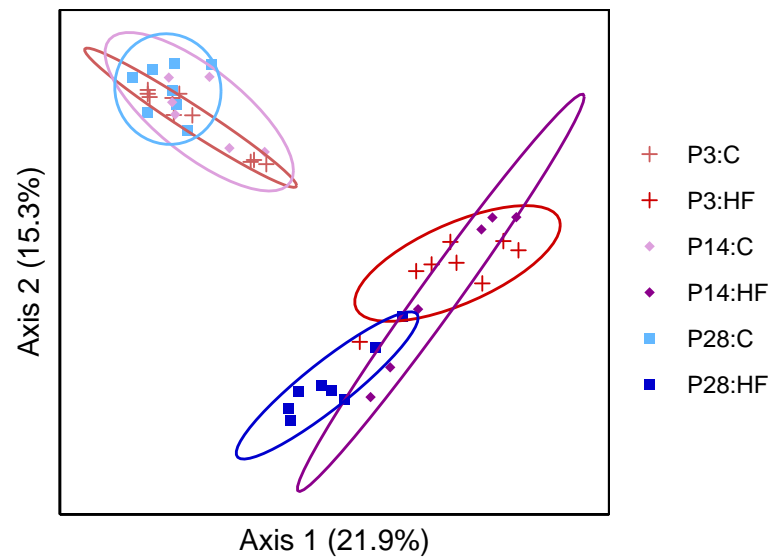
**Figure D.5. PCoA of maternal beta diversity by diet across
lactation** using Bray-Curtis dissimilarity. Points represent individual
samples and are coloured by sample time and diet (P3: HF red, C pink;
P14: HF purple, C mauve; P28: HF blue, C light blue; C=control,
HF=high-fat).
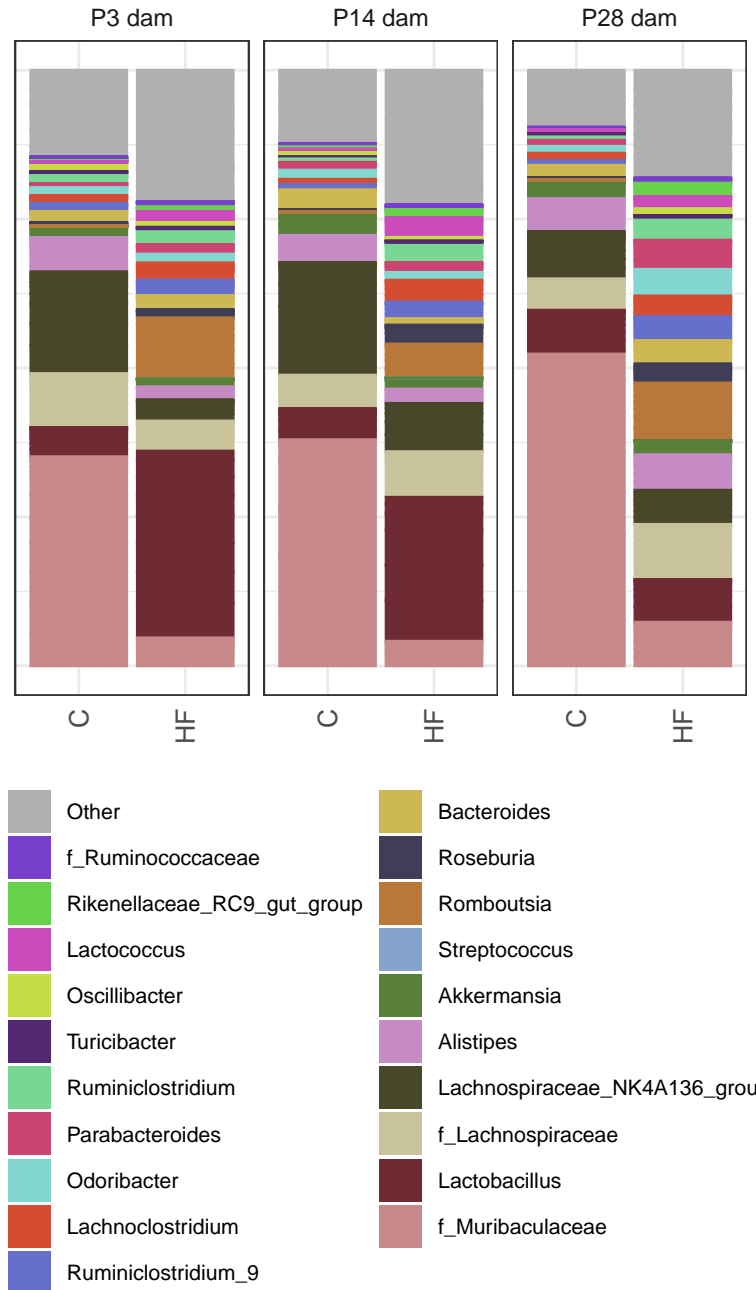
Figure D.6. Relative abundance of the 20 most abundant genera during lactation. Mean relative abundances were calculated for each sample time (P3, P14, and P28) and diet group (C=control and HF=high-fat) and plotted as stacked bar plots.
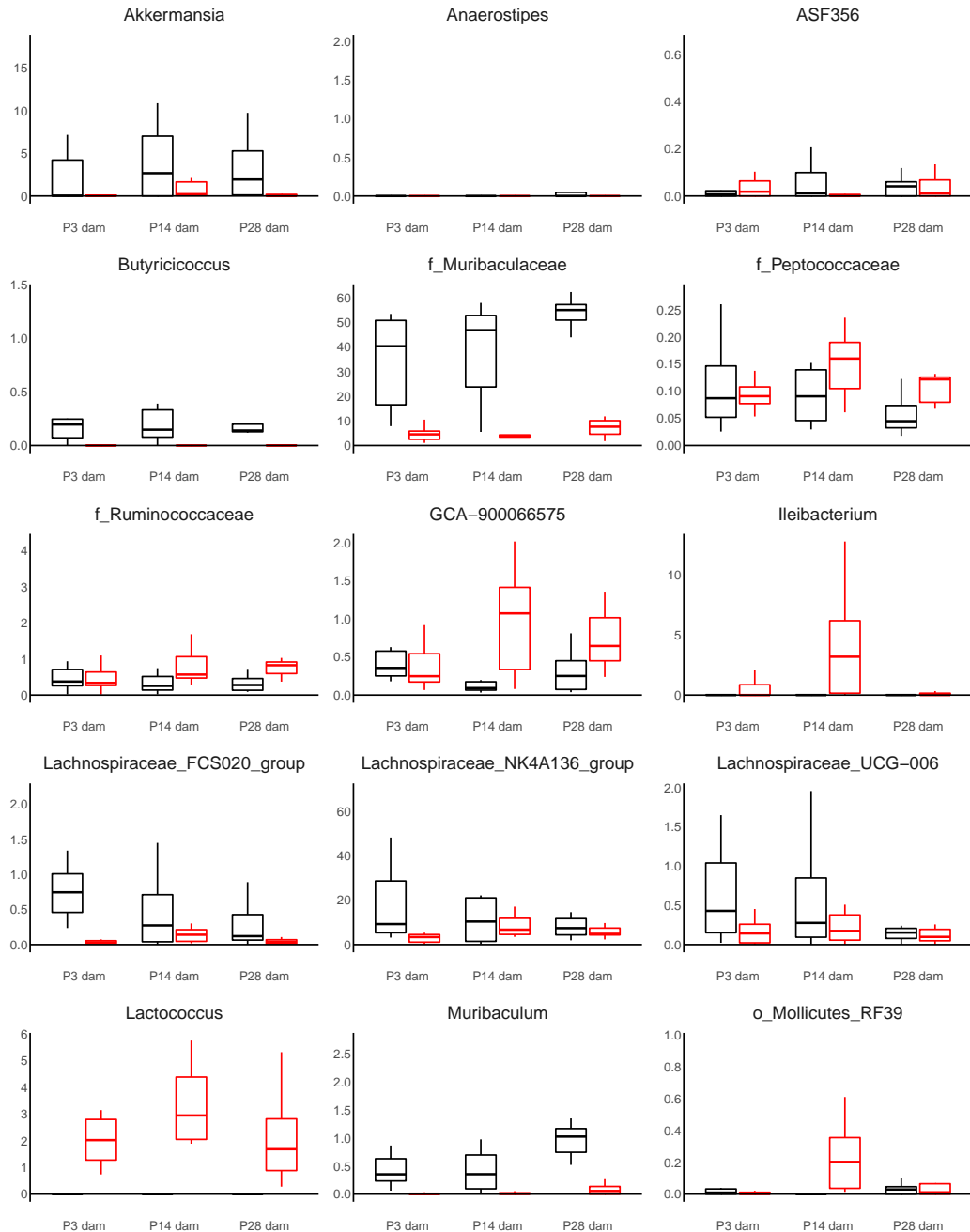
Figure D.7. Bacterial genera significantly enriched or depleted by diet during lactation. Legend on following page.
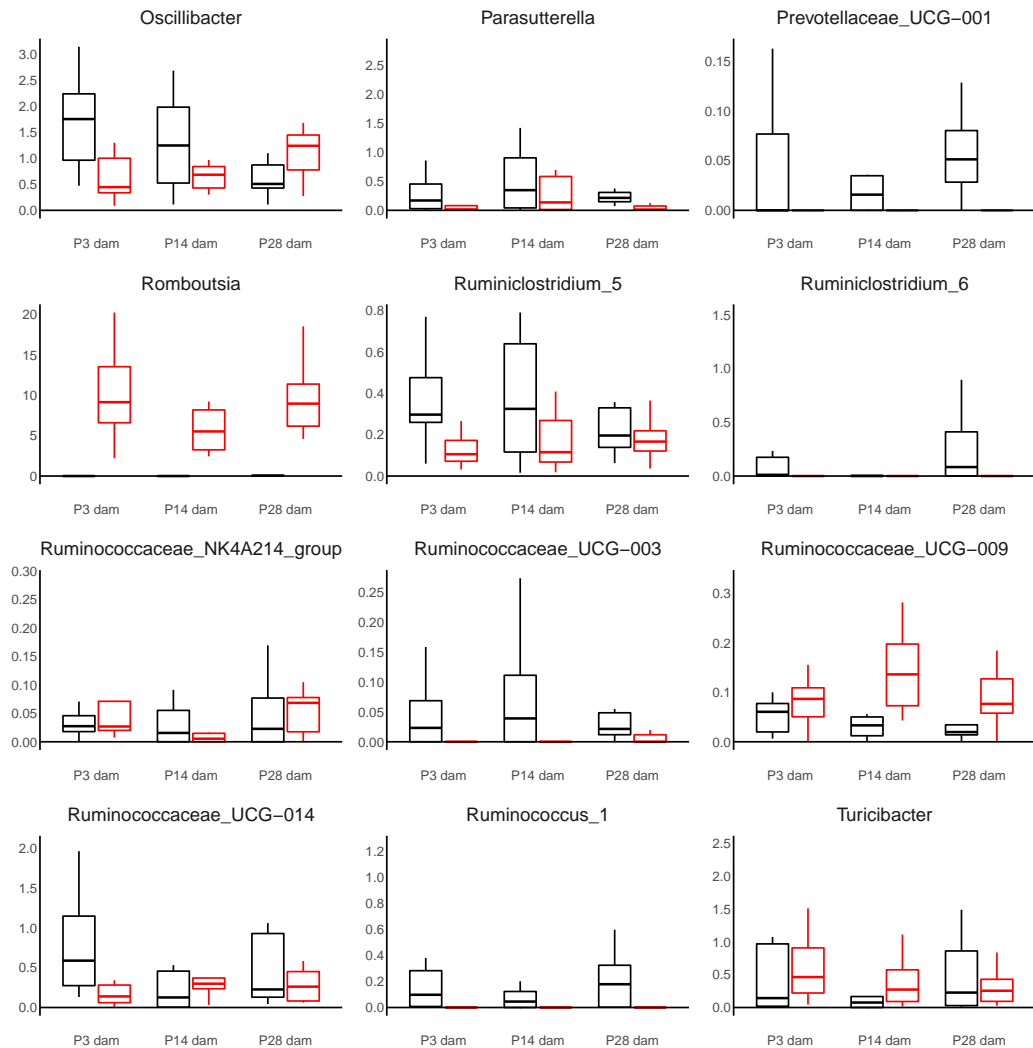
Figure D.7. Abundance in dam microbiota of genera significantly enriched or depleted in offspring microbiota Box plots of the relative abundance of each genus at each sample time points for control (black) and HF (red) wildtype (Wt) and are shown for genera significantly affected by diet in the gut microbiota of offspring. Significance was assessed by DESeq2.The box plot centre line represents the median; the box limits represent the upper and lower quartiles; the whiskers represent the 1.5x interquartile range.

Appendix E

Impact of COVID-19 pandemic

Aspects of the research contained within and absent from this thesis were affected by the COVID-19 pandemic. Although the majority of my animal work was completed prior to the pandemic my offspring experiments were concluded at the end of March 2020. The number of individuals present in the lab was limited by approximately 50% from March 2020 until August 2021. This limitation on the time I was able to be in the lab decreased the rate at which I was able to complete molecular and histological analysis of offspring, fetal, and maternal tissues and prevented the assessment of protein components of the intestinal epithelium through western blotting and immunohistochemistry due to time constraints.

Bibliography

[1] Kennedy, K., Selvaratnam, J. & Sloboda, D. Perinatal programming of disease risk: Maternal, microbial, and metabolic influences. In *The 116th Abbott Nutrition Research Conference*, 18 (static.abbottnutrition.com, 2017).

[2] Sender, R., Fuchs, S. & Milo, R. Revised estimates for the number of human and bacteria cells in the body. *PLoS Biol.* **14**, e1002533 (2016).

[3] Whitman, W. B., Coleman, D. C. & Wiebe, W. J. Prokaryotes: the unseen majority. *Proc. Natl. Acad. Sci. U. S. A.* **95**, 6578–6583 (1998).

[4] Sekirov, I., Russell, S. L., Antunes, L. C. M. & Finlay, B. B. Gut microbiota in health and disease. *Physiol. Rev.* **90**, 859–904 (2010).

[5] Fan, Y. & Pedersen, O. Gut microbiota in human metabolic health and disease. *Nat. Rev. Microbiol.* **19**, 55–71 (2020).

[6] Zoetendal, E. G., Akkermans, A. D. & De Vos, W. M. Temperature gradient gel electrophoresis analysis of 16S rRNA from human fecal samples reveals stable and host-specific communities of active bacteria. *Appl. Environ. Microbiol.* **64**, 3854–3859 (1998).

[7] Eckburg, P. B. *et al.* Diversity of the human intestinal microbial flora. *Science* **308**, 1635–1638 (2005).

[8] Human Microbiome Project Consortium. Structure, function and diversity of the healthy human microbiome. *Nature* **486**, 207–214 (2012).

[9] Hugenholtz, P., Goebel, B. M. & Pace, N. R. Impact of culture-independent studies on the emerging phylogenetic view of bacterial diversity. *J. Bacteriol.* **180**, 4765–4774 (1998).

[10] Ley, R. E., Peterson, D. A. & Gordon, J. I. Ecological and evolutionary forces shaping microbial diversity in the human intestine. *Cell* **124**, 837–848 (2006).

[11] Vandeputte, D. *et al.* Quantitative microbiome profiling links gut community variation to microbial load. *Nature* **551**, 507–511 (2017).

[12] Falony, G., Vieira-Silva, S. & Raes, J. Richness and ecosystem development across faecal snapshots of the gut microbiota. *Nat Microbiol* **3**, 526–528 (2018).

[13] Gill, S. R. *et al.* Metagenomic analysis of the human distal gut microbiome. *Science* **312**, 1355–1359 (2006).

[14] Sonnenburg, J. L. *et al.* Glycan foraging in vivo by an intestine-adapted bacterial symbiont. *Science* **307**, 1955–1959 (2005).

[15] Turnbaugh, P. J. *et al.* An obesity-associated gut microbiome with increased capacity for energy harvest. *Nature* **444**, 1027–1031 (2006).

[16] Round, J. L. & Mazmanian, S. K. The gut microbiota shapes intestinal immune responses during health and disease. *Nat. Rev. Immunol.* **9**, 313–323 (2009).

[17] Ulluwishewa, D. *et al.* Regulation of tight junction permeability by intestinal bacteria and dietary components. *J. Nutr.* **141**, 769–776 (2011).

[18] König, J. *et al.* Human intestinal barrier function in health and disease. *Clin. Transl. Gastroenterol.* **7**, e196 (2016).

[19] Grosheva, I. *et al.* High-Throughput screen identifies host and microbiota regulators of intestinal barrier function. *Gastroenterology* **159**, 1807–1823 (2020).

[20] Peng, L., Li, Z.-R., Green, R. S., Holzman, I. R. & Lin, J. Butyrate enhances the intestinal barrier by facilitating tight junction assembly via activation of AMP-activated protein kinase in caco-2 cell monolayers. *J. Nutr.* **139**, 1619–1625 (2009).

[21] Suzuki, T., Yoshida, S. & Hara, H. Physiological concentrations of short-chain fatty acids immediately suppress colonic epithelial permeability. *Br. J. Nutr.* **100**, 297–305 (2008).

[22] den Besten, G. *et al.* The role of short-chain fatty acids in the interplay between diet, gut microbiota, and host energy metabolism. *J. Lipid Res.* **54**, 2325–2340 (2013).

[23] Ríos-Covián, D. *et al.* Intestinal short chain fatty acids and their link with diet and human health. *Front. Microbiol.* **7**, 185 (2016).

[24] Roediger, W. E. The colonic epithelium in ulcerative colitis: an energy-deficiency disease? *Lancet* **2**, 712–715 (1980).

[25] Byndloss, M. X. *et al.* Microbiota-activated PPAR-γ signaling inhibits dysbiotic enterobacteriaceae expansion. *Science* **357**, 570–575 (2017).

[26] Tan, J. *et al.* The role of short-chain fatty acids in health and disease. *Adv. Immunol.* **121**, 91–119 (2014).

[27] Milligan, G., Stoddart, L. A. & Smith, N. J. Agonism and allosterism: the pharmacology of the free fatty acid receptors FFA2 and FFA3. *Br. J. Pharmacol.* **158**, 146–153 (2009).

[28] Chambers, E. S. *et al.* Effects of targeted delivery of propionate to the human colon on appetite regulation, body weight maintenance and adiposity in overweight adults. *Gut* **64**, 1744–1754 (2015).

[29] Pingitore, A. *et al.* The diet-derived short chain fatty acid propionate improves beta-cell function in humans and stimulates insulin secretion from human islets in vitro. *Diabetes Obes. Metab.* **19**, 257–265 (2017).

[30] Schwiertz, A. *et al.* Microbiota and SCFA in lean and overweight healthy subjects. *Obesity* **18**, 190–195 (2010).

[31] Bilotta, A. J. & Cong, Y. Gut microbiota metabolite regulation of host defenses at mucosal surfaces: implication in precision medicine. *Precis Clin Med* **2**, 110–119 (2019).

[32] Turner, J. R. Intestinal mucosal barrier function in health and disease. *Nat. Rev. Immunol.* **9**, 799–809 (2009).

[33] Johansson, M. E. V. *et al.* The inner of the two muc2 mucin-dependent mucus layers in colon is devoid of bacteria. *Proceedings of the National Academy of Sciences* **105**, 15064–15069 (2008).

[34] Finnie, I. A., Dwarakanath, A. D., Taylor, B. A. & Rhodes, J. M. Colonic mucin synthesis is increased by sodium butyrate. *Gut* **36**, 93–99 (1995).

[35] Burger-van Paassen, N. *et al.* The regulation of intestinal mucin MUC2 expression by short-chain fatty acids: implications for epithelial protection. *Biochem. J* **420**, 211–219 (2009).

[36] Cornick, S., Tawiah, A. & Chadee, K. Roles and regulation of the mucus barrier in the gut. *Tissue Barriers* **3**, e982426 (2015).

[37] Petersson, J. *et al.* Importance and regulation of the colonic mucus barrier in a mouse model of colitis. *Am. J. Physiol. Gastrointest. Liver Physiol.* **300**, G327–33 (2011).

[38] Ahn, D.-H. *et al.* TNF-alpha activates MUC2 transcription via NF-kappaB but inhibits via JNK activation. *Cell. Physiol. Biochem.* **15**, 29–40 (2005).

[39] Sassone-Corsi, M. & Raffatellu, M. No vacancy: how beneficial microbes cooperate with immunity to provide colonization resistance to pathogens. *J. Immunol.* **194**, 4081–4087 (2015).

[40] Roos, S. & Jonsson, H. A high-molecular-mass cell-surface protein from lactobacillus reuteri 1063 adheres to mucus components. *Microbiology* **148**, 433–442 (2002).

[41] Johansson, M. E. V. & Hansson, G. C. Immunological aspects of intestinal mucus and mucins. *Nat. Rev. Immunol.* **16**, 639–649 (2016).

[42] Bergstrom, K. S. B. & Xia, L. Mucin-type o-glycans and their roles in intestinal homeostasis. *Glycobiology* **23**, 1026–1037 (2013).

[43] Huang, I.-N. *et al.* New screening methods for probiotics with adhesion properties to sialic acid and sulphate residues in human colonic mucin using the biacore assay. *J. Appl. Microbiol.* **114**, 854–860 (2013).

[44] Freitas, M., Axelsson, L.-G., Cayuela, C., Midtvedt, T. & Trugnan, G. Microbial-host interactions specifically control the glycosylation pattern in intestinal mouse mucosa. *Histochem. Cell Biol.* **118**, 149–161 (2002).

[45] Etienne-Mesmin, L. *et al.* Experimental models to study intestinal microbes–mucus interactions in health and disease. *FEMS Microbiol. Rev.* **43**, 457–489 (2019).

[46] Qu, D. *et al.* The effects of diet and gut microbiota on the regulation of intestinal mucin glycosylation. *Carbohydr. Polym.* **258**, 117651 (2021).

[47] Arike, L. & Hansson, G. C. The densely O-Glycosylated MUC2 mucin protects the intestine and provides food for the commensal bacteria. *J. Mol. Biol.* **428**, 3221–3229 (2016).

[48] de Vos, W. M. Microbe profile: Akkermansia muciniphila: a conserved intestinal symbiont that acts as the gatekeeper of our mucosa. *Microbiology* **163**, 646–648 (2017).

[49] Wang, R. X., Lee, J. S., Campbell, E. L. & Colgan, S. P. Microbiota-derived butyrate dynamically regulates intestinal homeostasis through regulation of actin-associated protein synaptopodin. *Proc. Natl. Acad. Sci. U. S. A.* **117**, 11648–11657 (2020).

[50] Gao, Y. *et al.* Short-chain fatty acid butyrate, a breast milk metabolite, enhances immature intestinal barrier function genes in response to inflammation in vitro and in vivo. *Am. J. Physiol. Gastrointest. Liver Physiol.* **320**, G521–G530 (2021).

[51] Sprockett, D., Fukami, T. & Relman, D. A. Role of priority effects in the early-life assembly of the gut microbiota. *Nat. Rev. Gastroenterol. Hepatol.* **15**, 197–205 (2018).

[52] Martínez, I. *et al.* Experimental evaluation of the importance of colonization history in early-life gut microbiota assembly. *Elife* **7** (2018).

[53] Cox, L. M. *et al.* Altering the intestinal microbiota during a critical developmental window has lasting metabolic consequences. *Cell* **158**, 705–721 (2014).

[54] Ahmadizar, F. *et al.* Early-life antibiotic exposure increases the risk of developing allergic symptoms later in life: A meta-analysis. *Allergy* **73**, 971–986 (2018).

[55] Durack, J. *et al.* Delayed gut microbiota development in high-risk for asthma infants is temporarily modifiable by lactobacillus supplementation. *Nat. Commun.* **9**, 707 (2018).

[56] Benson, A. K. *et al.* Individuality in gut microbiota composition is a complex polygenic trait shaped by multiple environmental and host genetic factors. *Proc. Natl. Acad. Sci. U. S. A.* **107**, 18933–18938 (2010).

[57] Fulde, M. *et al.* Neonatal selection by toll-like receptor 5 influences long-term gut microbiota composition. *Nature* **560**, 489–493 (2018).

[58] Tamburini, S., Shen, N., Wu, H. C. & Clemente, J. C. The microbiome in early life: implications for health outcomes. *Nat. Med.* **22**, 713–722 (2016).

[59] Dominguez-Bello, M. G. *et al.* Delivery mode shapes the acquisition and structure of the initial microbiota across multiple body habitats in newborns. *Proc. Natl. Acad. Sci. U. S. A.* **107**, 11971–11975 (2010).

[60] Bäckhed, F. *et al.* Dynamics and stabilization of the human gut microbiome during the first year of life. *Cell Host Microbe* **17**, 690–703 (2015).

[61] Korpela, K. *et al.* Selective maternal seeding and environment shape the human gut microbiome. *Genome Res.* **28**, 561–568 (2018).

[62] Jakobsson, H. E. *et al.* Decreased gut microbiota diversity, delayed bacteroidetes colonisation and reduced th1 responses in infants delivered by caesarean section. *Gut* **63**, 559–566 (2014).

[63] Azad, M. B. *et al.* Impact of maternal intrapartum antibiotics, method of birth and breastfeeding on gut microbiota during the first year of life: a prospective cohort study. *BJOG* **123**, 983–993 (2016).

[64] Stewart, C. J. *et al.* Temporal development of the gut microbiome in early childhood from the TEDDY study. *Nature* **562**, 583–588 (2018).

[65] Reyman, M. *et al.* Impact of delivery mode-associated gut microbiota dynamics on health in the first year of life. *Nat. Commun.* **10**, 4997 (2019).

[66] Shao, Y. *et al.* Stunted microbiota and opportunistic pathogen colonization in caesarean-section birth. *Nature* **574**, 117–121 (2019).

[67] Mitchell, C. M. *et al.* Delivery mode affects stability of early infant gut microbiota. *Cell Rep Med* **1**, 100156 (2020).

[68] Martín, R. *et al.* Human milk is a source of lactic acid bacteria for the infant gut. *J. Pediatr.* **143**, 754–758 (2003).

[69] Martín, V. *et al.* Sharing of bacterial strains between breast milk and infant feces. *J. Hum. Lact.* **28**, 36–44 (2012).

[70] Azad, M. B. *et al.* Gut microbiota diversity and atopic disease: does breast-feeding play a role? *J. Allergy Clin. Immunol.* **131**, 247–248 (2013).

[71] Turroni, F. *et al.* Glycan utilization and Cross-Feeding activities by bifidobacteria. *Trends Microbiol.* **26**, 339–350 (2018).

[72] Chia, L. W. *et al.* Cross-feeding between bifidobacterium infantis and anaerostipes caccae on lactose and human milk oligosaccharides. *Benef. Microbes* **12**, 69–83 (2021).

[73] Yatsunenko, T. *et al.* Human gut microbiome viewed across age and geography. *Nature* **486**, 222–227 (2012).

[74] Koenig, J. E. *et al.* Succession of microbial consortia in the developing infant gut microbiome. *Proc. Natl. Acad. Sci. U. S. A.* **108 Suppl 1**, 4578–4585 (2011).

[75] Hooper, L. V. & Gordon, J. I. Commensal host-bacterial relationships in the gut. *Science* **292**, 1115–1118 (2001).

[76] Hooper, L. V., Xu, J., Falk, P. G., Midtvedt, T. & Gordon, J. I. A molecular sensor that allows a gut commensal to control its nutrient foundation in a competitive ecosystem. *Proc. Natl. Acad. Sci. U. S. A.* **96**, 9833–9838 (1999).

[77] Pham, T. A. N. *et al.* Epithelial IL-22RA1-mediated fucosylation promotes intestinal colonization resistance to an opportunistic pathogen. *Cell Host Microbe* **16**, 504–516 (2014).

[78] Gensollen, T., Iyer, S. S., Kasper, D. L. & Blumberg, R. S. How colonization by microbiota in early life shapes the immune system. *Science* **352**, 539–544 (2016).

[79] Sevelsted, A., Stokholm, J., Bønnelykke, K. & Bisgaard, H. Cesarean section and chronic immune disorders. *Pediatrics* **135**, e92–8 (2015).

[80] Kronman, M. P., Zaoutis, T. E., Haynes, K., Feng, R. & Coffin, S. E. Antibiotic exposure and IBD development among children: a population-based cohort study. *Pediatrics* **130**, e794–803 (2012).

[81] Metsälä, J. *et al.* Prenatal and post-natal exposure to antibiotics and risk of asthma in childhood. *Clin. Exp. Allergy* **45**, 137–145 (2015).

[82] Huh, S. Y. *et al.* Delivery by caesarean section and risk of obesity in preschool age children: a prospective cohort study. *Arch. Dis. Child.* **97**, 610–616 (2012).

[83] Saari, A., Virta, L. J., Sankilampi, U., Dunkel, L. & Saxen, H. Antibiotic exposure in infancy and risk of being overweight in the first 24 months of life. *Pediatrics* **135**, 617–626 (2015).

[84] Vatanen, T. *et al.* Variation in microbiome LPS immunogenicity contributes to autoimmunity in humans. *Cell* **165**, 842–853 (2016).

[85] Li, Y. *et al.* In utero human intestine harbors unique metabolome, including bacterial metabolites. *JCI Insight* **5** (2020).

[86] Vuillermin, P. J. *et al.* Maternal carriage of prevotella during pregnancy associates with protection against food allergy in the offspring. *Nat. Commun.* **11**, 1452 (2020).

[87] Vuong, H. E. *et al.* The maternal microbiome modulates fetal neurodevelopment in mice. *Nature* **586**, 281–286 (2020).

[88] Gomez de Agüero, M. *et al.* The maternal microbiota drives early postnatal innate immune development. *Science* **351**, 1296–1302 (2016).

[89] Tan, E. K. & Tan, E. L. Alterations in physiology and anatomy during pregnancy. *Best Pract. Res. Clin. Obstet. Gynaecol.* **27**, 791–802 (2013).

[90] Aatsinki, A.-K. *et al.* Gut microbiota composition in Mid-Pregnancy is associated with gestational weight gain but not prepregnancy body mass index. *J. Womens. Health* **27**, 1293–1301 (2018).

[91] Crusell, M. K. W. *et al.* Gestational diabetes is associated with change in the gut microbiota composition in third trimester of pregnancy and postpartum. *Microbiome* **6**, 89 (2018).

[92] Zacarías, M. F. *et al.* Pregestational overweight and obesity are associated with differences in gut microbiota composition and systemic inflammation in the third trimester. *PLoS One* **13**, e0200305 (2018).

[93] Koren, O. *et al.* Host remodeling of the gut microbiome and metabolic changes during pregnancy. *Cell* **150**, 470–480 (2012).

[94] Mukhopadhya, I., Hansen, R., El-Omar, E. M. & Hold, G. L. IBD-what role do proteobacteria play? *Nat. Rev. Gastroenterol. Hepatol.* **9**, 219–230 (2012).

[95] Nuriel-Ohayon, M. *et al.* Progesterone increases bifidobacterium relative abundance during late pregnancy. *Cell Rep.* **27**, 730–736.e3 (2019).

[96] Csapo, A. I., Knobil, E., van der Molen, H. J. & Wiest, W. G. Peripheral plasma progesterone levels during human pregnancy and labor. *Am. J. Obstet. Gynecol.* **110**, 630–632 (1971).

[97] Enomoto, T. *et al.* Effects of bifidobacterial supplementation to pregnant women and infants in the prevention of allergy development in infants and on fecal microbiota. *Allergol. Int.* **63**, 575–585 (2014).

[98] DiGiulio, D. B. *et al.* Temporal and spatial variation of the human microbiota during pregnancy. *Proc. Natl. Acad. Sci. U. S. A.* **112**, 11060–11065 (2015).

[99] Kumbhare, S. V. *et al.* Gut microbial diversity during pregnancy and early infancy: an exploratory study in the indian population. *FEMS Microbiol. Lett.* **367** (2020).

[100] Yang, Y., Gharaibeh, R. Z., Newsome, R. C. & Jobin, C. Amending microbiota by targeting intestinal inflammation with TNF blockade attenuates development of colorectal cancer. *Nat Cancer* **1**, 723–734 (2020).

[101] Berry, A. S. F. *et al.* Remodeling of the maternal gut microbiome during pregnancy is shaped by parity. *Microbiome* **9**, 146 (2021).

[102] García-Mantrana, I. *et al.* Distinct maternal microbiota clusters are associated with diet during pregnancy: impact on neonatal microbiota and infant growth during the first 18 months of life. *Gut Microbes* **11**, 962–978 (2020).

[103] Kuang, Y.-S. *et al.* Connections between the human gut microbiome and gestational diabetes mellitus. *Gigascience* **6**, 1–12 (2017).

[104] Ferrocino, I. *et al.* Changes in the gut microbiota composition during pregnancy in patients with gestational diabetes mellitus (GDM). *Sci. Rep.* **8**, 12216 (2018).

[105] Mokkala, K. *et al.* Gut microbiota aberrations precede diagnosis of gestational diabetes mellitus. *Acta Diabetol.* **54**, 1147–1149 (2017).

[106] Collado, M. C., Isolauri, E., Laitinen, K. & Salminen, S. Distinct composition of gut microbiota during pregnancy in overweight and normal-weight women. *Am. J. Clin. Nutr.* **88**, 894–899 (2008).

[107] Santacruz, A. *et al.* Gut microbiota composition is associated with body weight, weight gain and biochemical parameters in pregnant women. *Br. J. Nutr.* **104**, 83–92 (2010).

[108] Stanislawski, M. A. *et al.* Pre-pregnancy weight, gestational weight gain, and the gut microbiota of mothers and their infants. *Microbiome* **5**, 113 (2017).

[109] Gomez-Arango, L. F. *et al.* Connections between the gut microbiome and metabolic hormones in early pregnancy in overweight and obese women. *Diabetes* **65**, 2214–2223 (2016).

[110] Ganal-Vonarburg, S. C., Hornef, M. W. & Macpherson, A. J. Microbial–host molecular exchange and its functional consequences in early mammalian life. *Science* **368**, 604–607 (2020).

[111] Fröhlich, E., Mercuri, A., Wu, S. & Salar-Behzadi, S. Measurements of deposition, lung surface area and lung fluid for simulation of inhaled compounds. *Front. Pharmacol.* **7**, 181 (2016).

[112] Helander, H. F. & Fändriks, L. Surface area of the digestive tract - revisited. *Scand. J. Gastroenterol.* **49**, 681–689 (2014).

[113] Kimura, I. *et al.* Maternal gut microbiota in pregnancy influences offspring metabolic phenotype in mice. *Science* **367** (2020).

[114] Stanford, A. H. *et al.* A direct comparison of mouse and human intestinal development using epithelial gene expression patterns. *Pediatr. Res.* **88**, 66–76 (2020).

[115] Walton, K. D. *et al.* Hedgehog-responsive mesenchymal clusters direct patterning and emergence of intestinal villi. *Proc. Natl. Acad. Sci. U. S. A.* **109**, 15817–15822 (2012).

[116] Walton, K. D., Freddo, A. M., Wang, S. & Gumucio, D. L. Generation of intestinal surface: an absorbing tale. *Development* **143**, 2261–2272 (2016).

[117] Chin, A. M., Hill, D. R., Aurora, M. & Spence, J. R. Morphogenesis and maturation of the embryonic and postnatal intestine. *Semin. Cell Dev. Biol.* **66**, 81–93 (2017).

[118] Noah, T. K., Donahue, B. & Shroyer, N. F. Intestinal development and differentiation. *Exp. Cell Res.* **317**, 2702–2710 (2011).

[119] Yanai, H. *et al.* Intestinal stem cells contribute to the maturation of the neonatal small intestine and colon independently of digestive activity. *Sci. Rep.* **7**, 9891 (2017).

[120] Pellegrinet, L. *et al.* Dll1- and dll4-mediated notch signaling are required for homeostasis of intestinal stem cells. *Gastroenterology* **140**, 1230–1240.e1–7 (2011).

[121] Tian, H. *et al.* Opposing activities of notch and wnt signaling regulate intestinal stem cells and gut homeostasis. *Cell Rep.* **11**, 33–42 (2015).

[122] Chin, A. M. *et al.* A dynamic WNT/β-CATENIN signaling environment leads to WNT-Independent and WNT-Dependent proliferation of embryonic intestinal progenitor cells. *Stem Cell Reports* **7**, 826–839 (2016).

[123] He, X. C. *et al.* BMP signaling inhibits intestinal stem cell self-renewal through suppression of Wnt–β-catenin signaling. *Nat. Genet.* **36**, 1117 (2004).

[124] Carmon, K. S., Lin, Q., Gong, X., Thomas, A. & Liu, Q. LGR5 interacts and cointernalizes with wnt receptors to modulate Wnt/β-catenin signaling. *Mol. Cell. Biol.* **32**, 2054–2064 (2012).

[125] Tan, S. H. *et al.* A constant pool of lgr5+ intestinal stem cells is required for intestinal homeostasis. *Cell Rep.* **34**, 108633 (2021).

[126] Ghaleb, A. M., McConnell, B. B., Kaestner, K. H. & Yang, V. W. Altered intestinal epithelial homeostasis in mice with intestine-specific deletion of the krüppel-like factor 4 gene. *Dev. Biol.* **349**, 310–320 (2011).

[127] Katz, J. P. *et al.* The zinc-finger transcription factor klf4 is required for terminal differentiation of goblet cells in the colon. *Development* **129**, 2619–2628 (2002).

[128] Garcia, M. I. *et al.* LGR5 deficiency deregulates wnt signaling and leads to precocious paneth cell differentiation in the fetal intestine. *Dev. Biol.* **331**, 58–67 (2009).

[129] Kumar, N. *et al.* A YY1-dependent increase in aerobic metabolism is indispensable for intestinal organogenesis. *Development* **143**, 3711–3722 (2016).

[130] Donohoe, D. R. *et al.* The microbiome and butyrate regulate energy metabolism and autophagy in the mammalian colon. *Cell Metab.* **13**, 517–526 (2011).

[131] Stringari, C. *et al.* Metabolic trajectory of cellular differentiation in small intestine by phasor fluorescence lifetime microscopy of NADH. *Sci. Rep.* **2**, 568 (2012).

[132] Barker, D. J., Winter, P. D., Osmond, C., Margetts, B. & Simmonds, S. J. Weight in infancy and death from ischaemic heart disease. *Lancet* **2**, 577–580 (1989).

[133] Barker, D. J. The fetal and infant origins of adult disease. *BMJ* **301**, 1111–1111 (1990).

[134] Hales, C. N. *et al.* Fetal and infant growth and impaired glucose tolerance at age 64. *BMJ* **303**, 1019–1022 (1991).

[135] Phillips, D. I., Barker, D. J., Hales, C. N., Hirst, S. & Osmond, C. Thinness at birth and insulin resistance in adult life. *Diabetologia* **37**, 150–154 (1994).

[136] Ravelli, A. C. J., van der Meulen, J. H. P., Osmond, C., Barker, D. J. P. & Bleker, O. P. Obesity at the age of 50 y in men and women exposed to famine prenatally. *Am. J. Clin. Nutr.* **70**, 811–816 (1999).

[137] Gluckman, P. D. & Hanson, M. A. *The Fetal Matrix: Evolution, Development and Disease* (Cambridge University Press, 2004).

[138] Vickers, M. H., Breier, B. H., Cutfield, W. S., Hofman, P. L. & Gluckman, P. D. Fetal origins of hyperphagia, obesity, and hypertension and postnatal amplification by hypercaloric nutrition. *Am. J. Physiol. Endocrinol. Metab.* **279**, E83–7 (2000).

[139] Howie, G. J., Sloboda, D. M., Kamal, T. & Vickers, M. H. Maternal nutritional history predicts obesity in adult offspring independent of postnatal diet. *J. Physiol.* **587**, 905–915 (2009).

[140] Desai, M., Babu, J. & Ross, M. G. Programmed metabolic syndrome: prenatal undernutrition and postweaning overnutrition. *Am. J. Physiol. Regul. Integr. Comp. Physiol.* **293**, R2306–14 (2007).

[141] Bäckhed, F. *et al.* The gut microbiota as an environmental factor that regulates fat storage. *Proc. Natl. Acad. Sci. U. S. A.* **101**, 15718–15723 (2004).

[142] Dudenhausen, J. W., Grünebaum, A. & Kirschner, W. Prepregnancy body weight and gestational weight gain-recommendations and reality in the USA and in germany. *Am. J. Obstet. Gynecol.* **213**, 591–592 (2015).

[143] Hadden, D. R. & McLaughlin, C. Normal and abnormal maternal metabolism during pregnancy. *Semin. Fetal Neonatal Med.* **14**, 66–71 (2009).

[144] Christian, L. M. & Porter, K. Longitudinal changes in serum proinflammatory markers across pregnancy and postpartum: effects of maternal body mass index. *Cytokine* **70**, 134–140 (2014).

[145] Friedman, J. E. Developmental programming of obesity and diabetes in mouse, monkey, and man in 2018: Where are we headed? *Diabetes* **67**, 2137–2151 (2018).

[146] Guo, Y. *et al.* Diet induced maternal obesity affects offspring gut microbiota and persists into young adulthood. *Food Funct.* **9**, 4317–4327 (2018).

[147] Xie, R. *et al.* Maternal high fat diet alters gut microbiota of offspring and exacerbates DSS-Induced colitis in adulthood. *Front. Immunol.* **9**, 2608 (2018).

[148] Sela, D. A. *et al.* The genome sequence of bifidobacterium longum subsp. infantis reveals adaptations for milk utilization within the infant microbiome. *Proc. Natl. Acad. Sci. U. S. A.* **105**, 18964–18969 (2008).

[149] Zhao, Q. & Elson, C. O. Adaptive immune education by gut microbiota antigens. *Immunology* **154**, 28–37 (2018).

[150] Arrieta, M.-C. *et al.* Early infancy microbial and metabolic alterations affect risk of childhood asthma. *Sci. Transl. Med.* **7**, 307ra152 (2015).

[151] Yassour, M. *et al.* Natural history of the infant gut microbiome and impact of antibiotic treatment on bacterial strain diversity and stability. *Sci. Transl. Med.* **8**, 343ra81 (2016).

[152] Asnicar, F. *et al.* Studying vertical microbiome transmission from mothers to infants by Strain-Level metagenomic profiling. *mSystems* **2** (2017).

[153] Ferretti, P. *et al.* Mother-to-Infant microbial transmission from different body sites shapes the developing infant gut microbiome. *Cell Host Microbe* **24**, 133–145.e5 (2018).

[154] Yassour, M. *et al.* Strain-Level analysis of Mother-to-Child bacterial transmission during the first few months of life. *Cell Host Microbe* **24**, 146–154.e4 (2018).

[155] Rawls, J. F., Mahowald, M. A., Ley, R. E. & Gordon, J. I. Reciprocal gut microbiota transplants from zebrafish and mice to germ-free recipients reveal host habitat selection. *Cell* **127**, 423–433 (2006).

[156] Collado, M. C., Isolauri, E., Laitinen, K. & Salminen, S. Effect of mother's weight on infant's microbiota acquisition, composition, and activity during early infancy: a prospective follow-up study initiated in early pregnancy–. *Am. J. Clin. Nutr.* **92**, 1023–1030 (2010).

[157] Chu, D. M. *et al.* The early infant gut microbiome varies in association with a maternal high-fat diet. *Genome Med.* **8**, 77 (2016).

[158] Mueller, N. T. *et al.* Birth mode-dependent association between pre-pregnancy maternal weight status and the neonatal intestinal microbiome. *Sci. Rep.* **6**, 23133 (2016).

[159] Tun, H. M. *et al.* Roles of birth mode and infant gut microbiota in intergenerational transmission of overweight and obesity from mother to offspring. *JAMA Pediatr.* **172**, 368–377 (2018).

[160] Myles, I. A. *et al.* Parental dietary fat intake alters offspring microbiome and immunity. *J. Immunol.* **191**, 3200–3209 (2013).

[161] Goto, Y. *et al.* Segmented filamentous bacteria antigens presented by intestinal dendritic cells drive mucosal th17 cell differentiation. *Immunity* **40**, 594–607 (2014).

[162] Yan, X. *et al.* Maternal obesity induces sustained inflammation in both fetal and offspring large intestine of sheep. *Inflamm. Bowel Dis.* **17**, 1513–1522 (2011).

[163] Ruan, Q. *et al.* The th17 immune response is controlled by the Rel-RORγ-RORγ T transcriptional axis. *J. Exp. Med.* **208**, 2321–2333 (2011).

[164] Lee, J. S. *et al.* Interleukin-23-Independent IL-17 production regulates intestinal epithelial permeability. *Immunity* **43**, 727–738 (2015).

[165] Wang, Y., Mumm, J. B., Herbst, R., Kolbeck, R. & Wang, Y. IL-22 increases permeability of intestinal epithelial tight junctions by enhancing claudin-2 expression. *J. Immunol.* **199**, 3316–3325 (2017).

[166] Xue, Y., Wang, H., Du, M. & Zhu, M.-J. Maternal obesity induces gut inflammation and impairs gut epithelial barrier function in nonobese diabetic mice. *J. Nutr. Biochem.* **25**, 758–764 (2014).

[167] Campbell, E. L. *et al.* Transmigrating neutrophils shape the mucosal microenvironment through localized oxygen depletion to influence resolution of inflammation. *Immunity* **40**, 66–77 (2014).

[168] Gruber, L. *et al.* Maternal high-fat diet accelerates development of crohn's disease-like ileitis in TNFΔARE/WT offspring. *Inflamm. Bowel Dis.* **21**, 2016–2025 (2015).

[169] Bibi, S., Kang, Y., Du, M. & Zhu, M.-J. Maternal high-fat diet consumption enhances offspring susceptibility to DSS-induced colitis in mice. *Obesity* **25**, 901–908 (2017).

[170] Zindl, C. L. *et al.* IL-22–producing neutrophils contribute to antimicrobial defense and restitution of colonic epithelial integrity during colitis. *Proc. Natl. Acad. Sci. U. S. A.* **110**, 12768–12773 (2013).

[171] Pickert, G. *et al.* STAT3 links IL-22 signaling in intestinal epithelial cells to mucosal wound healing. *J. Exp. Med.* **206**, 1465–1472 (2009).

[172] Zheng, Y. *et al.* Interleukin-22 mediates early host defense against attaching and effacing bacterial pathogens. *Nat. Med.* **14**, 282–289 (2008).

[173] Eugene, S. P., Reddy, V. S. & Trinath, J. Endoplasmic reticulum stress and intestinal inflammation: A perilous union. *Front. Immunol.* **11**, 543022 (2020).

[174] Szegezdi, E., Logue, S. E., Gorman, A. M. & Samali, A. Mediators of endoplasmic reticulum stress-induced apoptosis. *EMBO Rep.* **7**, 880–885 (2006).

[175] Redman, C. W. G. The endoplasmic reticulum stress of placental impoverishment. *Am. J. Pathol.* **173**, 311–314 (2008).

[176] Yang, Q. *et al.* Tumour necrosis factor receptor 1 mediates endoplasmic reticulum stress-induced activation of the MAP kinase JNK. *EMBO Rep.* **7**, 622–627 (2006).

[177] Zhang, H.-S. *et al.* The endoplasmic reticulum stress sensor IRE1α in intestinal epithelial cells is essential for protecting against colitis. *J. Biol. Chem.* **290**, 15327–15336 (2015).

[178] Ozcan, U. *et al.* Endoplasmic reticulum stress links obesity, insulin action, and type 2 diabetes. *Science* **306**, 457–461 (2004).

[179] Sharma, N. K. *et al.* Endoplasmic reticulum stress markers are associated with obesity in nondiabetic subjects. *J. Clin. Endocrinol. Metab.* **93**, 4532–4541 (2008).

[180] Luo, K. & Cao, S. S. Endoplasmic reticulum stress in intestinal epithelial cell function and inflammatory bowel disease. *Gastroenterol. Res. Pract.* **2015**, 328791 (2015).

[181] Tréton, X. *et al.* Altered endoplasmic reticulum stress affects translation in inactive colon tissue from patients with ulcerative colitis. *Gastroenterology* **141**, 1024–1035 (2011).

[182] Kim, D. H. *et al.* Lactobacillus acidophilus suppresses intestinal inflammation by inhibiting endoplasmic reticulum stress. *J. Gastroenterol. Hepatol.* **34**, 178–185 (2019).

[183] Choi, J. H. *et al.* Lactobacillus paracasei-derived extracellular vesicles attenuate the intestinal inflammatory response by augmenting the endoplasmic reticulum stress pathway. *Exp. Mol. Med.* **52**, 423–437 (2020).

[184] Rodríguez, J. M. *et al.* The composition of the gut microbiota throughout life, with an emphasis on early life. *Microb. Ecol. Health Dis.* **26**, 26050 (2015).

[185] Cotillard, A. *et al.* Dietary intervention impact on gut microbial gene richness. *Nature* **500**, 585–588 (2013).

[186] David, L. A. *et al.* Diet rapidly and reproducibly alters the human gut microbiome. *Nature* **505**, 559–563 (2013).

[187] Belkaid, Y. & Hand, T. W. Role of the microbiota in immunity and inflammation. *Cell* **157**, 121–141 (2014).

[188] Claesson, M. J. *et al.* Gut microbiota composition correlates with diet and health in the elderly. *Nature* **488**, 178–184 (2012).

[189] Rakoff-Nahoum, S., Paglino, J., Eslami-Varzaneh, F., Edberg, S. & Medzhitov, R. Recognition of commensal microflora by toll-like receptors is required for intestinal homeostasis. *Cell* **118**, 229–241 (2004).

[190] Ijssennagger, N. *et al.* Gut microbiota facilitates dietary heme-induced epithelial hyperproliferation by opening the mucus barrier in colon. *Proc. Natl. Acad. Sci. U. S. A.* **112**, 10038–10043 (2015).

[191] Kelly, D. *et al.* Commensal anaerobic gut bacteria attenuate inflammation by regulating nuclear-cytoplasmic shuttling of PPAR-γ and RelA. *Nat. Immunol.* **5**, 104–112 (2003).

[192] Fulde, M. & Hornef, M. W. Maturation of the enteric mucosal innate immune system during the postnatal period. *Immunol. Rev.* **260**, 21–34 (2014).

[193] Tims, S. *et al.* Microbiota conservation and BMI signatures in adult monozygotic twins. *ISME J.* **7**, 707–717 (2013).

[194] Liu, R. *et al.* Gut microbiome and serum metabolome alterations in obesity and after weight-loss intervention. *Nat. Med.* **23**, 859–868 (2017).

[195] Ridaura, V. K. *et al.* Gut microbiota from twins discordant for obesity modulate metabolism in mice. *Science* **341**, 1241214 (2013).

[196] Ajslev, T. A., Andersen, C. S., Gamborg, M., Sørensen, T. I. A. & Jess, T. Childhood overweight after establishment of the gut microbiota: the role of delivery mode, pre-pregnancy weight and early administration of antibiotics. *Int. J. Obes.* **35**, 522–529 (2011).

[197] Mueller, N. T. *et al.* Does vaginal delivery mitigate or strengthen the intergenerational association of overweight and obesity? findings from the boston birth cohort. *Int. J. Obes.* **41**, 497–501 (2017).

[198] Cassidy-Bushrow, A. E. *et al.* Prenatal antimicrobial use and early-childhood body mass index. *Int. J. Obes.* **42**, 1–7 (2018).

[199] Korpela, K. *et al.* Childhood BMI in relation to microbiota in infancy and lifetime antibiotic use. *Microbiome* **5**, 26 (2017).

[200] Kalliomäki, M., Collado, M. C., Salminen, S. & Isolauri, E. Early differences in fecal microbiota composition in children may predict overweight. *Am. J. Clin. Nutr.* **87**, 534–538 (2008).

[201] He, Q. *et al.* The meconium microbiota shares more features with the amniotic fluid microbiota than the maternal fecal and vaginal microbiota. *Gut Microbes* **12**, 1794266 (2020).

[202] Stinson, L. *et al.* Comparison of bacterial DNA profiles in Mid-Trimester amniotic fluid samples from preterm and term deliveries. *Front. Microbiol.* **11**, 415 (2020).

[203] Younge, N. *et al.* Fetal exposure to the maternal microbiota in humans and mice. *JCI Insight* **4** (2019).

[204] Aagaard, K. *et al.* The placenta harbors a unique microbiome. *Sci. Transl. Med.* **6**, 237ra65 (2014).

[205] Blaser, M. J. *et al.* Lessons learned from the prenatal microbiome controversy. *Microbiome* **9**, 8 (2021).

[206] Perez-Muñoz, M. E., Arrieta, M.-C., Ramer-Tait, A. E. & Walter, J. A critical assessment of the "sterile womb" and "in utero colonization" hypotheses: implications for research on the pioneer infant microbiome. *Microbiome* **5**, 48 (2017).

[207] Bushman, F. D. De-Discovery of the placenta microbiome. *Am. J. Obstet. Gynecol.* **220**, 213–214 (2019).

[208] The Lancet Infectious Diseases. Microbiome studies and "blue whales in the himalayas". *Lancet Infect. Dis.* **18**, 925 (2018).

[209] de Goffau, M. C. *et al.* Human placenta has no microbiome but can contain potential pathogens. *Nature* **572**, 329–334 (2019).

[210] Kuperman, A. A. *et al.* Deep microbial analysis of multiple placentas shows no evidence for a placental microbiome. *BJOG* **127**, 159–169 (2020).

[211] Lauder, A. P. *et al.* Comparison of placenta samples with contamination controls does not provide evidence for a distinct placenta microbiota. *Microbiome* **4**, 29 (2016).

[212] Leiby, J. S. *et al.* Lack of detection of a human placenta microbiome in samples from preterm and term deliveries. *Microbiome* **6**, 196 (2018).

[213] Theis, K. R. *et al.* Does the human placenta delivered at term have a microbiota? results of cultivation, quantitative real-time PCR, 16S rRNA gene sequencing, and metagenomics. *Am. J. Obstet. Gynecol.* **220**, 267.e1–267.e39 (2019).

[214] Whelan, F. J. *et al.* The loss of topography in the microbial communities of the upper respiratory tract in the elderly. *Ann. Am. Thorac. Soc.* **11**, 513–521 (2014).

[215] Bartram, A. K., Lynch, M. D. J., Stearns, J. C., Moreno-Hagelsieb, G. & Neufeld, J. D. Generation of multimillion-sequence 16S rRNA gene libraries from complex microbial communities by assembling paired-end illumina reads. *Appl. Environ. Microbiol.* **77**, 3846–3852 (2011).

[216] Martin, M. Cutadapt removes adapter sequences from high-throughput sequencing reads. *EMBnet.journal* **17**, 10–12 (2011).

[217] Callahan, B. J. *et al.* DADA2: High-resolution sample inference from illumina amplicon data. *Nat. Methods* **13**, 581–583 (2016).

[218] Quast, C. *et al.* The SILVA ribosomal RNA gene database project: improved data processing and web-based tools. *Nucleic Acids Res.* **41**, D590–6 (2013).

[219] McMurdie, P. J. & Holmes, S. phyloseq: an R package for reproducible interactive analysis and graphics of microbiome census data. *PLoS One* **8**, e61217 (2013).

[220] Oksanen, J. *et al.* Vegan: Community ecology package. 2013. r-package version 2.0-10 (2013).

[221] Wickham, H. *ggplot2: Elegant Graphics for Data Analysis* (Springer, 2016).

[222] Kennedy, K. M. *et al.* Fetal meconium does not have a detectable microbiota before birth. *Nature Microbiology* **6**, 865–873 (2021).

[223] Weström, B., Arévalo Sureda, E., Pierzynowska, K., Pierzynowski, S. G. & Pérez-Cano, F.-J. The immature gut barrier and its importance in establishing immunity in newborn mammals. *Front. Immunol.* **11**, 1153 (2020).

[224] Rackaityte, E. *et al.* Viable bacterial colonization is highly limited in the human intestine in utero. *Nat. Med.* (2020).

[225] Mishra, A. *et al.* Microbial exposure during early human development primes fetal immune cells. *Cell* (2021).

[226] Olomu, I. N. *et al.* Elimination of "kitome" and "splashome" contamination results in lack of detection of a unique placental microbiome. *BMC Microbiol.* **20**, 157 (2020).

[227] Eisenhofer, R. *et al.* Contamination in low microbial biomass microbiome studies: Issues and recommendations. *Trends Microbiol.* **27**, 105–117 (2019).

[228] Turnbaugh, P. J. *et al.* The human microbiome project. *Nature* **449**, 804–810 (2007).

[229] Faucher, M. A. *et al.* Exploration of the vaginal and gut microbiome in african american women by body mass index, class of obesity, and gestational weight gain: A pilot study. *Am. J. Perinatol.* **37**, 1160–1172 (2020).

[230] Triunfo, S. & Lanzone, A. Impact of overweight and obesity on obstetric outcomes. *J. Endocrinol. Invest.* **37**, 323–329 (2014).

[231] Ludwig, D. S., Rouse, H. L. & Currie, J. Pregnancy weight gain and childhood body weight: a within-family comparison. *PLoS Med.* **10**, e1001521 (2013).

[232] Retnakaran, R. *et al.* Effect of maternal weight, adipokines, glucose intolerance and lipids on infant birth weight among women without gestational diabetes mellitus. *CMAJ* **184**, 1353–1360 (2012).

[233] Rasmussen, K. M. & Yaktine, A. L. (eds.) *Weight Gain During Pregnancy: Reexamining the Guidelines* (National Academies Press (US), Washington (DC), 2010).

[234] Whittaker, R. H. Evolution and measurement of species diversity. *Taxon* **21**, 213–251 (1972).

[235] Collado, M. C., Isolauri, E., Laitinen, K. & Salminen, S. Effect of mother's weight on infant's microbiota acquisition, composition, and activity during early infancy: a prospective follow-up study initiated in early pregnancy. *Am. J. Clin. Nutr.* **92**, 1023–1030 (2010).

[236] Galley, J. D., Bailey, M., Kamp Dush, C., Schoppe-Sullivan, S. & Christian, L. M. Maternal obesity is associated with alterations in the gut microbiome in toddlers. *PLoS One* **9**, e113026 (2014).

[237] Hu, J. *et al.* Diversified microbiota of meconium is affected by maternal diabetes status. *PLoS One* **8**, e78257 (2013).

[238] Gosalbes, M. J. *et al.* Meconium microbiota types dominated by lactic acid or enteric bacteria are differentially associated with maternal eczema and respiratory problems in infants. *Clin. Exp. Allergy* **43**, 198–211 (2013).

[239] Levin, A. M. *et al.* Joint effects of pregnancy, sociocultural, and environmental factors on early life gut microbiome structure and diversity. *Sci. Rep.* **6**, 31775 (2016).

[240] Rayfield, S. & Plugge, E. Systematic review and meta-analysis of the association between maternal smoking in pregnancy and childhood overweight and obesity. *J. Epidemiol. Community Health* **71**, 162–173 (2017).

[241] McLean, C., Jun, S. & Kozyrskyj, A. Impact of maternal smoking on the infant gut microbiota and its association with child overweight: a scoping review. *World J. Pediatr.* **15**, 341–349 (2019).

[242] Hill, C. J. *et al.* Evolution of gut microbiota composition from birth to 24 weeks in the INFANTMET cohort. *Microbiome* **5**, 4 (2017).

[243] Mueller, N. T., Differding, M. K., Østbye, T., Hoyo, C. & Benjamin-Neelon, S. E. Association of birth mode of delivery with infant faecal microbiota, potential pathobionts, and short chain fatty acids: a longitudinal study over the first year of life. *BJOG* **128**, 1293–1303 (2021).

[244] Singh, S. B. *et al.* Does birth mode modify associations of maternal pre-pregnancy BMI and gestational weight gain with the infant gut microbiome? *Int. J. Obes.* **44**, 23–32 (2020).

[245] Galazzo, G. *et al.* Development of the microbiota and associations with birth mode, diet, and atopic disorders in a longitudinal analysis of stool samples, collected from infancy through early childhood. *Gastroenterology* **158**, 1584–1596 (2020).

[246] Costello, E. K. *et al.* Bacterial community variation in human body habitats across space and time. *Science* **326**, 1694–1697 (2009).

[247] Yeoh, Y. K. *et al.* Impact of inter- and intra-individual variation, sample storage and sampling fraction on human stool microbial community profiles. *PeerJ* **7**, e6172 (2019).

[248] Sugino, K. Y., Paneth, N. & Comstock, S. S. Michigan cohorts to determine associations of maternal pre-pregnancy body mass index with pregnancy and infant gastrointestinal microbial communities: Late pregnancy and early infancy. *PLoS One* **14**, e0213733 (2019).

[249] Salonen, A. *et al.* Impact of diet and individual variation on intestinal microbiota composition and fermentation products in obese men. *ISME J.* **8**, 2218–2230 (2014).

[250] Henderson, G. *et al.* Improved taxonomic assignment of rumen bacterial 16S rRNA sequences using a revised SILVA taxonomic framework. *PeerJ* **7**, e6496 (2019).

[251] Kovatcheva-Datchary, P. *et al.* Dietary Fiber-Induced improvement in glucose metabolism is associated with increased abundance of prevotella. *Cell Metab.* **22**, 971–982 (2015).

[252] Pedersen, H. K. *et al.* Human gut microbes impact host serum metabolome and insulin sensitivity. *Nature* **535**, 376–381 (2016).

[253] Scher, J. U. *et al.* Expansion of intestinal prevotella copri correlates with enhanced susceptibility to arthritis. *Elife* **2**, e01202 (2013).

[254] Martínez-Cuesta, M. C., Del Campo, R., Garriga-García, M., Peláez, C. & Requena, T. Taxonomic characterization and Short-Chain fatty acids

production of the obese microbiota. *Front. Cell. Infect. Microbiol.* **11**, 598093 (2021).

[255] Oliphant, K. & Allen-Vercoe, E. Macronutrient metabolism by the human gut microbiome: major fermentation by-products and their impact on host health. *Microbiome* **7**, 91 (2019).

[256] Waters, J. L. & Ley, R. E. The human gut bacteria christensenellaceae are widespread, heritable, and associated with health. *BMC Biol.* **17**, 83 (2019).

[257] Gao, B. *et al.* Gut microbiota in early pregnancy among women with hyperglycaemia vs. normal blood glucose. *BMC Pregnancy Childbirth* **20**, 284 (2020).

[258] Goodrich, J. K. *et al.* Human genetics shape the gut microbiome. *Cell* **159**, 789–799 (2014).

[259] Morotomi, M., Nagai, F. & Watanabe, Y. Description of christensenella minuta gen. nov., sp. nov., isolated from human faeces, which forms a distinct branch in the order clostridiales, and proposal of christensenellaceae fam. nov. *Int. J. Syst. Evol. Microbiol.* **62**, 144–149 (2012).

[260] Gopalakrishna, K. P. *et al.* Maternal IgA protects against the development of necrotizing enterocolitis in preterm infants. *Nat. Med.* **25**, 1110–1115 (2019).

[261] Korpela, K. *et al.* Intestinal microbiota development and gestational age in preterm neonates. *Sci. Rep.* **8**, 2453 (2018).

[262] Chia, L. W. *et al.* Bacteroides thetaiotaomicron fosters the growth of Butyrate-Producing anaerostipes caccae in the presence of lactose and total human milk carbohydrates. *Microorganisms* **8** (2020).

[263] Pham, V. T., Lacroix, C., Braegger, C. P. & Chassard, C. Lactate-utilizing community is associated with gut microbiota dysbiosis in colicky infants. *Sci. Rep.* **7**, 11176 (2017).

[264] Hyman, P. E. *et al.* Childhood functional gastrointestinal disorders: neonate/toddler. *Gastroenterology* **130**, 1519–1526 (2006).

[265] Gohir, W. *et al.* High-fat diet intake modulates maternal intestinal adaptations to pregnancy and results in placental hypoxia, as well as altered fetal gut barrier proteins and immune markers. *J. Physiol.* **597**, 3029–3051 (2019).

[266] Gohir, W., Ratcliffe, E. M. & Sloboda, D. M. Of the bugs that shape us: maternal obesity, the gut microbiome, and long-term disease risk. *Pediatr. Res.* **77**, 196–204 (2015).

[267] Gluckman, P. D., Hanson, M. A. & Buklijas, T. A conceptual framework for the developmental origins of health and disease. *J. Dev. Orig. Health Dis.* **1**, 6–18 (2010).

[268] Catalano, P. M., Presley, L., Minium, J. & Hauguel-de Mouzon, S. Fetuses of obese mothers develop insulin resistance in utero. *Diabetes Care* **32**, 1076–1080 (2009).

[269] Eriksson, J. G., Sandboge, S., Salonen, M., Kajantie, E. & Osmond, C. Maternal weight in pregnancy and offspring body composition in late adulthood: findings from the helsinki birth cohort study (HBCS). *Ann. Med.* **47**, 94–99 (2015).

[270] Reynolds, R. M., Osmond, C., Phillips, D. I. W. & Godfrey, K. M. Maternal BMI, parity, and pregnancy weight gain: influences on offspring adiposity in young adulthood. *J. Clin. Endocrinol. Metab.* **95**, 5365–5369 (2010).

[271] Yu, Z. *et al.* Pre-pregnancy body mass index in relation to infant birth weight and offspring overweight/obesity: a systematic review and meta-analysis. *PLoS One* **8**, e61627 (2013).

[272] Bayol, S. A., Simbi, B. H., Bertrand, J. A. & Stickland, N. C. Offspring from mothers fed a 'junk food' diet in pregnancy and lactation exhibit exacerbated adiposity that is more pronounced in females. *J. Physiol.* **586**, 3219–3230 (2008).

[273] Desai, M. *et al.* Maternal obesity and high-fat diet program offspring metabolic syndrome. *Am. J. Obstet. Gynecol.* **211**, 237.e1–237.e13 (2014).

[274] Samuelsson, A.-M. *et al.* Diet-induced obesity in female mice leads to offspring hyperphagia, adiposity, hypertension, and insulin resistance: a novel murine model of developmental programming. *Hypertension* **51**, 383–392 (2008).

[275] Alfaradhi, M. Z. & Ozanne, S. E. Developmental programming in response to maternal overnutrition. *Front. Genet.* **2**, 27 (2011).

[276] Basu, S. *et al.* Pregravid obesity associates with increased maternal endotoxemia and metabolic inflammation. *Obesity* **19**, 476–482 (2011).

[277] Challier, J. C. *et al.* Obesity in pregnancy stimulates macrophage accumulation and inflammation in the placenta. *Placenta* **29**, 274–281 (2008).

[278] Shankar, K. *et al.* Maternal obesity promotes a proinflammatory signature in rat uterus and blastocyst. *Endocrinology* **152**, 4158–4170 (2011).

[279] Donnelly, J. M. *et al.* Perinatal inflammation and childhood adiposity - a gender effect? *J. Matern. Fetal. Neonatal Med.* **33**, 1203–1210 (2020).

[280] Radaelli, T. *et al.* Maternal interleukin-6: marker of fetal growth and adiposity. *J. Soc. Gynecol. Investig.* **13**, 53–57 (2006).

[281] Murabayashi, N. *et al.* Maternal high-fat diets cause insulin resistance through inflammatory changes in fetal adipose tissue. *Eur. J. Obstet. Gynecol. Reprod. Biol.* **169**, 39–44 (2013).

[282] Yan, X. *et al.* Up-regulation of toll-like receptor 4/nuclear factor-kappab signaling is associated with enhanced adipogenesis and insulin resistance in fetal skeletal muscle of obese sheep at late gestation. *Endocrinology* **151**, 380–387 (2010).

[283] Dijkstra, D. J. *et al.* Mid-gestation low-dose LPS administration results in female-specific excessive weight gain upon a western style diet in mouse offspring. *Sci. Rep.* **10**, 19618 (2020).

[284] Gohir, W. *et al.* Pregnancy-related changes in the maternal gut microbiota are dependent upon the mother's periconceptional diet. *Gut Microbes* **6**, 310–320 (2015).

[285] Soderborg, T. K. *et al.* The gut microbiota in infants of obese mothers increases inflammation and susceptibility to NAFLD. *Nat. Commun.* **9**, 4462 (2018).

[286] Zhou, L. & Xiao, X. The role of gut microbiota in the effects of maternal obesity during pregnancy on offspring metabolism. *Biosci. Rep.* **38** (2018).

[287] Melo, A. M. *et al.* Hypothalamic endoplasmic reticulum stress and insulin resistance in offspring of mice dams fed high-fat diet during pregnancy and lactation. *Metabolism* **63**, 682–692 (2014).

[288] Park, S., Jang, A. & Bouret, S. G. Maternal obesity-induced endoplasmic reticulum stress causes metabolic alterations and abnormal hypothalamic development in the offspring. *PLoS Biol.* **18**, e3000296 (2020).

[289] de Almeida-Faria, J. *et al.* Maternal obesity during pregnancy leads to adipose tissue ER stress in mice via mir-126-mediated reduction in lunapark. *Diabetologia* **64**, 890–902 (2021).

[290] Soeda, J. *et al.* Maternal obesity alters endoplasmic reticulum homeostasis in offspring pancreas. *J. Physiol. Biochem.* **72**, 281–291 (2016).

[291] Hu, P., Han, Z., Couvillon, A. D., Kaufman, R. J. & Exton, J. H. Autocrine tumor necrosis factor alpha links endoplasmic reticulum stress to the membrane death receptor pathway through IRE1α-mediated NF-κB activation and down-regulation of TRAF2 expression. *Mol. Cell. Biol.* **26**, 3071–3084 (2006).

[292] Levine, S. J. *et al.* Tumor necrosis factor-alpha induces mucin hypersecretion and MUC-2 gene expression by human airway epithelial cells. *Am. J. Respir. Cell Mol. Biol.* **12**, 196–204 (1995).

[293] Ding, S. *et al.* High-fat diet: bacteria interactions promote intestinal inflammation which precedes and correlates with obesity and insulin resistance in mouse. *PLoS One* **5**, e12191 (2010).

[294] Ma, J. *et al.* High-fat maternal diet during pregnancy persistently alters the offspring microbiome in a primate model. *Nat. Commun.* **5**, 3889 (2014).

[295] Zhu, A., Sunagawa, S., Mende, D. R. & Bork, P. Inter-individual differences in the gene content of human gut bacterial species. *Genome Biol.* **16**, 82 (2015).

[296] Ruder, B., Atreya, R. & Becker, C. Tumour necrosis factor alpha in intestinal homeostasis and gut related diseases. *Int. J. Mol. Sci.* **20** (2019).

[297] Lagkouvardos, I. *et al.* Sequence and cultivation study of muribaculaceae reveals novel species, host preference, and functional potential of this yet undescribed family. *Microbiome* **7**, 28 (2019).

[298] Pereira, F. C. *et al.* Rational design of a microbial consortium of mucosal sugar utilizers reduces clostridiodes difficile colonization. *Nat. Commun.* **11**, 5104 (2020).

[299] Li, L.-L. *et al.* Inulin with different degrees of polymerization protects against diet-induced endotoxemia and inflammation in association with gut microbiota regulation in mice. *Sci. Rep.* **10**, 978 (2020).

[300] Tailford, L. E., Crost, E. H., Kavanaugh, D. & Juge, N. Mucin glycan foraging in the human gut microbiome. *Front. Genet.* **6**, 81 (2015).

[301] Pruss, K. M. *et al.* Mucin-derived o-glycans supplemented to diet mitigate diverse microbiota perturbations. *ISME J.* **15**, 577–591 (2021).

[302] Bloom, S. M. *et al.* Commensal bacteroides species induce colitis in host-genotype-specific fashion in a mouse model of inflammatory bowel disease. *Cell Host Microbe* **9**, 390–403 (2011).

[303] Zhang, C. *et al.* Structural resilience of the gut microbiota in adult mice under high-fat dietary perturbations. *ISME J.* **6**, 1848–1857 (2012).

[304] Xie, G. *et al.* Dysregulated hepatic bile acids collaboratively promote liver carcinogenesis. *Int. J. Cancer* **139**, 1764–1775 (2016).

[305] Gamage, H. K. A. H. *et al.* Changes in dietary fiber intake in mice reveal associations between colonic mucin o-glycosylation and specific gut bacteria. *Gut Microbes* **12**, 1802209 (2020).

[306] Bisanz, J. E., Upadhyay, V., Turnbaugh, J. A., Ly, K. & Turnbaugh, P. J. Meta-Analysis reveals reproducible gut microbiome alterations in response to a High-Fat diet. *Cell Host Microbe* **26**, 265–272.e4 (2019).

[307] De Fabiani, E. *et al.* The negative effects of bile acids and tumor necrosis factor-α on the transcription of cholesterol 7α-hydroxylase gene (CYP7A1) converge to hepatic nuclear factor-4: a novel mechanism of feedback regulation of bile acid synthesis mediated by nuclear receptors. *J. Biol. Chem.* **276**, 30708–30716 (2001).

[308] Yamato, M. *et al.* High-fat diet-induced obesity and insulin resistance were ameliorated via enhanced fecal bile acid excretion in tumor necrosis factor-alpha receptor knockout mice. *Mol. Cell. Biochem.* **359**, 161–167 (2012).

[309] Labbé, A., Ganopolsky, J. G., Martoni, C. J., Prakash, S. & Jones, M. L. Bacterial bile metabolising gene abundance in crohn's, ulcerative colitis and type 2 diabetes metagenomes. *PLoS One* **9**, e115175 (2014).

[310] Smith, B. J. *et al.* Changes in the gut microbiome and fermentation products concurrent with enhanced longevity in acarbose-treated mice. *BMC Microbiol.* **19**, 130 (2019).

[311] Lee, S. H. Intestinal permeability regulation by tight junction: implication on inflammatory bowel diseases. *Intest Res* **13**, 11–18 (2015).

[312] Al-Sadi, R. *et al.* Occludin regulates macromolecule flux across the intestinal epithelial tight junction barrier. *Am. J. Physiol. Gastrointest. Liver Physiol.* **300**, G1054–64 (2011).

[313] Rosenthal, R. *et al.* Claudin-2, a component of the tight junction, forms a paracellular water channel. *J. Cell Sci.* **123**, 1913–1921 (2010).

[314] Schütte, A. *et al.* Microbial-induced meprin β cleavage in MUC2 mucin and a functional CFTR channel are required to release anchored small intestinal mucus. *Proc. Natl. Acad. Sci. U. S. A.* **111**, 12396–12401 (2014).

[315] Birchenough, G. M. H., Nyström, E. E. L., Johansson, M. E. V. & Hansson, G. C. A sentinel goblet cell guards the colonic crypt by triggering nlrp6-dependent muc2 secretion. *Science* **352**, 1535–1542 (2016).

[316] Gulhane, M. *et al.* High fat diets induce colonic epithelial cell stress and inflammation that is reversed by IL-22. *Sci. Rep.* **6**, 28990 (2016).

[317] Beyaz, S. *et al.* High-fat diet enhances stemness and tumorigenicity of intestinal progenitors. *Nature* **531**, 53–58 (2016).

[318] Guo, C. *et al.* Genetic ablation of tumor necrosis factor-alpha attenuates the promoted colonic wnt signaling in high fat diet-induced obese mice. *J. Nutr. Biochem.* **77**, 108302 (2020).

[319] Boney, C. M., Verma, A., Tucker, R. & Vohr, B. R. Metabolic syndrome in childhood: association with birth weight, maternal obesity, and gestational diabetes mellitus. *Pediatrics* **115**, e290–6 (2005).

[320] Heijmans, J. *et al.* ER stress causes rapid loss of intestinal epithelial stemness through activation of the unfolded protein response. *Cell Rep.* **3**, 1128–1139 (2013).

[321] Breznik, J. A. *et al.* Effects of Obesity-Associated chronic inflammation on peripheral blood immunophenotype are not mediated by TNF in female C57BL/6J mice. *Immunohorizons* **5**, 370–383 (2021).

[322] Jaipaul, J. V., Newburn-Cook, C. V., O'Brien, B. & Demianczuk, N. Modifiable risk factors for term large for gestational age births. *Health Care Women Int.* **30**, 802–823 (2009).

[323] Mathew, M., Machado, L., Al-Ghabshi, R. & Al-Haddabi, R. Fetal macrosomia. risk factor and outcome. *Saudi Med. J.* **26**, 96–100 (2005).

[324] Jones, H. N. *et al.* High-fat diet before and during pregnancy causes marked up-regulation of placental nutrient transport and fetal overgrowth in C57/BL6 mice. *FASEB J.* **23**, 271–278 (2009).

[325] Luo, Z.-C. *et al.* Maternal and fetal IGF-I and IGF-II levels, fetal growth, and gestational diabetes. *J. Clin. Endocrinol. Metab.* **97**, 1720–1728 (2012).

[326] Howell, K. R. & Powell, T. L. Effects of maternal obesity on placental function and fetal development. *Reproduction* **153**, R97–R108 (2017).

[327] Radulescu, L., Munteanu, O., Popa, F. & Cirstoiu, M. The implications and consequences of maternal obesity on fetal intrauterine growth restriction. *J. Med. Life* **6**, 292–298 (2013).

[328] Thagaard, I. N. *et al.* The effect of obesity on early fetal growth and pregnancy duration: a cohort study. *J. Matern. Fetal. Neonatal Med.* **31**, 2941–2946 (2018).

[329] van Duijn, L., Rousian, M., Laven, J. S. E. & Steegers-Theunissen, R. P. M. Periconceptional maternal body mass index and the impact on post-implantation (sex-specific) embryonic growth and morphological development. *Int. J. Obes.* (2021).

[330] de Barros Mucci, D. *et al.* Impact of maternal obesity on placental transcriptome and morphology associated with fetal growth restriction in mice. *Int. J. Obes.* **44**, 1087–1096 (2020).

[331] Thevaranjan, N. *et al.* Age-Associated microbial dysbiosis promotes intestinal permeability, systemic inflammation, and macrophage dysfunction. *Cell Host Microbe* **21**, 455–466.e4 (2017).

[332] Everard, A. *et al.* Cross-talk between akkermansia muciniphila and intestinal epithelium controls diet-induced obesity. *Proc. Natl. Acad. Sci. U. S. A.* **110**, 9066–9071 (2013).

[333] Belzer, C. & de Vos, W. M. Microbes inside–from diversity to function: the case of akkermansia. *ISME J.* **6**, 1449–1458 (2012).

[334] Agrawal, B., Reddish, M. A., Krantz, M. J. & Longenecker, B. M. Does pregnancy immunize against breast cancer? *Cancer Res.* **55**, 2257–2261 (1995).

[335] Mastrodonato, M. *et al.* High-fat diet alters the oligosaccharide chains of colon mucins in mice. *Histochem. Cell Biol.* **142**, 449–459 (2014).

[336] Sodhi, C. P. *et al.* Intestinal epithelial toll-like receptor 4 regulates goblet cell development and is required for necrotizing enterocolitis in mice. *Gastroenterology* **143**, 708–718.e5 (2012).

[337] Tawiah, A. *et al.* High MUC2 mucin expression and misfolding induce cellular stress, reactive oxygen production, and apoptosis in goblet cells. *Am. J. Pathol.* **188**, 1354–1373 (2018).

[338] Wankhade, U. D. *et al.* Maternal High-Fat diet programs offspring liver steatosis in a sexually dimorphic manner in association with changes in gut microbial ecology in mice. *Sci. Rep.* **8**, 16502 (2018).

[339] Mann, P. E., Huynh, K. & Widmer, G. Maternal high fat diet and its consequence on the gut microbiome: A rat model. *Gut Microbes* **9**, 143–154 (2018).

[340] Espín-Palazón, R. & Traver, D. The NF-κB family: Key players during embryonic development and HSC emergence. *Exp. Hematol.* **44**, 519–527 (2016).

[341] Nguyen, D. N. *et al.* Prenatal Intra-Amniotic endotoxin induces fetal gut and lung immune responses and postnatal systemic inflammation in preterm pigs. *Am. J. Pathol.* **188**, 2629–2643 (2018).

[342] Wolfs, T. G. A. M. *et al.* Endotoxin induced chorioamnionitis prevents intestinal development during gestation in fetal sheep. *PLoS One* **4**, e5837 (2009).

[343] Fricke, E. M. *et al.* Lipopolysaccharide-induced maternal inflammation induces direct placental injury without alteration in placental blood flow and induces a secondary fetal intestinal injury that persists into adulthood. *Am. J. Reprod. Immunol.* **79**, e12816 (2018).

[344] Vickers, M. H., Breier, B. H., McCarthy, D. & Gluckman, P. D. Sedentary behavior during postnatal life is determined by the prenatal environment and exacerbated by postnatal hypercaloric nutrition. *Am. J. Physiol. Regul. Integr. Comp. Physiol.* **285**, R271–3 (2003).

[345] O'Regan, D., Kenyon, C. J., Seckl, J. R. & Holmes, M. C. Prenatal dexamethasone 'programmes' hypotension, but stress-induced hypertension in adult offspring. *J. Endocrinol.* **196**, 343–352 (2008).

[346] Miyawaki, J., Sakayama, K., Kato, H., Yamamoto, H. & Masuno, H. Perinatal and postnatal exposure to bisphenol a increases adipose tissue mass and serum cholesterol level in mice. *J. Atheroscler. Thromb.* **14**, 245–252 (2007).

[347] Hsu, M.-H. *et al.* Effects of maternal resveratrol on maternal High-Fat Diet/Obesity with or without postnatal High-Fat diet. *Int. J. Mol. Sci.* **21** (2020).

[348] Page, K. C., Malik, R. E., Ripple, J. A. & Anday, E. K. Maternal and postweaning diet interaction alters hypothalamic gene expression and modulates response to a high-fat diet in male offspring. *Am. J. Physiol. Regul. Integr. Comp. Physiol.* **297**, R1049–57 (2009).

[349] Shankar, K. *et al.* Maternal obesity at conception programs obesity in the offspring. *Am. J. Physiol. Regul. Integr. Comp. Physiol.* **294**, R528–38 (2008).

[350] Mitra, A., Alvers, K. M., Crump, E. M. & Rowland, N. E. Effect of high-fat diet during gestation, lactation, or postweaning on physiological and behavioral indexes in borderline hypertensive rats. *Am. J. Physiol. Regul. Integr. Comp. Physiol.* **296**, R20–8 (2009).

[351] Chen, H., Simar, D. & Morris, M. J. Hypothalamic neuroendocrine circuitry is programmed by maternal obesity: interaction with postnatal nutritional environment. *PLoS One* **4**, e6259 (2009).

[352] Bayol, S. A., Simbi, B. H., Fowkes, R. C. & Stickland, N. C. A maternal "junk food" diet in pregnancy and lactation promotes nonalcoholic fatty liver disease in rat offspring. *Endocrinology* **151**, 1451–1461 (2010).

[353] Pruis, M. G. M. *et al.* Maternal western diet primes non-alcoholic fatty liver disease in adult mouse offspring. *Acta Physiol.* **210**, 215–227 (2014).

[354] Tsukahara, T., Iwasaki, Y., Nakayama, K. & Ushida, K. Stimulation of butyrate production in the large intestine of weaning piglets by dietary fructooligosaccharides and its influence on the histological variables of the large intestinal mucosa. *J. Nutr. Sci. Vitaminol. (Tokyo)* **49**, 414–421 (2003).

[355] Scheppach, W. Effects of short chain fatty acids on gut morphology and function. *Gut* **35**, S35–8 (1994).

[356] Al Nabhani, Z. *et al.* A weaning reaction to microbiota is required for resistance to immunopathologies in the adult. *Immunity* **50**, 1276–1288.e5 (2019).

[357] Al Nabhani, Z. & Eberl, G. Imprinting of the immune system by the microbiota early in life. *Mucosal Immunol.* **13**, 183–189 (2020).

[358] Timmerman, H. M. *et al.* Intestinal colonisation patterns in breastfed and formula-fed infants during the first 12 weeks of life reveal sequential microbiota signatures. *Sci. Rep.* **7**, 8327 (2017).

[359] Scholtens, P. A. M. J., Oozeer, R., Martin, R., Amor, K. B. & Knol, J. The early settlers: intestinal microbiology in early life. *Annu. Rev. Food Sci. Technol.* **3**, 425–447 (2012).

[360] Mackie, R. I., Sghir, A. & Gaskins, H. R. Developmental microbial ecology of the neonatal gastrointestinal tract. *Am. J. Clin. Nutr.* **69**, 1035S–1045S (1999).

[361] Wilczyńska, P., Skarżyńska, E. & Lisowska-Myjak, B. Meconium microbiome as a new source of information about long-term health and disease: questions and answers. *J. Matern. Fetal. Neonatal Med.* **32**, 681–686 (2019).

[362] Orrhage, K. & Nord, C. E. Factors controlling the bacterial colonization of the intestine in breastfed infants. *Acta Paediatr. Suppl.* **88**, 47–57 (1999).

[363] Underwood, M. A., German, J. B., Lebrilla, C. B. & Mills, D. A. Bifidobacterium longum subspecies infantis: champion colonizer of the infant gut. *Pediatr. Res.* **77**, 229–235 (2014).

[364] Sela, D. A. Bifidobacterial utilization of human milk oligosaccharides. *Int. J. Food Microbiol.* **149**, 58–64 (2011).

[365] Stearns, J. C. *et al.* Ethnic and diet-related differences in the healthy infant microbiome. *Genome Med.* **9**, 32 (2017).

[366] Mirpuri, J. *et al.* Proteobacteria-specific IgA regulates maturation of the intestinal microbiota. *Gut Microbes* **5**, 28–39 (2014).

[367] Kawai, T. & Akira, S. Toll-like receptors and their crosstalk with other innate receptors in infection and immunity. *Immunity* **34**, 637–650 (2011).

[368] Thorburn, A. N. *et al.* Evidence that asthma is a developmental origin disease influenced by maternal diet and bacterial metabolites. *Nat. Commun.* **6**, 7320 (2015).

[369] Hornef, M. W. & Torow, N. 'layered immunity' and the 'neonatal window of opportunity' - timed succession of non-redundant phases to establish mucosal host-microbial homeostasis after birth. *Immunology* **159**, 15–25 (2020).

[370] Arpaia, N. *et al.* Metabolites produced by commensal bacteria promote peripheral regulatory t-cell generation. *Nature* **504**, 451–455 (2013).

[371] Russell, S. L. *et al.* Early life antibiotic-driven changes in microbiota enhance susceptibility to allergic asthma. *EMBO Rep.* **13**, 440–447 (2012).

[372] Slykerman, R. F. *et al.* Exposure to antibiotics in the first 24 months of life and neurocognitive outcomes at 11 years of age. *Psychopharmacology* **236**, 1573–1582 (2019).

[373] Slykerman, R. F. *et al.* Antibiotics in the first year of life and subsequent neurocognitive outcomes. *Acta Paediatr.* **106**, 87–94 (2017).

[374] Wesolowski, S. R., Kasmi, K. C. E., Jonscher, K. R. & Friedman, J. E. Developmental origins of NAFLD: a womb with a clue. *Nat. Rev. Gastroenterol. Hepatol.* **14**, 81–96 (2016).

[375] Dogra, S. *et al.* Dynamics of infant gut microbiota are influenced by delivery mode and gestational duration and are associated with subsequent adiposity. *MBio* **6** (2015).

[376] Bailey, L. C. *et al.* Association of antibiotics in infancy with early childhood obesity. *JAMA Pediatr.* **168**, 1063–1069 (2014).

[377] Azad, M. B., Bridgman, S. L., Becker, A. B. & Kozyrskyj, A. L. Infant antibiotic exposure and the development of childhood overweight and central adiposity. *Int. J. Obes.* **38**, 1290–1298 (2014).

[378] Ribaroff, G. A., Wastnedge, E., Drake, A. J., Sharpe, R. M. & Chambers, T. J. G. Animal models of maternal high fat diet exposure and effects on

metabolism in offspring: a meta-regression analysis. *Obes. Rev.* **18**, 673–686 (2017).

[379] Pace, R. M. *et al.* Exposure to a high fat diet is associated with persistent alterations in behavior and the gut microbiome in juvenile offspring primates (2018).

[380] Pantoja-Feliciano, I. G. *et al.* Biphasic assembly of the murine intestinal microbiota during early development. *ISME J.* **7**, 1112–1115 (2013).

[381] Peng, C. *et al.* Sex-specific association between the gut microbiome and high-fat diet-induced metabolic disorders in mice. *Biol. Sex Differ.* **11**, 5 (2020).

[382] Campbell, C. L. *et al.* Modulation of fat metabolism and gut microbiota by resveratrol on high-fat diet-induced obese mice. *Diabetes Metab. Syndr. Obes.* **12**, 97–107 (2019).

[383] Feng, Y., Wang, Y., Wang, P., Huang, Y. & Wang, F. Short-Chain fatty acids manifest stimulative and protective effects on intestinal barrier function through the inhibition of NLRP3 inflammasome and autophagy. *Cell. Physiol. Biochem.* **49**, 190–205 (2018).

[384] Anitha, M. *et al.* Intestinal dysbiosis contributes to the delayed gastrointestinal transit in high-fat diet fed mice. *Cell. Mol. Gastroenterol. Hepatol.* **2**, 328–339 (2016).

[385] Li, B. *et al.* Intestinal epithelial tight junctions and permeability can be rescued through the regulation of endoplasmic reticulum stress by amniotic fluid stem cells during necrotizing enterocolitis. *FASEB J.* **35**, e21265 (2021).

[386] Heazlewood, C. K. *et al.* Aberrant mucin assembly in mice causes endoplasmic reticulum stress and spontaneous inflammation resembling ulcerative colitis. *PLoS Med.* **5**, e54 (2008).

[387] Steegenga, W. T. *et al.* Maternal exposure to a western-style diet causes differences in intestinal microbiota composition and gene expression of suckling mouse pups. *Mol. Nutr. Food Res.* **61** (2017).

[388] Min, Y. *et al.* Sex-specific association between gut microbiome and fat distribution. *Nat. Commun.* **10**, 2408 (2019).

[389] Foley, M. H. *et al.* Lactobacillus bile salt hydrolase substrate specificity governs bacterial fitness and host colonization. *Proc. Natl. Acad. Sci. U. S. A.* **118** (2021).

[390] Murakami, Y., Tanabe, S. & Suzuki, T. High-fat diet-induced intestinal hyperpermeability is associated with increased bile acids in the large intestine of mice. *J. Food Sci.* **81**, H216–22 (2016).

[391] Wang, X., Magkos, F. & Mittendorfer, B. Sex differences in lipid and lipoprotein metabolism: it's not just about sex hormones. *J. Clin. Endocrinol. Metab.* **96**, 885–893 (2011).

[392] Gälman, C., Angelin, B. & Rudling, M. Pronounced variation in bile acid synthesis in humans is related to gender, hypertriglyceridaemia and circulating levels of fibroblast growth factor 19. *J. Intern. Med.* **270**, 580–588 (2011).

[393] Selwyn, F. P., Csanaky, I. L., Zhang, Y. & Klaassen, C. D. Importance of large intestine in regulating bile acids and Glucagon-Like peptide-1 in Germ-Free mice. *Drug Metab. Dispos.* **43**, 1544–1556 (2015).

[394] Fu, Z. D., Csanaky, I. L. & Klaassen, C. D. Gender-divergent profile of bile acid homeostasis during aging of mice. *PLoS One* **7**, e32551 (2012).

[395] Sheng, L. *et al.* Gender differences in bile acids and microbiota in relationship with gender dissimilarity in steatosis induced by diet and FXR inactivation. *Sci. Rep.* **7**, 1748 (2017).

[396] Phelps, T., Snyder, E., Rodriguez, E., Child, H. & Harvey, P. The influence of biological sex and sex hormones on bile acid synthesis and cholesterol homeostasis. *Biol. Sex Differ.* **10**, 52 (2019).

[397] Huang, D. *et al.* Bile acids elevated by high-fat feeding induce endoplasmic reticulum stress in intestinal stem cells and contribute to mucosal barrier damage. *Biochem. Biophys. Res. Commun.* **529**, 289–295 (2020).

[398] Zheng, L. *et al.* Microbial-Derived butyrate promotes epithelial barrier function through IL-10 Receptor–Dependent repression of claudin-2. *The Journal of Immunology* **199**, 2976–2984 (2017).

[399] Hanson, M. A. *et al.* Developmental origins of health and disease. *Journal of Developmental Origins of Health and Disease (print ISSN* **2040**, 1744 (2010).

[400] de Goffau, M. C., Charnock-Jones, D. S., Smith, G. C. S. & Parkhill, J. Batch effects account for the main findings of an in utero human intestinal bacterial colonization study. *Microbiome* **9**, 6 (2021).

[401] Fujimura, K. E. *et al.* Neonatal gut microbiota associates with childhood multisensitized atopy and T cell differentiation. *Nat. Med.* **22**, 1187–1191 (2016).

[402] Ruohtula, T. *et al.* Maturation of gut microbiota and circulating regulatory T cells and development of IgE sensitization in early life. *Front. Immunol.* **10**, 2494 (2019).

[403] Nishikawa, J., Kudo, T., Sakata, S., Benno, Y. & Sugiyama, T. Diversity of mucosa-associated microbiota in active and inactive ulcerative colitis. *Scand. J. Gastroenterol.* **44**, 180–186 (2009).

[404] Manichanh, C. *et al.* Reduced diversity of faecal microbiota in crohn's disease revealed by a metagenomic approach. *Gut* **55**, 205–211 (2006).

[405] Stanislawski, M. A., Dabelea, D., Lange, L. A., Wagner, B. D. & Lozupone, C. A. Gut microbiota phenotypes of obesity. *NPJ Biofilms Microbiomes* **5**, 18 (2019).

[406] Abrahamsson, T. R. *et al.* Low gut microbiota diversity in early infancy precedes asthma at school age. *Clin. Exp. Allergy* **44**, 842–850 (2014).

[407] Abrahamsson, T. R. *et al.* Low diversity of the gut microbiota in infants with atopic eczema. *J. Allergy Clin. Immunol.* **129**, 434–40, 440.e1–2 (2012).

[408] Mirpuri, J. & Neu, J. Maternal microbial factors that affect the fetus and subsequent offspring. *Semin. Perinatol.* 151449 (2021).

[409] Coustan, D. R. *Maternal Metabolic Adaptation to Pregnancy*, 11–20 (2019).

[410] Soltani, H. & Fraser, R. B. A longitudinal study of maternal anthropometric changes in normal weight, overweight and obese women during pregnancy and postpartum. *Br. J. Nutr.* **84**, 95–101 (2000).

[411] Butte, N. F., Ellis, K. J., Wong, W. W., Hopkinson, J. M. & Smith, E. O. Composition of gestational weight gain impacts maternal fat retention and infant birth weight. *Am. J. Obstet. Gynecol.* **189**, 1423–1432 (2003).

[412] Butte, N. F., Wong, W. W., Treuth, M. S., Ellis, K. J. & O'Brian Smith, E. Energy requirements during pregnancy based on total energy expenditure and energy deposition. *Am. J. Clin. Nutr.* **79**, 1078–1087 (2004).

[413] Bronstein, M. N., Mak, R. P. & King, J. C. Unexpected relationship between fat mass and basal metabolic rate in pregnant women. *Br. J. Nutr.* **75**, 659–668 (1996).

[414] Breznik, J. A. *et al.* TNF, but not hyperinsulinemia or hyperglycemia, is a key driver of obesity-induced monocytosis revealing that inflammatory monocytes correlate with insulin in obese male mice. *Physiol Rep* **6**, e13937 (2018).

[415] Li, T. *et al.* Transgenic expression of cholesterol 7alpha-hydroxylase in the liver prevents high-fat diet-induced obesity and insulin resistance in mice. *Hepatology* **52**, 678–690 (2010).

[416] Laugerette, F. *et al.* Emulsified lipids increase endotoxemia: possible role in early postprandial low-grade inflammation. *J. Nutr. Biochem.* **22**, 53–59 (2011).

[417] Ghoshal, S., Witta, J., Zhong, J., de Villiers, W. & Eckhardt, E. Chylomicrons promote intestinal absorption of lipopolysaccharides. *J. Lipid Res.* **50**, 90–97 (2009).

[418] Cani, P. D. *et al.* Changes in gut microbiota control metabolic Endotoxemia-Induced inflammation in High-Fat Diet–Induced obesity and diabetes in mice. *Diabetes* **57**, 1470–1481 (2008).

[419] Fuke, N., Nagata, N., Suganuma, H. & Ota, T. Regulation of gut microbiota and metabolic endotoxemia with dietary factors. *Nutrients* **11** (2019).

[420] Pichler, M. J. *et al.* Butyrate producing colonic clostridiales metabolise human milk oligosaccharides and cross feed on mucin via conserved pathways. *Nat. Commun.* **11**, 3285 (2020).

[421] Van Herreweghen, F., De Paepe, K., Marzorati, M. & Van de Wiele, T. Mucin as a functional niche is a more important driver of in vitro gut microbiota composition and functionality than supplementation of akkermansia m uciniphila. *Appl. Environ. Microbiol.* **87** (2020).

[422] Van den Abbeele, P. *et al.* Butyrate-producing clostridium cluster XIVa species specifically colonize mucins in an in vitro gut model. *ISME J.* **7**, 949–961 (2013).

[423] Zhou, D. *et al.* Sodium butyrate attenuates high-fat diet-induced steatohepatitis in mice by improving gut microbiota and gastrointestinal barrier. *World J. Gastroenterol.* **23**, 60–75 (2017).

[424] Poritz, L. S., Garver, K. I., Tilberg, A. F. & Koltun, W. A. Tumor necrosis factor alpha disrupts tight junction assembly. *J. Surg. Res.* **116**, 14–18 (2004).

[425] Aiken, C. E. & Ozanne, S. E. Sex differences in developmental programming models. *Reproduction* **145**, R1–13 (2013).

[426] Hildebrandt, M. A. *et al.* High-fat diet determines the composition of the murine gut microbiome independently of obesity. *Gastroenterology* **137**, 1716–24.e1–2 (2009).

[427] Bell, A. *et al.* Elucidation of a sialic acid metabolism pathway in mucus-foraging ruminococcus gnavus unravels mechanisms of bacterial adaptation to the gut. *Nat Microbiol* **4**, 2393–2404 (2019).

[428] Lee, S. M. *et al.* Bacterial colonization factors control specificity and stability of the gut microbiota. *Nature* **501**, 426–429 (2013).

[429] Cheney, K., Berkemeier, S., Sim, K. A., Gordon, A. & Black, K. Prevalence and predictors of early gestational weight gain associated with obesity risk in a diverse australian antenatal population: a cross-sectional study. *BMC Pregnancy Childbirth* **17**, 296 (2017).

[430] Johnson, J. *et al.* Pregnancy outcomes with weight gain above or below the 2009 institute of medicine guidelines. *Obstet. Gynecol.* **121**, 969–975 (2013).

[431] Haugen, M. *et al.* Associations of pre-pregnancy body mass index and gestational weight gain with pregnancy outcome and postpartum weight retention: a prospective observational cohort study. *BMC Pregnancy Childbirth* **14**, 201 (2014).

[432] Armitage, J. A., Khan, I. Y., Taylor, P. D., Nathanielsz, P. W. & Poston, L. Developmental programming of the metabolic syndrome by maternal nutritional imbalance: how strong is the evidence from experimental models in mammals? *J. Physiol.* **561**, 355–377 (2004).

[433] Krych, L., Hansen, C. H. F., Hansen, A. K., van den Berg, F. W. J. & Nielsen, D. S. Quantitatively different, yet qualitatively alike: a meta-analysis of the mouse core gut microbiome with a view towards the human gut microbiome. *PLoS One* **8**, e62578 (2013).

[434] Gibbons, D. L. & Spencer, J. Mouse and human intestinal immunity: same ballpark, different players; different rules, same score. *Mucosal Immunol.* **4**, 148–157 (2011).

[435] McCafferty, J. *et al.* Stochastic changes over time and not founder effects drive cage effects in microbial community assembly in a mouse model. *ISME J.* **7**, 2116–2125 (2013).

[436] Perreault, M. *et al.* Structured diet and exercise guidance in pregnancy to improve health in women and their offspring: study protocol for the be healthy in pregnancy (BHIP) randomized controlled trial. *Trials* **19**, 691 (2018).

[437] Diop, K. *et al.* Characterization of a new ezakiella isolated from the human vagina: Genome sequence and description of ezakiella massiliensis sp. nov. *Curr. Microbiol.* **75**, 456–463 (2018).

[438] Knight, R. *et al.* Best practices for analysing microbiomes. *Nat. Rev. Microbiol.* **16**, 410–422 (2018).

[439] Brown, R. E., Mathieson, W. B., Stapleton, J. & Neumann, P. E. Maternal behavior in female C57BL/6J and DBA/2J inbred mice. *Physiol. Behav.* **67**, 599–605 (1999).

[440] Singer, J. R. *et al.* Preventing dysbiosis of the neonatal mouse intestinal microbiome protects against late-onset sepsis. *Nat. Med.* **25**, 1772–1782 (2019).